

UNIVERSITÀ
DEGLI STUDI
DI PADOVA

Sede Amministrativa: Università degli Studi di Padova

Dipartimento di Biologia

SCUOLA DI DOTTORATO DI RICERCA IN BIOSCIENZE E BIOTECNOLOGIE

INDIRIZZO BIOLOGIA CELLULARE

CICLO XXV

Regulation of the Mitochondrial Permeability Transition
Pore: Role of Outer Membrane and of Translocator Protein
(Peripheral Benzodiazepine Receptor)

Direttore della Scuola: Ch.mo Prof. Giuseppe Zanotti

Coordinatore d'indirizzo: Ch.mo Prof. Paolo Bernardi

Supervisore: Ch.mo Prof. Paolo Bernardi

Co-Supervisore: Dr. Fernanda Ricchelli

Dottoranda: Justina Šileikytė

DICEMBRE 2012

“Science, my lad, is made up of mistakes, but they are mistakes which it is useful to make, because they lead little by little to the truth.”

— Jules Verne, *Journey to the Center of the Earth*

Table of Contents

Summary	3
Riassunto.....	4
List of Publications	5
Abbreviations.....	7
Table of Figures.....	9
Table of Tables.....	9
1. Introduction	11
1.1. Mitochondria.....	11
1.1.1. Bioenergetics of mitochondria.....	13
1.1.2. Mitochondrial Ca ²⁺ : from uptake to signaling.....	16
1.1.3. Mitochondria as mediators of cell death.....	17
1.1.3.1. Apoptosis.....	17
1.2. Permeability transition pore.....	21
1.2.1. Regulation of the PTP.....	21
1.2.2. Molecular nature of the PTP.....	24
1.2.2.1. Voltage-dependent anion channel.....	25
1.2.2.2. Adenine nucleotide translocator.....	27
1.2.2.3. Phosphate carrier.....	28
1.2.2.4. Hexokinase.....	28
1.2.2.5. Cyclophilin D.....	29
1.2.3. PTP involvement in pathology.....	29
1.3. Translocator protein (TSPO).....	31
1.3.1. Biological roles.....	31
1.3.2. TSPO ligands.....	32
1.3.3. TSPO and Permeability transition.....	34
2. Results	35
2.1. The mitochondrial permeability transition is an inner membrane event.....	37
Paper 1	39
2.2. PTP regulation by photooxidative stress: implication for the role of TSPO.....	47
Paper 2	49
Paper 3	59
2.3. Characterization of PTP in TSPO-null liver mitochondria.....	71
2.3.1. Materials and methods.....	72
2.3.1.1. Reagents.....	72
2.3.1.2. Generation of TSPO-null mouse livers.....	72
2.3.1.3. Mice genotyping.....	76

2 | Table of Contents

2.3.1.4.	Isolation of mitochondria	77
2.3.1.5.	Western blotting.....	78
2.3.1.6.	Radioligand binding assay.....	78
2.3.1.7.	Measurement of mitochondrial respiration.....	79
2.3.1.8.	Estimation of mitochondrial membrane potential.....	79
2.3.1.9.	Ca ²⁺ retention capacity (CRC) test.....	80
2.3.1.10.	Permeability transition assessed on the osmotic swelling of mitochondria.....	81
2.3.1.11.	Photosensitization of mitochondria	81
2.3.2.	Results and Discussion	82
3.	Conclusions.....	89
4.	References	91
5.	Appendix	113
	Paper 4.....	115
	Paper 5.....	123

Summary

The mitochondrial permeability transition (PT) is a sudden increase in the permeability of the inner mitochondrial membrane (IMM) to solutes with molecular masses up to 1,500 Da. This process is due to opening of a voltage- and Ca^{2+} -dependent, cyclosporin (Cs) A-sensitive, high-conductance channel called the permeability transition pore (PTP). Its involvement in pathological states and in the loss of cell viability is widely recognized, but its molecular identity remains elusive. The long standing idea that the PTP may form at inner-outer membrane contact sites and that it may be constituted by the adenine nucleotide translocator (ANT) in the IMM and voltage dependent anion channel (VDAC) in the outer mitochondrial membrane (OMM) has not been confirmed by genetic ablation of these proteins. Yet, the PT can be regulated by proteins that interact with the OMM such as hexokinase, and by ligands of the OMM translocator protein of 18 kDa (TSPO, formerly known as peripheral benzodiazepine receptor). TSPO is highly conserved throughout evolution and was first identified as a binding site for benzodiazepines in tissues that lack GABA receptors, the clinical target of benzodiazepines in the central nervous system. Moreover, TSPO together with VDAC and ANT was included in the early models of PTP and as of today remains the only putative PTP component whose role has not been addressed by genetic inactivation. Thus, we first investigated the role of OMM in PTP regulation; and then created mice where *Tspo* gene could be inactivated.

We demonstrate that (i) PT is exclusively an IMM event, as it occurs in mitochondria (mitochondria stripped of outer membranes); (ii) in the presence of specific, high affinity TSPO-ligands, such as PK11195, Ro5-4864, FGIN1-27 and protoporphyrin (PP) IX the PT is observed in rat liver mitochondria, but not in mitoplasts; and (iii) upon photooxidative stress (achieved by photoirradiation after treatment with PP IX-like dicarboxylic porphyrins), low doses of light inactivate the PT both in mitochondria and in mitoplasts while high light doses activate the pore in mitochondria only. Conditional elimination of TSPO in mouse livers abolished high affinity binding of the TSPO ligand PK11195, but it did not prevent: (i) CsA-sensitive PTP formation; (ii) PT induction by TSPO ligands PK11195, Ro5-4864 and PP IX; (iii) PT induction by photooxidative stress. The latter findings are unequivocal demonstration that the ability of 'specific' TSPO ligands to regulate PTP is due to off-target effects, possibly at the F_0F_1 ATP synthase.

Riassunto

La transizione della permeabilità mitocondriale (PT) è un aumento della permeabilità della membrana mitocondriale interna (IMM) a soluti con massa molecolare fino a 1.500 Da. Questo processo è causato dall'apertura di un canale ad alta conduttanza, voltaggio e Ca^{2+} dipendente, sensibile alla ciclosporina (Cs) A, chiamato poro di transizione della permeabilità (PTP). Il suo coinvolgimento in varie patologie e nella perdita della vitalità cellulare è ampiamente riconosciuto, ma la sua identità molecolare rimane ancora da stabilire. L'ipotesi che il PTP possa essere costituito dal traslocatore ANT della IMM e da VDAC della membrana mitocondriale esterna (OMM), e che si formi nei siti di contatto tra le due membrane, è stata confutata da esperimenti di inattivazione genetica di queste proteine. Tuttavia, la PT può essere modulata da proteine che interagiscono con la OMM come le esochinasi e ligandi del traslocatore TSPO (noto in precedenza come recettore periferico delle benzodiazepine). TSPO è una proteina altamente conservata nel corso dell'evoluzione ed è stata identificata come recettore per le benzodiazepine in tessuti privi dei recettori GABA. Inoltre, fin dai primi modelli del PTP, TSPO è stato considerato come uno dei suoi componenti assieme a VDAC e ANT, anche se il suo ruolo non è ancora stato confermato. In questo progetto ci siamo focalizzati prima sullo studio del ruolo della OMM nella regolazione del PT, e poi abbiamo creato topicon abelezione genetica di *Tspo* (KO) per meglio caratterizzare il suo ruolo nella PT.

Abbiamo dimostrato che: (i) la PT interessa esclusivamente la IMM, dato che avviene nei mitopasti (mitocondri privi di OMM); (ii) i ligandi di TSPO ad alta affinità come PK11195, Ro5-4864 e protoporfirina (PP) IX inducono la PT in mitocondri di fegato di ratto ma non in mitoplasti; (iii) in condizioni di stress foto-ossidativo la PT è inattivata a basse dosi di luce sia in mitocondri che in mitoplasti, mentre è attivata con alte dosi di luce solo nei mitocondri. Il KO condizionale di *Tspo* in fegato di topo previene il legame ad alta affinità tra TSPO e il suo ligando PK11195, ma non impedisce: (i) la formazione di PTP sensibile alla CsA; (ii) l'induzione della PT da ligandi di TSPO (PK11195, Ro5-4864 e PP IX); (iii) l'induzione della PT da stress fotoossidativo. Questi risultati sono la dimostrazione inequivocabile che i ligandi specifici di TSPO regolano il PTP agendo in un altro bersaglio, che potrebbe essere la F_0F_1 ATP sintetasi.

List of Publications

Included in the Thesis

1. **Šileikytė J**, Petronilli V, Zulian A, Dabbeni-Sala F, Tognon G, Nikolov P, Bernardi P, Ricchelli F. Regulation of the inner membrane mitochondrial permeability transition by the outer membrane translocator protein (peripheral benzodiazepine receptor). *J Biol Chem*. 2011 Jan 14;286(2):1046-53.
2. Ricchelli F, **Šileikytė J**, Bernardi P. Shedding light on the mitochondrial permeability transition. *Biochim Biophys Acta*. 2011 May;1807(5):482-90.
3. **Šileikytė J**, Nikolov P, Bernardi P, Ricchelli F. The outer membrane-translocator protein mediates activation of the mitochondrial permeability transition by porphyrin based photooxidative stress. *Forum on Immunopathological Diseases and Therapeutics*, 2011; 2 (3):215-26.

Not included in the Thesis (see the Appendix)

4. Petronilli V, **Šileikytė J**, Zulian A, Dabbeni-Sala F, Jori G, Gobbo S, Tognon G, Nikolov P, Bernardi P, Ricchelli F. Switch from inhibition to activation of the mitochondrial permeability transition during hematoporphyrin-mediated photooxidative stress. Unmasking pore-regulating external thiols. *Biochim Biophys Acta*. 2009 Jul;1787(7):897-904.
5. Zulian A*, **Šileikytė J***, Petronilli V, Bova S, Dabbeni-Sala F, Cargnelli G, Rennison D, Brimble MA, Hopkins B, Bernardi P, Ricchelli F. The translocator protein (peripheral benzodiazepine receptor) mediates rat-selective activation of the mitochondrial permeability transition by norbormide. *Biochim Biophys Acta*. 2011 Dec;1807(12):1600-5.

*Co-first Authors

Abbreviations

AIF	apoptosis inducing factor
ANT	adenine nucleotide translocator
CoQ	coenzyme Q
CRC	Ca ²⁺ retention capacity
<i>Cre</i>	causes recombination
CsA	cyclosporin A
Cu(OP)₂	copper- <i>o</i> -phenantroline
CypD	cyclophilin D
Cyt <i>c</i>	cytochrome <i>c</i>
DP IX	deuteroporphyrin IX
EGTA	ethylene-bis (oxo-ethylene nitrilo) tetra-acetic acid
FCCP	carbonyl cyanide <i>p</i> -trifluoromethoxyphenylhydrazone
HK	hexokinase
IMM	inner mitochondrial membrane
IMS	intermembrane space
KO	knock out
<i>loxP</i>	locus of crossing (<i>x</i>) over P1
MCU	mitochondrial Ca ²⁺ uniporter
MOMP	mitochondrial outer membrane permeabilization
NEM	<i>N</i> -ethylmaleimide
OMM	outer mitochondrial membrane
OXPHOS	oxidative phosphorylation
PAGE	polyacrylamide gel electrophoresis
PCR	polymerase chain reaction
PhAsO	phenylarsine oxide
PN	pyridine nucleotides
PP IX	protoporphyrin IX
PT	permeability transition
PTP	permeability transition pore
RCR	respiratory control ratio
Rh123	rhodamine 123
SDS	sodium dodecyl sulphate

8 | Abbreviations

Smac / Diablo	second mitochondria-derived activator of caspases / direct IAP binding protein with low pI
TSPO	translocator protein
Ub0	ubiquinone 0
VDAC	voltage dependent anion channel
$\Delta\tilde{\mu}H$	electrochemical proton gradient
$\Delta\Psi$	membrane potential

Table of Figures

Figure 1. The morphology of mitochondrion.....	12
Figure 2. Cellular respiration: the electron transport chain and ATP synthase.	14
Figure 3. Intrinsic and extrinsic pathways of apoptosis.....	18
Figure 4. Schematic representation of PTP-regulating thiols.	23
Figure 5. The most widespread model of the permeability transition pore.....	26
Figure 6. The 34 bp <i>loxP</i> sequence.	73
Figure 7. Mouse <i>Tspo</i> locus and modifications.....	74
Figure 8. Generation of mice in which the <i>Tspo</i> gene was inactivated only in livers.	75
Figure 9. Structure of Rhodamine 123.....	80
Figure 10. Structure of Calcium Green-5N.....	80
Figure 11. TSPO-null mice have no obvious phenotype.....	83
Figure 12. The absence of TSPO does not affect mitochondrial respiration and development of $\Delta\Psi$	84
Figure 13. CRC of floxed and KO mouse liver mitochondria.....	85
Figure 14. Effect of PK11195, Ro5-4864 and PP IX on floxed and KO mouse liver mitochondria CRC.....	85
Figure 15. Effect of irradiation time in PP IX-treated floxed and KO mouse liver mitochondria.	86
Figure 16. [³ H]PK11195 binding to TSPO floxed and KO mitochondria.....	87

Table of Tables

Table 1. Ligand-binding affinities for TSPO.....	33
Table 2. Composition of the PCR reaction mixture.....	76
Table 3. The list of primers used in PCR. Fwd – forward, Rev – reverse.	77
Table 4. Cycling programs used to amplify <i>Tspo</i> gene region containing <i>loxP</i> sites and a part of Cre recombinase DNA.....	77

1. Introduction

1.1. Mitochondria

Situated in the cytoplasm of eukaryotic cells, mitochondria are essential for normal cell function. Originally studied mainly as the ‘powerhouses’ of the cell due to their ability to produce adenosine triphosphate (ATP, the key cellular fuel) nowadays they draw attention also for their role in Ca^{2+} homeostasis, inter-organelle communication, cell proliferation and senescence, and orchestration of various signaling pathways some of which determine cell commitment to death or survival [1]. Alterations in mitochondrial physiology are often synonyms of disease.

The earliest records of intracellular structures that probably were mitochondria date back to the 1840s, but their identification was the achievement of R. Altmann, who in 1890 observed cytoplasmic structures of ubiquitous occurrence resembling bacteria and functioning as “elementary organisms”, and called them bioblasts. The term “mitochondrion” was introduced eight years later by C. Benda and originates from the Greek “mitos” (thread) and “chondros” (granule) [2, 3]. Indeed, mitochondria not only look similar to bacteria in size (0.5-1 μm), they also replicate by fission and have their own genetic material, a circular DNA molecule that in *Homo Sapiens* codes for 22 tRNAs, 2 rRNAs and 13 respiratory chain proteins.

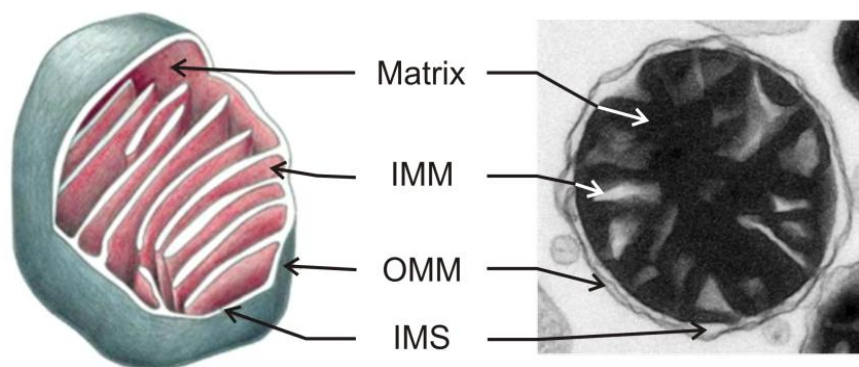


Figure 1. The morphology of mitochondrion.

IMM – inner mitochondrial membrane, OMM – outer mitochondrial membrane, IMS – intermembrane space. *Left:* modified from [4]

From a structural point of view, mitochondria possess two membranes (inner and outer) that are quite distinct in appearance and in physico-chemical properties, which determine the biochemical function of each. The membranes separate two aqueous compartments, the mitochondrial matrix and the intermembrane space (IMS) (Figure 1).

The outer mitochondrial membrane (OMM) is smooth and similar in composition to the plasma membrane. It is composed of phospholipids and proteins in similar proportion. The most abundant proteins in the OMM are membrane-spanning channels called voltage dependent anion channels (VDAC) or porins. They are 2-3 nm-wide in diameter and allow ions, metabolites and small proteins up to 5 kDa to freely diffuse from the cytosol to the IMS and *vice versa*. Higher molecular weight species (proteins) are transported by the OMM translocase complex TOM. Other proteins include enzymes involved in mitochondrial lipid synthesis and tryptophan degradation, transporters of cholesterol or heme precursors, receptors for apoptosis or mitochondrial fusion initiation.

At variance from the OMM, the inner mitochondrial membrane (IMM) has a very high protein-to-phospholipid ratio (~ 3:1 by weight) and its main lipid is cardiolipin. As such, the membrane is almost impermeable to ions and substrates; the only species able to cross it freely are H₂O, oxygen and carbon dioxide (CO₂). The IMM is highly convoluted and forms infoldings called *cristae*, dynamic structures that greatly increase the membrane's surface area allowing a wide range of proteins to be embedded in it [5]. The membrane contains proteins that perform redox reactions in the electron transport chain, the F₀F₁-ATP synthase and tightly controlled transport systems (translocase of inner membrane for protein import and various proteins that govern ion and metabolite transport *from or to* the matrix) [4].

The IMS is one of the two aqueous compartments of a mitochondrion and is in osmotic equilibrium with the cytosol. It hosts several proteins including cytochrome *c* (cyt *c*) and second mitochondria-derived activator of caspases (Smac)/ direct IAP binding protein with low pI (Diablo) that if released in the cytosol may initiate the apoptotic cascade leading to cell death [6]. IMS is also pivotal in exchange of lipids and ions between the matrix and the cytosol, scavenging of reactive oxygen species (ROS) produced by respiratory chain and the control of mitochondrial morphogenesis [7].

Since the matrix is enclosed by the almost impermeable IMM, it contains only a highly selected set of molecular species. It is the most protein-rich mitochondrial compartment, hosting about 2/3 of the organelle's protein contents including enzymes of the Krebs cycle, but also mitochondrial DNA, tRNAs and ribosomes [4].

1.1.1. Bioenergetics of mitochondria

The cellular energy currency, ATP, can be produced in 3 ways: (i) by anaerobic glycolysis (which takes place in the cytosol); when glucose is converted to pyruvate only a small fraction of total free energy potentially available for ATP synthesis is released with an overall net gain of 2 ATP molecules; (ii) by tricarboxylic acid (TCA), also known as citric acid or Krebs cycle, which takes place in mitochondrial matrix and yields one ATP molecule per cycle, (iii) by oxidative phosphorylation (OXPHOS), which takes place in the IMM and allows ~15 times more ATP to be made than that produced by glycolysis. This is because mitochondria house the major enzymatic systems used to complete the oxidation of sugars, fats and proteins that enter the Krebs cycle after being converted to acetyl-CoA. Pyruvate produced by glycolysis enters mitochondria, where pyruvate dehydrogenase catalyzes its conversion to acetyl-CoA, also reducing NAD⁺ to NADH; fatty acids are converted to acetyl-CoA by β oxidation; while various enzymes exist for the conversion of specific amino acids into pyruvate, acetyl-CoA or directly into specific citric acid cycle intermediates. Once in the TCA cycle, CoA causes the acetyl moiety to react with oxaloacetate to produce citrate. In a series of seven subsequent enzymatic steps, citrate is oxidized back to oxaloacetate while giving off two molecules of carbon in the form of CO₂, three NADH and one of flavin adenine dinucleotide FADH₂ [8]. The latter two carry the free energy liberated from the Krebs cycle to the mitochondrial electron transport chain made up of OXPHOS complexes I to V (Figure 2).

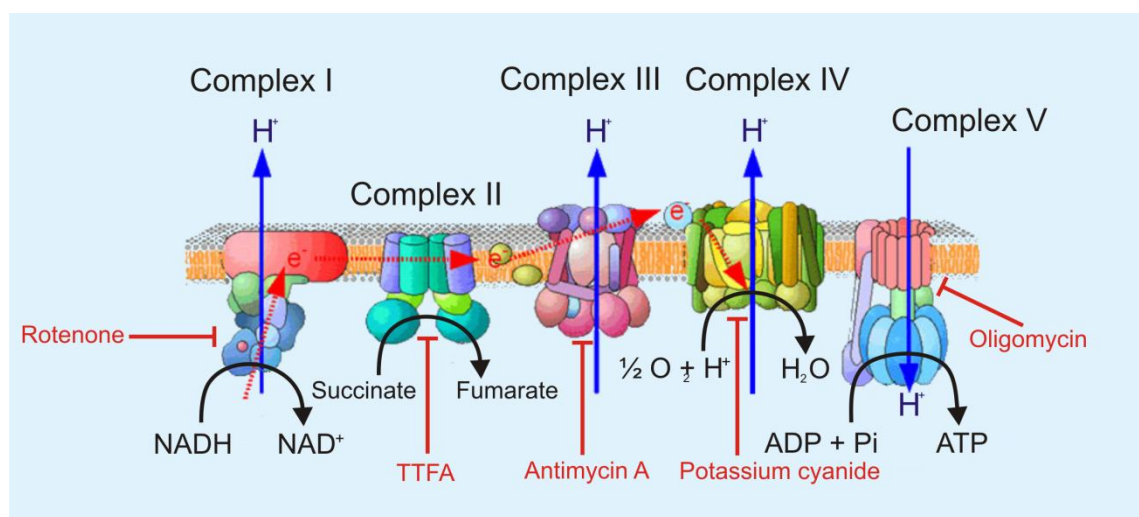


Figure 2. Cellular respiration: the electron transport chain and ATP synthase.

Complexes I-IV of electron transport chain (ETC) and the ATP synthase (Complex V) are embedded in the IMM. The ETC substrates coming from Krebs cycle feed the electrons to complexes I and II, electrons are then transferred along the chain due to the increasing redox potential of the OXPHOS enzymes. The flow of electrons is accompanied by proton pumping from the matrix to the intermembrane space creating the electrochemical proton gradient which then drives the synthesis of ATP. Complexes I to V can be inhibited by rotenone, thenoyltrifluoroacetone (TTFA), antimycin A, cyanide and oligomycin, respectively.

Modified from http://www.education-africa.com/wiki/index_en.php?title=Self-efficacy_and_its_practice

NADH donates electrons to respiratory complex I, also called NADH dehydrogenase, an L-shaped enzyme complex that contains a hydrophobic domain embedded in the IMM and a hydrophilic arm which protrudes into the mitochondrial matrix and contains the NADH binding site [9, 10]. The reduced cofactor donates two electrons to a flavin mononucleotide prosthetic group contained in the hydrophilic arm of complex I. These electrons are then passed down the arm via a series of iron-sulphur clusters to the lipid soluble redox carrier coenzyme Q (CoQ) [8]. The liberated energy is used to pump out four protons (H^+) from the matrix to the IMS against their concentration gradient. The other cofactor formed in the citric acid cycle ($FADH_2$) never leaves the complex, as the dehydrogenase itself is a part of the electron transport chain. The enzyme, also known as complex II, contains FAD as a prosthetic group alongside Fe-S clusters to catalyze of electron transfer to ubiquinone (CoQ) [11]. In contrast to complex I, no protons are pumped by this complex as the liberated energy is insufficient. The electrons coming either from complex I or II reduce CoQ; the ubiquinone diffuses through the IMM to complex III, also called cytochrome *c* reductase. This enzyme oxidizes CoQ and passes the liberated electrons to two molecules of cyt *c*. In total four protons are translocated to IMS – two coming from the oxidation of CoQ and two additional ones [12]. Finally electrons arrive to complex IV (cytochrome *c* oxidase) where

they are passed to oxygen to form water. Again, alongside this reaction, four protons are pumped from the mitochondrial matrix into the intermembrane space [13].

Because the IMM is impermeable to H^+ and charged species in general, the movement of protons across the inner mitochondrial membrane generates an electrochemical proton gradient or proton-motive force ($\Delta\tilde{\mu}H$), which can be calculated with the Nernst equation:

$$\Delta\tilde{\mu}H = zF\Delta\Psi_m + RT\ln \frac{[H^+]_{in}}{[H^+]_{out}}$$

It can be appreciated that the $\Delta\tilde{\mu}H$ results from the sum of the pH difference and the membrane potential difference ($\Delta\Psi_m$), which is negative inside [4]. ΔpH in mammalian cells is about 0.5-1 units, which corresponds to 30-60 mV; $\Delta\Psi_m$ is in the order of 180-200 mV, which makes it the major component of the proton-motive force [14]. As suggested by Peter Mitchell in 1961 [15], $\Delta\tilde{\mu}H$ is coupled to phosphorylation of ADP, which occurs at OXPHOS complex V, or ATP synthase. The enzyme consists of a membrane-spanning F_o domain, made of a variable number of c subunits organized in a ring-like structure. This proton-conducting ring allows proton influx back to the matrix, which results in F_o rotation. This is transmitted through a shaft to the F_1 portion, a matrix-exposed complex where conversion of ADP+Pi to ATP takes place. Of note, the ATP synthase can work in reverse, that is hydrolyze ATP and pump protons to intermembrane space when $n\Delta\tilde{\mu}H$ is lower than the phosphorylation potential (ΔG_p), where n is the H^+ /ATP stoichiometry [14].

The $\Delta\Psi_m$ also provides the major driving force for the electrophoretic Ca^{2+} uptake into mitochondria through a selective channel, the Ca^{2+} uniporter (MCU) [16-18]. Indeed, an obvious outcome of the chemiosmotic theory is that Ca^{2+} uptake across the inner membrane is greatly favored: based on the Nernst equation (and considering a $\Delta\Psi_m$ of -180 mV), the equilibrium would be reached only when Ca^{2+} in the matrix reaches a value 10^6 higher than that in the extramitochondrial space [19]. Hence, the rapid uptake of Ca^{2+} by energized mitochondria is observed.

1.1.2. Mitochondrial Ca²⁺: from uptake to signaling

Three major functions for mitochondrial Ca²⁺ transport have been proposed. First, matrix Ca²⁺ affects a wide range of metabolic reactions, including stimulation and control of oxidative phosphorylation. Ca²⁺ uptake by mitochondria stimulates three key enzymes of the cycle: (i) pyruvate dehydrogenase, where Ca²⁺ activates a phosphatase associated with the enzyme complex; (ii) isocitrate dehydrogenase; and (iii) α -ketoglutarate dehydrogenase. Ca²⁺ directly binds to the latter two and increases their affinity for the substrates [20-22]. Several studies also implied Ca²⁺ as a direct regulator of ATP synthase [23, 24]. Since increased matrix [Ca²⁺] is matched by increased activity of OXPHOS, uptake could represent a mechanism to couple ATP demand with supply [25]. Second, mitochondria act as cytosolic Ca²⁺ 'buffers'. This is achieved largely by the formation of Ca²⁺-Pi complexes in mitochondrial matrix, which are favored by alkaline pH, while the existence of specific Ca²⁺ binding proteins in the matrix is still unclear. Third, Ca²⁺ signaling is involved in cell death execution. It has long been recognized that mitochondrial Ca²⁺ overload can lead to a bioenergetic crisis associated with cell death by necrosis [26] as demonstrated by formation of Ca²⁺-Pi deposits, collapse of $\Delta\tilde{\mu}H$, rapid drop of ATP and production of ROS. Instead the role of Ca²⁺ in apoptosis was recognized only when it was discovered that the classical anti-apoptotic protein Bcl-2 was capable to affect mitochondrial Ca²⁺ signaling [27, 28]. Further, Ca²⁺ overload triggers the opening of the mitochondrial permeability transition pore (PTP), a phenomenon discussed more in detail in paragraph 1.2, which leads to ATP depletion and release of cyt *c*, apoptosis inducing factor (AIF) and Smac/Diablo.

Ca²⁺ fluxes must be tightly controlled. Ca²⁺ entry into mitochondria is mediated by a selective IMM channel, the MCU, whose molecular identity only recently has been unravelled [16, 17]. Ca²⁺ moves along its electrochemical gradient. According to the Nernst equation the equilibrium between the cytosol (given the Ca²⁺ concentration of 10⁻⁷ M there) and matrix would be reached only when matrix [Ca²⁺] becomes as high as 0.1 M, which is incompatible with cell physiology [29]. This is prevented by the low affinity for Ca²⁺ of MCU, which slows Ca²⁺ influx rates into mitochondria; and by operation of Na⁺/Ca²⁺ and/or H⁺/Ca²⁺ exchangers that release Ca²⁺ preventing electrochemical equilibrium from being reached and keeping the Ca²⁺ level at a steady state [30]. However, it must be mentioned that any change in cytosolic Ca²⁺ concentration would result in an alteration of this steady state [29]. Thus, when intracellular Ca²⁺ concentrations rise, *e.g.* under pathological conditions or due to the proximity of mitochondria to the endoplasmic reticulum, a fast mitochondrial Ca²⁺ uptake occurs.

1.1.3. Mitochondria as mediators of cell death

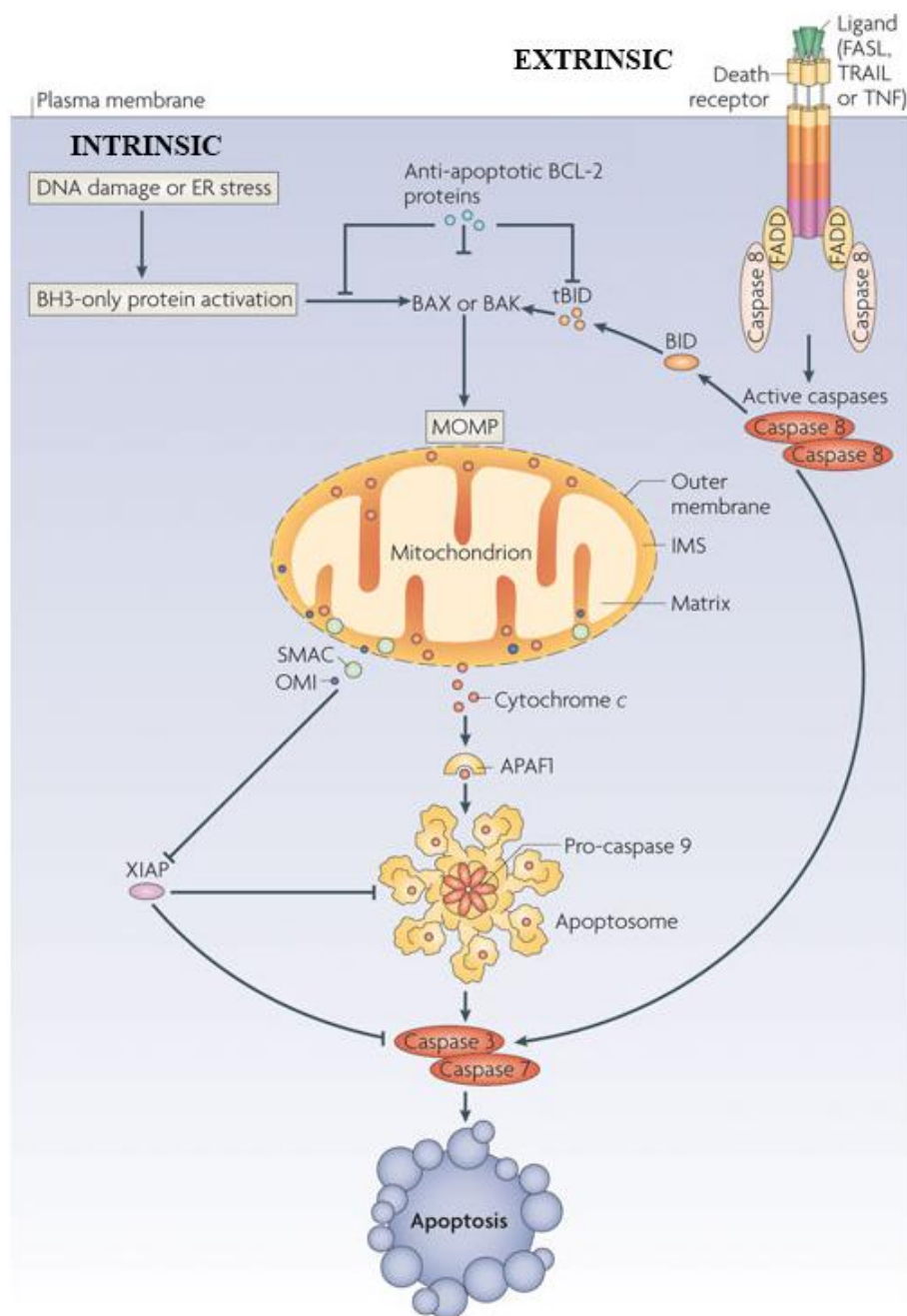
Cell death is an essential physiological process that it is required for the normal development of multicellular organisms [31]. However, if deregulated, it can contribute to diseases including cancer and degenerative diseases. Historically, cell death has been classified into two types: apoptosis (programmed cell death) and necrosis (accidental cell death). However, nowadays more and more evidence indicate that necrosis can be regulated as well (the new term necroptosis was introduced), and also that there are other forms of programmed cell death, such as autophagy, which otherwise is a process in which the cells recycle their own organelles and macromolecular components by engulfing them and then degrading by the lysosome. In general, it is an adaptive response of cells to sublethal stresses, like nutrient deprivation, meant to supply cells with metabolites for production of ATP [32]. Even if autophagy can serve as a protective mechanism against cell death by degrading organelles, both excessive and defective autophagy can be detrimental to the cell. The way in which the cell will die depends on the intensity of noxious signals, ATP concentration, cell type and other factors [33].

Necrosis is usually considered as accidental (that is, non-programmed) cell death and is characterized by the swelling of cytoplasm and its organelles and the rupture of cell membrane that causes release of cellular constituents followed by inflammation in the surrounding tissue. Necrosis usually results from metabolic failure that has coincided with rapid ATP depletion, *e.g.* it classically occurs in ischemia [34].

1.1.3.1. Apoptosis

Apoptosis is a genetically controlled and evolutionarily conserved form of cell death that is important for normal embryonic development and for maintenance of tissues homeostasis in the adult organism. In contrast to the swelling of the cell that defines necrosis, apoptosis occurs in a well organized sequence of morphological events [35]. First, the cytoplasm shrinks and the chromatin condenses, yet the organelles retain their integrity. Then the plasma membrane blebs, but stays intact, preventing the release of cellular components into extracellular medium. Ultimately, apoptotic cells fragment into membrane-enclosed vesicles (apoptotic bodies), that are recognized and removed by phagocytes, thereby avoiding inflammation [36]. Apoptotic cell death is triggered by extrinsic, receptor-mediated, or

intrinsic, mitochondria-mediated, signaling pathways that induce death-associated proteolytic and/or nucleolytic activities (Figure 3).



Nature Reviews | Molecular Cell Biology

Figure 3. Intrinsic and extrinsic pathways of apoptosis.

Two pathways of apoptotic cell death exist: one triggered by death receptor (extrinsic) which activates caspases 8, 3 and 7, culminating in apoptosis; and the mitochondrial (intrinsic) one. The intrinsic stimuli cause mitochondrial outer membrane permeabilization (MOMP) mediated either by interplay of the Bcl-2 family proteins or mitochondrial permeability transition, the release of proapoptotic proteins and activation of caspase 3 and caspase 7. The two pathways crosstalk through the ability of caspase 8 to cleave a Bcl-2 family member Bid, which then activates Bax and Bak and causes MOMP. From [37].

The **extrinsic** apoptotic pathway is activated when members of the tumor necrosis factor (TNF) superfamily (FasL, Trail, TNF) bind to cell surface “death receptors”, members of the TNF-receptor family [38-40]. Ligation of these receptors recruits adaptor molecules, such as Fas-associated death domain protein (FADD) and then initiator caspase, caspase 8, forming the multiprotein death-inducing signaling complex (DISC) [41-43]. This results in the dimerization and activation of caspase 8, which can then directly cleave and activate caspase 3 and caspase 7 and lead to apoptosis [32, 37], Figure 3.

The **intrinsic** pathway is activated by a variety of intrinsic stimuli, such as intracellular ROS, γ radiation, DNA damage, ER stress, which eventually target mitochondria and lead to loss in OMM integrity. This in turn results in the release of the proapoptotic proteins from the IMS, *e.g.* *cyt c*, AIF, Smac/Diablo, DNase endonuclease G (Endo G), high temperature requirement factor A2 (HtrA2)/Omi. *Cyt c* binds apoptotic protease-activating factor 1 (APAF1), inducing its oligomerization and thereby forming a structure termed apoptosome that recruits and activates an ATP-dependent initiator caspase, caspase 9. Caspase 9 cleaves and activates executor caspases (such as caspase 3 and caspase 7) leading to apoptosis. The release of Smac/Diablo and Omi/HtrA2 results in antagonizing the X-linked inhibitor of apoptosis protein (XIAP) ability to inhibit caspases (Figure 3). After release in the cytosol, AIF and EndoG translocate to the nucleus, where AIF causes DNA fragmentation and chromatin condensation [44] and EndoG cleaves DNA into nucleosomal fragments [45]; these proteins thus are part of caspase-independent, intrinsic cell death pathways. Release of the above mentioned proteins occurs through the mitochondrial outer membrane permeabilization (MOMP). The main mechanisms causing this event are: (i) direct membrane permeabilization by Bax and Bak, members of the B cell lymphoma 2 (Bcl-2) family; and (ii) indirect MOMP due to opening of the mitochondrial PTP (discussed in paragraph 1.2).

The pro-/anti- apoptotic function of Bcl-2 family proteins depends on the number of the Bcl-2 homology (BH) domains (four in total, BH1, BH2, BH3 and BH4) they contain. Prosurvival members (such as Bcl-2 and Bcl-xL) have as much as four, while proapoptotic ones are subdivided into the effectors (Bax, Bak and Bok) that share three homology domains and BH3-only, such as Bid and Bak, that by definition possess only BH3 domain [37]. Upon apoptosis inducing signals BH3-only proteins are activated which in turn leads to activation of proapoptotic Bax (Bcl-2-associated X protein) and Bak (Bcl-2 antagonist or killer). Bax and Bak change their conformation, oligomerize and form channels in the OMM leading to MOMP and the release of *cyt c* [37]. Anti-apoptotic Bcl-2 proteins prevent MOMP by binding BH3-only proteins and activated Bax or Bak. Although traditionally receptor mediated apoptosis pathway had been thought to be independent of mitochondrial one, the finding

that caspase 8 can trigger *cyt c* release has led to an integrated view where intrinsic and extrinsic pathways crosstalk through Bid. Caspase 8 is able to cleave the BH3-only protein Bid, leading to a smaller form of the protein, tBid, which now is able to translocate to OMM, where it inhibits the antiapoptotic members of Bcl-2 family and directly activates Bax and Bak, thus permeabilizing the OMM [2].

It needs to be stressed, however, that the formation of the channel in the OMM might not be enough to induce apoptosis. Indeed, the Bax/Bak pore size appears to be barely sufficient to release *cyt c*, but not other proapoptotic proteins. Furthermore, only about 15 % of the total *cyt c* is found in the IMS, while most of it is within *intracristal* compartments that communicate with the IMS through narrow openings of the so-called *cristae* junctions [46]. *Cristae* morphology and diameter of *cristae* junctions is regulated by a large dynamin-related protein, optic atrophy 1 (OPA1), and by presenilin-associated rhomboid like protein (PARL) [47]. The oligomers of OPA1 maintain the bottleneck configuration of *cristae*, thus keeping the *cyt c* compartmentalized [47, 48]. During apoptosis tBid causes *cristae* remodeling, which is favored by matrix swelling [46] and is inhibited by CsA [49], suggesting that opening of the CsA-sensitive PTP is an important step in *cristae* remodeling that can favor *cyt c* release through Bax/Bak channels [50].

1.2. Permeability transition pore

The mitochondrial permeability transition (PT) is a sudden increase of permeability of the otherwise impermeable IMM to ions and solutes with an exclusion size of about 1500 Da [51-54]. The prevailing view is that the PT is due to opening of a regulated high conductance protein channel, the PTP, which in the fully open state has an estimated diameter of about 3 nm [53, 55]. PTP opening requires the presence of matrix $[Ca^{2+}]$, which is an essential permissive factor, and of additional agents or conditions that are collectively termed “inducers”. Under the conditions used in most *in vitro* studies, PT is accompanied by depolarization, Ca^{2+} efflux, depletion of matrix pyridine nucleotides (PN), matrix swelling, *cristae* unfolding, outer membrane rupture and release of intermembrane space proteins, including *cyt c*, Smac/Diablo and AIF [2,56,57].

Apart from the long-lasting pore openings that can compromise cell viability, transient PTP openings occur both in isolated mitochondria [64] and *in situ* [65]. Besides *cristae* remodelling, our laboratory has proposed that PTP could also serve a physiological function as a mitochondrial Ca^{2+} release channel [66-68]. This hypothesis is consistent with early results on the effects of CsA in Ca^{2+} distribution in rat ventricular cardiomyocytes [69] and with recent findings in *Ppif*^{-/-} mice (*Ppif* is the gene encoding for the CsA target Cyclophilin D) whose heart mitochondria display a 2.6-fold elevation in total Ca^{2+} levels, and are more susceptible to heart failure after diverse stimuli that cause progressive Ca^{2+} overload [70]. The idea that the PTP may serve as a physiological Ca^{2+} release channel is also supported by recent work in mouse primary adult neurons showing that PTP is activated in response to the combined action of more than one physiological stimulus affecting cytosolic $[Ca^{2+}]$, and that under these conditions PTP opening does not induce neuronal death but rather takes part in physiological Ca^{2+} dynamics [71].

1.2.1. Regulation of the PTP

In spite of the fact that the molecular nature of the PTP remains elusive, a great deal of information is known regarding its regulation. The pore open-closed transitions are highly regulated by multiple effectors the main of which are discussed below (for reviews, see Refs. 1, 67, 61).

As already mentioned **matrix Ca²⁺** plays a key role in the induction of the PTP through a still-undefined mechanism. The Ca²⁺ binding site in the matrix can be competitively inhibited by other Me²⁺ ions, such as Mg²⁺, Sr²⁺ and Mn²⁺; while all these Me²⁺ ions, including Ca²⁺ itself, decrease the probability of pore opening through an external binding site [72].

The PT is strictly modulated by **matrix pH**. The optimum matrix pH for PT occurrence is about 7.3, and both an increase and decrease lead to decreased probability of PTP opening. An acidic pH locks the pore in the closed conformation through reversible protonation of His residues (that can be prevented by diethylpyrocarbonate, DEPC), whilst the mechanism of inhibition by pH > 7.4 is still unknown [73, 74].

The PTP is **voltage dependent** in the sense that that inside-negative $\Delta\Psi_m$ tends to stabilize the PTP in the closed conformation while the open state is favored by depolarization [75]. Our group has postulated the existence of a voltage sensor that decodes the changes of both the surface potential (through a set of charged residues) and of the trans-membrane voltage into changes of the PTP-open probability [1, 76]. Such a sensor would easily account for pore opening following depolarization as such, and for the effects of a large variety of membrane-perturbing agents that can either inhibit or promote the PT.

The voltage-dependence in turn is modulated by **redox events**. Pore opening is strongly promoted by an oxidized state of PN (NADH/NAD⁺ and NADPH/NADP⁺) [77], and through a dithiol-disulfide interconversion at two distinct, matrix- and intermembrane space- exposed sites (Figure 4). These can be discriminated by the use of proper oxidants and reductants. The membrane permeant dithiol phenylarsine oxide (PhAsO) cross-links matrix-exposed internal cysteins (Cys) and this can be prevented by low concentrations of *N*-ethylmaleimide (NEM) [78] or monobromobimane [79]. A second redox-sensitive site whose oxidation increases the probability of PTP opening is affected by membrane-impermeant oxidant copper-*o*-phenantroline [Cu(OP)₂]; oxidation of this site is inhibited by dithiotreitol and β-mercaptoethanol but not by monobromobimane, unless the latter one is in a cationic form [80].

PTP open-closed transitions are affected by **photooxidative stress**, which can be triggered by the use of protoporphyrin (PP)-like dicarboxylic porphyrins, such as hematoporphyrin (HP) IX, deuteroporphyrin (DP) IX and PP IX itself, and light. Short irradiation time of mitochondria treated with porphyrins prevents PTP opening by photomodifying matrix histidine residues, which in turn lowers the reactivity of critical PTP regulating dithiols; longer irradiation times instead cause opening of the PTP by direct oxidation of external

pore-regulating Cys [81]. For a detailed description of the photodynamic action and its effects on PTP, see **Paper 2**.

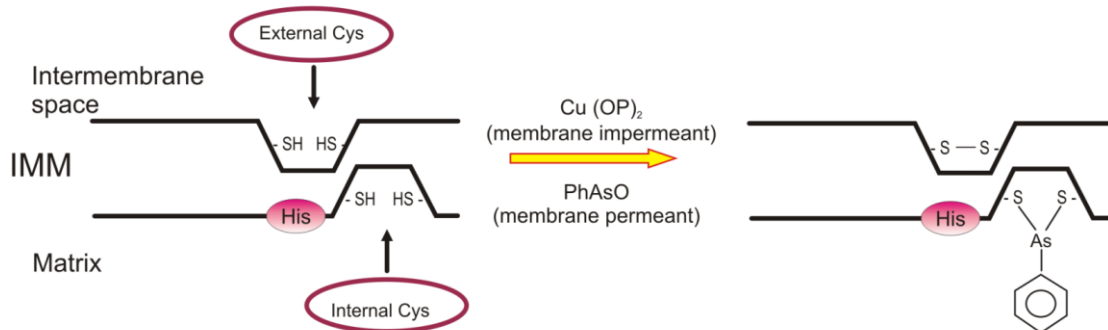


Figure 4. Schematic representation of PTP-regulating thiols.

The two sites can be distinguished by the use of proper oxidants and reductants. Cu(OP)_2 (copper-*o*-phenantroline) is a membrane-impermeant oxidant which selectively affects IMS-exposed (external) sulfhydryls. PhAsO (phenylarsine oxide) is a membrane permeant thiol cross-linker, also affecting matrix thiols.

Opening of the PTP is affected by the immunosuppressant **cyclosporin A** (CsA), a high-affinity inhibitor of cyclophilins (CyP) that desensitizes the pore to the inducing effects of Ca^{2+} and Pi through its binding to matrix CyPD [61,63,82,83]. The immunosuppressive effect of CsA is caused by a Ca^{2+} -calmodulin-dependent inhibition of calcineurin due to complex formation of the drug with cytosolic CyPA. In turn, this prevents dephosphorylation and nuclear translocation of nuclear factor of activated T cells and other transcription factors that are essential for the activation of T cells [84]. Available evidence indicates that CsA affects the pore independently of calcineurin, as non immunosuppressive CsA derivatives (Debio 025 and NIM811), that do not inhibit calcineurin, were found to be powerful PTP desensitizers [85-91].

Phosphate is a classical inducer of the PTP, but our group recently demonstrated that CyPD inhibition or its genetic ablation *sensitizes* the pore to the inhibitory effects of Pi, which would be an *inhibitor* of the pore under these conditions [92, 93]. This result is particularly intriguing because Pi is an inhibitor rather than an inducer of the PT in yeast [94, 95] and in *Drosophila melanogaster*, where the PTP cannot be desensitized by CsA [96].

Quinones may act both as inhibitors (the most potent is **Ubiquinone 0, Ub0**) or inducers; their structure-activity relationship for PTP inhibition is complex and has not yet been fully elucidated [97].

Provided that Pi is present, **rotenone** desensitizes the PTP by inhibiting complex I. The potency of the drug has been correlated with the CyPD expression levels, the less CyPD mitochondria express, the more potent rotenone is in inhibiting the PTP. In tissues that have high levels of CyPD expressed, rotenone is not effective; however, the inhibitory potency of it can be restored by CyPD ablation or treatment with CsA [98].

PTP is regulated by two inhibitors of the adenine nucleotide translocator (ANT): **bongkrekate**, which is an inhibitor and **atractylate**, which is an inducer.

The pore is also affected by **amphipathic compounds**. They modify surface membrane potential fitting well with the idea of PTP regulation by voltage. In general, amphipathic anions, such as fatty acids produced by phospholipase A₂ (PLA₂) (*e.g.* arachidonic acid) mimic a depolarization and favor the PT. Instead, polycations such as spermine, amphipathic cations such as sphingosine and trifluoroperazine, and positively charged peptides mimic a hyperpolarization and inhibit pore opening [1, 61].

1.2.2. Molecular nature of the PTP

The key features of the permeability transition were described almost fifty years ago by Crofts and Chappell, who reported that energized mitochondria exposed to high loads of Ca²⁺ can undergo a massive swelling, which can be partially reverted by Ca²⁺ chelation [99, 100]. Ever since, identification of the basis for this phenomenon has been a challenge, and in spite of many efforts the molecular nature of the PTP remains elusive. The regulation of the PTP is so complex that no model has so far been able to account for the huge variety of pore inducers and inhibitors (more than 50 classes were already listed in 1990 [101]).

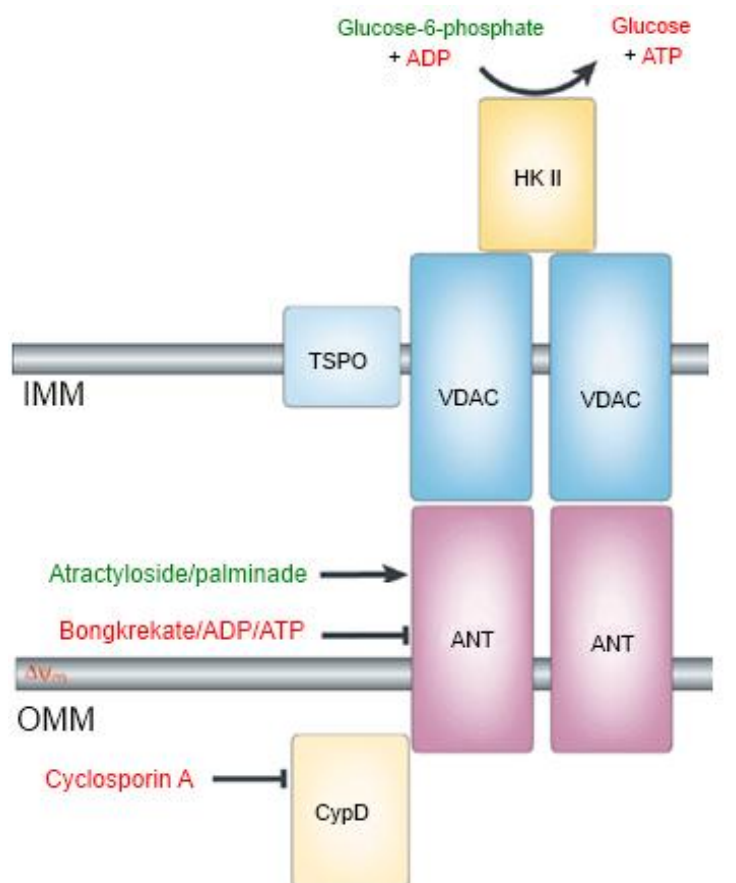
Over the years several models to explain the PT have been proposed. Haworth and Hunter suggested that PT is caused by opening of a proteinaceous pore in the IMM, with inhibitors and activators of the transition binding to the pore at specific sites affecting the tendency to open or close in an allosteric fashion, and proposed that it may serve an undefined physiological role [51-54]. Unfortunately, at the time this proposal did not get much attention, in part at least as a consequence of the general acceptance of the chemiosmotic theory and of the prevailing view that mitochondria did not possess cation channels; existence of a large unspecific pore in the IMM seemed to contradict the basic tenets of chemiosmosis [61]. Pfeiffer and co-workers proposed that changes in membrane permeability can occur from accumulating PLA₂ reaction products. In this view, a substrate

cycle of phospholipid deacylation-reacylation establishes the steady state of free fatty acid and lysophospholipids which, in turn, alters permeability; Ca^{2+} uptake activates PLA_2 , and inducing agents inhibit reacylation, either directly [102, 103] or indirectly by raising the matrix content of reduced glutathione [104]. The PLA_2 reaction product levels would then rise leading to increased membrane permeability. However, the observation that CsA is a potent PT inhibitor, but has no effect on PLA_2 activity led to conclude that PLA_2 activation is not a primary cause of the PT [101]. The 'modern' model of the PTP was introduced by Brdiczka's lab. It suggests that the pore forms at the contact sites between the IMM and OMM and itself spans both the membranes [107]. The basis for this hypothesis is the presence of ANT and VDAC (together with many other proteins, however) in detergent membrane extracts that possess hexokinase (HK) activity and display properties that resemble those of the PTP after reconstitution in liposomes [108, 109]. Similar preparations (which were, however, not even enriched in ANT and VDAC) had been previously shown to possess electrophysiological properties similar to those of the PTP, although atractylate caused channel closure [110] rather than the opening that would be expected based on studies in intact mitochondria [53]. The findings that the PT can be inhibited by low concentrations of CsA [63]; and that the translocator protein (TSPO; previously known as the peripheral benzodiazepine receptor, PBR) co-purify with VDAC and ANT [111] added CyPD and TSPO to the most widespread PTP model to date (Figure 5). Each of the putative components of this PTP model is discussed more in detail below. It must also be mentioned that both He & Lemasters and Vercesi and co-workers have suggested that the PTP might not consist of a specific protein. They rather hypothesized that the pore may be formed by aggregation of different misfolded integral membrane proteins that have been damaged by oxidant or by other stresses [105, 106]. In the model of He & Lemasters binding of CyPD blocks the conductance through these proteins, and upon the increase of matrix Ca^{2+} this binding is somehow perturbed, which favors the PTP 'open' conformation [105]. While interesting, the model fails to explain the PTP regulation by voltage and matrix pH.

1.2.2.1. Voltage-dependent anion channel

The earliest indication that the OMM is involved in the PT was the finding that swelling induced by high concentrations of sulfhydryl reagents (like NEM and other substituted maleimides) is not observed in mitoplasts, *i.e.* preparations where the OMM has been removed [112]. VDAC is the most abundant protein of the OMM, and in mammals is present in three isoforms (VDAC1, VDAC2 and VDAC3). It functions as a gatekeeper for the entry and

exit of mitochondrial metabolites and thus controls the cross-talk between mitochondria and the cytosol. Several lines of evidence suggested that the OMM component contributing to the PTP is VDAC. Purified VDAC forms channels with a pore diameter of 2.5-3.0 nm and possesses electrophysiological properties similar to those of the PTP [113, 114]. VDAC is modulated by many factors that also affect the PTP, such as NADH, Ca^{2+} , glutamate and hexokinase [115]. Moreover, Crompton *et al* reported that GST-CyPD pulled down both the ANT and VDAC, and that after reconstitution in liposomes these proteins formed a Ca^{2+} -activated, CsA-sensitive pore [116], although only ANT, but not VDAC was detected by others in similar experiments [117]. In spite of these results, mice lacking VDAC1, VDAC3 or VDAC1 and VDAC3 developed normally; and mitochondria isolated from *Vdac1*^{-/-} mice underwent CsA-sensitive PTP, which was also inhibited by Ub0 [118] and Ro 68-3400 [119],



Nature Reviews | Molecular Cell Biology

Figure 5. The most widespread model of the permeability transition pore.

This model suggests that PTP is formed by matrix cyclophilin D (CypD), adenine nucleotide translocator in the inner mitochondrial membrane (IMM), outer membrane voltage dependant anion channel (VDAC), translocator protein (TSPO) and membrane bound hexokinase (HK) II. *Modified from* [72].

and retained all basic features of PTP modulation, including inhibition by CsA [120]. Since non-conditional ablation of *Vdac2* led to embryonic death, this gene was silenced in *Vdac1/Vdac3-null* background mouse embryonic fibroblasts; again, no relevant differences on PTP formation were observed [121]. Thus, it appears that VDAC is not an essential component of the PTP.

1.2.2.2. Adenine nucleotide translocator

The ANT, as the name indicates, catalyses the selective exchange ADP for ATP. Under physiological conditions matrix ATP is swapped with cytosolic ADP, and the reaction is favoured by the membrane potential. However, if mitochondrial respiration is compromised (and thus unable to maintain $\Delta\Psi_m$), ATP synthase steps in by hydrolyzing glycolytic ATP taken up by ANT working in reverse, *i.e.* transporting cytosolic ATP in exchange for matrix ADP. The ANT is the most abundant protein in the IMM.

Based on the finding that PT is modulated by atractylate and bongkrekate (inhibitors of ANT) it was suggested that this protein is a core component of the PTP complex. Atractylate inhibits the ANT and stabilizes it in the *c* (cytosol-facing) conformation, and favors PTP opening. On the other hand, bongkrekate inhibits the ANT, stabilizes it in *m* (matrix-facing) conformation and favors PTP closure [122]. The purified ANT reconstituted into liposomes formed a Ca^{2+} -activated channel measured by patch clamp [123]. Although the data supporting ANT involvement in the pore formation seemed reasonable, unequivocal evidence that the ANT is not essential for the PT was obtained in a detailed study of liver mitochondria prepared from mice lacking both ANT1 and ANT2. The ANT-null mitochondria underwent a Ca^{2+} - and CsA-sensitive PT with matrix swelling, the only difference being its lack of sensitivity to the ligands of ANT and the requirement of a higher Ca^{2+} load. Thus, the study revealed that ANT is not an obligatory binding partner of CyPD [124]. Consistent with these findings, recent work has shown that the polyclonal antibody used to identify a CyPD binding protein as ANT1 in fact labelled the Pi carrier, which has now been incorporated in the model of the PTP proposed by the Halestrap laboratory [125, 126].

1.2.2.3. Phosphate carrier

The physiological role of the phosphate carrier (PiC) is to mediate the co-transport of Pi and H⁺ to the mitochondrial matrix [127], where Pi is essential for the phosphorylation of ADP to ATP. Interestingly, Pi has long been known to be a PTP sensitizer, too. This fact and the findings that PiC (i) associates with ANT in the so called “ATP synthasome”[128]; (ii) upon reconstitution in liposomes it can yield a non specific pore under certain conditions [129]; (iii) is inhibited by the PTP inhibitors Ub0, Ro 68-3400 and NEM [126]; (iv) is found among the proteins that bind a PhAsO affinity matrix, and could be eluted with GST-CyPD in a CsA-sensitive manner [126] led Halestrap to propose a PTP model in which the pore is formed by ANT, PiC and CyPD [130, 131]. However, these agents might affect other mitochondrial transporters; and Basso *et al.* demonstrated that the PTP can be desensitized to Ca²⁺ by Ub0 and Ro 68-3400 even if the Pi is substituted by arsenate or vanadate [92]. We think that the genetic approach should be used to unequivocally establish the importance of the PiC in the PTP. This was partially addressed in *Saccharomyces cerevisiae* lacking PiC. Mersalyl, which inhibits PiC and triggers PT, induced opening of the decavanadate-sensitive Yeast Mitochondrial Unselective Channel (YMUC) in WT, but not the ΔPiC strain, although the latter could still undergo a decavanadate sensitive permeabilization through a pore of smaller size [132]. It is fair to say however, that there is an open debate as to whether YMUC can be considered a *bona fide* equivalent of the mammalian PTP.

1.2.2.4. Hexokinase

HK initiates intracellular glucose utilization by catalyzing its phosphorylation to glucose-6-phosphate [133]. In mammals there are four important isozymes, type II (HK II) being the most represented. It is highly expressed in most cancer cells, where it localizes on the OMM. In highly glycolytic tumors HK II fosters cell growth in the hypoxic conditions of the primary tumor mass [134]. As already mentioned, it was found to form complexes with VDAC and ANT [108], and direct binding of HK I and II to VDAC was demonstrated [135]. The detachment of HK from mitochondria triggered PTP opening and cell death [136], and this was also observed in mitochondria devoid of VDAC [135].

1.2.2.5. Cyclophilin D

CyPD (which in the mouse is encoded by the *Ppif* gene) is the mitochondrial isoform of a large family of proteins endowed with peptidylprolyl *cis-trans* isomerase activity that is blocked by CsA. CyPD involvement in PTP regulation was suggested by the finding that similar amounts of CsA are needed both to desensitize the pore and to inhibit CyPD enzymatic activity [137, 140]. Several genetic studies revealed that the protein is a powerful PTP regulator rather than a pore component. Inactivation of the *Ppif* gene didn't prevent PTP opening, although more Ca²⁺ was required to induce the PT, matching the Ca²⁺ load required in wild-type mitochondria treated with CsA [141, 144]. As expected, sensitivity to CsA was no longer present, while inhibitors acting at different sites (such as Ub0 and Ro 68-3400) were still active [144].

1.2.3. PTP involvement in pathology

The role of the PTP as a mediator of cell death in paradigms relevant to human health is no longer questioned. A word of caution about an exclusive causative role of the pore is in order about early studies based on the effects of CsA alone because (i) inhibition of calcineurin prevents mitochondrial fission by inhibiting mitochondrial translocation of Drp1, a cytoprotective event that occurs independent of PTP inhibition [145]; and (ii) CyPD displays multiple regulatory interactions in mitochondria including CsA-sensitive binding to Hsp90 and TRAP1 [146], modulation of the F₀F₁ ATP synthase [147] and binding to Bcl-2 [148, 149]. Yet a role of the PTP is generally supported by studies of *Ppif*^{-/-} mice and of their cross-breeding with several disease genotypes.

Ppif^{-/-} mice were protected from ischemia-reperfusion injury of the heart [141, 142] and brain [143, 150], infarct size being reduced in CyPD-null adults compared to wild-type or littermate controls. These studies do corroborate the conclusions of previous studies based on the use of CsA in ischemic isolated hearts [151] and in infarcted patients [152], in brain damage by hypoglycemia [153], hyperglycemia [154], middle cerebral artery occlusion [155,156], and traumatic injury [157,158]. *Ppif*^{-/-} mice also display resistance to development of axonopathy in autoimmune encephalomyelitis [159] and to disease progression after crossing with superoxide dismutase 1 mutant mice [160], suggesting that CyPD-dependent (and possibly PTP-dependent) mechanisms are critical in the neurodegenerative aspects of demyelinating and motor neuron diseases. Ablation of CyPD

substantially improved learning, memory and synaptic function, and alleviated decreased long-term potentiation by the amyloid β peptide in a mouse model of Alzheimer's disease [161].

Perhaps the best case involving CyPD in pathology in vivo is represented by collagen VI diseases [162], a set of genetically heterogeneous conditions that cause Bethlem myopathy [163], Ullrich congenital muscular dystrophy [164] and myosclerosis myopathy [165]. The rodent model of the disease (*Col6a1*^{-/-} mice lacking collagen VI [166]) displays mitochondrial alterations in affected muscles that could be cured with CsA [167] or with the CyP inhibitor Debio 025 [87]; and *Ppif*^{-/-} *Col6a1*^{-/-} mice lacking both CyPD and collagen VI became indistinguishable from syngenic wild type mice [168], a clear indication that CyPD is involved in the development of the disease downstream of the lack of collagen VI in a process that is amplified by defective autophagy [169]. These results match those obtained in patient cultures [170] and in a pilot clinical trial with CsA [171], and in *Ppif*^{-/-} *Scgd*^{-/-} and *Ppif*^{-/-} *Lama2*^{-/-} mice modeling sarcoglycan deficiency and congenital muscular dystrophy due to lack of laminin, respectively [172].

1.3. Translocator protein (TSPO)

The Translocator protein (TSPO), previously known as peripheral benzodiazepine receptor (PBR), is an 18 kDa, nuclear-encoded, highly hydrophobic protein located in the OMM [173], although minute amounts were also found in plasma membrane and nucleus [174–176]. TSPO is highly conserved throughout evolution from bacteria to humans [174, 175]. Although it is ubiquitously expressed, protein levels differ in different tissues; the highest levels are found in steroid-synthesizing ones [177]. Hydropathy profile analysis of the 169-amino-acid TSPO sequence suggested a putative five transmembrane helix structure, N-terminus and C-terminus facing IMS and cytosol respectively, a model that is supported by experiments [177–181].

TSPO was first identified in 1977 by Braestrup and Squires in binding studies of the benzodiazepine diazepam in the central nervous system (CNS). While looking for a control tissue, they observed that the drug also binds rat kidney membranes [182, 183]. Benzodiazepine binding was also observed in other peripheral tissues and led to the denomination ‘peripheral benzodiazepine receptor – PBR’, to stress its expression in the periphery as opposed to the ‘central’ benzodiazepine receptor expressed in CNS [174, 176, 184, 185].

In 2006 the Human Genome Organization Gene Nomenclature Committee renamed the PBR to translocator protein of 18 kDa (TSPO) [184]. The rationale for this was:

- i) ‘peripheral’ does not reflect the tissue distribution of the protein, as it is also expressed in glial and ependymal cells, located in the CNS;
- ii) the protein does bind other structures, such as the isoquinoline carboxamide PK11195, cholesterol and PP IX, but not all benzodiazepines;
- iii) the protein is not a receptor in the traditional sense; its primary location is the OMM, where it does not only bind but also facilitates transport molecules of such as cholesterol and PP IX.

1.3.1. Biological roles

Although TSPO was suggested to play a role in a wide variety of biological processes (such as regulation of mitochondrial membrane potential and respiration, cell proliferation, Ca^{2+}

signaling, apoptosis, control of immune response [174-176, 184-188]), its best characterized features are cholesterol and porphyrin transport [184].

Perhaps the most studied function of TSPO is cholesterol transport from the outer to inner mitochondrial membranes, a rate-limiting step in steroidogenesis [174, 176, 184, 189]. Steroids are formed from cholesterol by several sequential enzymatic steps. The first takes place in the IMM and is the conversion of cholesterol to pregnenolone by cholesterol side chain cleavage catalyzed by cytochrome P450. Then pregnenolone leaves the mitochondrion to enter the endoplasmic reticulum, where it undergoes further enzymatic transformations that give rise to the final steroids [176]. Evidence exists to show that TSPO may function as a channel, accommodating a cholesterol molecule in the space delimited by the five transmembrane helices [178]. A cholesterol recognition amino acid consensus (CRAC) domain in the cytosolic C-terminus of the TSPO was identified [190].

TSPO also binds and transports porphyrins involved in mammalian tetrapyrrole metabolism, and thus participates in heme biosynthesis [184, 191, 192]. In most eukaryotes heme synthesis is initiated in the mitochondrion where δ -aminolevulinic acid (ALA) is produced from succinyl-CoA and glycine. ALA is exported to the cytosol, where it is converted to coproporphyrinogen III. This molecule crosses the OMM, presumably at least in part through TSPO [191, 193], is oxidized in the IMS and imported into the mitochondrial matrix where it is further oxidized to PP IX. Heme synthesis is completed by the incorporation of iron into PP IX [193]. A bacterial homolog of TSPO, a tryptophan-rich sensory transducer of oxygen (*TspO*), regulates photosynthetic membrane complex formation in *Rhodobacter sphaeroides* and is involved in *Rhodobacter* transport of porphyrin intermediates [195].

1.3.2. TSPO ligands

Ligands of TSPO have been extensively used to characterize TSPO function and to explore its role in cell pathophysiology; they are generally classified as endogenous and synthetic ones. The putative **endogenous ligands** include cholesterol, porphyrins (PP IX, mesoporphyrin IX, DP IX, hemin), which exhibit a nM affinity (Table 1) [196- 198], diazepam binding inhibitor (DBI), trikontatetraneuropeptide (TTN) and PLA₂ [188].

Porphyrins are a group of organic compounds. The core of the porphyrin molecule is a tetrapyrrolic macrocycle, while peripheral substituents control drug biodistribution and

pharmacokinetics. Tetrapyrroles are naturally occurring pigments and vital constituents of oxidation–reduction and oxygen transport–related proteins such as hemoglobins, cytochromes, apoferritin, catalase, ferrichrome and peroxidases. Free base porphyrins proved to be good photosensitizers, *i.e.* compounds which upon absorption of light transfer energy to a substrate rather than giving it away as heat or light. Due to the efficient formation of the triplet state (quantum yield ~ 0.7 – 0.9 in a monomeric state [199]) and the low energy gap between the triplet states of tetrapyrroles and molecular oxygen, a large fraction of triplets (0.7 – 1.0) leads to the generation of singlet oxygen ($^1\text{O}_2$), a highly reactive oxygen species whose diffusion distance in biological systems is only about 10–20 nm [200]. Consequently, photodamage occurs in close proximity to the porphyrin. *For an extensive description of the photodynamic effect, of porphyrins and of their involvement in photosensitization see Paper 2.*

Table 1. Ligand-binding affinities for TSPO.

Ligand	K_d , nM
PK11195	0.6–2.0*
Ro5-4864	1.1–7.3*
FGIN1-27	15.0*
PP IX	$14.5 \pm 10.7^\$$
DP IX	$31.3 \pm 2^\$$
Cholesterol	6.14#

From: *[201], $^\$$ [202], #[197].

The classical **synthetic ligands** of TSPO include 1-(2-chlorophenyl)-N-methyl-N-(1-methylpropyl)isoquinoline-3-carboxamide (PK11195) and 4-chlorodiazepam (Ro5-4864). Although both of them exhibit nanomolar affinity for the protein, the former binds exclusively to TSPO across all species and shows high levels of stereoselectivity and specificity [203–204], whereas benzodiazepine Ro5-4864 binding differs between species [205–209] and may require additional mitochondrial proteins, such as VDAC, for full binding [185]. The distinctive properties the two compounds suggest that their binding sites are not identical. Based on the entropy- and enthalpy- driven nature of the ligand-receptor interactions, PK11195 was originally classified as an antagonist and Ro5-4864 as an agonist [204]. However, both ligands are able to induce similar effects under certain conditions. Moreover, additional TSPO ligands were developed, such as the indole derivative FGIN1-27 (N,N-dihexyl-2-(4-fluorophenyl) indole-3-acetamide) [177, 210]. In contrast with

cholesterol, which binds to the C-terminus of TSPO, all other drug ligands (and presumably porphyrins) bind near the N-terminus [190, 208, 211].

1.3.3. TSPO and Permeability transition

Involvement of TSPO in the 'PTP' complex was suggested by its co-purification with the putative pore components VDAC and ANT [111], and was tested by what are considered to be high affinity TSPO ligands. It was demonstrated that TSPO ligands, such as PK11195, Ro5-4864 and PP IX, cause PTP opening both in isolated mitochondria and in cells [212-219], although the potency depended on the cell type and the concentration used, which varied from nM to μ M. Further complexity was uncovered with the demonstration that the same compounds could instead inhibit PTP and/or protect cells from apoptosis in other models [220, 221]; and that individual TSPO ligands can have the opposite effect on the same cell. For example, Ro5-4864 and PK11195 can either stimulate or inhibit apoptosis, respectively, with addition of Ro5-4864 overcoming the antiapoptotic effect of PK11195 [213, 222]. Furthermore, evidence exists that TSPO ligands can cause cellular responses that are independent of the TSPO [223-225], calling into question the specificity of TSPO ligands in general and the conclusions (such as the involvement of the TSPO in the PT) that were made based on the use of these drugs. Initial attempts to generate animals lacking expression of TSPO have indicated that non-conditional elimination of protein expression results in embryonic lethality [226], although details of the stage at which development arrests, and whether any specific phenotypes precede lethality have not been reported. We therefore generated mice in which the *Tspo* gene was conditionally eliminated. *Our results are reported in paragraph 2.3.1.2.*

2. Results

2.1. The mitochondrial permeability transition is an inner membrane event

The long-standing idea that the PTP may form at inner-outer membrane contact sites and that it may be constituted by the ANT in the IMM and VDAC in the OMM has not been confirmed by genetic ablation of these proteins, yet the PT can be regulated by proteins that interact with the OMM such as hexokinase and by ligands of the OMM TSPO. As of today, however, it is not clear whether the OMM is necessary for the PT to occur and what regulatory properties, if any, it may contribute to the PTP. Intriguingly, apart from early studies of Lê-Quôc and Lê-Quôc demonstrating that the OMM is necessary to induce mitochondrial swelling upon treatment with maleimide derivatives [112], the question of whether a PT can occur in mitoplasts (mitochondria stripped of the OMM) has never been addressed.

We thus studied the properties of the PTP in rat liver mitochondria and in mitoplasts retaining IMM ultrastructure and energy-linked functions. Like mitochondria, mitoplasts readily underwent a PT following Ca^{2+} uptake and upon treatment with classical PT inducers PhAsO and Cu(OP)_2 (which affect two distinct PTP-regulatory sites) in a process that maintained sensitivity to CsA, demonstrating that PT is exclusively an IMM event. On the other hand, major differences between mitochondria and mitoplasts emerged in PTP regulation by ligands of the OMM TSPO. Indeed, mitoplasts became resistant (i) to the photodamage induced by the treatment with dicarboxylic porphyrins endowed with PP IX configuration (which bind TSPO in intact mitochondria) and irradiation (see also Ref. 81 and **Papers 2** and **3**); and (ii) to PTP-induction by the selective TSPO-ligands FGIN1-27, Ro5-4864 and PK11195, suggesting that the OMM plays an important regulatory role through specific interactions with TSPO.

Paper 1:

Šileikytė J, Petronilli V, Zulian A, Dabbeni-Sala F, Tognon G, Nikolov P, Bernardi P, Ricchelli F. Regulation of the inner membrane mitochondrial permeability transition by the outer membrane translocator protein (peripheral benzodiazepine receptor). *J Biol Chem*. 2011 Jan 14; 286(2):1046-53.

Regulation of the Inner Membrane Mitochondrial Permeability Transition by the Outer Membrane Translocator Protein (Peripheral Benzodiazepine Receptor)*

Received for publication, August 9, 2010, and in revised form, November 8, 2010. Published, JBC Papers in Press, November 9, 2010, DOI 10.1074/jbc.M110.172486

Justina Šileikytė^{†1}, Valeria Petronilli[‡], Alessandra Zulian[‡], Federica Dabbeni-Sala[§], Giuseppe Tognon[¶], Peter Nikolov^{||}, Paolo Bernardi^{‡2}, and Fernanda Ricchelli^{¶3}

From the [†]Consiglio Nazionale delle Ricerche Institute of Neuroscience and Department of Biomedical Sciences, the [§]Department of Pharmacology and Anesthesiology, and the [¶]Consiglio Nazionale delle Ricerche Institute of Biomedical Technologies and Department of Biology, University of Padova, I-35121 Padova, Italy and the ^{||}Institute of Organic Chemistry, Bulgarian Academy of Sciences, 1000 Sofia, Bulgaria

We studied the properties of the permeability transition pore (PTP) in rat liver mitochondria and in mitoplasts retaining inner membrane ultrastructure and energy-linked functions. Like mitochondria, mitoplasts readily underwent a permeability transition following Ca^{2+} uptake in a process that maintained sensitivity to cyclosporin A. On the other hand, major differences between mitochondria and mitoplasts emerged in PTP regulation by ligands of the outer membrane translocator protein of 18 kDa, TSPO, formerly known as the peripheral benzodiazepine receptor. Indeed, (i) in mitoplasts, the PTP could not be activated by photo-oxidation after treatment with dicarboxylic porphyrins endowed with protoporphyrin IX configuration, which bind TSPO in intact mitochondria; and (ii) mitoplasts became resistant to the PTP-inducing effects of *N,N*-dihexyl-2-(4-fluorophenyl)indole-3-acetamide and of other selective ligands of TSPO. Thus, the permeability transition is an inner membrane event that is regulated by the outer membrane through specific interactions with TSPO.

The mitochondrial permeability transition (PT)⁴ is a sudden increase in the permeability of the inner mitochondrial membrane to solutes with molecular masses of up to 1500 Da. This process is due to opening of a voltage- and Ca^{2+} -dependent, cyclosporin A (CsA)-sensitive, high conductance chan-

nel called the permeability transition pore (PTP). Its involvement in pathological states and in the loss of cell viability is widely recognized, but its molecular identity remains elusive (1). The long-standing idea that the PTP may form at inner-outer membrane contact sites and that it may be constituted by the adenine nucleotide translocator (ANT) in the inner mitochondrial membrane (IMM) and the voltage-dependent anion channel (VDAC) in the outer mitochondrial membrane (OMM) has not been confirmed by genetic ablation of these proteins (2–4), yet the PT can be regulated by proteins that interact with the OMM such as hexokinase (5, 6) and by ligands of the OMM translocator protein of 18 kDa, TSPO (formerly known as the peripheral benzodiazepine receptor) (7–17). As of today, however, it is not clear whether the OMM is necessary for the PT to occur and what regulatory properties, if any, it may contribute to the PTP.

Among the variety of effectors that regulate the PTP open-closed transitions, oxidizing agents have received considerable attention, and changes in the redox state of pyridine nucleotides, glutathione, and sulfhydryl groups have been shown to play a prominent regulatory role (18–23). We have used chemical modifiers, photosensitizing agents, and light to explore PTP regulation by redox events. As photodamage is restricted to sites in close proximity to the photosensitizer, irradiation offered a unique opportunity to explore the role of specific protein residues in PT regulation (24–26). One remarkable finding was that hematoporphyrin IX (HP), which produces mainly singlet oxygen ($^1\text{O}_2$) upon irradiation, results in PT inhibition or activation depending on the light dose (24–26). For low light doses, HP inhibits the PT through photomodification of matrix-exposed His residues (24), followed by a drop in reactivity of critical matrix Cys residues (26). For higher doses, HP instead causes PTP reactivation through modification of distinct surface Cys residues (26). HP belongs to the class of dicarboxylic porphyrins endowed with protoporphyrin IX (PP) configuration. These porphyrins bind mitochondria with nanomolar affinity through TSPO (17, 27–31), and intriguingly, PP is a potent inducer of PTP opening (32). Given the long-standing proposals that the PTP is regulated by the OMM and that it may include TSPO itself (7–9, 11, 32–34), we studied the properties of the PTP in rat liver mitochondria and in digitonin-treated mitoplasts that retain

* This work was supported in part by grants from the Consiglio Nazionale delle Ricerche within the framework of Italy-Bulgaria (BAN) bilateral cooperation, by the Ministry for University and Research (MIUR/FIRB CINECA RBAU01YLSR and PRIN), and the Università di Padova Progetto Strategico "Models of Mitochondrial Diseases."

¹ Supported by a fellowship from the Fondazione Cariparo, Padova, Italy. Performed this work in partial fulfillment of the requirements for a Ph.D.

² To whom correspondence may be addressed: Dept. of Biomedical Sciences, University of Padova, Viale Giuseppe Colombo 3, I-35121 Padova, Italy. Fax: 39-49-827-6361; E-mail: bernardi@bio.unipd.it.

³ To whom correspondence may be addressed: Consiglio Nazionale delle Ricerche Inst. of Biomedical Technologies and Dept. of Biology, University of Padova, Via Ugo Bassi 58B, I-35121 Padova, Italy. Fax: 39-49-827-6348; E-mail: rchielli@bio.unipd.it.

⁴ The abbreviations used are: PT, permeability transition; CsA, cyclosporin A; PTP, permeability transition pore; ANT, adenine nucleotide translocator; IMM, inner mitochondrial membrane; VDAC, voltage-dependent anion channel; OMM, outer mitochondrial membrane; HP, hematoporphyrin IX; PP, protoporphyrin IX; DP, deuteroporphyrin IX; CP, coproporphyrin III; PhAsO, phenylarsine oxide; Cu(OP)₂, copper-*o*-phenanthroline; MAO, monoamine oxidase; W, watts.

IMM ultrastructure and energy-linked functions. Our results indicate that mitoplasts undergo a Ca^{2+} -induced and CsA-sensitive PT and that the OMM plays a regulatory role exerted in part at least through TSPO.

EXPERIMENTAL PROCEDURES

Reagents—HP, PP, deuteroporphyrin IX (DP), and coproporphyrin III (CP) were obtained from Frontier Scientific (Logan, UT), and stock solutions were prepared in dimethyl sulfoxide. FGIN1-27 (*N,N*-dihexyl-2-(4-fluorophenyl)indole-3-acetamide) and PK11195 (1-(2-chlorophenyl)-*N*-methyl-*N*-(1-methylpropyl)isoquinoline-3-carboxamide) were generous gifts of Prof. Pietro Giusti (Department of Pharmacology and Anesthesiology, University of Padova). Digitonin, phenylarsine oxide (PhAsO), and Ro 5-4864 (4'-chlorodiazepam; 7-chloro-5-(4-chlorophenyl)-1,3-dihydro-1-methyl-2*H*-1,4-benzodiazepin-2-one) were from Sigma. Copper-*o*-phenanthroline ($\text{Cu}(\text{OP})_2$) was prepared just before use by mixing CuSO_4 with *o*-phenanthroline at a molar ratio of 1:2 in bidistilled water. All chemicals were of the highest purity commercially available.

Preparation of Mitochondria—Liver mitochondria from Wistar rats were prepared by standard differential centrifugation. The final pellet was suspended in isolation buffer (250 mM sucrose, 0.5 mM EGTA/Tris, and 10 mM Tris-HCl, pH 7.4) to give a protein concentration of 80–100 mg/ml as measured by the biuret method. The quality of mitochondrial preparations was established as described previously (26).

Preparation of Mitoplasts—The mitochondrial suspension was added to solutions of varying digitonin concentrations in isolation buffer at a final protein concentration of 20 mg/ml. The resulting mixtures were then cooled in an ice-water bath and gently stirred for 20 min. The suspensions were centrifuged at $10,000 \times g$ for 5 min, and the resulting pellets were washed twice with isolation buffer and finally resuspended in the same medium. The extent of OMM extraction was assessed based on the activity of monoamine oxidase (MAO) using benzylamine as a substrate (35). Extraction of MAO activity was ~90% after treatment of mitochondria with 0.09–0.12 mg of digitonin/mg of mitochondrial protein (see Fig. 2).

Western Blotting—Proteins were solubilized in Laemmli gel sample buffer, separated by 15% SDS-PAGE, and transferred electrophoretically to nitrocellulose membranes using a Mini Trans-Blot system (Bio-Rad). Western blotting was performed in phosphate-buffered saline containing 3% nonfat dry milk with polyclonal antibodies prepared in rabbits against purified bovine heart F_1 -ATPase, anti-GRIM19 monoclonal antibody (Santa Cruz Biotechnology), anti-apoptosis-inducing factor polyclonal antibody (Exalpha Biologicals, Inc.), anti-Bcl- x_L polyclonal antibody (Cell Signaling Technology), and anti-VDAC1 monoclonal antibody (a generous gift of Dr. F. Thinnes). Immunoreactive bands were detected by enhanced chemiluminescence (Millipore).

Permeability Transition and Calcium Retention Capacity—PT was induced at 25 °C in standard medium (250 mM sucrose, 10 mM Tris/MOPS, 5 mM succinate, 1 mM P_i /Tris, 10 μM EGTA/Tris, 0.5 $\mu\text{g}/\text{ml}$ oligomycin, and 2 μM rotenone,

pH 7.4). Osmotic swelling was followed as the decrease in 90° light scattering at 540 nm with a PerkinElmer Life Sciences LS50 spectrofluorometer (36). The calcium retention capacity of mitochondria and mitoplasts was measured in the same medium supplemented with 0.5 μM calcium green-5N (excitation at 480 nm and emission at 530 nm).

Mitochondrial and Mitoplast Membrane Potential—Changes in membrane potential difference ($\Delta\psi_m$) in mitochondria and mitoplasts were followed based on the accumulation of pyronin G (3 μM) as monitored by the changes in emission fluorescence intensity at $\lambda = 580$ nm (excitation, $\lambda = 520$ nm) (37).

Porphyrin Uptake and Photosensitization of Mitochondria and Mitoplasts—Mitochondria and mitoplasts were suspended in standard medium, and porphyrins were added under gentle stirring at room temperature. After 2 min, the suspensions were centrifuged at $4000 \times g$ for 2 min, and porphyrin concentrations were determined fluorometrically by calibration plots after extraction of supernatants and pellets with 2% SDS. Porphyrin-mediated photosensitization of mitochondria and mitoplasts was achieved as described previously (26). Briefly, preparations were incubated for 1–2 min in the dark with the desired concentration of porphyrin and then irradiated at 365 nm in a thermostatted glass reaction vessel with a Philips HPW 125-watt lamp. The fluence rate at the level of the preparations (40 watts (W)/ m^2) was measured with a calibrated quantum photo radiometer (Delta OHM HD 9021). All irradiations were performed at 25 °C under magnetic stirring. Proper controls were carried out to verify that neither incubation with the photosensitizer in the dark nor illumination in the absence of porphyrin produced any appreciable changes in the parameters under study. The structures of the porphyrins studied in this work are shown in Fig. 1.

To compare the photoactivity of these different porphyrins on the PTP, it was essential to establish first how much of each was taken up by mitochondria and mitoplasts. Determinations of porphyrin uptake revealed that HP, PP, and DP exhibited higher incorporation yields in mitochondria (~30–40% of the total added) than in mitoplasts (~20–30%) (see Table 1; see also Ref. 38 for HP and PP). The membrane affinity of the highly hydrophilic tetracarboxylic CP was much lower and equal for mitochondria and mitoplasts (incorporation yield of ~10–13%). For each porphyrin, the concentration was adjusted in the range of 0.2–1.5 nmol of porphyrin taken up per mg of protein to obtain comparable amounts of membrane-bound compound, which was measured spectrofluorometrically. The rates of permeabilization were then studied after irradiation times ranging from 10 to 240 s at 40 W/m^2 (total light doses between 0.04 and 0.96 J/cm^2). Under these conditions, (i) porphyrins were bound to mitochondria and mitoplasts as monomers, the only species that is appreciably photoactive (39); (ii) no measurable effects were induced in the dark (data not shown); and (iii) the molar absorption at the irradiation wavelength used (365 nm) was very similar for all porphyrins (difference within 10%), which reflects an equivalent number of absorbed photons (data not shown).

Modulation of the Mitochondrial Permeability Transition by TSP0

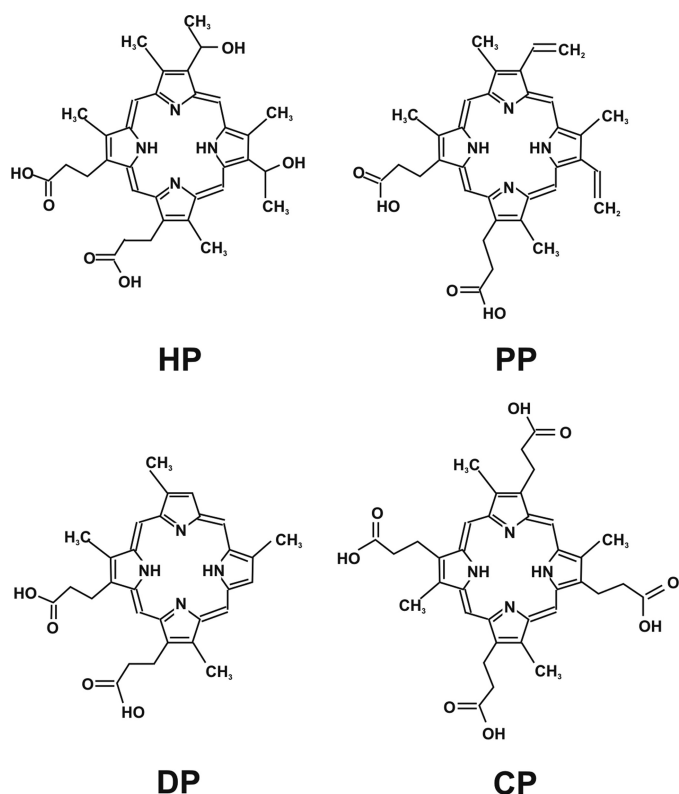


FIGURE 1. **Structure of porphyrins.** The chemical structures of HP, PP, DP, and CP are shown.

Transmission Electron Microscopy—Mitochondria and mitoplasts were fixed for 30 min at 4 °C using glutaraldehyde at a final concentration of 1.5% (v/v) in 0.1 M cacodylate buffer, pH 7.2, and post-fixed with 1% OsO₄. Thin sections (60–80 nm) were stained with uranyl acetate in alcohol (50%) and lead citrate. Observations were made with an FEI Tecnai F12 transmission electron microscope.

RESULTS

We carried out a titration of mitochondria with increasing concentrations of digitonin, and we assessed the release of MAO and maintenance of the $\Delta\psi_m$ by the resulting organelle preparation. About 90% of MAO activity was solubilized between 0.09 and 0.12 mg of digitonin/mg of mitochondrial protein, and a lower $\Delta\psi_m$ was detected only with the highest digitonin concentration (Fig. 2A).

Ultrastructural observation by transmission electron microscopy showed that treatment with 0.04 mg/mg digitonin caused partial removal of the OMM (Fig. 2B, panel b, compare with intact mitochondria in panel a), whereas with 0.09 mg/mg digitonin, the OMM was effectively removed. The electron-dense matrix was preserved and delimited by a highly convoluted, slightly unwound IMM (Fig. 2B, panel c). At this concentration of digitonin, characteristic features of mitoplasts were also foldings or finger-like protrusions of the IMM and the absence of cristae and intracristal spaces projecting into the matrix typically found in mitochondria. A few mitoplasts were round and swollen, and this population became predominant after treatment with 0.12 mg/mg digito-

nin, which resulted in the formation of spherical vesicles (Fig. 2B, panel d).

We also studied the profile of marker proteins at increasing digitonin concentrations. We found that 0.09 mg/mg digitonin extracted all of OMM Bcl-x_L and nearly all VDAC, with a marginal effect on the intermembrane apoptosis-inducing factor, whereas it left an intact amount of IMM GRIM19 and the β -subunit of the ATP synthase complex, which resides largely in the matrix space (Fig. 2C). We also tested an anti-TSP0 antibody (a generous gift of Dr. Vassilios Papadopoulos), which unfortunately did not react with the rat protein. However, similar digitonin titrations performed in mouse liver mitochondria revealed an identical digestion pattern as in rats and led to the complete disappearance of TSP0 at 0.09 mg/mg digitonin (data not shown). On the basis of the ultrastructural data and protein profiles, we therefore chose 0.09 mg of digitonin/mg of mitochondrial protein for subsequent experiments.

We tested the ability of mitoplasts to undergo the PT with the sensitive calcium retention capacity test, which measures the threshold Ca²⁺ load required to open the pore. Like mitochondria (Fig. 2D, trace a), mitoplasts readily took up a train of Ca²⁺ pulses (Fig. 2D, trace a') in a process that was fully sensitive to ruthenium red, an inhibitor of the Ca²⁺ uniporter (data not shown). In mitoplasts, the threshold Ca²⁺ required for opening of the PTP, which is marked by a precipitous release of the previously accumulated Ca²⁺, was about one-third of that necessary to open the pore in intact mitochondria. In both preparations, the Ca²⁺ threshold was more than doubled in the presence of 1 μ M CsA (data not shown). Mitoplast Ca²⁺ uptake could not be explained by residual intact mitochondria after digitonin treatment. Indeed, a titration with concentrations of mitochondria ranging between 0.1 and 1 mg/ml revealed that 0.4 mg/ml mitochondria was necessary to match the calcium retention capacity of 1 mg/ml mitoplasts (data not shown). This is well above the residual MAO activity, which would account for a maximum of 0.10 mg/ml intact mitochondria. Given that intact mitochondria were not seen in EM images of preparations treated with 0.09 mg/mg digitonin, we concluded that Ca²⁺ uptake was entirely due to mitoplasts (see also below).

A set of experiments was carried out to study PT regulation in mitoplasts. Specifically, we checked whether the pore could still be regulated by two distinct classes of matrix- and surface-exposed sulfhydryl groups previously identified in intact mitochondria (20, 22, 26). These thiols can be discriminated based on their reactivity with the membrane-permeant dithiol cross-linker PhAsO and the membrane-impermeant thiol oxidant Cu(OP)₂, respectively (20, 22, 26). Both mitochondria (Fig. 3A) (22) and mitoplasts (Fig. 3A') underwent permeabilization and swelling upon addition of PhAsO (traces a), in a process that was prevented by CsA (traces b) or by 20 μ M N-ethylmaleimide (traces c), indicating that the PhAsO-reactive matrix thiols (19) maintained their PTP regulatory activity after removal of the OMM. PTP-dependent permeabilization of both mitochondria (Fig. 3B) and mitoplasts (Fig. 3B') was also seen after the addition of Cu(OP)₂ (traces a) in a process that maintained its sensitivity to CsA (traces b) but was not

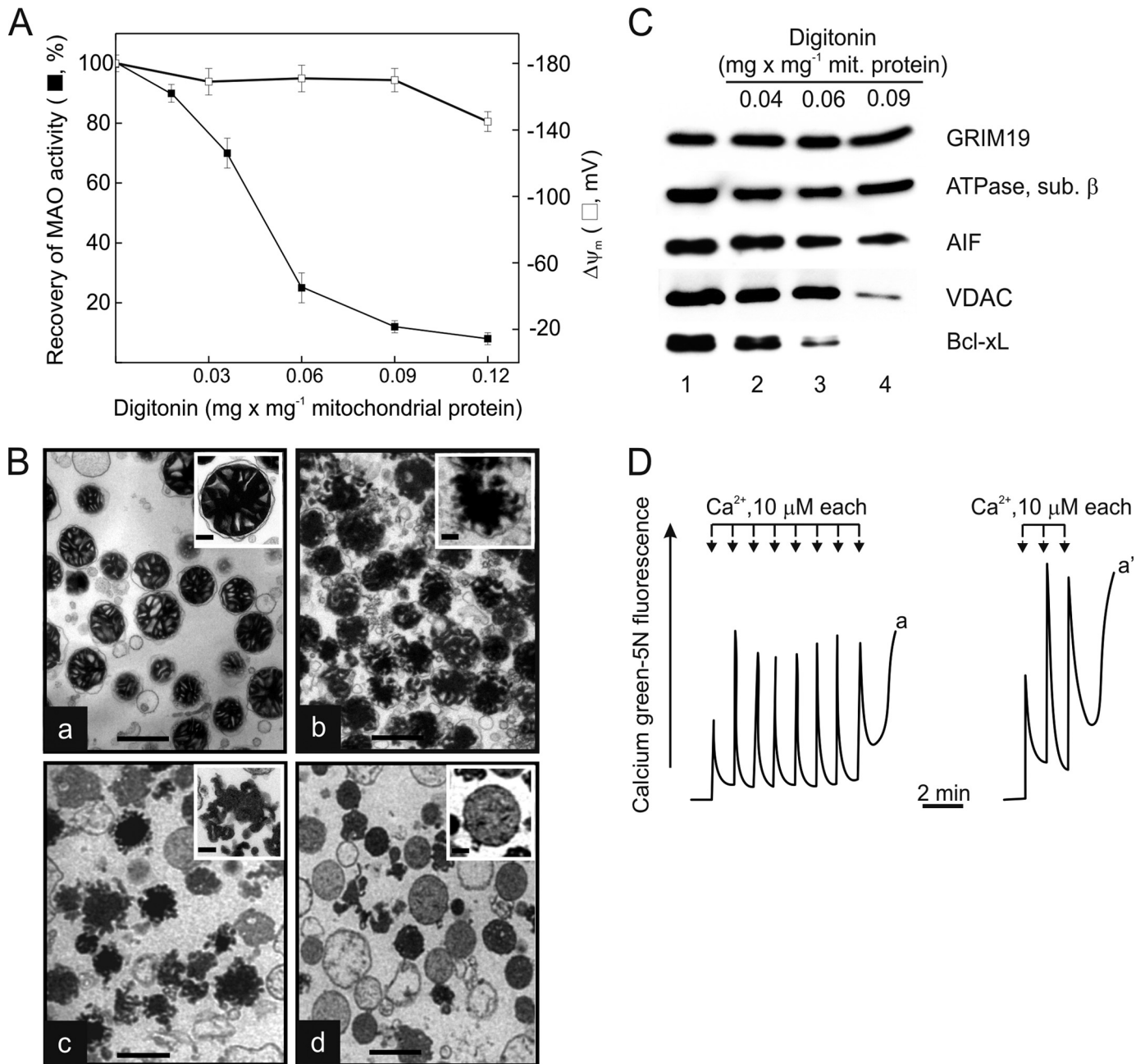


FIGURE 2. Properties of mitochondria and digitonin-treated mitoplasts. *A*, mitochondria (20 mg/ml) were incubated for 20 min with the indicated amounts of digitonin. The suspensions were then diluted and pelleted by centrifugation as described under "Experimental Procedures." For each preparation, MAO activity (■) and $\Delta\psi_m$ (□) were determined. The activity was calculated as percent of the starting untreated mitochondria. Error bars represent means \pm S.D. of four experiments. *B*, transmission electron microscopy of mitochondrial preparations without treatment with digitonin (*panel a*) and after treatment with 0.04 (*panel b*), 0.09 (*panel c*), and 0.12 mg (*panel d*) of digitonin/mg of protein. Scale bars = 1 μ m in the main panels and 0.2 μ m in the insets. *C*, Western blot analysis of untreated mitochondria (*lane 1*) and of preparations obtained after treatment of mitochondria with the indicated amounts of digitonin (*lanes 2–4*). AIF, apoptosis-inducing factor; mit., mitochondrial; sub., subunit. *D*, the incubation medium contained 250 mM sucrose, 10 mM Tris/MOPS, 5 mM succinate, 1 mM P_i, 10 μ M EGTA/Tris, 0.5 μ M calcium green-5N, 0.5 μ g/ml oligomycin, and 2 μ M rotenone, pH 7.4, at 25 °C. The calcium retention capacity was measured in mitochondria (1 mg/ml; *trace a*) or mitoplasts prepared with 0.09 mg of digitonin/mg of protein (1 mg/ml; *trace a'*) by the sequential addition of a train of 10 μ M Ca²⁺ pulses at 1-min intervals (arrows).

inhibited by 20 μ M *N*-ethylmaleimide (*traces c*), as also described in detail previously for intact mitochondria (22, 26). These results prove that the Cu(OP)₂-reactive external thiols are located in the outer face of the IMM rather than in the OMM.

In intact mitochondria, the PT can be either inhibited or activated by photo-oxidative stress mediated by HP depending on whether low or high doses of light are applied, respec-

tively (26). We tested whether these peculiar photosensitizing properties of HP are maintained in mitoplasts. Mitochondria or mitoplasts (Fig. 4, *closed* and *open squares*, respectively) were incubated with 2 μ M HP and irradiated for times ranging between 30 and 240 s at 40 W/m², corresponding to light doses between 0.12 and 0.96 J/cm². PTP opening was then triggered by Ca²⁺. These experiments showed that irradiation for up to 100 s inactivated the PTP in both mitochondria (26)

Modulation of the Mitochondrial Permeability Transition by TSPO

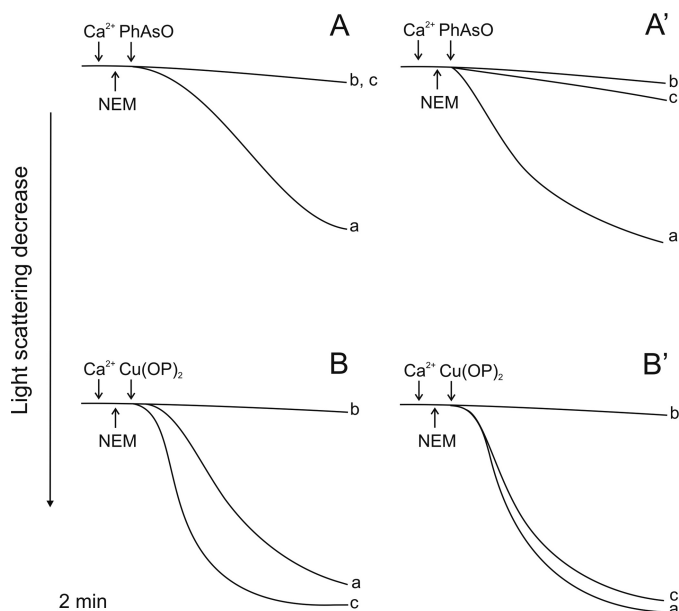


FIGURE 3. Effect of PhAsO and Cu(OP)₂ on light scattering in mitochondria and mitoplasts. The experimental conditions were as described for Fig. 2C, except that calcium green-5N was omitted. Light scattering was measured at 540 nm in mitochondria (1 mg/ml; A and B) or mitoplasts (1 mg/ml; A' and B'). A and A', 5 μ M Ca²⁺ and 5 μ M PhAsO were added where indicated (traces a); 1 μ M CsA was added before (traces b); and 20 μ M *N*-ethylmaleimide (NEM) was added where indicated (traces c). B and B', 5 μ M Ca²⁺ and 3 μ M Cu(OP)₂ were added where indicated (traces a); 1 μ M CsA was added before the organelles (traces b); and 20 μ M *N*-ethylmaleimide was added where indicated (traces c).

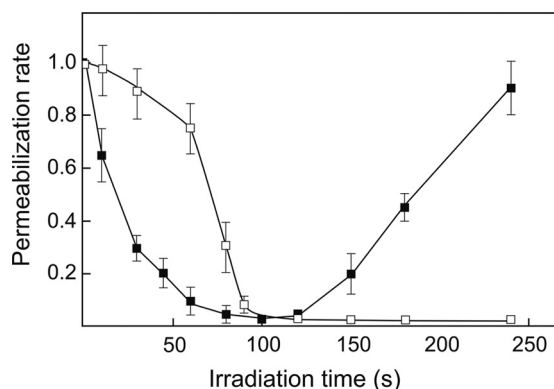


FIGURE 4. Effect of the irradiation time in mitochondria and mitoplasts loaded with HP. Mitochondria (■) and mitoplasts (□) at 0.5 mg/ml were loaded with 2 μ M HP for 1 min at 25 °C in standard medium before irradiation at 40 W/m² for the indicated times; permeabilization was then studied as the light scattering change at 540 nm following the addition of 60 μ M (mitochondria) or 30 μ M (mitoplasts) Ca²⁺. The permeabilization rates were normalized to that of the control (non-irradiated organelles). Error bars represent the mean \pm S.D. of four experiments.

and mitoplasts, although the latter were significantly more resistant (Fig. 4). In both preparations, inactivation occurred through photomodification of His residues, as indicated by the counteracting effect of diethyl pyrocarbonate, which prevents the addition of ¹O₂ to the His imidazole ring and its irreversible degradation (data not shown, but see Ref. 26). On the other hand, mitoplasts were strikingly resistant to the activation of the PTP that in mitochondria follows irradiation for times longer than 100 s (Fig. 4). It must be stressed that the mitoplast preparations (i) maintained the ability to take up Ca²⁺ in the full range of light doses investigated, indicat-

TABLE 1

Porphyrin incorporation in mitochondria and mitoplasts

Mitochondria and mitoplasts (1 mg/ml protein) were incubated for 2 min in standard medium in the presence of HP, PP, DP, and CP ranging from 1 to 6 nmol of porphyrin/mg of protein. After 2 min, the suspensions were centrifuged at 4000 \times g for 2 min, and porphyrin concentrations were determined fluorometrically by calibration plots after extraction of supernatants and pellets with 2% SDS. All data are the average of at least three independent experiments and are expressed as percent of the total amount of porphyrin added.

	Mitochondria	Mitoplasts
HP	30 \pm 4	20 \pm 2
PP	37 \pm 5	25 \pm 4
DP	40 \pm 5	30 \pm 5
CP	13 \pm 3	10 \pm 3

ing that they retained energy coupling and a membrane potential, and (ii) readily underwent large amplitude swelling upon addition of alamethicin, indicating that they maintained their structural integrity (data not shown). We deduce that in intact mitochondria HP interferes with PTP-regulating OMM sites that are lost in mitoplasts.

HP binds TSPO with nanomolar affinity (27). To test whether this OMM protein mediates HP-dependent PTP photoactivation, we extended our investigation to DP and PP, dicarboxylic porphyrins that display even higher affinity than HP in binding TSPO (27). We also tested CP (Table 1; see "Experimental Procedures" for details), a tetracarboxylic porphyrin whose binding to TSPO is very weak (27).

Like HP, photoactivated PP and DP caused a concentration-dependent PT inhibition in both mitochondria and mitoplasts (Fig. 5, A and A', respectively). PP and DP were more effective than HP, whereas CP was totally inactive. As the efficiency of ¹O₂ production is very similar for all porphyrins in the monomeric state (\sim 0.7) (39), the resulting effects (or lack thereof) must depend on the different localization of specific porphyrins in the mitochondrial and mitoplast membranes. It should be noted that the PTP-active porphyrins were more effective in mitochondria than in mitoplasts (Fig. 5, compare A and A'), suggesting the TSPO facilitates their diffusion to the "internal" PTP regulatory sites.

We next investigated the effects of these porphyrins on PTP after prolonged irradiation. Mitochondria and mitoplasts were allowed to accumulate a very small Ca²⁺ load (10 nmol/mg of protein) that was not sufficient for spontaneous PTP opening yet was permissive for the subsequent effect of irradiation. In mitochondria, PTP opening was readily detected with PP, DP, and HP (Fig. 6, closed symbols); of note, the relative potency of porphyrins in eliciting photosensitization of the PTP closely correlated with their relative affinities for TSPO binding (27). Strikingly, in these protocols, all porphyrins were instead totally inactive in mitoplasts (Fig. 6, open symbols).

Several TSPO ligands have been reported to cause PTP opening (7–9, 11, 13, 16). We tested the effects of PP, PK11195, Ro 5-4864, and FGIN1-27 (40) on Ca²⁺ release in Ca²⁺-loaded mitochondria treated with ruthenium red, a sensitive measure of pore opening (41). In these protocols, the uncoupler carbonyl cyanide *p*-trifluoromethoxyphenylhydrazone caused Ca²⁺ release in both mitochondria and mitoplasts (Fig. 7, A and A', respectively, traces b) through a fully CsA-sensitive process (traces a). Strikingly, the addition of 40

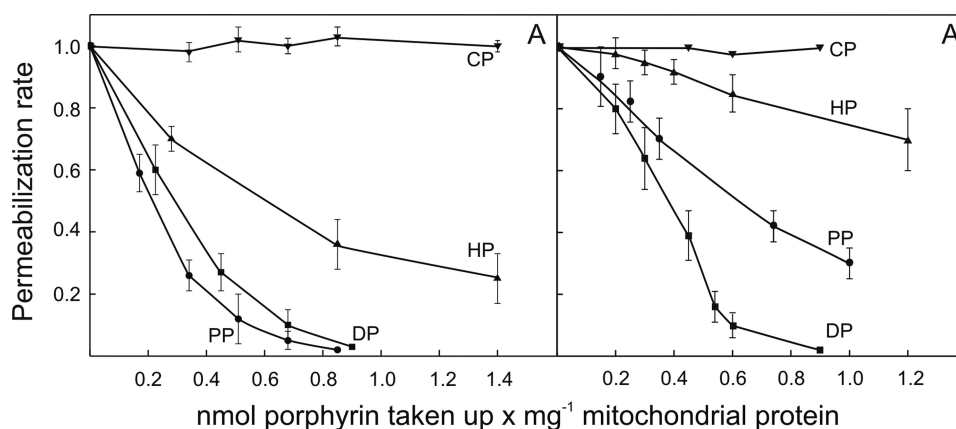


FIGURE 5. **Effect of DP, HP, PP, and CP on light-dependent inactivation of the permeability transition.** Mitochondria (A) and mitoplasts (A') at 0.5 mg/ml were incubated for 1 min with concentrations of each porphyrin giving a loading of 0.2–1.5 nmol of porphyrin/mg of protein at 25 °C (for details, see Table 1 and "Experimental Procedures"). Preparations were irradiated for 45 s at a fluence rate of 40 W/m² and then supplemented with 60 μM (A) or 30 μM (A') Ca²⁺ to trigger the PT, which was followed as the changes in 90° light scattering at 540 nm. The permeabilization rate was normalized to that of the control (in the absence of porphyrins). Error bars represent the mean ± S.D. of three experiments.

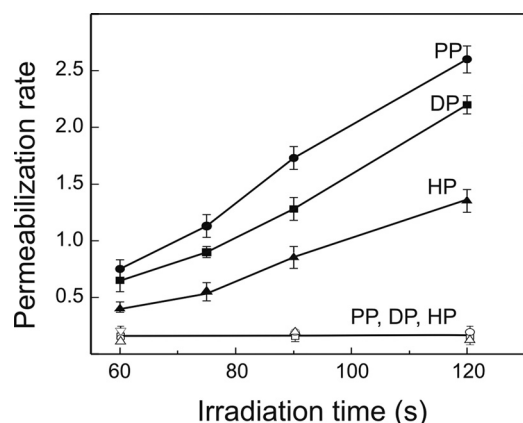


FIGURE 6. **Effect of DP, HP, and PP on light-dependent activation of the permeability transition.** Mitochondria (closed symbols) or mitoplasts (open symbols) at 0.5 mg/ml were incubated for 1 min at 25 °C with concentrations of each porphyrin (PP, circles; DP, squares; HP, triangles) giving a loading of 1.2 nmol of porphyrin/mg of protein (for details, see Table 1 and "Experimental Procedures"). Preparations were then supplemented with 5 μM Ca²⁺ (a concentration not sufficient to induce PTP opening *per se*) and irradiated for the indicated times at a fluence rate of 40 W/m². The PT was followed as the change in 90° light scattering at 540 nm. Error bars represent the mean ± S.D. of three experiments.

μM FGIN1-27 caused CsA-sensitive PTP opening in mitochondria but not in mitoplasts (Fig. 7, A and A', respectively, traces c). A full titration was carried out with FGIN1-27, Ro 5-4864, and PK11195, which confirmed the striking resistance of digitonin-treated mitoplasts to the PTP-inducing effects of TSPO ligands (Fig. 8). Similar results were obtained for concentrations of PP above ~6 μM (data not shown).

DISCUSSION

An important result of this work is the demonstration that a CsA-sensitive PT can occur in digitonin-treated mitoplasts, *i.e.* in the absence of an intact OMM. The PT of mitoplasts maintains most of the basic features of the PT observed in mitochondria (Ca²⁺ dependence, desensitization by CsA, activation by oxidants, inactivation by HP at low irradiation times), thus indicating that the PT is fundamentally an IMM event that can occur in the absence of an intact OMM. These findings heavily bear on our understanding of the nature and

location of the PTP and call into question the widespread conviction that the pore forms at contact sites between the IMM and OMM and that the pore itself spans both membranes (42).

The basis for this model of the PTP is the presence of ANT and VDAC (together with many other proteins) in detergent membrane extracts that possess hexokinase activity and display transport properties that resemble those of the PTP after reconstitution in liposomes (43). Similar preparations (which were, however, not even enriched in ANT and VDAC) had been previously shown to possess electrophysiological properties similar to those of the PTP, although atractylate caused channel closure (44) rather than the opening that would be expected based on studies in intact mitochondria (45). We believe that this model should be abandoned because (i) a Ca²⁺-dependent and CsA-sensitive PT can occur in mice in which both isoforms of ANT have been genetically ablated (2); (ii) the PTP of VDAC1-null mice is indistinguishable from that of wild-type animals (3); (iii) a PT can occur in mitochondria of cells in which the genes for all three VDAC isoforms have been deleted or silenced (4); (iv) the 32-kDa protein binding to the PTP modulator cyclophilin D under conditions that favor pore opening is not ANT (46); and (v) the PT can occur in the absence of an intact OMM (this study). Although trace amounts of VDAC could be detected in our mitoplasts (Fig. 2C), we would like to stress that the absence of an intact OMM was documented by electron microscopy (Fig. 2B) and, most importantly, by the lack of effects of TSPO ligands (see below).

These results should not be taken to imply that the OMM is not relevant for PTP modulation. On the contrary, another important result of this work is the demonstration that the OMM plays a prominent regulatory role and that this is in part at least exerted through TSPO. Our data are consistent with a dual role of TSPO (i) as a *regulatory protein* for PTP modulation when it binds its selective ligands such as FGIN1-27, PK11195, Ro 5-4864, and PP and (ii) as a *transport protein* for PTP-active compounds that are then transferred to their PTP regulatory site(s) in the IMM or in the matrix.

Modulation of the Mitochondrial Permeability Transition by TSPO

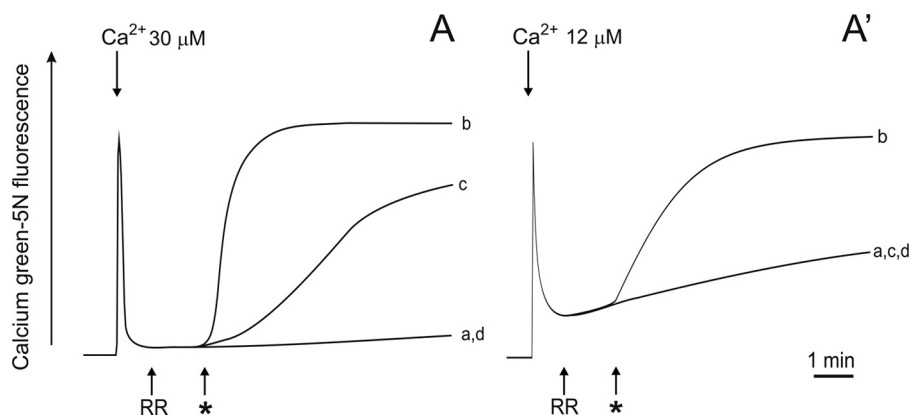


FIGURE 7. **Effect of uncoupler and FGIN1-27 on PTP-dependent Ca^{2+} release in mitochondria and mitoplasts.** Mitochondria (1 mg/ml; A) or mitoplasts (1 mg/ml; A') were incubated as described for Fig. 2D. In traces a and d, the medium was supplemented with $1 \mu\text{M}$ CsA. Where indicated, Ca^{2+} was added, followed by $0.1 \mu\text{M}$ ruthenium red (RR) and, at the asterisk, by $0.5 \mu\text{M}$ carbonyl cyanide *p*-trifluoromethoxyphenylhydrazone (traces a and b) or $40 \mu\text{M}$ FGIN1-27 (traces c and d).

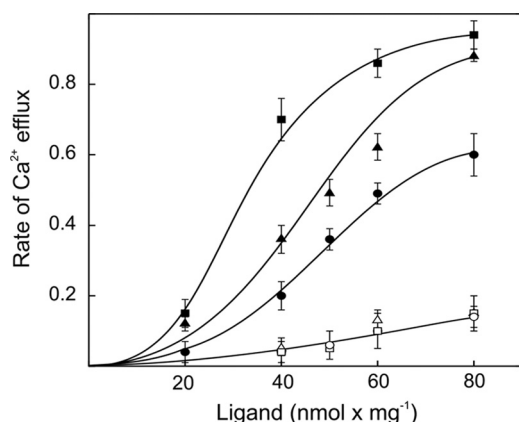


FIGURE 8. **Effect of TSPO ligands on PTP-dependent Ca^{2+} release in mitochondria and mitoplasts.** Mitochondria or mitoplasts (1 mg/ml) were incubated as described for Fig. 2D, and experiments were performed as shown in Fig. 7 by adding the stated amounts of FGIN1-27 (squares), Ro 5-4864 (triangles), or PK11195 (circles) after ruthenium red to mitochondria (closed symbols) or mitoplasts (open symbols). The rate of Ca^{2+} efflux was normalized to that obtained after the addition of $0.5 \mu\text{M}$ carbonyl cyanide *p*-trifluoromethoxyphenylhydrazone.

The first role is exemplified by the lack of pore reactivation by light in mitoplasts treated with porphyrins that bind TSPO in intact mitochondria (Figs. 4 and 6). This remarkable finding demonstrates that high light doses in mitochondria treated with HP, DP, and PP do not cause unspecific damage to the IMM because damage should be more prominent, rather than absent, in preparations that are not protected by the OMM. Instead, our data show that porphyrin- and light-dependent PTP reactivation is a specific event mediated by the OMM and suggest that the PTP regulatory sites are contributed by TSPO. In keeping with this hypothesis, in intact mitochondria, PTP activation could be induced in the presence of porphyrins characterized by a PP-like configuration that bind TSPO with nanomolar affinity (27, 28), whereas the PP-unrelated CP was ineffective (data not shown). Furthermore, the photoactivity of dicarboxylic porphyrins (PP > DP >> HP) followed exactly their order of affinity for TSPO, as calculated from the values of their inhibition constants for [^3H]PK11195 binding (27). Selectivity is the basis for the physiological role of TSPO, which allows the transport of nat-

ural dicarboxylic porphyrins (such as PP), heme precursors, heme itself, and cholesterol to mitochondria (28, 47–50). Strong evidence in favor of a regulatory role of TSPO in inner membrane permeability is provided by the observation that FGIN1-27, PK11195, Ro 5-4864, and relatively high concentrations of PP ($\sim 6 \mu\text{M}$ or higher) cause PTP opening in mitochondria (7–16) but not in mitoplasts (Figs. 7 and 8). We believe that the liganded state of TSPO modulates the PTP through protein-protein interactions that may be similar to those described for dephosphorylated Bad and Bcl- x_L (51).

The second role of TSPO is revealed by the effects of PP, DP, and HP, which at low concentrations do not affect the pore yet are able to induce PTP inhibition through photo-oxidation of matrix His residues in both mitochondria and mitoplasts (Fig. 5). Higher porphyrin concentrations are required in mitoplasts, indicating that transport through TSPO facilitates diffusion of porphyrins to their relevant matrix or IMM sites of action. In other words, these data demonstrate that compounds whose PTP-dependent effects are facilitated via transport through TSPO do not necessarily exert their effects through TSPO itself.

TSPO is a member of an evolutionarily conserved family of ubiquitous proteins able to bind small molecule drugs, cholesterol, and porphyrins (17). TSPO has been conserved from bacteria to mammals, and its inactivation induces an early embryonic-lethal phenotype in mice (52). In mammals, TSPO is highly expressed in the adrenal cortex (53), particularly in the zona glomerulosa (54), which is consistent with its role in steroid hormone synthesis. Its ubiquitous distribution suggests, however, more general functions, including heme biosynthesis, apoptosis, cell proliferation, and PTP modulation (49). A thorough study is under way to define which PTP ligands of pathophysiological relevance act through TSPO.

REFERENCES

- Bernardi, P., Krauskopf, A., Basso, E., Petronilli, V., Blachly-Dyson, E., Di Lisa, F., and Forte, M. A. (2006) *FEBS J.* **273**, 2077–2099
- Kokoszka, J. E., Waymire, K. G., Levy, S. E., Sligh, J. E., Cai, J., Jones, D. P., MacGregor, G. R., and Wallace, D. C. (2004) *Nature* **427**, 461–465
- Krauskopf, A., Eriksson, O., Craigen, W. J., Forte, M. A., and Bernardi, P. (2006) *Biochim. Biophys. Acta* **1757**, 590–595
- Baines, C. P., Kaiser, R. A., Sheiko, T., Craigen, W. J., and Molkenin,

- J. D. (2007) *Nat. Cell Biol.* **9**, 550–555
5. Pastorino, J. G., Shulga, N., and Hoek, J. B. (2002) *J. Biol. Chem.* **277**, 7610–7618
 6. Chiara, F., Castellaro, D., Marin, O., Petronilli, V., Brusilow, W. S., Juhászova, M., Sollott, S. J., Forte, M., Bernardi, P., and Rasola, A. (2008) *PLoS ONE* **3**, e1852
 7. McEnery, M. W., Snowman, A. M., Trifiletti, R. R., and Snyder, S. H. (1992) *Proc. Natl. Acad. Sci. U.S.A.* **89**, 3170–3174
 8. Kinnally, K. W., Zorov, D. B., Antonenko, Y. N., Snyder, S. H., McEnery, M. W., and Tedeschi, H. (1993) *Proc. Natl. Acad. Sci. U.S.A.* **90**, 1374–1378
 9. Hirsch, T., Decaudin, D., Susin, S. A., Marchetti, P., Larochette, N., Resche-Rigon, M., and Kroemer, G. (1998) *Exp. Cell Res.* **241**, 426–434
 10. Berson, A., Descatoire, V., Sutton, A., Fau, D., Maulny, B., Vadrot, N., Feldmann, G., Berthon, B., Tordjmann, T., and Pessayre, D. (2001) *J. Pharmacol. Exp. Ther.* **299**, 793–800
 11. Chelli, B., Falleni, A., Salvetti, F., Gremigni, V., Lucacchini, A., and Martini, C. (2001) *Biochem. Pharmacol.* **61**, 695–705
 12. Jayakumar, A. R., Panickar, K. S., and Norenberg, M. D. (2002) *J. Neurochem.* **83**, 1226–1234
 13. Azarashvili, T., Grachev, D., Krestinina, O., Evtodienko, Y., Yurkov, I., Papadopoulos, V., and Reiser, G. (2007) *Cell Calcium* **42**, 27–39
 14. Li, J., Wang, J., and Zeng, Y. (2007) *Eur. J. Pharmacol.* **560**, 117–122
 15. Krestinina, O. V., Grachev, D. E., Odinkova, I. V., Reiser, G., Evtodienko, Y. V., and Azarashvili, T. S. (2009) *Biochemistry* **74**, 421–429
 16. Azarashvili, T., Stricker, R., and Reiser, G. (2010) *Biol. Chem.* **391**, 619–629
 17. Papadopoulos, V., Baraldi, M., Guilarte, T. R., Knudsen, T. B., Lacapère, J. J., Lindemann, P., Norenberg, M. D., Nutt, D., Weizman, A., Zhang, M. R., and Gavish, M. (2006) *Trends Pharmacol. Sci.* **27**, 402–409
 18. Beatrice, M. C., Stiers, D. L., and Pfeiffer, D. R. (1984) *J. Biol. Chem.* **259**, 1279–1287
 19. Petronilli, V., Costantini, P., Scorrano, L., Colonna, R., Passamonti, S., and Bernardi, P. (1994) *J. Biol. Chem.* **269**, 16638–16642
 20. Costantini, P., Chernyak, B. V., Petronilli, V., and Bernardi, P. (1996) *J. Biol. Chem.* **271**, 6746–6751
 21. Halestrap, A. P., Woodfield, K. Y., and Connern, C. P. (1997) *J. Biol. Chem.* **272**, 3346–3354
 22. Costantini, P., Colonna, R., and Bernardi, P. (1998) *Biochim. Biophys. Acta* **1365**, 385–392
 23. Kowaltowski, A. J., Castilho, R. F., and Vercesi, A. E. (2001) *FEBS Lett.* **495**, 12–15
 24. Salet, C., Moreno, G., Ricchelli, F., and Bernardi, P. (1997) *J. Biol. Chem.* **272**, 21938–21943
 25. Moreno, G., Poussin, K., Ricchelli, F., and Salet, C. (2001) *Arch. Biochem. Biophys.* **386**, 243–250
 26. Petronilli, V., Sileikyte, J., Zulian, A., Dabbeni-Sala, F., Jori, G., Gobbo, S., Tognon, G., Nikolov, P., Bernardi, P., and Ricchelli, F. (2009) *Biochim. Biophys. Acta* **1787**, 897–904
 27. Verma, A., Nye, J. S., and Snyder, S. H. (1987) *Proc. Natl. Acad. Sci. U.S.A.* **84**, 2256–2260
 28. Verma, A., and Snyder, S. H. (1988) *Mol. Pharmacol.* **34**, 800–805
 29. Hirsch, J. D., Beyer, C. F., Malkowitz, L., Loullis, C. C., and Blume, A. J. (1989) *Mol. Pharmacol.* **35**, 164–172
 30. Garnier, M., Dimchev, A. B., Boujrad, N., Price, J. M., Musto, N. A., and Papadopoulos, V. (1994) *Mol. Pharmacol.* **45**, 201–211
 31. Kessel, D., and Luo, Y. (1999) *Cell Death Differ.* **6**, 28–35
 32. Pastorino, J. G., Simbula, G., Gilfor, E., Hoek, J. B., and Farber, J. L. (1994) *J. Biol. Chem.* **269**, 31041–31046
 33. Castedo, M., Perfettini, J. L., and Kroemer, G. (2002) *J. Exp. Med.* **196**, 1121–1125
 34. Galiegue, S., Tinel, N., and Casellas, P. (2003) *Curr. Med. Chem.* **10**, 1563–1572
 35. Ragan, C. I., Wilson, M. T., Darley-Usmar, V. M., and Lowe, P. N. (1987) in *Mitochondria: A Practical Approach* (Darley-Usmar, V. M., Rickwood, D., and Wilson, M. T., eds) pp. 79–112, IRL Press, Oxford
 36. Ricchelli, F., Gobbo, S., Moreno, G., and Salet, C. (1999) *Biochemistry* **38**, 9295–9300
 37. Tomov, T. C. (1986) *J. Biochem. Biophys. Methods* **13**, 29–38
 38. Ricchelli, F., Gobbo, S., Jori, G., Moreno, G., Vinzens, F., and Salet, C. (1993) *Photochem. Photobiol.* **58**, 53–58
 39. Ricchelli, F. (1995) *J. Photochem. Photobiol. B* **29**, 109–118
 40. Raghavendra Rao, V. L., and Butterworth, R. F. (1997) *Eur. J. Pharmacol.* **340**, 89–99
 41. Petronilli, V., Cola, C., and Bernardi, P. (1993) *J. Biol. Chem.* **268**, 1011–1016
 42. Kroemer, G., Galluzzi, L., and Brenner, C. (2007) *Physiol. Rev.* **87**, 99–163
 43. Marzo, I., Brenner, C., Zamzami, N., Susin, S. A., Beutner, G., Brdiczka, D., Rémy, R., Xie, Z. H., Reed, J. C., and Kroemer, G. (1998) *J. Exp. Med.* **187**, 1261–1271
 44. Beutner, G., Ruck, A., Riede, B., Welte, W., and Brdiczka, D. (1996) *FEBS Lett.* **396**, 189–195
 45. Haworth, R. A., and Hunter, D. R. (1979) *Arch. Biochem. Biophys.* **195**, 460–467
 46. Leung, A. W., and Halestrap, A. P. (2008) *Biochim. Biophys. Acta* **1777**, 946–952
 47. Wendler, G., Lindemann, P., Lacapère, J. J., and Papadopoulos, V. (2003) *Biochem. Biophys. Res. Commun.* **311**, 847–852
 48. Krueger, K. E. (1995) *Biochim. Biophys. Acta* **1241**, 453–470
 49. Batarseh, A., and Papadopoulos, V. (2010) *Mol. Cell. Endocrinol.* **327**, 1–12
 50. Taketani, S., Kohno, H., Furukawa, T., and Tokunaga, R. (1995) *J. Biochem.* **117**, 875–880
 51. Roy, S. S., Madesh, M., Davies, E., Antonsson, B., Danial, N., and Hajnóczky, G. (2009) *Mol. Cell* **33**, 377–388
 52. Papadopoulos, V., Amri, H., Boujrad, N., Cascio, C., Culty, M., Garnier, M., Hardwick, M., Li, H., Vidic, B., Brown, A. S., Reversa, J. L., Bernasau, J. M., and Drieu, K. (1997) *Steroids* **62**, 21–28
 53. Anholt, R. R., De Souza, E. B., Oster-Granite, M. L., and Snyder, S. H. (1985) *J. Pharmacol. Exp. Ther.* **233**, 517–526
 54. De Souza, E. B., Anholt, R. R., Murphy, K. M., Snyder, S. H., and Kuhar, M. J. (1985) *Endocrinology* **116**, 567–573

2.2. PTP regulation by photooxidative stress: implication for the role of TSPO

As already mentioned, PTP appears to be modulated by specific interactions with the OMM TSPO. Indeed, (i) TSPO ligands induce PTP opening in a CsA-sensitive manner in mitochondria, but not mitoplasts; (ii) PTP is modulated by photooxidative stress upon treatment with PP IX-like dicarboxylic porphyrins and irradiation with UV/visible light; indeed, the PT can be first inactivated at low irradiation times and then reactivated at longer times [81, **Paper 1**].

Porphyrin photoactivity correlated with its affinity for TSPO: the higher the affinity, the lower light dose was needed for both PT inactivation and reactivation. In mitoplasts (that by definition should lack TSPO) the PTP could still be inactivated by porphyrins plus light. Strikingly, however, IMM preparations that should have become more fragile were instead completely resistant to PT reactivation by high light doses, suggesting that PTP occurred through the OMM, and was most likely mediated by TSPO.

In **Paper 2**, which also includes original data, we review the basic principles of the photodynamic effect, the mechanisms of phototoxicity, and discuss the unique properties of $^1\text{O}_2$ generated by porphyrins in discrete mitochondrial domains. We also cover the characterization of the PTP by chemical modification of specific residues through photoirradiation of mitochondria after treatment with porphyrins. Finally, we propose a dual role of TSPO in PT: (i) as a transport protein for PTP-active compounds like porphyrins that are thus transferred to their PTP regulatory site(s) in the IMM or in the matrix; (ii) as a PTP regulatory protein when it binds its selective ligands like porphyrins. Moreover, results presented in **Paper 3** provide additional evidence on a regulatory role of TSPO in PT. There we demonstrate that (i) PT activation by photodynamic events can be prevented by low μM concentrations of TSPO ligand FGIN1-27; and (ii) PP IX itself can induce the PT in mitochondria but not in mitoplasts.

Paper 2:

Ricchelli F, Šileikytė J, Bernardi P. Shedding light on the mitochondrial permeability transition. *Biochim Biophys Acta*. 2011 May; 1807(5):482-90.

Paper 3:

Šileikytė J, Nikolov P, Bernardi P, Ricchelli F. The outer membrane-translocator protein mediates activation of the mitochondrial permeability transition by porphyrin based photooxidative stress. *Forum on Immunopathological Diseases and Therapeutics*, 2011; 2 (3):215-26.



Review

Shedding light on the mitochondrial permeability transition

Fernanda Ricchelli^{a,*}, Justina Šileikytė^b, Paolo Bernardi^{b,**}^a CNR Institute of Biomedical Technologies, Department of Biology, University of Padova, Italy^b CNR Institute of Neurosciences, Department of Biomedical Sciences, University of Padova, Italy

ARTICLE INFO

Article history:

Received 27 January 2011

Received in revised form 21 February 2011

Accepted 28 February 2011

Available online 4 March 2011

Keywords:

Mitochondria

Permeability transition pore

Photodynamic effect

ABSTRACT

The mitochondrial permeability transition is an increase of permeability of the inner mitochondrial membrane to ions and solutes with an exclusion size of about 1500 Da. It is generally accepted that the permeability transition is due to opening of a high-conductance channel, the permeability transition pore. Although the molecular nature of the permeability transition pore remains undefined, a great deal is known about its regulation and role in pathophysiology. This review specifically covers the characterization of the permeability transition pore by chemical modification of specific residues through photoirradiation of mitochondria after treatment with porphyrins. The review also illustrates the basic principles of the photodynamic effect and the mechanisms of phototoxicity and discusses the unique properties of singlet oxygen generated by specific porphyrins in discrete mitochondrial domains. These experiments provided remarkable information on the role, interactions and topology of His and Cys residues in permeability transition pore modulation and defined an important role for the outer membrane 18 kDa translocator protein (formerly known as the peripheral benzodiazepine receptor) in regulation of the permeability transition.

© 2011 Elsevier B.V. All rights reserved.

1. The mitochondrial permeability transition

The mitochondrial permeability transition (PT) is an increase of permeability of the inner mitochondrial membrane (IMM) to ions and solutes with an exclusion size of about 1500 Da [1–4]. The prevailing view is that the PT is due to opening of a regulated protein channel, the PT pore (PTP), which in the fully open state has an estimated diameter of about 3 nm [3,5]. PTP opening requires the presence of matrix $[Ca^{2+}]$,

Abbreviations: ANT, adenine nucleotide translocase; CP, coproporphyrin III; CRC, Ca^{2+} retention capacity; CsA, cyclosporin A; CyPD, cyclophilin D; Cu(OP)₂, copper-*o*-phenanthroline; DP, deuteroporphyrin IX; DTT, dithiothreitol; EGTA, [ethylenebis(oxoethylenitrilo)] tetraacetic acid; EP, etioporphyrin; FGIN1-27, N,N-dihexyl-2-(4-fluorophenyl) indole-3-acetamide; HP, hematoporphyrin IX; IMM, inner mitochondrial membrane; MBM⁺, trimethylammonium monobromobimane; MOPS, 4-morpholinepropanesulfonic acid; NEM, N-ethylmaleimide; ¹O₂, singlet oxygen; O₂^{•-}, superoxide anion; OMM, outer mitochondrial membrane; PhAsO, phenylarsine oxide; PK11195, 1-(2-chlorophenyl)-N-methyl-N-(1-methyl-propyl)-3-isoquinolinecarboxamide; PP, protoporphyrin IX; PT, permeability transition; PTP, permeability transition pore; RCR, respiratory control ratio; Ro5-4864, 7-chloro-5-(4-chlorophenyl)-1,3-dihydro-1-methyl-2H-1,4-benzodiazepin-2-one; ROS, reactive oxygen species; TEM, transmission electron microscopy; TSPO, 18 kDa translocator protein; UP, uroporphyrin I; VDAC, voltage-dependent anion channel

* Correspondence to: F. Ricchelli, CNR Institute of Biomedical Technologies/Padova Unit, Department of Biology, University of Padova, Via Ugo Bassi 58B, 35121 Padova, Italy. Tel.: +39 049 827 6336; fax: +39 049 827 6348.

** Correspondence to: P. Bernardi, Department of Biomedical Sciences, Viale Giuseppe Colombo 3, I-35121 Padova, Italy. Tel.: +39 049 827 6365; fax: +39 049 827 6361.

E-mail addresses: rchielli@mail.bio.unipd.it (F. Ricchelli), bernardi@bio.unipd.it (P. Bernardi).

which is an essential permissive factor, and of additional agents or conditions that are collectively termed “inducers” [6–15]. In spite of major efforts the molecular nature of the PTP remains undefined. Earlier candidates such as the IMM adenine nucleotide translocator (ANT) and the outer mitochondrial membrane (OMM) VDAC appear to be regulators rather than constituents of the PTP, as their genetic ablation did not prevent PTP opening [16–18] nor its sensitivity to cyclosporin A (CsA) [19–22], a high-affinity inhibitor of cyclophilins (CyP) that desensitizes the PTP to the inducing effects of Ca^{2+} and Pi through its binding to matrix CyPD [23–25]. Consistent with these findings, recent work has shown that the polyclonal antibody used to identify a CyPD-binding protein as ANT1 in fact labeled the Pi carrier, which has now been incorporated in the model of the PTP proposed by the Halestrap laboratory [12,26].

Ablation of the *Ppif* gene encoding CyPD has similar effects as CsA, in the sense that a higher of Ca^{2+} load and Pi is required for PTP opening in isolated mitochondria [27–30]. Pi is a classical inducer of the PTP, but we recently found that CyPD inhibition or its genetic ablation sensitizes the pore to the *inhibitory* effects of Pi, which would be the actual inhibitor of the pore under these conditions [31]. The evolutionary implications of this finding and their importance in reevaluating the yeast PTP (which is inhibited by Pi) as a model for the mammalian pore have been discussed in greater detail elsewhere [32].

1.1. The PTP as a fast Ca^{2+} release channel

Transient pore openings occur both in isolated mitochondria [33] and *in situ* [34], and we have proposed that the PTP could serve a

physiological function as a mitochondrial Ca^{2+} release channel [8,35]. This hypothesis is consistent with early results on the effects of CsA on Ca^{2+} distribution in rat ventricular cardiomyocytes [36] and with recent findings in *Ppif*^{-/-} mice whose heart mitochondria display a 2.6-fold elevation in total Ca^{2+} levels and consequent activation of intramitochondrial Ca^{2+} -dependent dehydrogenases resulting in stimulation of glucose oxidation at the expense of fatty acids [37]. Strikingly, CyPD ablation resulted in increased propensity to heart failure after transaortic constriction, overexpression of Ca^{2+} /calmodulin-dependent protein kinase II δ c and swimming exercise [37], findings that suggest a progressive Ca^{2+} overload due to decreased probability of PTP opening. That the PTP may serve as a physiological Ca^{2+} release channel is also supported by recent work in mouse primary adult neurons showing that PTP is activated in response to the combined action of more than one physiological stimulus affecting cytosolic [Ca^{2+}] and that under these conditions PTP opening does not induce neuronal death but rather takes part in physiological Ca^{2+} dynamics [38].

1.2. Role of the PTP in disease

The role of the PTP as a mediator of cell death in paradigms relevant to human health is no longer questioned. A word of caution about an *exclusive* causative role of the pore is in order about early studies based on the effects of CsA alone because (i) inhibition of calcineurin prevents mitochondrial fission by inhibiting mitochondrial translocation of Drp1, a cytoprotective event that occurs independent of PTP inhibition [39]; and (ii) CyPD displays multiple regulatory interactions in mitochondria including CsA-sensitive binding to Hsp90 and TRAP1 [40], modulation of the F_0F_1 ATP synthase [41] and binding to Bcl2 [42] (see Ref. [43] for a review). Yet a role of the PTP is generally supported by studies of *Ppif*^{-/-} mice and of their cross-breeding with several disease genotypes.

Ppif^{-/-} mice were protected from ischemia-reperfusion injury of the heart [27,29] and brain [30,44], infarct size being reduced in CyPD-null adults compared to wild-type or littermate controls. These studies do corroborate the conclusions of previous studies based on the use of CsA in ischemic isolated hearts [45] and in infarcted patients [46], in brain damage by hypoglycemia [47], hyperglycemia [48], middle cerebral artery occlusion [49,50], and traumatic injury [51,52]. *Ppif*^{-/-} mice also display resistance to development of axonopathy in autoimmune encephalomyelitis [53] and to disease progression after crossing with superoxide dismutase 1 mutant mice [54], suggesting that CyPD-dependent (and possibly PTP-dependent) mechanisms are critical in the neurodegenerative aspects of demyelinating and motor neuron diseases. Ablation of CyPD substantially improved learning, memory, and synaptic function, and alleviated decreased long-term potentiation by the amyloid β peptide in a mouse model of Alzheimer's disease [55].

Perhaps the best case involving CyPD in pathology *in vivo* is represented by collagen VI diseases [56], a set of genetically heterogeneous conditions that cause Bethlem myopathy [57], Ullrich congenital muscular dystrophy [58,59] and myosclerosis [60]. The rodent model of the disease (*Col6a1*^{-/-} mice lacking collagen VI [61]) displays mitochondrial alterations in affected muscles that could be cured with CsA [62] or with the CyP inhibitor Debio 025 [63], and *Ppif*^{-/-} *Col6a1*^{-/-} mice lacking both CyPD and collagen VI became indistinguishable from syngenic wild type mice [64], a clear indication that CyPD is involved in the development of the disease downstream of the lack of collagen VI in a process that is amplified by defective autophagy [65]. These results match those obtained in patient cultures [66] and in a pilot clinical trial with CsA [67], and in *Ppif*^{-/-} *Scgd*^{-/-} and *Ppif*^{-/-} *Lama2*^{-/-} mice modeling sarcoglycan deficiency and congenital muscular dystrophy due to lack of laminin, respectively [68].

1.3. Modulation of the PTP by specific amino acid residues

As mentioned above, the molecular nature of the PTP is not known, yet we understand in some detail how the pore is modulated by key pathophysiological effectors like voltage, matrix pH and oxidative stress through specific Cys and His residues [8,10]. The PTP is voltage-dependent in the sense that the open conformation is favored by depolarization [69] while an acidic matrix pH locks the pore in the closed conformation through reversible protonation of His residues even in depolarized mitochondria [70,71]. The voltage-dependence in turn is modulated by redox events through a dithiol-disulfide interconversion at a matrix site that can be prevented by N-ethylmaleimide (NEM) [72] or monobromobimane [73]. A second redox-sensitive site whose oxidation increases the probability of PTP opening has been identified based on the effects of the IMM-impermeant reagent copper-*o*-phenanthroline ($\text{Cu}(\text{OP})_2$) [74]. Oxidation of this site promotes PTP opening that was inhibited by dithiotreitol (DTT) and β -mercaptoethanol but not monobromobimane [74]. Conclusive evidence that this site is located on the outer surface of the IMM rather than in the OMM was recently obtained in digitonin mitoplasts, which displayed an identical inducing effect of $\text{Cu}(\text{OP})_2$ as intact mitochondria [75].

Characterization of the PTP by chemical modification of specific residues has recently been pursued by a novel approach, i.e. photoirradiation of mitochondria after treatment with porphyrins [75–78]. The results of these experiments provided remarkable information on the role and interactions of His and Cys residues in PTP modulation, as well as on their topology, and suggested an important role for the 18 kDa translocator protein (TSPO), formerly known as the peripheral benzodiazepine receptor [79]. Before covering in greater detail the picture emerging from these studies, we will illustrate the basic principles of the photodynamic effect and the mechanisms of phototoxicity and discuss the unique properties of singlet oxygen ($^1\text{O}_2$) generated by specific porphyrins in discrete mitochondrial domains.

2. The photodynamic effect

Photosensitization is a process induced by highly noxious reactive species (free radicals and reactive oxygen species, ROS) which are generated by molecules (called photosensitizers) after they have adsorbed UV/visible light of appropriate wavelengths. When oxygen is required for photosensitization to occur, the overall process is defined as “photodynamic.” Photosensitization can lead to severe cell damage or death [80]. Nearly all organisms contain potential photosensitizers (e.g., bilirubin, chlorophylls and porphyrins), but under physiological conditions the photodynamic effect does not occur because the concentration of these compounds is low or because they are sequestered in complexes that inhibit photosensitization reactions. Photosensitization from these natural substances is only observed under extreme conditions such as the porphyrias, a group of diseases that causes severe skin lesions through overproduction of porphyrins. In addition to endogenous sensitizers, a broad variety of exogenous photosensitizers (present in food, cosmetics, plants or their juices, chemicals, drugs, etc.) can enter the body through ingestion, inhalation, injection or direct contact with the skin or exposed mucosa, causing photodamage in the presence of light.

Early last century scientists realized that the harmful effects of photosensitizers could be a tool for medicine [81,82]. Since then, the photochemical approach has primarily been developed as a treatment for cancer and for ophthalmologic and dermatologic disorders [83–88]. Although the term photodynamic therapy (PDT) was only defined at the beginning of the 20th century, this form of therapy can be dated back over 3000 years. In one of India's sacred books Atharva-Veda (1400 BC) a description is found of how

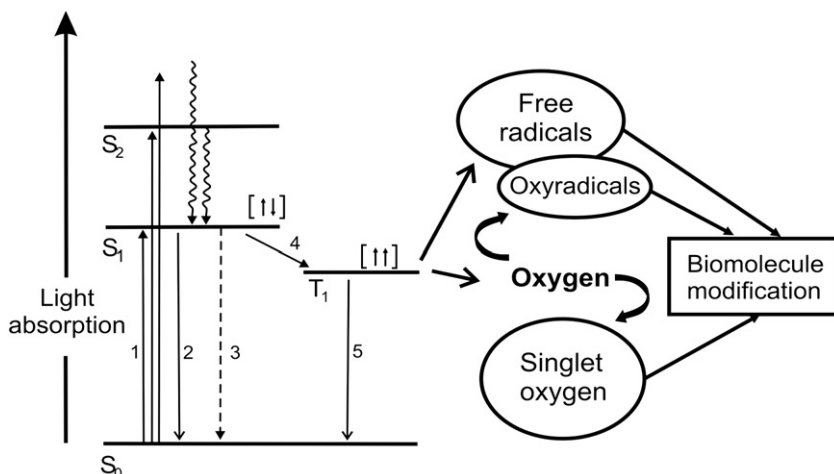


Fig. 1. Energy level diagram and photophysical and photobiological processes involving a photosensitizer. For explanation see text.

Psoralea corylifolia could be used for the treatment of vitiligo, which ancient Egyptians cured with extracts of *Ammi majus* growing on the banks of the Nile. The seeds of both plants contain psoralens, their photoactive components [81,82]. The modern history of PDT started with the observation that the combination of a chemical (acridine red) and visible light had a lethal effect on the microorganism *Infusoria*, a species of *Paramecium* [81,82]. The clinical potential of this discovery was not explored for several decades also because of the beginning of the antibiotic era. Today PDT (which inactivates many classes of pathogens) is a promising tool to overcome the problem of bacterial (multi-)drug resistance and to treat viral, fungal and parasitic infections [87,89,90].

2.1. Mechanisms of phototoxicity

The physical processes involved in sensitizer phototoxicity are illustrated in Fig. 1. The ground electronic state of the photosensitizer is a singlet state (S_0). On absorption of light of appropriate wavelength (1) the photosensitizer is excited to one of its short-lived singlet excited states, and rapid thermal relaxation leads to the lowest singlet excited state (S_1). The photosensitizer can then relax back to its ground state by fluorescence emission (2) and internal conversion (3), or can undergo intersystem crossing (4) to its lowest triplet excited state (T_1). This latter transition is spin-forbidden, but a good photosensitizer has a high probability of triplet-state formation after excitation. The T_1 -state is sufficiently long-lived to take part in chemical reactions, and therefore the photosensitizing action is mostly mediated by the T_1 -state. The T_1 -photosensitizer can also return to the S_0 -state by emitting phosphorescence (5). Activated photosensitizers in the excited triplet state can induce photochemical changes in a neighboring molecule via two competing pathways (Fig. 1). If oxygen is present in the environment, the photosensitizer can transfer its energy to form the highly reactive 1O_2 in a reaction defined as a type II mechanism [91]. The type I mechanism becomes important at low oxygen concentration or in a more polar environment. In this process the photosensitizer reacts directly with organic substrates, the solvent or another photosensitizer molecule via electron or hydrogen transfer to yield free radicals. These species are highly reactive and can easily interact with molecular oxygen to generate intermediates such as the superoxide anion ($O_2^- \cdot$), which can convert to H_2O_2 , the immediate precursor of the hydroxyl radical, the most dangerous member of the ROS family [91–93]. Both type I and type II reactions cause oxidation of cellular biomolecules. Frequently they occur simultaneously, and the ratio depends on

several parameters, the type of photosensitizer and the oxygen concentration being the most important [91,93]. For most photosensitizers employed in PDT, the type II photochemical reaction is the dominant process [94,95].

2.2. Singlet oxygen

In contrast to the vast majority of molecules, molecular oxygen in its ground state has an electronic triplet configuration with two unpaired electrons occupying two degenerate π antibonding orbitals (Fig. 2). In the two forms of excited singlet states ($^1\Sigma_g^+O_2$ and $^1\Delta_gO_2$) these electrons have opposite spin. The $^1\Delta_gO_2$ form (noted for simplicity as 1O_2) is involved in photosensitization, while $^1\Sigma_g^+O_2$ is too short-lived (10^{-11} – 10^{-9} s in solution) to be biologically relevant [93,96]. Electrophilic 1O_2 is seeking electrons to fill its vacant molecular orbital, and it thus reacts readily with electron-rich molecules. Targets for oxidation are lipids (cholesterol and phospholipids), amino acids (Trp, Tyr, His) and nucleic acid bases (guanine and guanosine) that have double bonds, as well as sulfur-containing amino acids (Cys, Met) [95,96]. In biological systems proteins are the main intracellular targets for 1O_2 owing to their abundance and fast rates of reaction, which are two orders of magnitude faster than those displayed with unsaturated lipids [97,98]. The reaction of 1O_2 with proteins can result in multiple effects including oxidation of side-chains, backbone fragmentation, dimerization/aggregation, unfolding

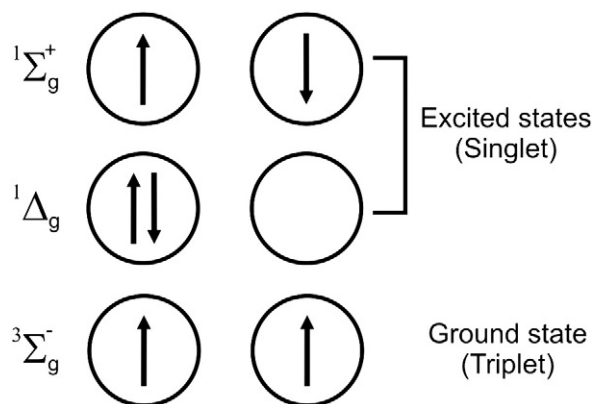


Fig. 2. Simplified representation of the electronic configurations of molecular oxygen lowest triplet and singlet states. The scheme depicts only π antibonding orbitals, for further explanation see text.

or other conformational changes, enzymatic inactivation, and alterations in cellular handling and turnover [97].

$^1\text{O}_2$ has unique features compared to other ROS. Being an electronically excited state it is generally produced when exogenous or endogenous photosensitizers absorb the appropriate wavelength of visible or UV-radiation; in contrast, other ROS such as H_2O_2 and O_2^- are produced in cells during normal physiological processes or are formed by activated neutrophils and macrophages. These “physiological” ROS can readily interconvert, making it difficult to discern which ROS is responsible for a particular cellular response, while $^1\text{O}_2$ does not interconvert to other ROS. Finally, the lifetime of $^1\text{O}_2$ has an inherent upper value (i.e. how long $^1\text{O}_2$ exists in the absence of reactive molecules) which poses an upper limit to its mobility from the site of generation. Based on the $^1\text{O}_2$ lifetime of $\sim 4\ \mu\text{s}$ a maximal diffusion radius of a mere $\sim 220\ \text{nm}$ in water has been calculated [98]. After this period of time $^1\text{O}_2$ returns to the ground state and loses reactivity by transferring its energy to the solvent. In contrast, other cellular ROS retain their activity until they hit a target or are destroyed by enzymes [98].

The lifetime of $^1\text{O}_2$ in homogeneous solutions is between 10^{-6} and $10^{-3}\ \text{s}$ [99]. This value is considerably shorter in cellular systems, ranging from 100 ns in the lipid regions of membranes to 250 ns in the cytoplasm. The shorter intracellular lifetime of $^1\text{O}_2$ indicates efficient quenching of this species by reaction with susceptible intracellular targets (for a review see Ref. [93]). Due to the abundance of these reactive molecules, the diffusion distance of $^1\text{O}_2$ in cells and tissues has been estimated to be in the order of $0.01\text{--}0.02\ \mu\text{m}$ [100–102]. Given a cell diameter of $10\text{--}30\ \mu\text{m}$, it can be reasonably assumed that the primary site of photodamage is also the site where $^1\text{O}_2$ has been generated. Thus, the intracellular localization of the photosensitizer is the major determinant in dictating which subcellular structures will be reached and attacked. Generally, mitochondrial photosensitizers are able to induce apoptosis very rapidly, lysosomal photosensitizers can elicit either a necrotic or an apoptotic response, and plasma membrane photosensitizers can lead to cell rescue or initiate apoptosis and/or necrosis (for a review, see Ref. [103]).

2.3. Porphyrins as photosensitizers

Porphyrins were identified in the mid-19th century, but it was not until the early 20th century that they were used in Medicine. Between 1908 and 1913 a number of photobiological experiments were carried out with hematoporphyrin (HP), demonstrating how it sensitized paramecia, erythrocytes, mice, and guinea pigs to light [81,82]. The pioneering report of human photosensitization by porphyrins was published in 1913 by Friedrich Meyer-Betz, who injected himself with 200 mg of HP and reported swelling and prolonged pain in light-exposed areas [82,104]. The subsequent discovery of the tumor-localizing properties of porphyrins and of the phototoxic effects on tumor tissues led to the development of modern clinical PDT [105–110].

The “photoactive core” of porphyrin-based compounds is the tetrapyrrolic macrocycle (porphine), while peripheral substituents control drug biodistribution and pharmacokinetics. Tetrapyrroles are naturally occurring pigments and vital constituents of oxidation–reduction and oxygen transport-related proteins such as hemoglobins, cytochromes, apoferritin, catalase, ferrichrome and peroxidases. Within these proteins tetrapyrroles are not able to induce photochemical reactions due to the presence of metal ions (Fe^{3+} , Al^{3+} , Mg^{2+}) which increase the probability of non-radiative decay of the triplet state. Indeed, the most efficient porphyrin-based photosensitizers (free base porphyrins) lack coordinated metal ions.

In the monomeric state free base porphyrins are potent photosensitizers with long lifetimes and high quantum yields of triplet

formation ($\Phi_T \sim 0.7\text{--}0.9$) while aggregation decreases the probability of photoexcitation. Because of the low energy gap between the triplet states of tetrapyrroles and molecular oxygen, a large fraction of triplets ($0.7\text{--}1.0$) leads to $^1\text{O}_2$ generation by energy transfer. Thus, $^1\text{O}_2$ is the predominant phototoxic species involved in porphyrin-photosensitized processes with a quantum yield of $^1\text{O}_2$ production (Φ_Δ) between about 0.7 and 0.9 for carboxylic porphyrins [111]. Alternative pathways for oxygen activation by photoexcited porphyrins (e.g. generation of O_2^- by electron transfer) usually have an efficiency lower than 0.1 [112].

Under the same experimental conditions, monomeric porphyrins exhibit quite similar photophysical properties and photosensitizing efficiency, independent of their chemical structure and the nature of the surrounding environment [111,113]. In particular, the yield of $^1\text{O}_2$ is similar for monomeric porphyrins with various degrees of hydrophobicity [111]. In spite of their similar basic structure and photophysical characteristics, however, porphyrins in cells display a wide range of activities even when they target the same organelle; and small differences (e.g. of peripheral substituents) result in different physicochemical properties that modulate the affinity for binding sites dictating uptake, subcellular distribution and therefore the final target of the photoprocess [111,114]. For these reasons a clever use of porphyrins can yield a wealth of information on biological processes.

2.4. Mitochondria as targets of porphyrin photodynamic activity

Studies with porphyrin-loaded cells indicate that hydrophobic porphyrins tend to concentrate in mitochondria, especially after prolonged incubation [115]. Mitochondrial damage is a major determinant of porphyrin phototoxicity [116–118] to which cells with few mitochondria are refractory [119]. Several mitochondrial components are affected by photoirradiation [115,116,119–121]. Light- and dose-dependence studies using dicarboxylic porphyrins (mainly HP) indicate that ATP synthesis is the first function to be lost because the F_0F_1 ATP synthase [115] and the adenine nucleotide translocator (ANT) [120] are the most vulnerable $^1\text{O}_2$ targets whereas respiration, Ca^{2+} uptake, OMM, matrix and intermembrane enzyme activities are more resistant in this order.

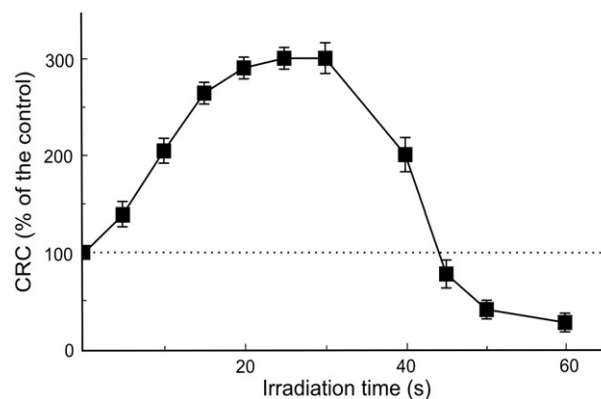


Fig. 3. Effect of increasing irradiation times on the Ca^{2+} retention capacity of HP-loaded mouse liver mitochondria. CD1 mouse liver mitochondria (0.5 mg/ml) were incubated for 2 min at $25\ ^\circ\text{C}$ in a medium containing 250 mM sucrose, 10 mM Tris–Mops pH 7.4, 5 mM succinate–Tris, 1 mM P_i –Tris, 10 μM EGTA–Tris, 3 μM HP, 2 μM rotenone, 0.5 $\mu\text{g}/\text{ml}$ oligomycin, 0.5 μM Calcium Green-5N. After irradiation for the indicated periods of time at a fluence rate of $40\ \text{W}/\text{m}^2$, mitochondria were loaded with a series of 10 μM Ca^{2+} pulses at 1 min intervals. PTP opening was determined as the Ca^{2+} retention capacity (CRC, expressed as the % of the CRC of non-irradiated organelles) measured at excitation 480 nm and emission 530 nm. The CRC decrease at high doses of light was prevented by 1 μM CSA (data not shown, see also Ref. [75]). Error bars refer to the mean \pm S.D. of four experiments.

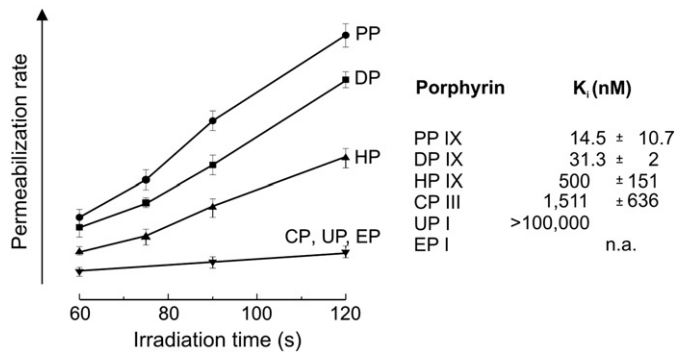


Fig. 4. Effect of PP-like (DP, HP, PP) and PP-unrelated (CP, EP, UP) porphyrins on light-dependent activation of the permeability transition. Wistar rat liver mitochondria (0.5 mg/ml) were incubated for 2 min at 25 °C in a medium containing 250 mM sucrose, 10 mM Tris–Mops, 5 mM succinate, 1 mM P_i -Tris, 10 μ M EGTA–Tris, 0.5 μ g/ml oligomycin, 2 μ M rotenone, pH 7.4 plus concentrations of each porphyrin giving a loading of 1.2 nmol of porphyrin/mg of protein (see also Ref. [75]). Preparations were then supplemented with 5 μ M Ca^{2+} (a concentration not sufficient to induce PTP opening per se) and irradiated for the indicated times at a fluence rate of 40 W/m². The PT was followed as the change in 90° light scattering at 540 nm. Error bars represent the mean \pm S.D. of three experiments. K_d values for porphyrins were taken from Ref. [123].

In 1992 Verma et al. [122] observed that the potencies of porphyrins at catalyzing cellular photodamage correlated closely with their affinities for the TSPO. Among a wide variety of porphyrins and porphyrin-like compounds the most photoactive were dicarboxylic porphyrins endowed with PP-like configuration such as PP itself,

mesoporphyrin IX, deuteroporphyrin (DP) and HP, which bind TSPO with nanomolar affinities [123]. Such selectivity for PP-like porphyrins has been ascribed to the major physiological role of TSPO to mediate mitochondrial uptake of naturally occurring dicarboxylic porphyrins such as PP, other heme precursors as well as heme itself [123,124]. TSPO is an 18 kDa OMM protein that may be located at junctional sites with the IMM [124–126]. Such a localization could influence substrate transfer between cytosolic and mitochondrial compartments, and porphyrins with the highest affinity for TSPO would be expected to accumulate best. The notion of TSPO mediating porphyrin phototoxicity was confirmed by our recent results in mitoplasts [75] while it has been challenged by other authors [127]. A key role of TSPO in controlling mitochondrial internalization and photoactivity of porphyrins is supported by the finding that high-affinity ligands of TSPO (such as 1-(2-chlorophenyl)-N-methyl-N-(1-methyl-propyl)-3-isoquinolinecarboxamide, PK11195, and 7-chloro-5-(4-chlorophenyl)-1,3-dihydro-1-methyl-2H-1,4-benzodiazepin-2-one, Ro5-4864) as well as cholesterol, prevent porphyrin-induced phototoxicity [128–131] probably by inhibiting translocation of porphyrins into mitochondria [129,131] (see also the following paragraphs).

3. Light on the PTP

In 1997 Salet et al. [76] and later Moreno et al. [77] exploited the photodynamic effect to study the PT. This approach provided detailed information on critical residues regulating the PT and helped to understand the role of IMM and OMM in PTP modulation [75–78]. The first observation was that a short photoirradiation of mitochondria

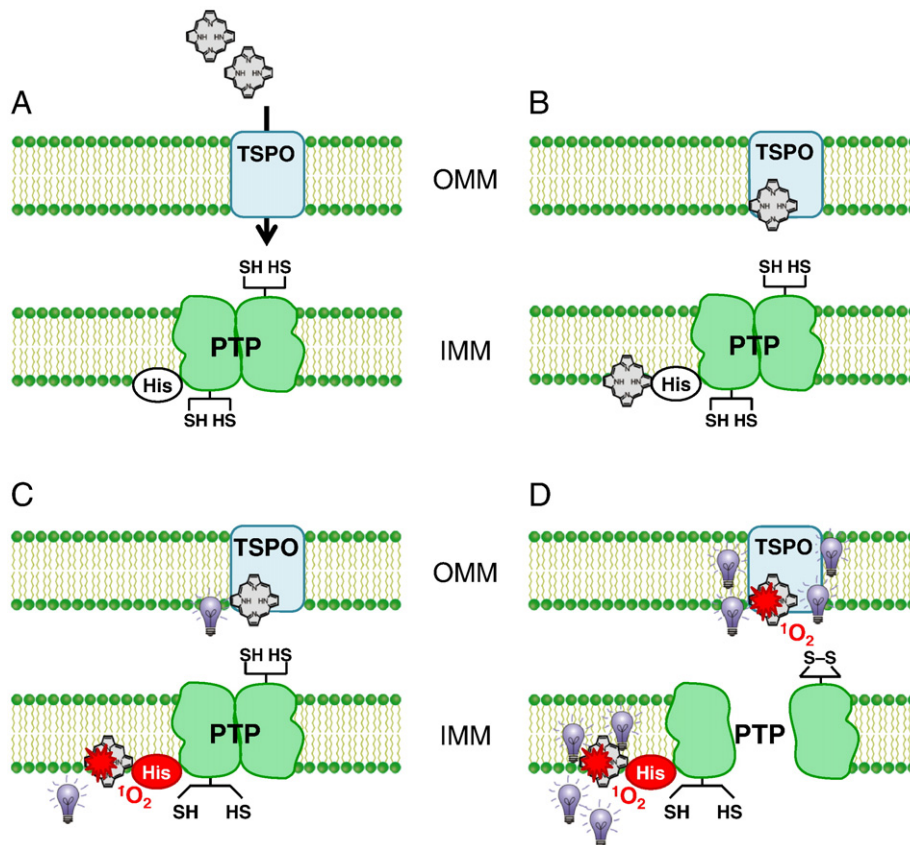


Fig. 5. Photodynamic events mediated by porphyrins at PTP-regulating His and Cys residues. (A) Porphyrins with PP-like configuration are transported inside mitochondria through TSPO. (B) Matrix-facing IMM porphyrin-binding sites are located in close proximity to critical His residues, and additional binding sites are adjacent to external thiols in close proximity to TSPO. In the dark, HP does not affect the structural properties of His- and Cys-containing domains, and PTP can open through selective oxidation of internal or external Cys when PhAsO or Cu(OP)₂ are added (omitted for clarity from the scheme, but see Refs. [75,78]). (C) After mitochondrial irradiation with moderate light doses, photoactivated HP generates ¹O₂ in the proximity of critical His residues which undergo modification and cause a structural rearrangement of the internal dithiol which can no longer undergo oxidation, thus resulting in PTP inhibition. (D) Irradiation with high light doses causes TSPO-dependent photoactivation of porphyrins in the OMM leading to oxidation of IMM surface thiols by ¹O₂, resulting in PTP opening. For further explanation see text.

loaded with HP caused inactivation of the ANT, yet mitochondria retained their ability to form a proton electrochemical gradient, and accumulated Ca^{2+} and Pi at the same rate as non-irradiated mitochondria. Strikingly, the oxidative effects of photodynamic action prevented opening of the PTP, which is normally induced by Ca^{2+} plus Pi, in the first example of pore inactivation by an oxidant [76], which is at variance with what is generally observed under oxidizing conditions [132–135]. The inactivating effect could be traced to photomodification of matrix His residues (the direct target of $^1\text{O}_2$) by vicinal porphyrin; this in turn lowered the reactivity of critical dithiols whose oxidation (e.g. by diamide) causes opening of the PTP [72]. Irradiation of HP-loaded mitochondria thus represents an example of site-selective inactivation of discrete pore functional domains comprising critical His and Cys residues in close structural and functional correlation [76].

The next finding was that irradiation with higher light doses caused instead opening of the PTP, which was attributed to photooxidation of IMM external thiols [75,78]. The effect of light dose on the Ca^{2+} retention capacity (CRC) of mouse liver mitochondria (a sensitive measure of the propensity of the PTP to open) is illustrated in Fig. 3. The initial increase of CRC (i.e. pore desensitization) was offset by a sharp decrease as the irradiation time increased. Since at high light dose the previously identified His and Cys residues have already been inactivated by matrix porphyrin, reactivation must depend on a different porphyrin site, which is specifically contributed by the OMM through TSPO [75]. The properties of this site are illustrated in the experiments of Fig. 4, where irradiation times of more than 60 s were applied to rat liver mitochondria preincubated with concentrations of PP, DP, HP, coproporphyrin III (CP), uroporphyrin I (UP) and etioporphyrin (EP) yielding an identical loading of 1.2 nmol of porphyrin \times mg^{-1} of protein. The relative potency of PP-related porphyrins at sensitizing the PTP (measured here as the rate of mitochondrial permeabilization to sucrose) matched their affinity for TSPO, as based on the Ki displayed by each porphyrin for inhibition of binding of PK11195, a classical ligand of TSPO (see also Ref. [136]). The process of PTP activation was specific to porphyrins characterized by a PP-like configuration that bind TSPO with nanomolar affinity (PP, DP and HP), whereas PP-unrelated porphyrins such as tetracarboxylic CP, octacarboxylic UP and EP, which lacks carboxylic groups, were ineffective (Fig. 4 and Ref. [75]). It is also remarkable that porphyrin-mediated PTP photoactivation is suppressed (results not shown) by low concentrations of the high-affinity, porphyrin-competitive TSPO ligand FG1N1-27 [136].

The regulatory role of the OMM and TSPO on the PTP was confirmed by a study of mitoplasts prepared with digitonin concentrations that allowed selective removal of the OMM without interfering with mitochondrial energy-linked functions [75]. Like mitochondria, mitoplasts readily underwent PTP opening following Ca^{2+} uptake in a CsA-sensitive process, but major differences emerged in PTP regulation by ligands of TSPO. In mitoplasts the PTP could not be activated by photooxidation after treatment with dicarboxylic porphyrins endowed with PP configuration, and mitoplasts became resistant to the PTP-inducing effects of selective ligands of TSPO [75].

4. Summary and conclusions

In photosensitization of biological materials by $^1\text{O}_2$ the photo-damage is strictly limited to the immediate surroundings of the sensitizer because of the short diffusion distance and high reactivity of the photogenerated species. This peculiar oxidation mechanism provided novel information on residues regulating the PTP. Studies with this approach, whose results are summarized in Fig. 5, allowed to characterize the PTP-modulating properties of sites which exhibit different sensitivity towards oxidation by photoactivated porphyrins. Under basal conditions (Fig. 5A) the PTP favors the closed conforma-

tion. Porphyrins transported through TSPO are transferred to matrix, IMM and OMM sites, but in the absence of photoirradiation they do not affect the reactivity and pore-modulating properties of internal (matrix-exposed) and external cysteines located on the outer surface of the IMM [75] (Fig. 5B). Photoirradiation for short periods of time hits the most vulnerable site, which comprises matrix-exposed His and causes a secondary drop of reactivity of internal Cys, thus stabilizing the PTP in the closed conformation (Fig. 5C). Inactivation of internal Cys by His photodegradation allowed to establish the role of (i) external regulatory Cys, which can still undergo oxidation and thus increase the probability of PTP opening and (ii) of TSPO, which is essential for reactivation of the PTP by high light doses, an effect mediated in part at least by oxidation of regulatory thiols on the outer surface of the IMM (Fig. 5D).

TSPO thus fulfills a dual role in PTP modulation (i) as a *transport protein* for PTP-active compounds that are transferred to their PTP regulatory site(s) in the IMM or in the matrix and (ii) as a *PTP regulatory protein* when it binds its selective ligands like porphyrins. TSPO belongs to a family of ubiquitous proteins conserved from bacteria to mammals that bind small drugs, cholesterol, and porphyrins [79]. Consistent with its role in steroid hormone synthesis, in mammals TSPO is highly expressed in the adrenal cortex [137,138], and its inactivation induces an early embryonic-lethal phenotype in the mouse [139]. Establishing a role for TSPO in PTP modulation, which was also made possible by the unique features of the photodynamic effect, holds great promise for our continuing studies on the nature of the PTP, and on the development of drugs that can modulate its probability of opening.

Acknowledgements

This manuscript is in partial fulfillment of the requirements for the PhD of JS, who was supported by a Fellowship from the Fondazione Cariparo, Padova. The work was supported in part by grants from the Ministry for University and Research (MIUR/PRIN) and Fondazione Cariparo Progetti di Eccellenza "Models of Mitochondrial Diseases".

References

- [1] D.R. Hunter, R.A. Haworth, J.H. Southard, Relationship between configuration, function, and permeability in calcium-treated mitochondria, *J. Biol. Chem.* 251 (1976) 5069–5077.
- [2] D.R. Hunter, R.A. Haworth, The Ca^{2+} -induced membrane transition in mitochondria. I. The protective mechanisms, *Arch. Biochem. Biophys.* 195 (1979) 453–459.
- [3] R.A. Haworth, D.R. Hunter, The Ca^{2+} -induced membrane transition of rat liver mitochondria. II. Nature of the Ca^{2+} trigger site, *Arch. Biochem. Biophys.* 195 (1979) 460–467.
- [4] D.R. Hunter, R.A. Haworth, The Ca^{2+} -induced membrane transition in mitochondria. III. Transitional Ca^{2+} release, *Arch. Biochem. Biophys.* 195 (1979) 468–477.
- [5] S. Massari, G.F. Azzone, The equivalent pore radius of intact and damaged mitochondria and the mechanism of active shrinkage, *Biochim. Biophys. Acta* 283 (1972) 23–29.
- [6] T.E. Gunter, D.R. Pfeiffer, Mechanisms by which mitochondria transport calcium, *Am. J. Physiol.* 258 (1990) C755–C786.
- [7] J.J. Lemasters, A.L. Nieminen, T. Qian, L. Trost, S.P. Elmore, Y. Nishimura, R.A. Crowe, W.E. Cascio, C.A. Bradham, D.A. Brenner, B. Herman, The mitochondrial permeability transition in cell death: a common mechanism in necrosis, apoptosis and autophagy, *Biochim. Biophys. Acta* 1366 (1998) 177–196.
- [8] P. Bernardi, Mitochondrial transport of cations: channels, exchangers and permeability transition, *Physiol. Rev.* 79 (1999) 1127–1155.
- [9] M. Crompton, The mitochondrial permeability transition pore and its role in cell death, *Biochem. J.* 341 (1999) 233–249.
- [10] P. Bernardi, A. Krauskopf, E. Basso, V. Petronilli, E. Blachly-Dyson, F. Di Lisa, M.A. Forte, The mitochondrial permeability transition from in vitro artifact to disease target, *FEBS J.* 273 (2006) 2077–2099.
- [11] A. Rasola, P. Bernardi, The mitochondrial permeability transition pore and its involvement in cell death and in disease pathogenesis, *Apoptosis* 12 (2007) 815–833.
- [12] A.W. Leung, A.P. Halestrap, Recent progress in elucidating the molecular mechanism of the mitochondrial permeability transition pore, *Biochim. Biophys. Acta* 1777 (2008) 946–952.
- [13] C.P. Baines, The molecular composition of the mitochondrial permeability transition pore, *J. Mol. Cell. Cardiol.* 46 (2009) 850–857.

- [14] D.B. Zorov, M. Juhaszova, Y. Yaniv, H.B. Nuss, S. Wang, S.J. Sollott, Regulation and pharmacology of the mitochondrial permeability transition pore, *Cardiovasc. Res.* 83 (2009) 213–225.
- [15] A. Rasola, M. Sciacovelli, B. Pantic, P. Bernardi, Signal transduction to the permeability transition pore, *FEBS Lett.* 584 (2010) 1989–1996.
- [16] J.E. Kokoszka, K.G. Waymire, S.E. Levy, J.E. Sligh, J. Cai, D.P. Jones, G.R. MacGregor, D.C. Wallace, The ADP/ATP translocator is not essential for the mitochondrial permeability transition pore, *Nature* 427 (2004) 461–465.
- [17] A. Krauskopf, O. Eriksson, W.J. Craigen, M.A. Forte, P. Bernardi, Properties of the permeability transition in VDAC1^{-/-} mitochondria, *Biochim. Biophys. Acta Bioenerg.* 1757 (2006) 590–595.
- [18] C.P. Baines, R.A. Kaiser, T. Sheiko, W.J. Craigen, J.D. Molkentin, Voltage-dependent anion channels are dispensable for mitochondrial-dependent cell death, *Nat. Cell Biol.* 9 (2007) 550–555.
- [19] N. Fournier, G. Ducet, A. Crevat, Action of cyclosporine on mitochondrial calcium fluxes, *J. Bioenerg. Biomembr.* 19 (1987) 297–303.
- [20] M. Crompton, H. Ellinger, A. Costi, Inhibition by cyclosporin A of a Ca²⁺-dependent pore in heart mitochondria activated by inorganic phosphate and oxidative stress, *Biochem. J.* 255 (1988) 357–360.
- [21] K.M. Broekemeier, M.E. Dempsey, D.R. Pfeiffer, Cyclosporin A is a potent inhibitor of the inner membrane permeability transition in liver mitochondria, *J. Biol. Chem.* 264 (1989) 7826–7830.
- [22] A.P. Halestrap, A.M. Davidson, Inhibition of Ca²⁺-induced large-amplitude swelling of liver and heart mitochondria by cyclosporin is probably caused by the inhibitor binding to mitochondrial-matrix peptidyl-prolyl cis-trans isomerase and preventing it interacting with the adenine nucleotide translocase, *Biochem. J.* 268 (1990) 153–160.
- [23] C.P. Connern, A.P. Halestrap, Purification and N-terminal sequencing of peptidyl-prolyl cis-trans-isomerase from rat liver mitochondrial matrix reveals the existence of a distinct mitochondrial cyclophilin, *Biochem. J.* 284 (1992) 381–385.
- [24] A. Nicoli, E. Basso, V. Petronilli, R.M. Wenger, P. Bernardi, Interactions of cyclophilin with the mitochondrial inner membrane and regulation of the permeability transition pore, a cyclosporin A-sensitive channel, *J. Biol. Chem.* 271 (1996) 2185–2192.
- [25] K.Y. Woodfield, N.T. Price, A.P. Halestrap, cDNA cloning of rat mitochondrial cyclophilin, *Biochim. Biophys. Acta* 1351 (1997) 27–30.
- [26] A.W. Leung, P. Varanyuwatana, A.P. Halestrap, The mitochondrial phosphate carrier interacts with cyclophilin D and may play a key role in the permeability transition, *J. Biol. Chem.* 283 (2008) 26312–26323.
- [27] C.P. Baines, R.A. Kaiser, N.H. Purcell, N.S. Blair, H. Osinska, M.A. Hambleton, E.W. Brunskill, M.R. Sayen, R.A. Gottlieb, G.W. Dorn, J. Robbins, J.D. Molkentin, Loss of cyclophilin D reveals a critical role for mitochondrial permeability transition in cell death, *Nature* 434 (2005) 658–662.
- [28] E. Basso, L. Fante, J. Fowlkes, V. Petronilli, M.A. Forte, P. Bernardi, Properties of the permeability transition pore in mitochondria devoid of Cyclophilin D, *J. Biol. Chem.* 280 (2005) 18558–18561.
- [29] T. Nakagawa, S. Shimizu, T. Watanabe, O. Yamaguchi, K. Otsu, H. Yamagata, H. Inohara, T. Kubo, Y. Tsujimoto, Cyclophilin D-dependent mitochondrial permeability transition regulates some necrotic but not apoptotic cell death, *Nature* 434 (2005) 652–658.
- [30] A.C. Schinzel, O. Takeuchi, Z. Huang, J.K. Fisher, Z. Zhou, J. Rubens, C. Hetz, N.N. Danial, M.A. Moskowitz, S.J. Korsmeyer, Cyclophilin D is a component of mitochondrial permeability transition and mediates neuronal cell death after focal cerebral ischemia, *Proc. Natl Acad. Sci. USA* 102 (2005) 12005–12010.
- [31] E. Basso, V. Petronilli, M.A. Forte, P. Bernardi, Phosphate is essential for inhibition of the mitochondrial permeability transition pore by cyclosporin A and by cyclophilin D ablation, *J. Biol. Chem.* 283 (2008) 26307–26311.
- [32] L. Azzolin, S. von Stockum, E. Basso, V. Petronilli, M.A. Forte, P. Bernardi, The mitochondrial permeability transition from yeast to mammals, *FEBS Lett.* 584 (2010) 2504–2509.
- [33] J. Hüser, L.A. Blatter, Fluctuations in mitochondrial membrane potential caused by repetitive gating of the permeability transition pore, *Biochem. J.* 343 (Pt 2) (1999) 311–317.
- [34] V. Petronilli, G. Miotto, M. Canton, M. Brini, R. Colonna, P. Bernardi, F. Di Lisa, Transient and long-lasting openings of the mitochondrial permeability transition pore can be monitored directly in intact cells by changes in mitochondrial calcein fluorescence, *Biophys. J.* 76 (1999) 725–734.
- [35] P. Bernardi, V. Petronilli, The permeability transition pore as a mitochondrial calcium release channel: a critical appraisal, *J. Bioenerg. Biomembr.* 28 (1996) 131–138.
- [36] R.A. Altschuld, C.M. Hohl, L.C. Castillo, A.A. Garleb, R.C. Starling, G.P. Brierley, Cyclosporin inhibits mitochondrial calcium efflux in isolated adult rat ventricular cardiomyocytes, *Am. J. Physiol.* 262 (1992) H1699–H1704.
- [37] J.W. Elrod, R. Wong, S. Mishra, R.J. Vagnozzi, B. Sakthivel, S.A. Goonasekera, J. Karch, S. Gabel, J. Farber, T. Force, J.H. Brown, E. Murphy, J.D. Molkentin, Cyclophilin D controls mitochondrial pore-dependent Ca²⁺ exchange, metabolic flexibility, and propensity for heart failure in mice, *J. Clin. Invest.* 120 (2010) 3680–3687.
- [38] A. Barsukova, A. Komarov, G. Hajnóczky, P. Bernardi, D. Bourdette, M. Forte, Activation of the mitochondrial permeability transition pore modulates Ca²⁺ responses to physiological stimuli in adult neurons, *Eur. J. Neurosci.* 33 (2011) 831–842.
- [39] G.M. Cereghetti, A. Stangherlin, O. Martins de Brito, C.R. Chang, C. Blackstone, P. Bernardi, L. Scorrano, Dephosphorylation by calcineurin regulates translocation of Drp1 to mitochondria, *Proc. Natl Acad. Sci. USA* 105 (2008) 15803–15808.
- [40] B.H. Kang, J. Plescia, T. Dohi, J. Rosa, S.J. Duxsey, D.C. Altieri, Regulation of tumor cell mitochondrial homeostasis by an organelle-specific Hsp90 chaperone network, *Cell* 131 (2007) 257–270.
- [41] V. Giorgio, E. Bisetto, M.E. Soriano, F. Dabbeni-Sala, E. Basso, V. Petronilli, M.A. Forte, P. Bernardi, G. Lippe, Cyclophilin D modulates mitochondrial FOF1-ATP synthase by interacting with the lateral stalk of the complex, *J. Biol. Chem.* 284 (2009) 33982–33988.
- [42] R.A. Eliseev, J. Malecki, T. Lester, Y. Zhang, J. Humphrey, T.E. Gunter, Cyclophilin D interacts with Bcl2 and exerts an anti-apoptotic effect, *J. Biol. Chem.* 284 (2009) 9692–9699.
- [43] V. Giorgio, M.E. Soriano, E. Basso, E. Bisetto, G. Lippe, M.A. Forte, P. Bernardi, Cyclophilin D in mitochondrial pathophysiology, *Biochim. Biophys. Acta* 1797 (2010) 1113–1118.
- [44] X. Wang, Y. Carlsson, E. Basso, C. Zhu, C.I. Rousset, A. Rasola, B.R. Johansson, K. Blomgren, C. Mallard, P. Bernardi, M.A. Forte, H. Hagberg, Developmental shift of cyclophilin D contribution to hypoxic-ischemic brain injury, *J. Neurosci.* 29 (2009) 2588–2596.
- [45] E.J. Griffiths, A.P. Halestrap, Protection by Cyclosporin A of ischemia/reperfusion-induced damage in isolated rat hearts, *J. Mol. Cell. Cardiol.* 25 (1993) 1461–1469.
- [46] C. Piot, P. Croisille, P. Staat, H. Thibault, G. Rioufol, N. Mewton, R. Elbelghiti, T.T. Cung, E. Bonnefoy, D. Angoulvant, C. Macia, F. Racza, C. Sportouch, G. Gahide, G. Finet, X. André-Fouët, D. Revel, G. Kirkorian, J.-P. Monassier, G. Derumeaux, M. Ovize, Effect of cyclosporine on reperfusion injury in acute myocardial infarction, *New Engl. J. Med.* 359 (2008) 473–481.
- [47] H. Friberg, M. Ferrand-Drake, F. Bengtsson, A.P. Halestrap, T. Wieloch, Cyclosporin A, but not FK 506, protects mitochondria and neurons against hypoglycemic damage and implicates the mitochondrial permeability transition in cell death, *J. Neurosci.* 18 (1998) 5151–5159.
- [48] J. Folbergrova, P.A. Li, H. Uchino, M.L. Smith, B.K. Siesjo, Changes in the bioenergetic state of rat hippocampus during 2.5 min of ischemia, and prevention of cell damage by cyclosporin A in hyperglycemic subjects, *Exp. Brain Res.* 114 (1997) 44–50.
- [49] H. Uchino, E. Elmer, K. Uchino, P.A. Li, Q.P. He, M.L. Smith, B.K. Siesjo, Amelioration by cyclosporin A of brain damage in transient forebrain ischemia in the rat, *Brain Res.* 812 (1998) 216–226.
- [50] S. Matsumoto, H. Friberg, M. Ferrand-Drake, T. Wieloch, Blockade of the mitochondrial permeability transition pore diminishes infarct size in the rat after transient middle cerebral artery occlusion, *J. Cereb. Blood Flow Metab.* 19 (1999) 736–741.
- [51] D.O. Okonkwo, J.T. Povlishock, An intrathecal bolus of cyclosporin A before injury preserves mitochondrial integrity and attenuates axonal disruption in traumatic brain injury, *J. Cereb. Blood Flow Metab.* 19 (1999) 443–451.
- [52] S.W. Scheff, P.G. Sullivan, Cyclosporin A significantly ameliorates cortical damage following experimental traumatic brain injury in rodents, *J. Neurotrauma* 16 (1999) 783–792.
- [53] M. Forte, B.G. Gold, G. Marracci, P. Chaudhary, E. Basso, D. Johnsen, X. Yu, J. Fowlkes, M. Rahder, K. Stem, P. Bernardi, D. Bourdette, Cyclophilin D inactivation protects axons in experimental autoimmune encephalomyelitis, an animal model of multiple sclerosis, *Proc. Natl Acad. Sci. USA* 104 (2007) 7558–7563.
- [54] L.J. Martin, B. Gertz, Y. Pan, A.C. Price, J.D. Molkentin, Q. Chang, The mitochondrial permeability transition pore in motor neurons: involvement in the pathobiology of ALS mice, *Exp. Neurol.* 218 (2009) 333–346.
- [55] H. Du, L. Guo, F. Fang, D. Chen, A.A. Sosunov, G.M. McKhann, Y. Yan, C. Wang, H. Zhang, J.D. Molkentin, F.J. Gunn-Moore, J.P. Vonsattel, O. Arancio, J.X. Chen, S.D. Yan, Cyclophilin D deficiency attenuates mitochondrial and neuronal perturbation and ameliorates learning and memory in Alzheimer's disease, *Nat. Med.* 14 (2008) 1097–1105.
- [56] A.K. Lampe, K.M. Bushby, Collagen VI related muscle disorders, *J. Med. Genet.* 42 (2005) 673–685.
- [57] G.J. Jöbbs, H. Keizers, J.P. Vreijling, M. de Visser, M.C. Speer, R.A. Wolterman, F. Baas, P.A. Bolhuis, Type VI collagen mutations in Bethlem myopathy, an autosomal dominant myopathy with contractures, *Nat. Genet.* 14 (1996) 113–115.
- [58] O. Ullrich, Kongenitale, atonisch-sklerotische Muskeldystrophie, ein weiterer Typus der hereditären Erkrankungen des neuromuskulären Systems, *Z. Ges. Neurol. Psychiatr.* 126 (1930) 171–201.
- [59] O. Camacho Vanegas, E. Bertini, R.Z. Zhang, S. Petrini, C. Minosse, P. Sabatelli, B. Giusti, M.L. Chu, G. Pepe, Ullrich scleroatonic muscular dystrophy is caused by recessive mutations in collagen type VI, *Proc. Natl Acad. Sci. USA* 98 (2001) 7516–7521.
- [60] L. Merlini, E. Martoni, P. Grumati, P. Sabatelli, S. Squarzoni, A. Urciuolo, A. Ferlini, F. Gualandi, P. Bonaldo, Autosomal recessive myosclerosis myopathy is a collagen VI disorder, *Neurology* 71 (2008) 1245–1253.
- [61] P. Bonaldo, P. Braghetta, M. Zanetti, S. Piccolo, D. Volpin, G.M. Bressan, Collagen VI deficiency induces early onset myopathy in the mouse: an animal model for Bethlem myopathy, *Hum. Mol. Genet.* 7 (1998) 2135–2140.
- [62] W.A. Irwin, N. Bergamin, P. Sabatelli, C. Reggiani, A. Megighian, L. Merlini, P. Braghetta, M. Columbaro, D. Volpin, G.M. Bressan, P. Bernardi, P. Bonaldo, Mitochondrial dysfunction and apoptosis in myopathic mice with collagen VI deficiency, *Nat. Genet.* 35 (2003) 267–271.
- [63] T. Tiepolo, A. Angelin, E. Palma, P. Sabatelli, L. Merlini, L. Nicolosi, F. Finetti, P. Braghetta, G. Vuagniaux, J.M. Dumont, C.T. Baldari, P. Bonaldo, P. Bernardi, The cyclophilin inhibitor Debio 025 normalizes mitochondrial function, muscle apoptosis and ultrastructural defects in *Col6a1*^{-/-} myopathic mice, *Br. J. Pharmacol.* 157 (2009) 1045–1052.
- [64] E. Palma, T. Tiepolo, A. Angelin, P. Sabatelli, N.M. Maraldi, E. Basso, M.A. Forte, P. Bernardi, P. Bonaldo, Genetic ablation of cyclophilin D rescues mitochondrial

- defects and prevents muscle apoptosis in collagen VI myopathic mice, *Hum. Mol. Genet.* 18 (2009) 2024–2031.
- [65] P. Grumati, L. Coletto, P. Sabatelli, M. Cescon, A. Angelin, E. Bertaggia, B. Blaauw, A. Urciuolo, T. Tiepolo, L. Merlini, N.M. Maraldi, P. Bernardi, M. Sandri, P. Bonaldo, Autophagy is defective in collagen VI muscular dystrophies, and its reactivation rescues myofiber degeneration, *Nat. Med.* 16 (2010) 1313–1320.
- [66] A. Angelin, T. Tiepolo, P. Sabatelli, P. Grumati, N. Bergamin, C. Golfieri, E. Mattioli, F. Gualandi, A. Ferlini, L. Merlini, N.M. Maraldi, P. Bonaldo, P. Bernardi, Mitochondrial dysfunction in the pathogenesis of Ullrich congenital muscular dystrophy and prospective therapy with cyclosporins, *Proc. Natl Acad. Sci. USA* 104 (2007) 991–996.
- [67] L. Merlini, A. Angelin, T. Tiepolo, P. Braghetta, P. Sabatelli, A. Zamparelli, A. Ferlini, N.M. Maraldi, P. Bonaldo, P. Bernardi, Cyclosporin A corrects mitochondrial dysfunction and muscle apoptosis in patients with collagen VI myopathies, *Proc. Natl Acad. Sci. USA* 105 (2008) 5225–5229.
- [68] D.P. Millay, M.A. Sargent, H. Osinsky, C.P. Baines, E.R. Barton, G. Vuagniaux, H.L. Sweeney, J. Robbins, J.D. Molkentin, Genetic and pharmacologic inhibition of mitochondrial-dependent necrosis attenuates muscular dystrophy, *Nat. Med.* 14 (2008) 442–447.
- [69] P. Bernardi, Modulation of the mitochondrial cyclosporin A-sensitive permeability transition pore by the proton electrochemical gradient. Evidence that the pore can be opened by membrane depolarization, *J. Biol. Chem.* 267 (1992) 8834–8839.
- [70] A. Nicolli, V. Petronilli, P. Bernardi, Modulation of the mitochondrial cyclosporin A-sensitive permeability transition pore by matrix pH. Evidence that the pore open-closed probability is regulated by reversible histidine protonation, *Biochemistry* 32 (1993) 4461–4465.
- [71] V. Petronilli, C. Cola, P. Bernardi, Modulation of the mitochondrial cyclosporin A-sensitive permeability transition pore. II. The minimal requirements for pore induction underscore a key role for transmembrane electrical potential, matrix pH, and matrix Ca^{2+} , *J. Biol. Chem.* 268 (1993) 1011–1016.
- [72] V. Petronilli, P. Costantini, L. Scorrano, R. Colonna, S. Passamonti, P. Bernardi, The voltage sensor of the mitochondrial permeability transition pore is tuned by the oxidation–reduction state of vicinal thiols. Increase of the gating potential by oxidants and its reversal by reducing agents, *J. Biol. Chem.* 269 (1994) 16638–16642.
- [73] P. Costantini, B.V. Chernyak, V. Petronilli, P. Bernardi, Selective inhibition of the mitochondrial permeability transition pore at the oxidation–reduction sensitive dithiol by monobromobimane, *FEBS Lett.* 362 (1995) 239–242.
- [74] P. Costantini, R. Colonna, P. Bernardi, Induction of the mitochondrial permeability transition pore by N-ethylmaleimide depends on secondary oxidation of critical thiol groups. Potentiation by copper-*ortho*-phenanthroline without dimerization of the adenine nucleotide translocase, *Biochim. Biophys. Acta* 1365 (1998) 385–392.
- [75] J. Šileikyte, V. Petronilli, A. Zulian, F. Dabbeni-Sala, G. Tognon, P. Nikolov, P. Bernardi, F. Ricchelli, Regulation of the inner membrane mitochondrial permeability transition by the outer membrane translocator protein (peripheral benzodiazepine receptor), *J. Biol. Chem.* 286 (2011) 1046–1053.
- [76] C. Salet, G. Moreno, F. Ricchelli, P. Bernardi, Singlet oxygen produced by photodynamic action causes inactivation of the mitochondrial permeability transition pore, *J. Biol. Chem.* 272 (1997) 21938–21943.
- [77] G. Moreno, K. Poussin, F. Ricchelli, C. Salet, The effects of singlet oxygen produced by photodynamic action on the mitochondrial permeability transition differ in accordance with the localization of the sensitizer, *Arch. Biochem. Biophys.* 386 (2001) 243–250.
- [78] V. Petronilli, J. Šileikyte, A. Zulian, F. Dabbeni-Sala, G. Jori, S. Gobbo, G. Tognon, P. Nikolov, P. Bernardi, F. Ricchelli, Switch from inhibition to activation of the mitochondrial permeability transition during hematoporphyrin-mediated photooxidative stress. Unmasking pore-regulating external thiols, *Biochim. Biophys. Acta* 1787 (2009) 897–904.
- [79] V. Papadopoulos, M. Baraldi, T.R. Guilarte, T.B. Knudsen, J.J. Lacapere, P. Lindemann, M.D. Norenberg, D. Nutt, A. Weizman, M.R. Zhang, M. Gavish, Translocator protein (18 kDa): new nomenclature for the peripheral-type benzodiazepine receptor based on its structure and molecular function, *Trends Pharmacol. Sci.* 27 (2006) 402–409.
- [80] J.D. Spikes, in: K.C. Smith (Ed.), *Photosensitization, The Science of Photobiology*, Plenum Press, New York and London, 1989, pp. 79–110.
- [81] J. Moan, Q. Peng, An outline of the history of PDT, in: Patrice Thierry (Ed.), *An Outline of the History of PDT, Photodynamic Therapy, Comprehensive Series in Photochemistry and Photobiology*, 2, 2003, pp. 1–18.
- [82] R. Ackroyd, C. Kelty, N. Brown, M. Reed, The history of photodetection and photodynamic therapy, *Photochem. Photobiol.* 74 (2001) 656–669.
- [83] T.J. Dougherty, C.J. Gomer, B.W. Henderson, G. Jori, D. Kessel, M. Korbelik, J. Moan, Q. Peng, Photodynamic therapy, *J. Natl Cancer Inst.* 90 (1998) 889–905.
- [84] D.T. Mody, Pharmaceutical development and medical applications of porphyrin-type macrocycles, *J. Porphyrins Phthalocyanines* 4 (2000) 362–367.
- [85] A.P. Castano, T.N. Demidova, M.R. Hamblin, Mechanisms in photodynamic therapy: part one—photosensitizers, photochemistry and cellular localization, *Photodiagn. Photodyn. Ther.* 1 (2004) 279–293.
- [86] S. Verma, G.M. Watt, Z. Mai, T. Hasan, Strategies for enhanced photodynamic therapy effects, *Photochem. Photobiol.* 83 (2007) 996–1005.
- [87] T. Dai, Y.-Y. Huang, M.R. Hamblin, Photodynamic therapy for localized infections—state of the art, *Photodiagn. Photodyn. Ther.* 6 (2009) 170–188.
- [88] K. Plaetzer, B. Krammer, J. Berlanda, F. Berr, T. Kiesslich, Photochemistry and photochemistry of photodynamic therapy: fundamental aspects, *Lasers Med. Sci.* 24 (2009) 259–268.
- [89] M.R. Hamblin, T. Hasan, Photodynamic therapy: a new antimicrobial approach to infectious disease? *Photochem. Photobiol. Sci.* 3 (2004) 436–450.
- [90] G. Jori, C. Fabris, M. Soncin, S. Ferro, O. Coppellotti, D. Dei, L. Fantetti, G. Chiti, G. Roncucci, Photodynamic therapy in the treatment of microbial infections: basic principles and perspective applications, *Lasers Surg. Med.* 38 (2006) 468–481.
- [91] C.S. Foote, Definition of type I and type II photosensitized oxidation, *Photochem. Photobiol.* 54 (1991) 659.
- [92] B. Halliwell, Oxygen radicals: a commonsense look at their nature and medical importance, *Med. Biol.* 62 (1984) 71–77.
- [93] M. Ochsner, Photophysical and photobiological processes in the photodynamic therapy of tumours, *J. Photochem. Photobiol. B* 39 (1997) 1–18.
- [94] T. Ito, Cellular and subcellular mechanisms of photodynamic action: the 102 hypothesis as a driving force in recent research, *Photochem. Photobiol.* 28 (1978) 493–508.
- [95] D.P. Valenzano, Photomodification of biological membranes with emphasis on singlet oxygen mechanisms, *Photochem. Photobiol.* 46 (1987) 147–160.
- [96] A. Michaeli, J. Feitelson, Reactivity of singlet oxygen toward amino acids and peptides, *Photochem. Photobiol.* 59 (1994) 284–289.
- [97] M.J. Davies, Singlet oxygen-mediated damage to proteins and its consequences, *Biochem. Biophys. Res. Commun.* 305 (2003) 761–770.
- [98] R.W. Redmond, I.E. Kochevar, Spatially resolved cellular responses to singlet oxygen, *Photochem. Photobiol.* 82 (2006) 1178–1186.
- [99] M.C. DeRosa, R.J. Crutchley, Photosensitized singlet oxygen and its applications, *Coord. Chem. Rev.* 233–234 (2002) 351–371.
- [100] J. Moan, On the diffusion length of singlet oxygen in cells and tissues, *J. Photochem. Photobiol. B Biol.* 6 (1990) 334–343.
- [101] J. Moan, K. Berg, The photodegradation of porphyrins in cells can be used to estimate the lifetime of singlet oxygen, *Photochem. Photobiol.* 53 (1991) 549–553.
- [102] M. Niedre, M.S. Patterson, B.C. Wilson, Direct near-infrared luminescence detection of singlet oxygen generated by photodynamic therapy in cells in vitro and tissues in vivo, *Photochem. Photobiol.* 75 (2002) 382–391.
- [103] A.C.E. Moor, Signaling pathways in cell death and survival after photodynamic therapy, *J. Photochem. Photobiol. B* 57 (2000) 1–13.
- [104] F. Meyer-Betz, Untersuchungen über die biologische (photodynamische) Wirkung des Haematoporphyrins und anderer Derivate des Blut- und Gallenfarbstoffs, *Dtsch Arch. Klin. Med.* 112 (1913) 476–503.
- [105] D. Kessel, P. Thompson, B. Musselman, C.K. Chang, Chemistry of hematoporphyrin-derived photosensitizers, *Photochem. Photobiol.* 46 (1987) 563–568.
- [106] T.J. Dougherty, Photosensitizers: therapy and detection of malignant tumors, *Photochem. Photobiol.* 45 (1987) 879–889.
- [107] E.S. Nyman, P.H. Hynninen, Research advances in the use of tetrapyrrolic photosensitizers for photodynamic therapy, *J. Photochem. Photobiol. B* 73 (2004) 1–28.
- [108] H. Mojziso, S. Bonneau, D. Brault, Structural and physico-chemical determinants of the interactions of macrocyclic photosensitizers with cells, *Eur. Biophys. J.* 36 (2007) 943–953.
- [109] I.J. MacDonald, T.J. Dougherty, Basic principles of photodynamic therapy, *J. Porphyrins Phthalocyanines* 5 (2001) 105–129.
- [110] J.C. Kennedy, R.H.P. Pottier, Photodynamic therapy with endogenous photoporphyrin IX: basic principles and present clinical experience, *J. Photochem. Photobiol. B* 6 (1990) 143–148.
- [111] F. Ricchelli, Photophysical properties of porphyrins in biological membranes, *J. Photochem. Photobiol. B* 29 (1995) 109–118.
- [112] E. Reddi, G. Jori, Steady-state and time-resolved spectroscopic studies of photodynamic sensitizers: porphyrins and phthalocyanines, *Rev. Chem. Intermed.* 10 (1988) 241–268.
- [113] C.R. Lambert, E. Reddi, J.D. Spikes, M.A. Rodgers, G. Jori, The effects of porphyrin structure and aggregation state on photosensitization processes in aqueous and micellar media, *Photochem. Photobiol.* 44 (1986) 595–601.
- [114] F. Ricchelli, S. Gobbo, G. Jori, G. Moreno, F. Vinzens, C. Salet, Photosensitization of mitochondria by liposome-bound porphyrins, *Photochem. Photobiol.* 58 (1993) 53–58.
- [115] R. Hilf, Mitochondria are targets of photodynamic therapy, *J. Bioenerg. Biomembr.* 39 (2007) 85–89.
- [116] J. Morgan, A.R. Oseroff, Mitochondria-based photodynamic anti-cancer therapy, *Adv. Drug Deliv. Rev.* 49 (2001) 71–86.
- [117] D.S. Perlin, R.S. Murant, S.L. Gibson, R. Hilf, Effects of photosensitization by hematoporphyrin derivative on mitochondrial adenosine triphosphatase-mediated proton transport and membrane integrity of R3230AC mammary adenocarcinoma, *Cancer Res.* 45 (1985) 653–658.
- [118] R. Hilf, R.S. Murant, U. Narayanan, S.L. Gibson, Relationship of mitochondrial function and cellular adenosine triphosphate levels to hematoporphyrin derivative-induced photosensitization in R3230AC mammary tumors, *Cancer Res.* 46 (1986) 211–217.
- [119] A.D. Munday, A. Sriratana, J.S. Hill, S.B. Kahl, P. Nagley, Mitochondria are the functional intracellular target for a photosensitizing boronated porphyrin, *Biochim. Biophys. Acta* 1311 (1996) 1–4.
- [120] A. Atlante, S. Passarella, E. Quagliariello, G. Moreno, C. Salet, Haematoporphyrin derivative (Photofrin II) photosensitization of isolated mitochondria: inhibition of ADP/ATP translocator, *J. Photochem. Photobiol. B* 4 (1989) 35–46.
- [121] C. Salet, G. Moreno, Photosensitization of mitochondria. Molecular and cellular aspects, *J. Photochem. Photobiol. B* 5 (1990) 133–150.
- [122] A. Verma, S.L. Facchina, D.J. Hirsch, S.Y. Song, L.F. Dillahey, J.R. Williams, S.H. Snyder, Photodynamic tumor therapy: mitochondrial benzodiazepine receptors as a therapeutic target, *Mol. Med.* 4 (1998) 40–45.

- [123] A. Verma, J.S. Nye, S.H. Snyder, Porphyrins are endogenous ligands for the mitochondrial (peripheral-type) benzodiazepine receptor, *Proc. Natl Acad. Sci. USA* 84 (1987) 2256–2260.
- [124] A. Verma, S.H. Snyder, Peripheral type benzodiazepine receptors, *Annu. Rev. Pharmacol. Toxicol.* 29 (1989) 307–322.
- [125] M.W. McEnery, A.M. Snowman, R.R. Trifiletti, S.H. Snyder, Isolation of the mitochondrial benzodiazepine receptor: association with the voltage-dependent anion channel and the adenine nucleotide carrier, *Proc. Natl Acad. Sci. USA* 89 (1992) 3170–3174.
- [126] M. Garnier, A.B. Dimchev, N. Boujrad, J.M. Price, N.A. Musto, V. Papadopoulos, In vitro reconstitution of a functional peripheral-type benzodiazepine receptor from mouse Leydig tumor cells, *Mol. Pharmacol.* 45 (1994) 201–211.
- [127] D. Kessel, M. Antolovich, K.M. Smith, The role of the peripheral benzodiazepine receptor in the apoptotic response to photodynamic therapy, *Photochem. Photobiol.* 74 (2001) 346–349.
- [128] M. Mesenholler, E.K. Matthews, A key role for the mitochondrial benzodiazepine receptor in cellular photosensitisation with delta-aminolaevulinic acid, *Eur. J. Pharmacol.* 406 (2000) 171–180.
- [129] G. Wendler, P. Lindemann, J.J. Lacapere, V. Papadopoulos, Protoporphyrin IX binding and transport by recombinant mouse PBR, *Biochem. Biophys. Res. Commun.* 311 (2003) 847–852.
- [130] I.E. Furre, S. Shahzidi, Z. Luksiene, M.T. Moller, E. Borgen, J. Morgan, K. Tkacz-Stachowska, J.M. Nesland, Q. Peng, Targeting PBR by hexaminolevulinate-mediated photodynamic therapy induces apoptosis through translocation of apoptosis-inducing factor in human leukemia cells, *Cancer Res.* 65 (2005) 11051–11060.
- [131] S.L. Ratcliffe, E.K. Matthews, Modification of the photodynamic action of delta-aminolaevulinic acid (ALA) on rat pancreatoma cells by mitochondrial benzodiazepine receptor ligands, *Br. J. Cancer* 71 (1995) 300–305.
- [132] A.J. Kowaltowski, R.F. Castilho, A.E. Vercesi, Mitochondrial permeability transition and oxidative stress, *FEBS Lett.* 495 (2001) 12–15.
- [133] P. Costantini, B.V. Chernyak, V. Petronilli, P. Bernardi, Modulation of the mitochondrial permeability transition pore by pyridine nucleotides and dithiol oxidation at two separate sites, *J. Biol. Chem.* 271 (1996) 6746–6751.
- [134] G.P. McStay, S.J. Clarke, A.P. Halestrap, Role of critical thiol groups on the matrix surface of the adenine nucleotide translocase in the mechanism of the mitochondrial permeability transition pore, *Biochem. J.* 367 (2002) 541–548.
- [135] A.P. Halestrap, K.Y. Woodfield, C.P. Connern, Oxidative stress, thiol reagents, and membrane potential modulate the mitochondrial permeability transition by affecting nucleotide binding to the adenine nucleotide translocase, *J. Biol. Chem.* 272 (1997) 3346–3354.
- [136] E. Romeo, J. Auta, A.P. Kozikowski, D. Ma, V. Papadopoulos, G. Puia, E. Costa, A. Guidotti, 2-Aryl-3-indoleacetamides (FGIN-1): a new class of potent and specific ligands for the mitochondrial DBI receptor (MDR), *J. Pharmacol. Exp. Ther.* 262 (1992) 971–978.
- [137] R.R. Anholt, E.B. De Souza, M.L. Oster-Granite, S.H. Snyder, Peripheral-type benzodiazepine receptors: autoradiographic localization in whole-body sections of neonatal rats, *J. Pharmacol. Exp. Ther.* 233 (1985) 517–526.
- [138] E.B. De Souza, R.R. Anholt, K.M. Murphy, S.H. Snyder, M.J. Kuhar, Peripheral-type benzodiazepine receptors in endocrine organs: autoradiographic localization in rat pituitary, adrenal, and testis, *Endocrinology* 116 (1985) 567–573.
- [139] V. Papadopoulos, H. Amri, N. Boujrad, C. Cascio, M. Culty, M. Garnier, M. Hardwick, H. Li, B. Vidic, A.S. Brown, J.L. Reversa, J.M. Bernassau, K. Drieu, Peripheral benzodiazepine receptor in cholesterol transport and steroidogenesis, *Steroids* 62 (1997) 21–28.

The Outer Membrane-Translocator Protein Mediates Activation of the Mitochondrial Permeability Transition by Porphyrin-Based Photooxidative Stress

Justina Šileikytė,¹ Peter Nikolov,² Paolo Bernardi,¹ & Fernanda Ricchelli^{1,}*

¹C.N.R. Institute of Neurosciences at the Department of Biomedical Sciences, University of Padova, Padova, Italy; ²Institute of Organic Chemistry, Bulgarian Academy of Sciences, Sofia, Bulgaria

*Address all correspondence to: Fernanda Ricchelli; CNR, Institute of Biomedical Technologies at the Department of Biology, University of Padova, Italy, Viale Giuseppe Colombo 3, I-35121 Padova, Italy; Tel.: +39 0498276336, Fax: +39 0498276348; rchielli@bio.unipd.it

ABSTRACT: A prominent feature of successful photodynamic therapy (PDT) is the targeting of mitochondria, because these organelles are critical sites for initiating both necrotic and apoptotic cell death. Among the variety of structures identified as targets for PDT, the outer membrane (OMM)-bound translocator protein, TSPO (formerly known as the peripheral benzodiazepine receptor), is of particular interest because it binds photosensitizers such as dicarboxylic porphyrins with nanomolar affinity and it is present at elevated levels in cancer cells. TSPO has also been postulated to be a component of the mitochondrial permeability transition (PT) pore (PTP), a protein channel that opens in the inner membrane (IMM) under the action of various stimuli, mainly matrix Ca^{2+} overload and oxidative stress, leading the cell toward death. In this study, photooxidation experiments with porphyrins indicated a strict correlation between porphyrin affinity for TSPO and the extent of mitochondrial photosensitization; moreover, they revealed a dual role of TSPO: (1) as a transport protein that facilitates diffusion of porphyrins into IMM, and (2) as a PTP regulatory protein when it binds porphyrins at its selective sites. Only photoactivation of TSPO-bound porphyrins leads to the opening of the PTP and mitochondrial dysfunction, whereas photoactivation of IMM-bound porphyrins maintains the PTP in the closed state.

KEY WORDS: mitochondria, mitoplasts, porphyrins, TSPO, photooxidative stress

ABBREVIATIONS

ANT: adenine nucleotide translocase; **CP:** coproporphyrin III; **CyP-D:** cyclophilin D; **DP:** deuteroporphyrin IX; **EGTA:** [ethylenebis(oxoethylenetriolo)] tetraacetic acid; **EP:** etioporphyrin; **FGIN1-27:** N,N-dihexyl-2-(4-fluorophenyl) indole-3-acetamide; **HP:** hematoporphyrin IX; **IMM:** inner mitochondrial membrane; **MOPS:** 4-morpholinepropanesulfonic acid; **¹O₂:** singlet oxygen; **OMM:** outer mitochondrial membrane; **PDT:** photodynamic therapy; **PK11195:** 1-(2-chlorophenyl)-N-methyl-N-(1-methyl-propyl)-3-isoquinolinecarboxamide; **PP:** protoporphyrin IX; **PT:** permeability transition; **PTP:** permeability transition pore; **Ro5-4864:** 7-chloro-5-(4-chlorophenyl)-1,3-dihydro-1-methyl-2H-1,4-benzodiazepin-2-one; **ROS:** reactive oxygen species; **TSPO:** 18 kDa translocator protein; **UP:** uroporphyrin I; **VDAC:** voltage-dependent anion channel

I. INTRODUCTION

Mitochondria have a major role in various aspects of cell metabolism, particularly in energy production and maintenance of calcium homeostasis. The continuous growth of tumor cells is highly energy dependent, so disruption of mitochondrial function could be a significant therapeutic target.¹ Many photosensitizers used in PDT can rapidly induce apoptosis. Works elucidating apoptotic mechanisms of various cytotoxic agents have revealed that many of the triggers converge on mitochondrial events that lead to downstream effector pathways, such as activation of the caspase cascade, culminating in apoptotic death.² A major mechanism responsible for these events is the opening of the permeability transition (PT) pore (PTP) in the inner mitochondrial membrane (IMM). PTP opening causes a sudden increase in the permeability of the IMM to solutes with molecular mass less than 1.5 kDa and is mainly induced by matrix calcium overload and oxidative stress. Under the conditions used in most *in vitro* studies, PT is accompanied by depolarization, matrix swelling, Ca²⁺ efflux, depletion of matrix pyridine nucleotides (PN), outer membrane (OMM) rupture, and release of intermembrane proteins, including cytochrome c, Smac/DIABLO, and apoptosis inducing factor (AIF).³⁻⁷

The molecular composition of the PTP remains elusive. In the classical view, the pore frame was thought to be formed by a complex comprising the adenine nucleotide translocase (ANT; a component of the IMM), the voltage dependent anion channel (VDAC; the most abundant protein in the OMM), the cyclophilin D (CyP-D; a component of the matrix) and located at the contact sites between IMM and OMM (Figure 1A).⁸⁻¹⁰ The

OMM translocator protein, TSPO (previously known as the peripheral benzodiazepine receptor-PBR),^{11,12} was also included in the PTP structure by some investigators.^{13,14} This PTP model was recently abandoned for two reasons: (1) the PT can still occur in the mitochondria of mice in which ANT, VDAC, and CyP-D have been genetically ablated or silenced,¹⁵⁻¹⁷ and (2) the PT can occur in the absence of an intact OMM (in mitoplasts).¹⁸ In the current view, the PTP is considered an IMM event and the elements comprising its structure remain unidentified but are probably regulated by ANT, VDAC, and CyP-D (Figure 1B). The role of TSPO in the PT, as well as of other putative regulatory proteins, remains an open question.

Involvement of TSPO in PTP function was initially suggested following the activity of TSPO-specific ligands, notably the benzodiazepine, Ro5-4864, the isoquinoline carboxamide, PK11195, the indole derivative FGIN1-27 and the endogenous ligand protoporphyrin (PP), which were shown to promote the PT in isolated mitochondria and apoptosis in a variety of cells. Other studies, however, have shown that TSPO ligands, particularly in combination with other pathological stimuli, inhibit, rather than promote, the PT and apoptosis.^{5,13,14} To circumvent these contradictions, we explored the regulatory properties of TSPO on PTP function using a novel methodology. This approach takes advantage of the ability of some PP-like porphyrins, such as hematoporphyrin (HP), deuteroporphyrin (DP), as well as PP itself, to bind to TSPO with high affinity (nanomolar range) and to produce reactive oxygen species [ROSs, mainly singlet oxygen (¹O₂)] upon irradiation with UV/visible light. The ¹O₂ transient photogenerated *in situ* can easily oxidize electron-rich protein targets,

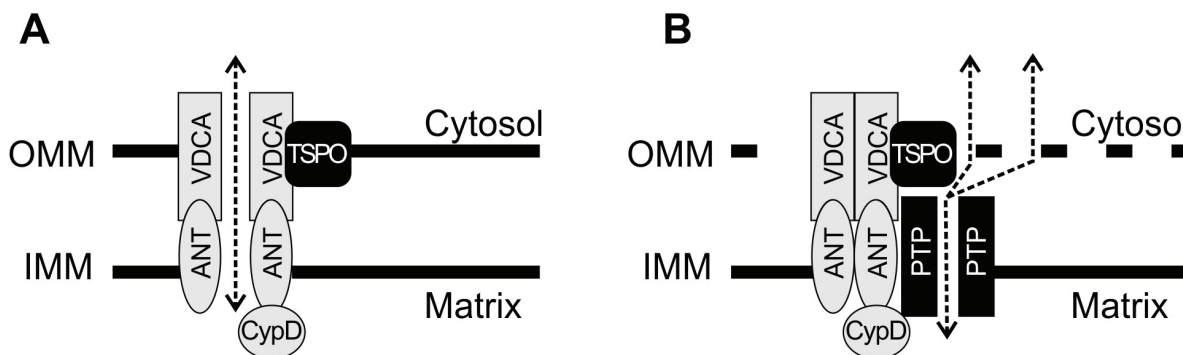


FIGURE 1. Proposed PTP complex architecture. (A) Classical model. The pore structure is formed by the VDAC-ANT-CyP-D complex, which is located at the contact sites between IMM and OMM. TSPO is included as a putative regulatory component. Other putative regulators (hexokinase II, creatine kinase, and Bcl-2-family members -Bcl-2, Bcl-xL and Bax) are not shown. (B) Current model. ANT, VDAC and CyP-D are no longer seen as pore components based on recent genetic evidence and studies on mitoplasts. The elements comprising the PTP itself (exclusively located in the IMM) are presently unidentified, but they are probably regulated by the adjacent elements as indicated.

provided that the substrate and the sensitizer are situated in close proximity. Interestingly, two of the targets readily oxidized by $^1\text{O}_2$, Cys, and His have been shown to have a critical role in regulation of the PT.^{19,20}

In our studies, we also aimed to define whether and how TSPO regulates porphyrin-induced mitochondrial phototoxicity. Actually, the affinity of several porphyrins for TSPO and the high amount of TSPO in tumor cells suggest that binding of sensitizers to this site may be important for cell killing.

II. MATERIAL AND METHODS

II.A. Reagents

Hematoporphyrin IX (HP), protoporphyrin IX (PP), deuteroporphyrin IX (DP), copropor-

phyrin III (CP) and uroporphyrin I (UP) were obtained from Frontier Scientific (Logan, UT), and stock solutions were prepared in dimethylsulfoxide. N,N-dihexyl-2-(4-fluorophenyl) indole-3-acetamide (FGIN1-27), digitonin and etioporphyrin I (EP) were from Sigma-Aldrich. Calcium Green-5N was from Invitrogen. All chemicals were of the highest purity commercially available.

II.B. Preparation of Mitochondria and Mitoplasts

Liver mitochondria from Wistar rats were prepared by standard differential centrifugation. The final pellet was suspended in a medium containing 250 mM sucrose, 0.5 mM EGTA-Tris, and 10 mM Tris-HCl pH 7.4 (isolation buffer), and the protein concentration

was determined using the biuret method. Mitoplasts were prepared by treating mitochondrial suspensions with proper amounts of digitonin, as described by Šileikytė et al.¹⁸

II.C. Permeability Transition

PT was induced at 25°C in a medium containing 250 mM sucrose, 10 mM Tris-Mops, 5 mM succinate, 1 mM P_i-Tris, 10 μM EGTA-Tris, 0.5 μg/ml oligomycin, and 2 μM rotenone, pH 7.4 (standard medium). PT-related osmotic swelling was measured by the decrease in 90° light scattering at 540 nm, measured with a Perkin-Elmer LS50 spectrofluorometer. PT-related Ca²⁺ efflux was measured in the same medium supplemented with 0.5 μM of the fluorescent, membrane-impermeant Ca²⁺-indicator, calcium green-5N (excitation 480 nm and emission 530 nm). In all experimental conditions, occurrence of the PT was verified by the desensitizing effect of cyclosporin A.¹⁸

II.D. Porphyrin-Based Photosensitization of Mitochondria and Mitoplasts

Porphyrin-mediated photosensitization of mitochondria and mitoplasts was achieved as described by Šileikytė et al.¹⁸ and Petronilli et al.²¹ Briefly, preparations were incubated for 1–2 min in the dark with the desired concentration of porphyrin and then irradiated at 365 nm in a thermostated glass reaction vessel with a Philips HPW 125W lamp (Philips, Eindhoven, The Netherlands). The fluence rate of the preparations (40 W/m²) was measured using a calibrated quantum-photo-radiometer (Delta OHM HD 9021). All irradiations were performed at 25°C under magnetic stirring. Proper controls were conducted to verify that neither incubation with the photosensitizer in

the dark nor illumination in the absence of porphyrin produced any appreciable changes in the parameters under study. Photooxidation experiments were performed in a range of concentrations of 0.2–1.8 nmoles of porphyrin taken up per milligram protein. Under these conditions, porphyrins were bound to mitochondria and mitoplasts as monomers, the only species appreciably photoactive; moreover, they did not induce detrimental effects on the organelles in the dark. In addition, we determined that the molar absorptivities at the irradiation wavelength used (365 nm) were very similar (within 10%) for all porphyrins, which reflects an equivalent number of photons absorbed (data not shown). Thus, for comparative investigations the sensitizer concentrations were properly adjusted to obtain an equivalent amount of dyes effectively taken up by the organelles, which ensured a similar photosensitizing effectiveness upon irradiation. Determinations of porphyrin uptake were performed as described previously.¹⁸

III. RESULTS AND DISCUSSION

III.A. Photooxidation of PTP-Regulating His and Cys in Mitochondria

PTP opening is strongly promoted by an oxidized state of critical Cys at discrete sites of the IMM. So far, at least two sites have been identified as being involved in the PT process. The first site resides in internal, matrix-exposed regions of IMM (internal Cys) and is in close structural and functional correlation with critical His, whereas the second site is located on the outer surface of the IMM (external Cys) (see scheme in Figure 2).¹⁸

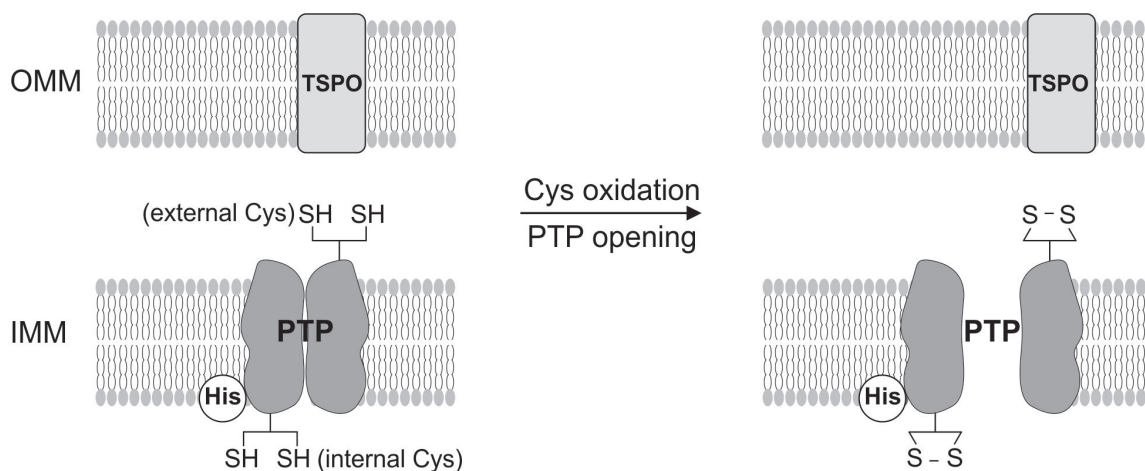


FIGURE 2. Distribution of critical His and Cys in the PTP. A group of Cys is located in matrix-exposed regions of the IMM (internal Cys), in close structural and functional correlation with critical His; another group of Cys is located on the outer surface of the IMM (external Cys). Opening of the PTP by oxidative stress is mainly due to modifications of one or both Cys sites.

In sharp contrast with other activated oxygen species such as H_2O_2 or superoxide, porphyrin-photogenerated $^1\text{O}_2$ does not induce the PT, which follows Cys oxidation, when relatively low doses of light are used. Rather, photodynamic action leads to suppression of the PT.¹⁹ As shown in Figure 3, photoactivation of HP at increasing irradiation times induces a gradual decrease of the rate of Ca^{2+} -triggered membrane permeabilization until IMM becomes fully impermeable to external solutes. Irradiation for times longer than 45 s, however, counteracts the inhibitory effect and reactivates the PTP. The peculiar effects of porphyrin-based photooxidative stress on the PT can be easily explained by the fact that photodamage is restricted to sites that are in close proximity to the photosensitizer.²⁰ Therefore, the properties of the region surrounding the photosensitizer binding site may be criti-

cal in determining the molecular events involved in the PT. The inactivating effect can be traced back to critical His (the most photovulnerable target), whose photomodification by vicinal HP causes a drop in reactivity of internal, PTP-regulating Cys, thus stabilizing the pore in a closed conformation.²¹ On the other hand, photooxidation of external Cys (the most photoresistant target) promoted by vicinal HP reactivates the PTP after the block caused by His photodegradation (*see* Petronilli et al.²¹). The processes of PTP inhibition and/or reactivation are specific to porphyrins characterized by a PP-like configuration that bind TSPO with nanomolar affinity such as HP, PP, and DP. Interestingly, their potencies in eliciting both PT-photoinhibition and PT-photoreactivation strictly match the affinities for the OMM-TSPO (Table 1).

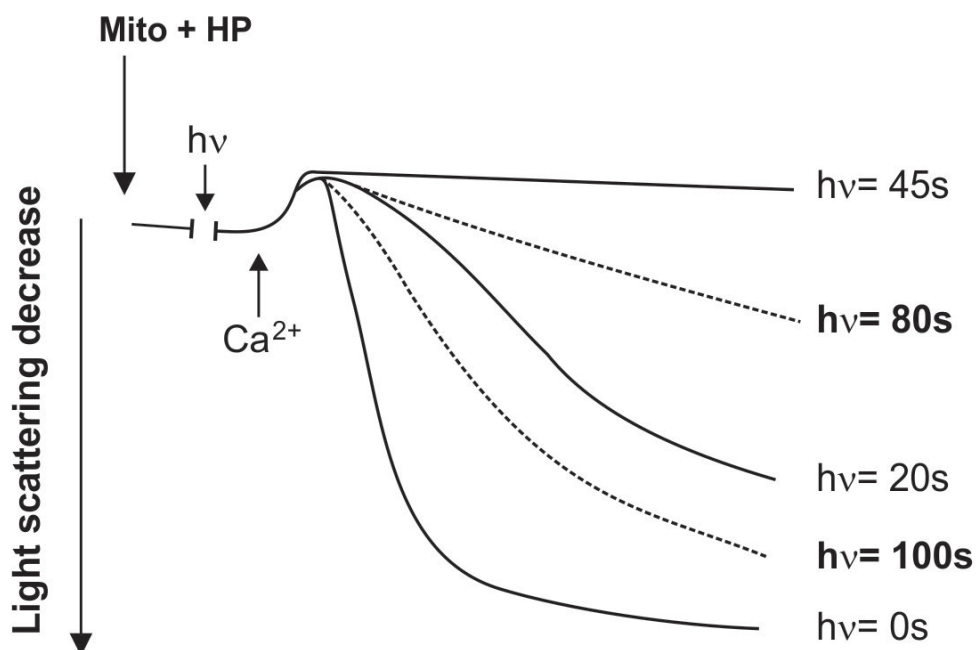


FIGURE 3. Mitochondrial PT inhibition and reactivation at increasing irradiation times in HP-loaded mitochondria. Mitochondria (0.5 mg/ml) labelled with 3 μM HP (corresponding to 1.8 nmol HP taken up/mg protein) (m+HP) were incubated for 2 min at 25°C in the standard medium. Irradiation ($h\nu$) was performed for the indicated periods of time at a fluence rate of 40 W/m². PT was triggered by 80 μM Ca²⁺. PT-induced matrix swelling was followed as the decrease of 90° light scattering at 540 nm.

TABLE 1. Relationship Between Porphyrin Photosensitizing Effects and TSPO Affinity

Porphyrin	Light dose (J/cm ²) for PT inhibition ^a	Light dose (J/cm ²) for PT reactivation ^b	TSPO K _i (nM) ^c
PP	0.05±0.01	0.12± 0.03	14.5 ± 10.7
DP	0.07±0.005	0.15±0.02	31.3 ± 2
HP	0.18±0.01	0.35±0.05	500.0 ±151

^aMinimal dose of light required to obtain full PT inhibition and ^bminimal dose of light required to start PT reactivation for 1.8 nmol porphyrin taken up per milligram mitochondrial protein; ^cK_i is the value of the constant displayed by each porphyrin for inhibition of binding of PK11195, a classical ligand of TSPO.²⁸

PP-unrelated porphyrins (such as the tetracarboxylic coproporphyrin III (CP), the octacarboxylic uroporphyrin I (UP) and etio-porphyrin I (EP) that lacks carboxylic groups), which exhibit negligible affinity for TSPO, are ineffective on the PT (data not shown).

III.B. Photooxidation of PTP-Regulating His and Cys in Mitoplasts

The photodynamic events observed in mitochondria using PP-like porphyrins as sensitizers were only partly retained in mitoplasts, which lacked OMM-bound TSPO. Irradiation of porphyrin-loaded mitoplasts with low doses of light caused inactivation of the PTP, although mitoplasts were significantly more resistant to photosensitization than mitochondria. As shown in Figure 4, which shows the results obtained with HP, higher doses of light were required to inhibit the PT in mitoplasts, compared to mitochondria. Also DP and PP were more effective in mitochondria than in mitoplasts (data not shown), suggesting that TSPO facilitates the diffusion of PTP-active porphyrins to the “internal” PTP regulatory sites.

Unlike mitochondria, pore reactivation by high light doses in mitoplasts treated with PP-like porphyrins were not observed (data not shown). Therefore, PTP reactivation is a specific event mediated by the OMM, and importantly, PTP regulatory, porphyrin-binding sites are contributed by TSPO.

III.C. Photooxidation of Mitochondria in the Presence of Porphyrin Competitive, TSPO-Ligands

To further prove the role of TSPO on the PTP-related photooxidative events, we tested

whether the presence of other TSPO ligands could influence porphyrin photoactivity in mitochondria. As shown in Figure 5 B, porphyrin-mediated PTP photoactivation (at high light doses) was suppressed by low concentrations of the high affinity, porphyrin competitive, TSPO ligand FGIN1-27, indicating that FGIN1-27 protects external cysteines from being converted to cystines. Probably, competition with other ligands displaces porphyrins from their selective binding sites on TSPO. Specific involvement of TSPO in FGIN1-27 effects was demonstrated by the fact that this ligand did not partition into PTP sites; actually, it neither interfered with the process of PT inhibition (Figure 5A), which involves “internal” PTP domains, nor modified the reactivity of external Cys in mitoplasts (data not shown).

III.D. Effects of TSPO Ligands on the Mitochondrial and Mitoplast PT in the Dark

At the concentrations we used in our photooxidation experiments, TSPO ligands did not affect the PTP in the dark. At relatively high concentrations, however, several TSPO ligands were potent inducers of the PT *per se*.^{22–26} In the experiments shown in Figure 6, we tested the effect of PP on the PT-related Ca²⁺ release in Ca²⁺-loaded mitochondria and mitoplasts. Doses of PP higher than 2 nmol/mg protein caused PTP opening in mitochondria but not in mitoplasts. A full titration conducted with other compounds that bind to TSPO with nanomolar affinity, including FGIN1-27, Ro-4864, and PK11195, confirmed the striking resistance of mitoplasts to the PTP-inducing effects of TSPO ligands (*see Šileikytė et al.*¹⁸). In the absence

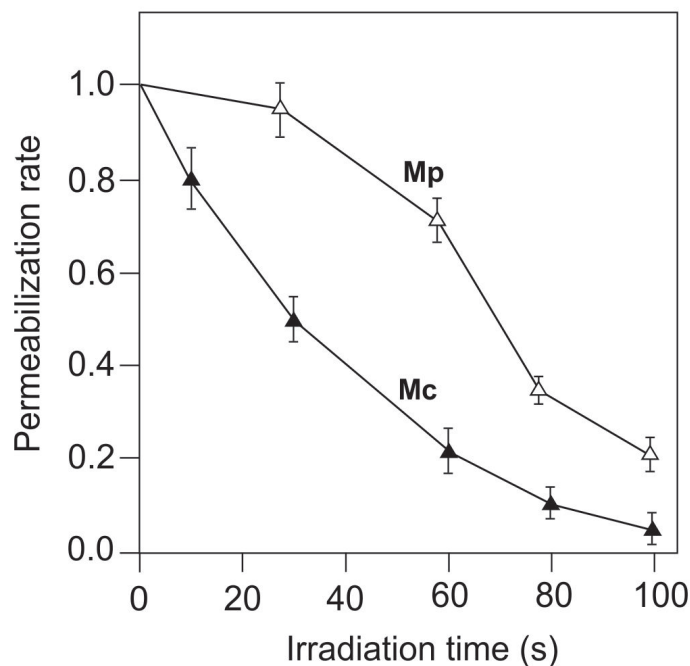


FIGURE 4. PT inhibition in mitochondria and mitoplasts loaded with HP. Mitochondria (Mc) and mitoplasts (Mp) at 0.5 mg/ml were incubated for 2 min with a concentration of HP (2 μ M), giving a loading of 1.2 nmol/mg of protein at 25°C. Preparations were irradiated for the indicated times at a fluence rate of 40 W/m² and then supplemented with 60 μ M (Mc) or 30 μ M (Mp) Ca²⁺ to trigger the PT, which was followed by the changes in 90° light scattering at 540 nm. The permeabilization rate was normalized to that of the control (in the absence of porphyrins). Error bars represent the mean \pm S.D. of the three experiments.

of a clear PT inducer (such as the oxidant ¹O₂) in the dark, we postulate that TSPO in its liganded state can regulate the PTP activity *per se*, likely through conformational changes of specific domains closely associated with the pore.

IV. CONCLUSIONS

TSPO is an 18-kDa OMM protein highly conserved throughout evolution, from bacteria to humans. It is involved in a variety

of biological functions such as apoptosis, cell proliferation, mitochondrial respiration, ischemia, microglial activation, immune response, and steroidogenesis (transport of cholesterol). Consistent with this latter function, TSPO is particularly present (up to 20- to 50-fold) in tissues in which steroids are synthesized.^{11–13} In addition, TSPO mediates mitochondrial uptake of naturally occurring dicarboxylic porphyrins such as protoporphyrin IX (PP), other heme precursors, as well as heme itself.^{26,27}

Our results provide evidence for the involvement of TSPO in PTP opening as well.

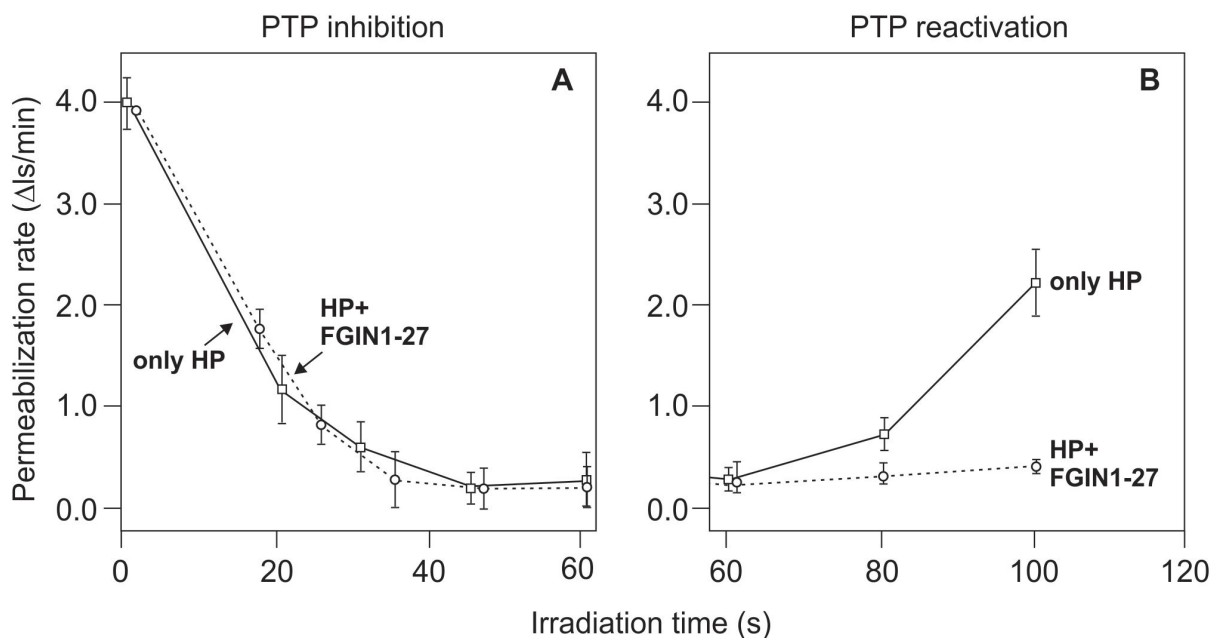


FIGURE 5. Effects of FGIN1-27 on PTP inhibition (A) and PTP reactivation (B) in HP-loaded mitochondria. A. The experiments were performed as described in Figure 4, except that an HP loading of 1.8 nmol/mg of protein was used; FGIN1-27 was added after HP at 5 μ M concentration; B. HP-labelled mitochondria were supplemented with 5 μ M Ca^{2+} (a concentration not sufficient to induce PTP opening per se), then irradiated for the indicates times at 40 W/m² to activate the PT. The permeabilization rates are expressed as the changes of light scattering intensity at 540 nm (Δ ls) per min.

TSPO plays a dual role in PTP modulation (1) as a transport protein for PTP-active compounds that are transferred to their PTP regulatory site(s) in the IMM or in the matrix and (2) as a PTP regulatory protein when it binds its selective ligands like porphyrins. These modes of action of TSPO result in modulation of porphyrin phototoxicity on PT-related mitochondrial dysfunction. Actually, porphyrin-based photodynamic effects can either inhibit (by porphyrin channeled to internal domains by TSPO) or, oppositely, open (by porphyrin bound to TSPO) the PTP.

ACKNOWLEDGMENTS

This paper partially fulfills the requirements for the PhD of JS, who was supported by a Fellowship from the Fondazione Cariparo, Padova. This research was supported by the Italian National Research Council (CNR) within the framework of the Italy-Bulgaria (BAN) bilateral cooperation, and, in part, by grants from the Ministry for University and Research (MIUR/PRIN) and Fondazione Cariparo Progetti di Eccellenza “Models of Mitochondrial Diseases.”

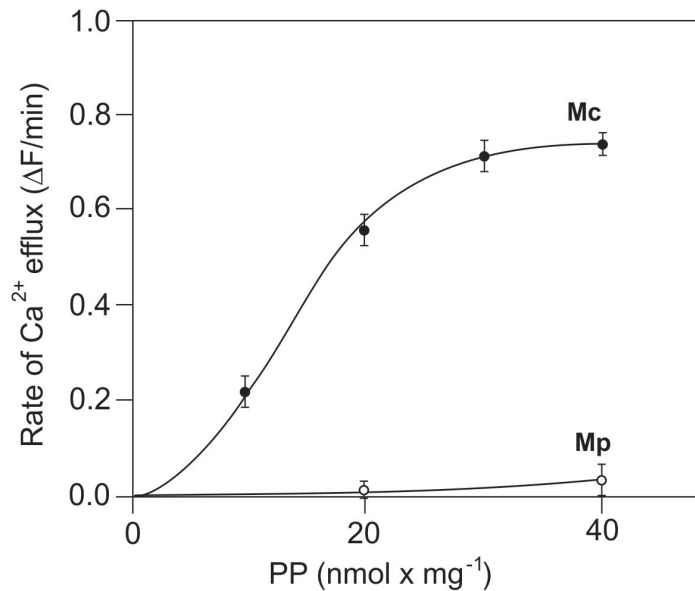


FIGURE 6. Effect of PP on PTP-dependent Ca^{2+} release in mitochondria and mitoplasts in the dark. Mitochondria or mitoplasts (1 mg/ml) were incubated in the standard medium containing the fluorescent Ca^{2+} -indicator, calcium green-5N, then supplemented with a pulse of Ca^{2+} (30 μM) which was retained by the organelles. The PT was triggered by adding different PP concentrations giving the stated amounts of incorporated porphyrin. The rates of PT-induced Ca^{2+} efflux are expressed as the fluorescence changes of the probe (ΔF) per min..

REFERENCES

- Hilf R. Mitochondria are targets of photodynamic therapy. *J Bioenerg Biomembr.* 2007; 39:85–9.
- Morgan J, Oseroff AR. Mitochondria-based photodynamic anti-cancer therapy. *Adv Drug Deliv Rev.* 2001; 49:71–86.
- Lemasters JJ, Nieminen AL, Qian T, Trost L, Elmore SP, Nishimura Y, Crowe RA, Cascio WE, Bradham CA, Brenner DA, Herman B. The mitochondrial permeability transition in cell death: a common mechanism in necrosis, apoptosis and autophagy. *Biochim Biophys Acta.* 1998;1366:177–96.
- Bernardi P. Mitochondrial transport of cations: channels, exchangers and permeability transition. *Physiol Rev.* 1999;79:1127–55.
- Bernardi P, Krauskopf A, Basso E, Petronilli V, Blachly-Dyson E, Di Lisa F, Forte MA. The mitochondrial permeability transition from in vitro artifact to disease target. *FEBS J.* 2006;273:2077–99.
- Crompton M. The mitochondrial permeability transition pore and its role in cell death. *Biochem J.* 1999; 341:233–49.
- Rasola A, Bernardi P. The mitochondrial

- permeability transition pore and its involvement in cell death and in disease pathogenesis. *Apoptosis*. 2007;12:815–33.
8. Juhaszova M, Wang SU, Zorov DB, Bradley Nuss H, Gleichmann M, Mattson M, Soltott SJ. The identity and regulation of the mitochondrial permeability transition pore. Where the known meets the unknown. *Ann NY Acad Sci*. 2008;1123:197–212.
 9. Baines CP. The molecular composition of the mitochondrial permeability transition pore. *J Mol Cell Cardiol*. 2009;46:850–857.
 10. Kroemer G, Galluzzi L, and Brenner C. Mitochondrial membrane permeabilization in cell death. *Physiol Rev*. 2007;87(1):99–163.
 11. Papadopoulos A, Baraldi M, Guilarte TR, Knudsen TB, Lacapère JJ, Lindemann P, Norenberg MD, Nutt D, Weizman A, Zhang MR, Gavish M. Translocator protein (18kDa): new nomenclature for the peripheral-type benzodiazepine receptor based on its structure and molecular function. *Trends Pharmacol Sci*. 2006;27(8):402–9.
 12. Bourdeley-Thomas A, Miccoli L, Oudard S, Dutrillaux B, Poupon MF. The peripheral benzodiazepine receptor: a review. *J Neuro-Oncol*. 2000;46:45–56.
 13. Veenman L, Papadopoulos V, and Gavish M. Channel-like functions of the 18-kDa translocator protein (TSPO): regulation of apoptosis and steroidogenesis as part of the host-defense response. *Curr Pharm Design*. 2007;13:2385–405.
 14. Casellas P, Galiegue, Basile AS. Peripheral benzodiazepine receptors and mitochondrial function. *Neurochem Int*. 2002;40:475–86.
 15. Kokoszka JE, Waymire KG, Levy SE, Sligh JE, Cai J, Jones DP, MacGregor GR, Wallace DC. The ADP/ATP translocator is not essential for the mitochondrial permeability transition pore. *Nature*. 2004;427:461–5.
 16. Krauskopf A, Eriksson O, Craigen WJ, Forte MA, Bernardi P. Properties of the permeability transition in VDAC1(-/-) mitochondria. *Biochim Biophys Acta*. 2006;1757:590–5.
 17. Nakagawa T, Shimizu S, Watanabe T, Yamaguchi O, Otsu K, Yamagata H, Inohara H, Kubo T, Tsujimoto Y. Cyclophilin D-dependent mitochondrial permeability transition regulates some necrotic but not apoptotic cell death. *Nature*. 2005;434:652–8.
 18. Šileikytė J, Petronilli V, Zulian Z, Dabbeni-Sala F, Tognon G, Nikolov P, Bernardi P, and Ricchelli F. Regulation of the inner membrane mitochondrial permeability transition by the outer membrane translocator protein (peripheral benzodiazepine receptor). *J Biol Chem*. 2011;286:1046–53.
 19. Salet C, Moreno G, Ricchelli F, and Bernardi P. Singlet oxygen produced by photodynamic action causes inactivation of the mitochondrial permeability transition pore. *J Biol Chem*. 1997;272(35):21938–43.
 20. Ricchelli F, Šileikytė J, Bernardi P. Shedding light on the mitochondrial permeability transition. *Biochim Biophys Acta*. 2011;1807:482–90.
 21. Petronilli V, Šileikytė J, Zulian A, Dabbeni-Sala F, Jori G, Gobbo S, Tognon G, Nikolov P, Bernardi P, Ricchelli F. Switch from inhibition to activation of the mitochondrial permeability transition during hematoxylin-mediated photooxidative stress. Unmasking pore-regulating external thiols. *Biochim Biophys Acta*. 2009;1787:897–904.
 22. McEnery MW, Snowman AM, Trifiletti RR, Snyder SH. Isolation of the mitochondrial benzodiazepine receptor: association with the voltage-dependent anion channel and

- the adenine nucleotide carrier. *Proc Natl Acad Sci USA*. 1992;89:3170–4.
23. Hirsch T, Decaudin D, Susin SA, Marchetti P, Larochette N, Resche-Rigon M, Kroemer G. PK11195, a ligand of the mitochondrial benzodiazepine receptor, facilitates the induction of apoptosis and reverses Bcl-2-mediated cytoprotection. *Exp Cell Res*. 1998;241:426–34.
 24. Chelli B, Falleni A, Salvetti F, Gremigni V, Lucacchini A, Martini C. Peripheral-type benzodiazepine receptor ligands: mitochondrial permeability transition induction in rat cardiac tissue. *Biochem Pharmacol*. 2001;61:695–705.
 25. Azarashvili T, Stricker R, Reiser G. The mitochondria permeability transition pore complex in the brain with interacting proteins—promising targets for protection in neurodegenerative diseases. *Biol Chem*. 2010;39:619–29.
 26. Pastorino JG, Simbula G, Gilfor E, Hoek JB, and Farber JL. Protoporphyrin IX, an endogenous ligand of the peripheral benzodiazepine receptor, potentiates induction of the mitochondrial permeability transition and the killing of cultured hepatocytes by rotenone. *J Biol Chem*. 1994;269:31041–6.
 27. Verma A, Nye J, Snyder SH. Porphyrins are endogeneous ligands for the mitochondrial (peripheral-type) benzodiazepine receptor. *Proc Natl Acad Sci USA*. 1987;84:2256–60.

2.3. Characterization of PTP in TSPO-null liver mitochondria

As also mentioned before, TSPO was attributed a variety of biological functions including taking part (or at least regulating) the mitochondrial PTP. As the initial attempts to generate TSPO-null animals led to early embryonic death, the “golden standard” in the field has been the use of high affinity TSPO ligands, such as PP IX, PK11195 and Ro5-4864. On this basis the involvement of TSPO in PT was suggested by others [214, 216, 217] and was also supported by our own results (see *Papers 1, 2 and 3*). We have shown that all of these compounds can activate the PT in a CsA-sensitive manner in isolated rat liver mitochondria, but not mitoplasts.

In order to investigate the role of TSPO in PTP regulation directly, in collaboration with Dr. M. Forte (Vollum Institute, Portland, Oregon) we created a mouse line in which the *Tspo* gene could be conditionally inactivated. We characterized TSPO-null mitochondria from these mice and showed that: (i) isolated TSPO-null liver mitochondria possess a CsA-sensitive PTP, ruling out that TSPO is required for the PT to occur; (ii) TSPO ligands PP IX, PK11195 and Ro5-4864 induced the PT in isolated liver mitochondria lacking TSPO with the same concentration-dependence as they did in littermate controls; and (iii) upon photooxidative stress in mitochondria treated with PP IX (high light dose) PT was also induced in TSPO-null mitochondria. The latter findings are the first unequivocal demonstration that the ability of ‘specific’ TSPO ligands to regulate PTP is due to off-target effects.

The details of this study, which is being submitted for publication (Šileikytė J et al.), are reported in the following sections.

2.3.1. Materials and methods

2.3.1.1. Reagents

PP IX, DP IX and HP IX were obtained from Frontier Scientific (Logan, UT) and stock solutions were prepared in dimethylsulfoxide. Cu(OP)₂ was prepared just before use by mixing CuSO₄ with *o*-phenanthroline at a molar ratio of 1:2 in bidistilled water. PK11195, Ro5-4864, PhAsO, oligonucleotides and all generic reagents were from Sigma-Aldrich. Calcium Green-5N was from Invitrogen. [³H]PK11195 (85.7 Ci/mmol) and Ultima Gold scintillation cocktail were from Perkin Elmer. Genomic mouse DNA was isolated with DNeasy Blood and Tissue Kit from QIAGEN, Finnzymes 2X Phusion HF master mix was used for PCR. Nitrocellulose membrane was from GE Healthcare, Enhanced chemiluminence kit – from Millipore.

All chemicals were of the highest purity commercially available.

2.3.1.2. Generation of TSPO-null mouse livers

In the mouse genome, the TSPO is encoded by the nuclear *Tspo* gene, located on Chromosome 15. Initial attempts to generate animals lacking expression of the TSPO have indicated that non-conditional elimination of TSPO expression results in embryonic lethality. Consequently, our group (led by Dr. M. Forte Vollum Institute, Portland, Oregon) used *Cre/loxP* site-specific recombination system to conditionally eliminate *Tspo* gene in the mouse liver.

2.3.1.2.1. *Cre-loxP* recombination system

Routinely, the *Cre/loxP* site-specific recombination has proven to be a powerful tool to achieve tissue-specific manipulations of genes in mice. It was discovered in P1 bacteriophage as part of this organism's normal viral live cycle [227, 228]. The bacteriophage uses *Cre/loxP* recombination to circularize and facilitate replication of its genomic DNA when reproducing. The system requires only two components:

- 1) *Cre* recombinase, a 38 kDa enzyme that catalyzes the recombination between two its recognition sites, called *loxP* sites;

2) *LoxP* (locus of X-over P1) sites, which are bacteriophage specific 34 bp sequences. They consist of an 8 bp core sequence, where recombination takes place, and two flanking 13 bp inverted repeats [229]. (Figure 6)

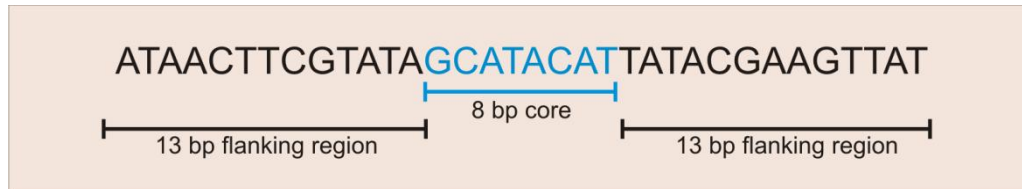


Figure 6. The 34 bp *loxP* sequence.

2.3.1.2.2. Modification of mouse *Tspo* locus

In order to generate *Tspo* replacement gene for the use of the *Cre/loxP* conditional gene elimination strategies, bacterial artificial chromosome (BAC) clones containing the *Tspo* gene on Chrom-15 from C57Bl/6J mice (C57) were obtained from libraries maintained by the Children's Hospital Oakland Research Institute (clone number RP23-121MC).

The *Tspo* gene (Figure 7A) spans 4 exons (exon1 is a non-translated exon) and encompasses 10.6 kB of genomic DNA. Subclones containing *Tspo* protein coding exons were modified in two ways:

- 1) the insertion of *loxP* sites in intronic sequence flanking exons 2 and 3, resulting in the elimination of residues encoding the translational start site through amino acid 124 on *Cre*-mediated recombination *and*
- 2) the addition of the *neo* gene (that renders cells resistant to antibiotic G418) between *loxP* sites and flanked by flippase recognition target (*FRT*) sites that are recognized by the *FRT* recombinase (*FLP*) from yeast [230-232] (Figure 7B, C).

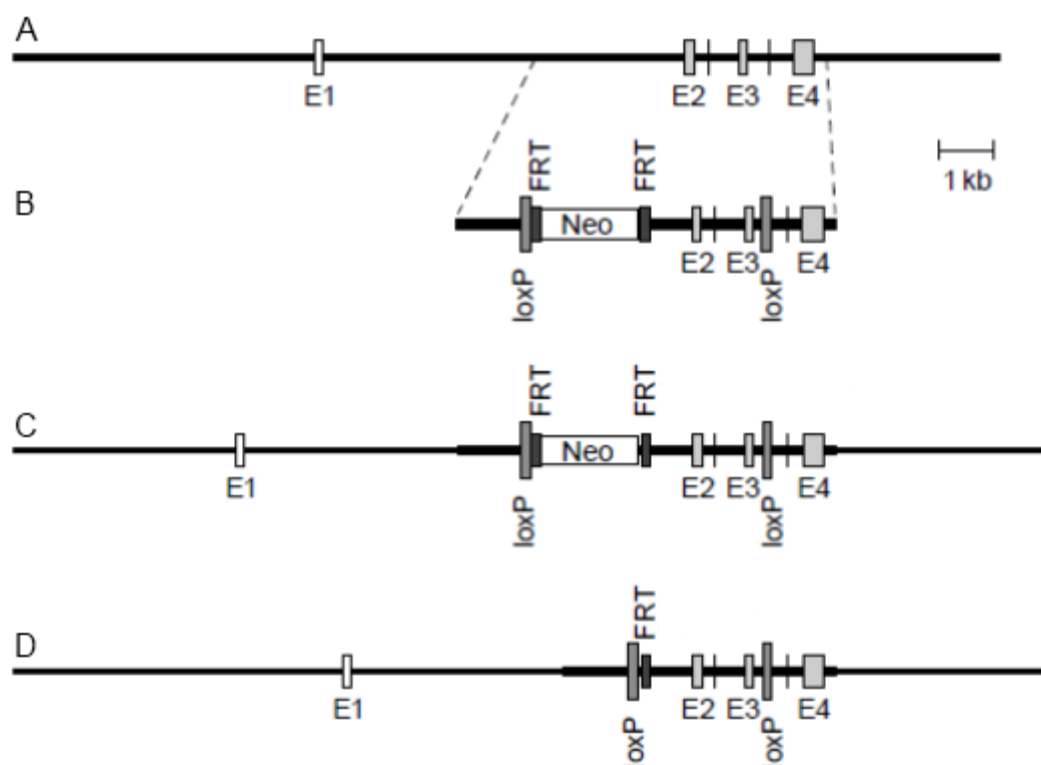


Figure 7. Mouse *Tspo* locus and modifications.

A, map of the mouse *Tspo* locus. E1-E4 indicate exons 1-4; E1 is a non-coding exon.

B, modified *Tspo* DNA construct used to transfect ES cells. *Neo* is the neomycin resistance gene; FRT, FLP recombination sites; *loxP*, *Cre* recombination sites.

C, mouse *Tspo* locus after recombination with construct *B*.

D, *Tspo* locus as in *C*, but after recombination at FRT sites to remove the *neo* gene.

2.3.1.2.3. Generation of mice in which the *Tspo* gene contains *loxP* sites

To generate mice in which the expression of TSPO has been eliminated, C57 ES cells were cultured using standard conditions, transfected by electroporation with the targeting construct described in Figure 7B, transfectants selected with appropriate antibiotic (G418), and candidate ES cells screened for replacement of the endogenous *Tspo* gene with the targeting construct by PCR analysis and Southern blotting. Five candidate ES cell lines were identified, injected into C57 MF-1 blastocysts (an albino variant of black C57) and evaluated for the ability to generate chimeric offspring (black coat color on a normally white background). Of the five ES cell lines identified, two were able to successfully generate chimeric offspring ($\geq 95\%$ black). Male chimeras were subsequently mated with C57 female mice and all offspring evaluated for germ line transmission. Several of the males from two targeted ES cell lines were able to pass the modified *Tspo* gene to progeny.

F1 heterozygotes carrying the targeted allele were mated to mice expressing the FLP1 recombinase from yeast driven by the Gt(ROSA)26Sor promoter. In this “deletor strain”, FLP1 recombinase is constitutively expressed from pre-implantation onward resulting in progeny in which the *neo* gene used for selection of ES cells containing modified *Tspo* genes has been eliminated. The progeny was tested for the elimination of the *neo* gene by PCR analysis of genomic DNA (final gene shown in Figure 7D) and homozygotes for the *Tspo* containing *loxP* sites were established.

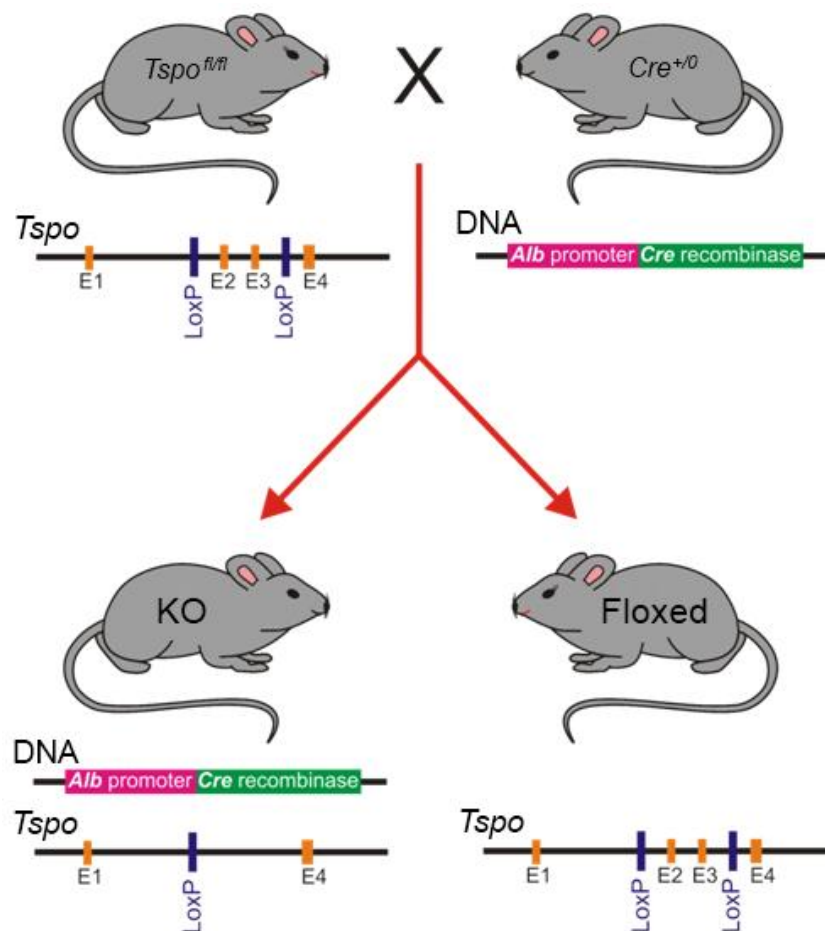


Figure 8. Generation of mice in which the *Tspo* gene was inactivated only in livers.

Simplified version, for details see the text.

Tspo^{fl/fl} – mouse lines homozygous for the *Tspo* gene containing *loxP* sites.

Cre^{+/0} – mouse lines heterozygous for the *Cre* recombinase driven by *Albumin* promoter.

KO – the progeny that acquired both of the above mentioned constructs, Floxed – the ones that express only *Tspo* gene containing *loxP* sites, but no *Cre* recombinase.

Finally, the above mentioned mice were mated to mice heterozygous for *Cre* recombinase driven by hepatocyte specific albumin (*Alb*) promoter. The offspring that were positive for *Cre* were then mated to each other to establish lines that were *Cre* positive and homozygous for a *Tspo* gene containing flanking *loxP* sites. Lastly, the latter were mated to each other or to homozygotes carrying only modified *Tspo* allele and the progeny that had an *Alb-Cre* recombinase expressed, had an inactivated *Tspo* in hepatocytes (thus generating TSPO-null liver) while retaining normal gene function in all other types of cells, and are called 'KO' throughout this Thesis, while their littermates that contain only the modified *Tspo* gene, but no *Cre*, are called 'floxed' (Figure 8).

2.3.1.3. Mice genotyping

In order to distinguish the TSPO KO mice from their littermate controls the mice were genotyped by the polymerase chain reaction (PCR).

Briefly, the pups were numbered and tailed at weaning and their genomic DNA was extracted with *DNeasy Blood and Tissue Kit* from *QIAGEN* according to manufacturer's instructions. Afterwards, the PCRs for the *Tspo* containing *loxP* sites (TSPO) and *Cre* recombinase (*Cre*) were performed. Each PCR reaction tube contained in Table 2 reported components. The sequences of the primers used are indicated in Table 3. The PCR reaction mixtures were loaded into thermocycler (Bio-rad) and cycling programs denoted in Table 4 were run. PCR products were analyzed by electrophoresis on a Syber Safe stained 1% agarose gel, followed by visualization under UV light with the ChemiDoc XRS System (Bio-Rad).

Table 2. Composition of the PCR reaction mixture.

Component	Volume (μ l)	Final concentration
2X Phusion HF Master mix	12.5	1X
Working Primer mix*	11.5	1 μ M each
DNA	11	

*Working Primer mix contained 2.17 μ M of both Forward and Reverse primers.

Table 3. The list of primers used in PCR. Fwd – forward, Rev – reverse.

Primer name	Sequence (5'-3')
TSPO Fwd	ACCCAGAGTTTGCCAATTGC
TSPO Rev	CTCTGGGCTGAAATCAAGAC
Cre Fwd	GCGTCTGGCAGTAAAACTATC
Cre Rev	GTGAAACAGCATTGCTGTCACTT

Table 4. Cycling programs used to amplify *Tspo* gene region containing *loxP* sites (TSPO) and a part of Cre recombinase DNA (Cre).

Cycle step	TSPO			Cre		
	Temp °C	Time	Cycle	Temp °C	Time	Cycle
Denaturation	96	2 min	-	94	3 min	-
Denaturation	96	1min		94	30 sec	
Annealing	55	45 sec	34	51.7	1 min	35
Extention	72	1 min		72.1	1 min	
Final Anneling	72	2 min	-	72	2 min	-

2.3.1.4. Isolation of mitochondria

TSPO-null and floxed mouse liver mitochondria were prepared by standard differential centrifugation. Livers were removed and placed in a glass beaker containing ice-cold 0.25 M sucrose, 10 mM Tris-HCl pH 7.4, 0.1 mM EGTA-Tris buffer (Isolation buffer -IB-) supplemented with a small amount of Bovine serum albumin.

Livers were then cut into small pieces with scissors, rinsed with ice-cold IB (to remove as much blood as possible) and passed through a pre-chilled Potter homogenizer with theflon pestle. The homogenate (~ 60 ml) per liver was transferred to 2 Beckman F0650 rotor centrifuge tubes. Unbroken cells and nuclei were removed by centrifugation at 2700 RPM (685 *g*) for 10 minutes in a refrigerated Beckman Allegra-64R centrifuge at 4°C. The supernatant containing mitochondria and other organelles was transferred to new tubes and centrifuged at 8000 RPM (6010 *g*) for 10 minutes at the same temperature. The resulting supernatant was discarded, mitochondrial pellet carefully suspended in ice-cold IB

buffer and spun at 10000 RPM (9390 *g*) for 5 minutes at 4°C. The mitochondrial pellet was suspended in IB to give a protein concentration of about 60-80 mg/ml and stored on ice.

2.3.1.4.1. Protein determination by Biuret method

Mitochondrial protein concentration was determined by Biuret method as follows: 20 µl of mitochondria (*sample*; omitted for the *reference*) were suspended in 1 ml of H₂O + 0.5 ml of 1% deoxycholic acid + 1.5 ml of Biuret reagent [233]. Both solutions were put in a thermostated bath (100 °C) for 1 minute and then cooled with cold water. Next, the absorbance of the sample solution was read at 540 nm and the total protein concentration was determined using standard calibration curve.

2.3.1.5. Western blotting

Mitochondrial proteins were solubilized in loading buffer (2 % SDS, 50 mM Tris-HCl, pH 6.8, 10% glycerol, 2,5% β-mercaptoethanol, 0.002% bromphenol blue), boiled for 5 min and separated by 15% SDS-PAGE. The proteins were then electrophoretically transferred to nitrocellulose membrane (GE Healthcare) using a Mini Trans-Blot system (Bio-Rad).

To minimize the non specific binding, the membrane was blocked with TBST (10 mM Tris-HCl, pH 7.4, 150 mM NaCl, 0.01% Tween 20) buffer containing 5% nonfat dry milk at room temperature for 1 h, followed by an overnight incubation with an anti-TSPO (a generous gift of Dr. V. Papadopoulos) or monoclonal anti-ANT (MitoSciences) antibody. The membrane was then washed in TBST and subjected to 1 h incubation with appropriate secondary antibody conjugated to horseradish peroxidase. The membrane was washed again in TBST buffer and immunoreactive bands were detected by enhanced chemiluminescence (Millipore).

2.3.1.6. Radioligand binding assay

The presence of the TSPO in mitochondrial membranes was assayed by the use of [³H]PK11195 (85.7 Ci/mmol), a specific TSPO ligand [203]. Liver mitochondria were isolated as described in paragraph 2.3.1.4 and mitochondrial protein was adjusted to 0.1 mg/ml in Tris buffer (50 mM Tris-HCl, pH 7.4, 4°C) to a final assay volume of 200 µl. The

suspensions were incubated with 0.05-9.6 nM radioligand or 10 μ M PK11195 (for background correction) for 60 min at 4°C. Assays were terminated by the rapid vacuum filtration through Whatman GF/C glass microfiber filters. The filters were immediately washed first with 1 ml of 10 μ M PK11195 in Tris buffer (in order to wash-out filter bound radioligand), then with additional 15 ml of ice cold 50 mM Tris-HCl, pH 7.4. Subsequently the membranes were dried, placed in 5ml of liquid scintillation counting cocktail Ultima gold (Perkin Elmer), vortexed and assayed for ^3H using Packard Tri-Carb 1500 Liquid Scintillation Analyzer.

2.3.1.7. Measurement of mitochondrial respiration

Experiments were initiated by the addition of 2 ml of Assay buffer (250 mM sucrose, 10 mM MOPS-Tris, 10 μ M EGTA-Tris, 5 mM succinate-Tris, 1 mM Pi-Tris and 1 μ M rotenone, pH7.4) to the chamber. When the recorded trace was stable, an aliquot of mitochondrial suspension to give a final concentration of 1.0 mg/ml was added. The chamber was then sealed with a frosted glass stopper and further additions were made through a small syringe port in the stopper. Basal mitochondrial respiration (analogous to respiratory state 4, as described by Chance and Williams [234]) was measured, followed by the addition of 0.3 mM ADP, which allowed to measure state 3 [234] respiration, and finally oligomycin (0.5 μ g/ml) and carbonyl cyanide *p*-trifluoromethoxyphenylhydrazone (FCCP; 0.1 μ M). The respiratory control ratio (RCR) was calculated as the ratio between ADP-stimulated and basal respiratory rates. All experiments were performed at 25 °C under magnetic stirring.

2.3.1.8. Estimation of mitochondrial membrane potential

Mitochondrial inner membrane potential ($\Delta\psi$) was assessed with the potentiometric fluorescent probe Rhodamine 123 (Rh123, Figure 9) [235], a lipophilic cation, which readily equilibrates across the IMM and accumulates in the matrix of energized mitochondria because of the inside negative $\Delta\psi$. The accumulation was shown to follow Nernst equation [236], and can be monitored because the probe concentrates in the matrix forming aggregates that cause a process of fluorescence quenching.

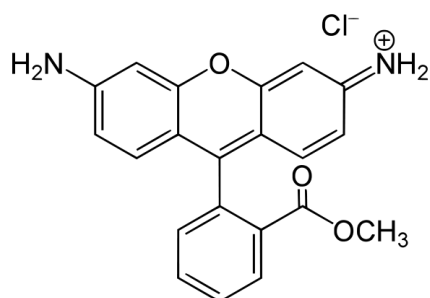


Figure 9. Structure of Rhodamine 123.

Rh123 ($\lambda_{\text{excitation}}=503$ nm, $\lambda_{\text{emission}}=523$ nm) fluorescence intensity changes were monitored with a PerkinElmer Life Sciences LS50 spectrofluorimeter: 2 ml of assay buffer (250 mM sucrose, 10 mM MOPS-Tris, 10 μ M EGTA-Tris, 1 mM Pi-Tris and 1 μ M rotenone) was supplemented with 0.3 μ M Rh123, followed by the addition 0.5 mg/ml mitochondria, 5 mM succinate and 0.5 μ M FCCP. All experiments were performed at 25 °C under magnetic stirring.

2.3.1.9. Ca^{2+} retention capacity (CRC) test

The Ca^{2+} retention capacity (CRC) is one of the most sensitive assays to assess the propensity of the PTP to open [58]. The test measures the amount of Ca^{2+} that mitochondria can accumulate and retain before the precipitous release that marks PTP opening.

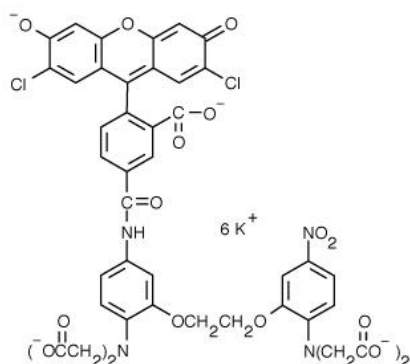


Figure 10. Structure of Calcium Green-5N.

Extramitochondrial Ca^{2+} fluxes were measured fluorimetrically using Calcium Green-5N (excitation-emission λ : 505-535 nm) (Figure 10), a low affinity membrane-impermeant probe which increases its fluorescence emission upon Ca^{2+} binding. Mitochondria (0.5 mg/ml) were suspended in 2 ml of Assay buffer that also contained 0.5 μM Calcium Green-5N and the suspension was subjected to train of Ca^{2+} pulses (typically 40 μM each).

2.3.1.10. Permeability transition assessed on the osmotic swelling of mitochondria

A classical approach to detect occurrence of the PT is to follow osmotic swelling of isolated mitochondria as measured by the decrease of light scattering at 540 nm. Indeed, the amount of light scattering (LS) by mitochondrial suspension depends on matrix volume [237], which increases during PT lowering the refraction index of the suspension. This results in a large decrease in LS, as measured at 90° using Perkin Elmer Life Sciences LS50 spectrofluorimeter equipped with magnetic stirring and thermostatic control. The experiments were performed at 25 $^\circ\text{C}$ in Assay buffer (*see* paragraph 2.3.1.7) supplemented with 0.5 mg/ml mitochondria. Permeabilization rates were calculated as the rate of change of LS immediately after addition of Ca^{2+} .

2.3.1.11. Photosensitization of mitochondria

Mitochondria were suspended in Assay buffer, and porphyrins were added under gentle stirring at room temperature. After 5 min, the suspensions were centrifuged at 10,000 g for 1 min. Supernatant was diluted 1:1 ratio with 2% SDS, pellet was suspended in 2% SDS and the OD of the suspensions at Soret band was registered. Porphyrin concentrations were determined by Lambert-Beer law based of the extinction coefficient of the porphyrins. Porphyrin-mediated photosensitization of mitochondria achieved as described previously [81]. Briefly, preparations were incubated for 1–2 min in the dark with the desired concentration of porphyrin and then irradiated at 365 nm with a Philips HPW 125-watt lamp. The fluence rate at the level of the preparations (56 W/m^2) was measured with a calibrated quantum photo radiometer (Delta OHM HD9021). All irradiations were performed at 25 $^\circ\text{C}$ under magnetic stirring.

2.3.2. Results and Discussion

As already mentioned, most studies on TSPO have been performed using high-affinity ligands, and only few of them were complemented by manipulation of TSPO expression. Many conclusions in the field of cell death have been undermined by the demonstration that similar effects of 'TSPO ligands' can be observed in cells where expression of TSPO has been suppressed [184, 225]. Thus, there is emerging evidence of TSPO-independent effects of 'TSPO ligands'. To directly investigate the role of TSPO in PTP, we created mice in which the protein was eliminated specifically in the livers. The mice were viable, developed normally and had no apparent phenotype, Figure 11A.

PCR analysis of genomic DNA from *Tspo*^{+/+} (WT), *Tspo*^{fl/fl} (floxed) and *Tspo*^{fl/fl} *Cre*^{+/-} (KO) mice confirmed that: (i) neither *loxP* nor *Cre* is expressed in WT mice; (ii) only *loxP* is expressed in floxed mice; (iii) both of the constructs are expressed in KO mice (Figure 11B, *upper panel*). The TSPO protein levels were assessed by SDS-PAGE and subsequent western blotting. TSPO expression in *Tspo*^{fl/fl} animal liver mitochondria was not altered by the insertion of *loxP* sites, while TSPO was undetectable in *Tspo*^{fl/fl} *Cre*^{+/-} mice liver mitochondria; on the other hand, expression of ANT was identical in the three genotypes (Figure 11B, *lower panel*). Transmission electron microscopy (TEM) analysis revealed no obvious ultrastructural difference between floxed and KO mouse liver mitochondria. Both of them possessed a well defined OMM, finger-like *cristae* infoldings and an electron dense matrix (Figure 11C, D).

TSPO ligands were demonstrated to increase state 4 and decrease state 3 respiration rates resulting in a decrease in respiratory control ratio (RCR) [240]. Thus, we wondered if the absence of TSPO had any effect on oxygen consumption rates. Mitochondria were isolated from floxed and KO mouse livers and assayed in sucrose-based medium (250 mM sucrose, 10 mM MOPS-Tris, 10 μ M EGTA-Tris, 1 mM Pi-Tris, pH7.4) supplemented with complex II substrate succinate-Tris (5 mM) and complex I inhibitor rotenone (1 μ M). The KO mitochondria most often displayed slightly lower rates of basal, ADP- and uncoupler-stimulated respiration compared with mitochondria isolated from floxed animal livers (results not shown); however, the difference in the RCRs were not significant (Figure 12A). Further, we measured mitochondrial membrane potential based on the changes in fluorescence quenching of Rh123. Both mitochondrial preparations readily developed $\Delta\Psi$

(~ -180 mV) upon addition of succinate; and $\Delta\Psi$ could be abolished by the uncoupler FCCP (Figure 12).

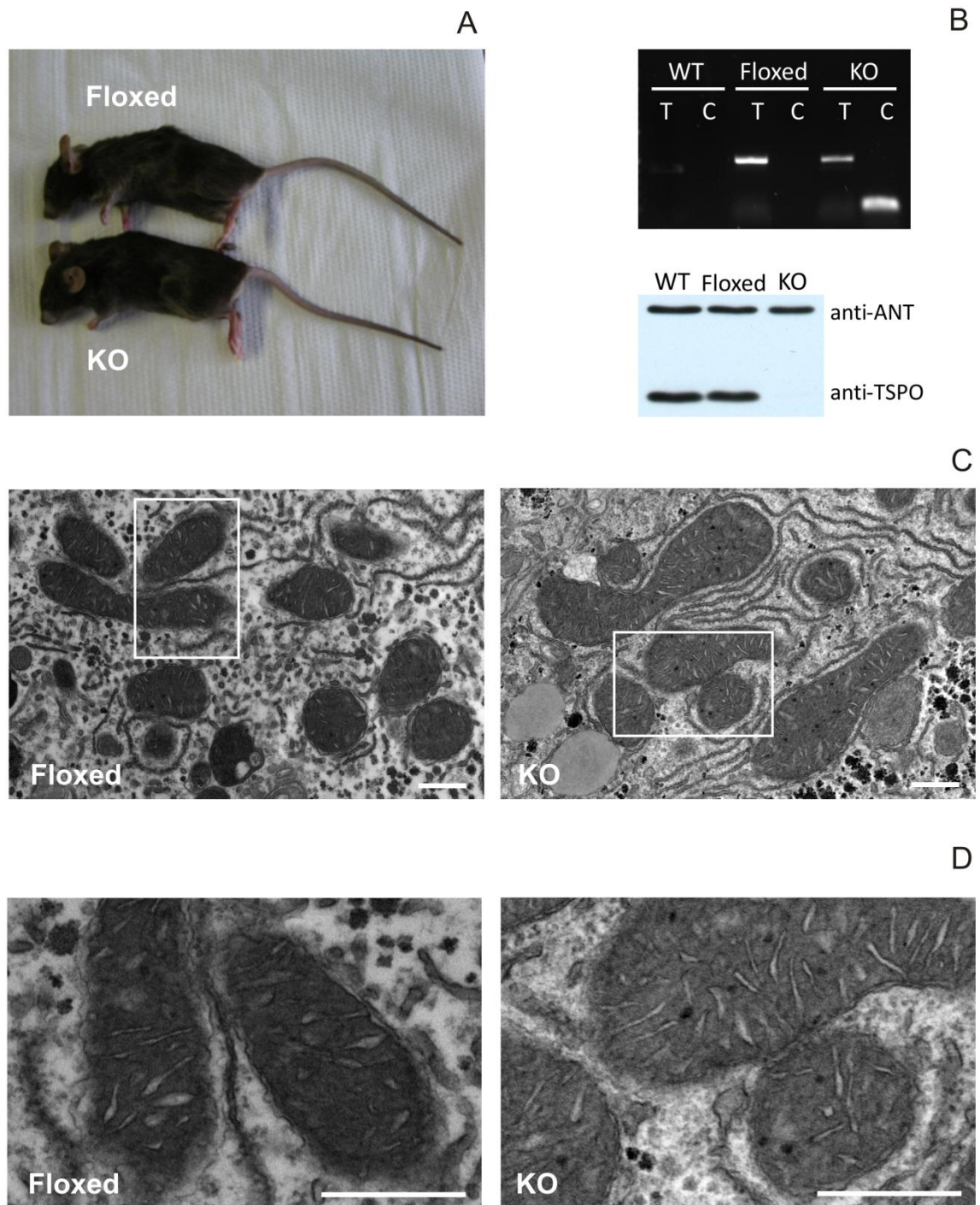


Figure 11. TSP0-null mice have no obvious phenotype.

A, *Tspo*^{*f/f*} (Floxed) and *Tspo*^{*f/f*} *Cre*^{*+/-*} (KO) animals. *B*, upper panel: agarose gel electrophoresis of PCR amplification products of mice genomic DNA; T – primer set for *Tspo*^{*f/f*}, C – for *Cre* recombinase; lower panel: western blot analysis of mitochondria isolated from *Tspo*^{*+/+*} (WT), Floxed and KO mice livers. ANT antibody was used as a loading control. *C* and *D*, transmission electron microscopy of floxed and KO mice livers, bars: 500 nm. Panel *D* represents the 3X magnification of the areas boxed in panel *C*.

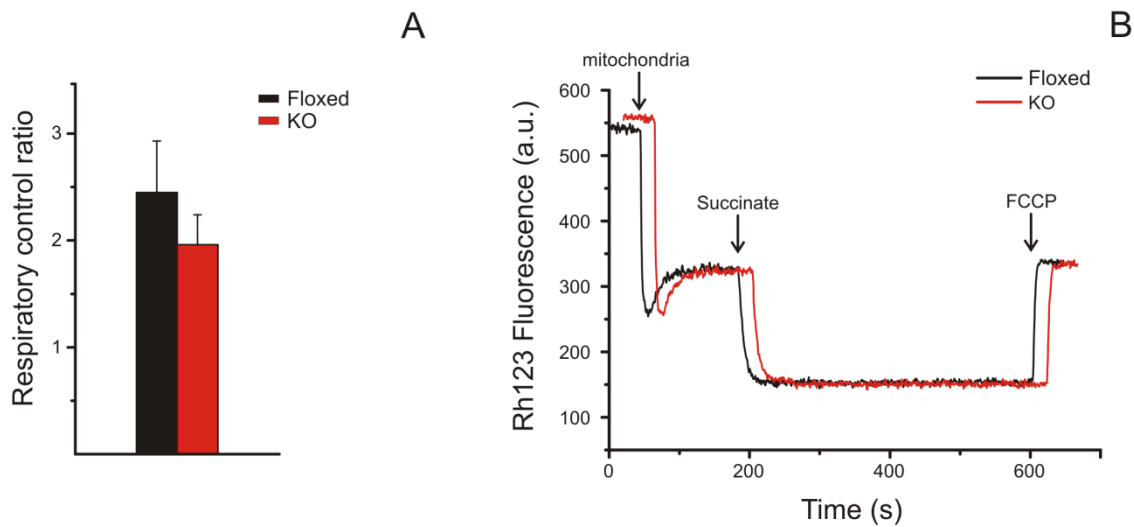


Figure 12. The absence of TSPO does not affect mitochondrial respiration and development of $\Delta\Psi$.

A, respiratory control ratios, *i.e.* ratios between ADP-stimulated and basal oxygen consumption rates (OCR), of *Tspo* ^{β/β (Floxed) and *Tspo* ^{β/β *Cre*^{+/⁰ (KO) mitochondria. Error bars represent the mean \pm S.D. of at least three independent experiments. B, typical traces of $\Delta\Psi$ measurement of floxed and KO liver mitochondria. Additions were made as indicated in the graph.}}}

The OCR and $\Delta\Psi$ were measured as described in Materials and Methods.

We next tested the ability of TSPO-null mitochondria to undergo PT with the sensitive CRC test. KO mitochondria readily took up a train of Ca^{2+} pulses (Figure 13B, *trace a*) in a process that was sensitive to CsA (Figure 13B, *trace b*). The Ca^{2+} load required to trigger PTP opening, as well as the desensitizing effect of CsA, was indistinguishable from that of floxed mitochondria (Figure 13A) ruling out that TSPO is required for the PTP to occur.

In order to investigate whether TSPO plays a regulatory role in the PT, we challenged floxed and KO mouse liver mitochondria with TSPO-ligands PK11195 (100 μM), Ro5-4864 (100 μM) and PP IX (8 μM) (Figure 14 *traces b, c* and *d*, respectively) and tested their effect on the CRC. As expected, all of the compounds lowered the CRC of floxed liver mitochondria (Figure 14A). Surprisingly, however, we observed exactly the same response of TSPO-null mitochondria to the inducing effects of PK11195, Ro5-4864 and PP IX (Figure 14B *traces b, c* and *d*, respectively), which could be prevented by 1 μM CsA (data not shown).

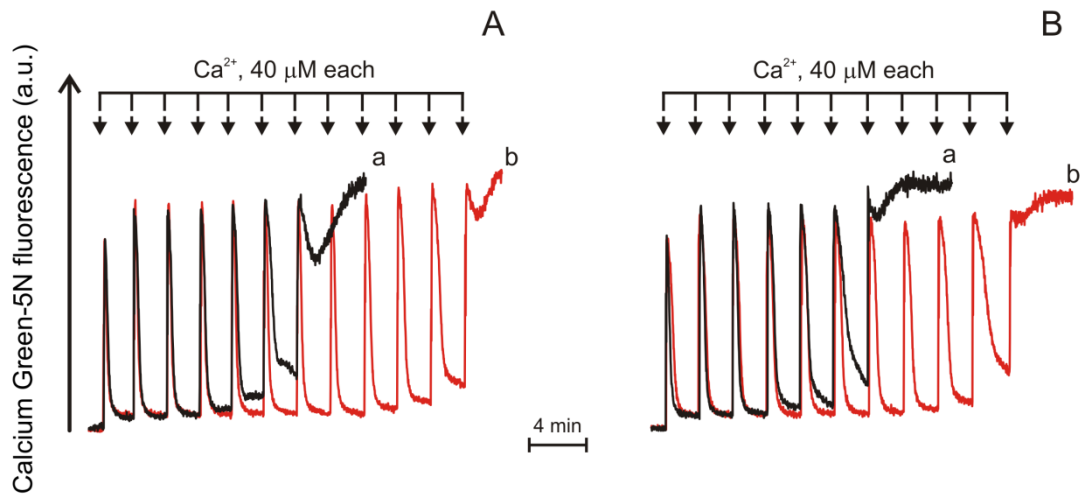


Figure 13. CRC of floxed and KO mouse liver mitochondria.

Floxed (A) and KO (B) mouse liver mitochondria (0.5 mg/ml) were suspended in Assay buffer supplemented with 0.5 μM Calcium Green-5N, and loaded with a train of Ca^{2+} pulses, *traces a*. In *traces b* medium was supplemented with 1 μM CsA. Representative traces of at least five independent experiments.

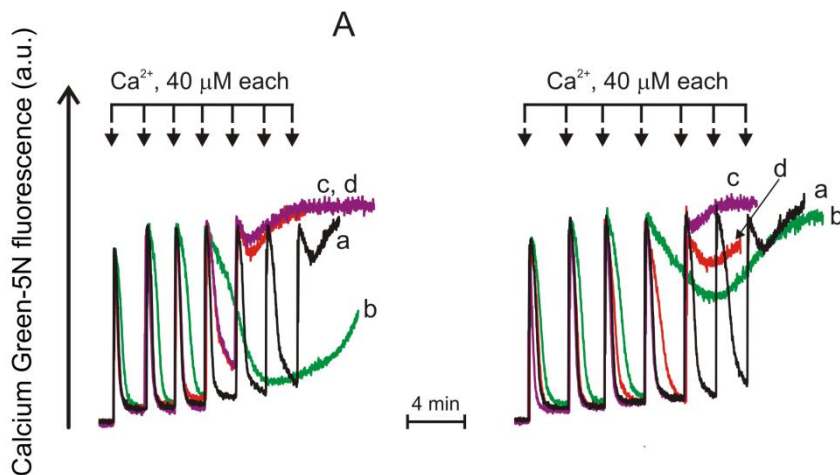


Figure 14. Effect of PK11195, Ro5-4864 and PP IX on floxed and KO mouse liver mitochondria CRC.

Floxed (A) and KO (B) mouse liver mitochondria (0.5 mg/ml) were suspended in Assay buffer containing 0.5 μM Calcium Green-5N and loaded with a train of Ca^{2+} pulses, *traces a*. In *traces b, c* and *d* 100 μM PK11195, 100 μM Ro5-4864 and 8 μM PP IX, respectively, were added immediately prior to mitochondria. Representative traces of three independent experiments.

In isolated mitochondria PT can be modulated by photooxidative stress mediated by PP IX-like dicarboxylic porphyrins. Low doses of light inactivate the PTP, while higher light doses activate it [81]. As already mentioned, pore activation occurs through the OMM, since (unlike PTP inactivation) in mitoplasts the PT cannot be triggered after prolonged irradiation. Since porphyrins are ligands of TSPO, we proposed that PT photoactivation occurs through TSPO [238]. To test this hypothesis, we assessed the PT (measured as a decrease of light scattered at 540 nm) in floxed and KO mouse liver mitochondria upon photooxidative stress. Liver mitochondria

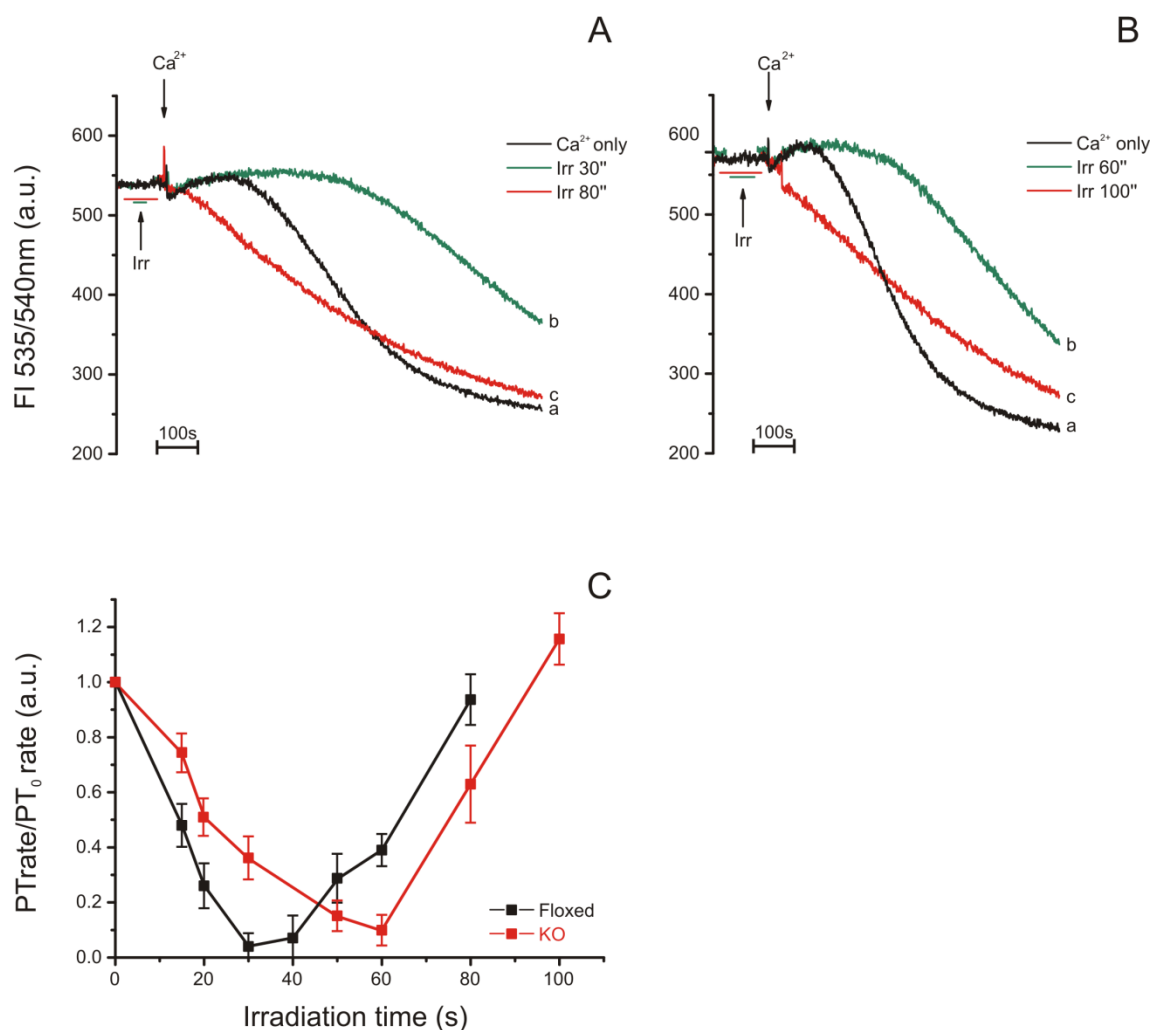


Figure 15. Effect of irradiation time in PP IX-treated floxed and KO mouse liver mitochondria. A, B, 0.5 mg/ml of PP IX-treated (0.5 μ M) floxed (A) or KO (B) liver mitochondria were challenged with 220 μ M Ca²⁺ (traces a); in traces b and c mitochondria were irradiated for the indicated time prior to Ca²⁺ addition. C, experiments were performed as in A and B, and permeabilization rates were normalized to those of non-irradiated mitochondria. A, B, represent typical traces, C, error bars mean \pm S.D. of three independent experiments.

from floxed (Figure 15A) or KO (Figure 15B) mice were incubated with 0.5 μM PP IX in Assay buffer in the dark; and PT was triggered with 220 μM Ca^{2+} (Figure 15A and B, traces *a*). Irradiation for short times expectedly [81, 238, 239] inhibited the PT in both genotypes (Figure 15A and B, traces *b*). The totally unexpected finding was that irradiation for longer times activated the PTP irrespective of the presence of TSPO (Figure 15A, B, traces *c*). When a full range of irradiation times was investigated, both inactivation and activation were somewhat shifted to the right, yet at striking variance from mitoplasts [238], activation did occur in TSPO-null mitochondria (Figure 15C). Since TSPO was implicated in porphyrin transport from OMM to IMM, we suspected that the difference might be explained by different amounts of porphyrin accumulated by the two types of mitochondria. This was not the case, as identical amounts of porphyrin were found in KO and in floxed mouse liver mitochondria. Furthermore, in both genotypes uptake was completed in less than 30 s (results not shown). We suspected that KO mice could express other TSPO isoforms [241]. We therefore studied binding profiles of [^3H]PK11195 in TSPO floxed and KO mitochondria (Figure 16). [^3H]PK11195 labelled floxed, but not KO liver mitochondria (Figure 16A), and Scatchard plots confirmed the existence of high affinity binding sites ($K_d = 1.2$ nM) only in TSPO floxed mitochondria (Figure 16B).

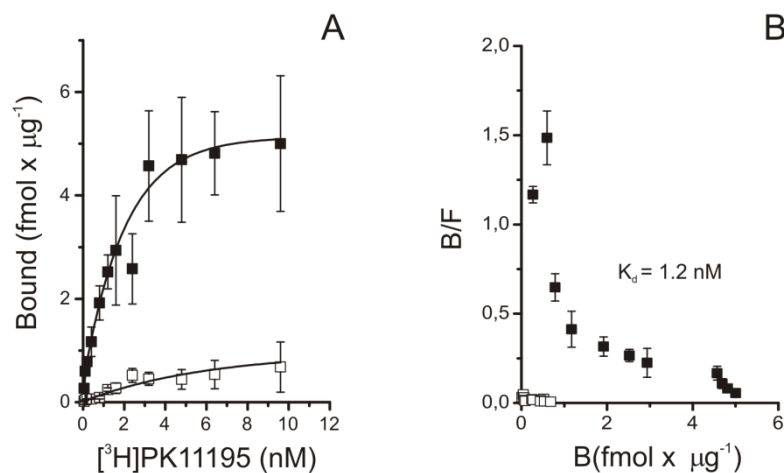


Figure 16. [^3H]PK11195 binding to TSPO floxed and KO mitochondria.

A, [^3H]PK11195 binding to floxed (*full squares*) and KO (*open squares*) liver mitochondria was assessed as described in Materials and Methods. *B*, Scatchard plots of experiments described in *A*. Error bars represent the mean \pm S.D. of three independent experiments performed in duplicate.

3. Conclusions

The results of the work presented in this Thesis are remarkable in many respects, and open a set of new questions both on the nature and function of the PTP and on the physiological role(s) of TSPO.

The first point is the demonstration that a PT can take place in the absence of an intact OMM. This finding in turn bears on the nature of the PTP, and on the mechanism(s) through which its opening affects mitochondrial pathophysiology. Indeed, we can predict that the pore will turn out to be an IMM protein or protein complex, whose opening causes membrane depolarization, Ca^{2+} release, changes of matrix volume, cristae junction rearrangement and mobilization of cyt *c*. Damage/rupture of the OMM leading to release of IMS proteins would be a secondary consequence of matrix expansion, and would occur only for extreme degrees of swelling. Thus, the PTP does not span the OMM and IMM, a physical arrangement that would be expected to release matrix solutes but certainly not cyt *c*, which would be in fact sealed off in the IMS [61]. Swelling must not necessarily take place in all mitochondria in the cell, resulting in a graded response. Indeed, affected mitochondria may release proapoptotic factors and intact mitochondria provide the ATP required for execution of apoptosis, while the involvement of the majority or of all mitochondria may switch the process toward necrosis, in keeping with earlier results demonstrating the key role of mitochondrial function in dictating the shape of cell death [244].

The second issue concerns the regulatory role of the OMM on PTP function, and how is this exerted. Our group as well as others have demonstrated that interactions of HK with the OMM decrease the probability of PTP opening [135, 136, 245] suggesting that OMM-IMM protein-protein interactions influence the propensity of the pore to open. As remarkably, our results demonstrate that the OMM can also **sensitize** the PTP to opening, since mitoplasts are protected from the pore-inducing effects of photosensitization by TSPO-binding porphyrins seen in intact mitochondria [238, 246]. In spite of our own predictions, the sensitizing effect cannot be due to the TSPO because it is observed in TSPO-null mitochondria which demonstrably lack high affinity binding sites for [^3H]PK11195. These results are very puzzling, and indicate that the inducing effects of FGIN1-27, PK11195, Ro5-4864, and PP IX on the PTP must be mediated by a different target. Data from the Glick laboratory show that many ligands of TSPO (such as the benzodiazepine Bz-423 and PK11195 analogs) bind to and inhibit the mitochondrial F_0F_1 ATP synthase [247, 248].

While the affinity displayed toward TSPO is in the nanomolar range, *i.e.* about 4 orders of magnitude lower than that required to sensitize the PTP, the concentrations required for the inhibitory effect on the ATP synthase match those on the PTP [238, 246]. Consistent with these findings, our laboratory has strong data supporting the idea that the PTP forms from dimers of the mitochondrial ATP synthase (Giorgio et al., submitted). While these results would explain the effects of 'TSPO ligands' on the PTP, what protein(s) mediate pore activation through the protoporphyrin-dependent photodynamic effect remains an open question.

The third issue concerns the lack of phenotypic effects of TSPO ablation. It must be stressed that gene inactivation was specific for the liver, *i.e.* an organ that is actively involved in steroid catabolism rather than production. Given the fact that TSPO is important in steroidogenesis but also in heme biosynthesis [249], we were surprised that no phenotypic alteration was detectable at the macroscopic, functional or ultrastructural level. It may well be that subtle differences exist that escaped our attention, or that other proteins may play a compensatory role. These issues, as well as the production of adrenal cortex TSPO-null mice, can now be addressed starting from our floxed strains.

4. References

1. Rasola A, Bernardi P. The mitochondrial permeability transition pore and its involvement in cell death and in disease pathogenesis. *Apoptosis*. 2007 May;12(5):815-33.
2. Ulivieri C. Cell death: insights into the ultrastructure of mitochondria. *Tissue Cell*. 2010 Dec;42(6):339-47.
3. Ernster L, Schatz G. Mitochondria: a historical review. *J Cell Biol*. 1981 Dec;91(3 Pt 2):227s-255s.
4. Alberts B, Johnson A, Lewis J, et al. *Molecular Biology of the Cell*. 4th edition. New York: Garland Science; 2002.
5. Frey TG, Renken CW, Perkins GA. Insight into mitochondrial structure and function from electron tomography. *Biochim Biophys Acta*. 2002 Sep 10;1555(1-3):196-203.
6. Elmore S. Apoptosis: a review of programmed cell death. *Toxicol Pathol*. 2007 Jun;35(4):495-516.
7. Herrmann JM, Riemer J. The intermembrane space of mitochondria. *Antioxid RedoxSignal*. 2010 Nov 1;13(9):1341-58.
8. Osellame LD, Blacker TS, Duchon MR. Cellular and molecular mechanisms of mitochondrial function. *Best Pract Res Clin Endocrinol Metab*. 2012 Dec;26(6):711-23.

9. Efremov RG, Baradaran R, Sazanov LA. The architecture of respiratory complex I. *Nature*. 2010 May 27;465(7297):441-5.
10. Efremov RG, Sazanov LA. Structure of the membrane domain of respiratory complex I. *Nature*. 2011 Aug 7;476(7361):414-20.
11. Zhou Q, Zhai Y, Lou J, Liu M, Pang X, Sun F. Thiabendazole inhibits ubiquinone reduction activity of mitochondrial respiratory complex II via a water molecule mediated binding feature. *Protein Cell*. 2011 Jul;2(7):531-42.
12. Crofts AR. The cytochrome bc₁ complex: function in the context of structure. *Annu Rev Physiol*. 2004;66:689-733.
13. Liu J, Qin L, Ferguson-Miller S. Crystallographic and online spectral evidence for role of conformational change and conserved water in cytochrome oxidase proton pump. *Proc Natl Acad Sci U S A*. 2011 Jan 25;108(4):1284-9.
14. Nicholls DG and Ferguson SJ. *Bioenergetics 3*. London: Academic Press; 2002.
15. Mitchell P. Coupling of phosphorylation to electron and hydrogen transfer by a chemi-osmotic type of mechanism. *Nature*. 1961 Jul 8;191:144-8.
16. De Stefani D, Raffaello A, Teardo E, Szabò I, Rizzuto R. A forty-kilodalton protein of the inner membrane is the mitochondrial calcium uniporter. *Nature*. 2011 Jun 19;476(7360):336-40.
17. Baughman JM, Perocchi F, Girgis HS, Plovanich M, Belcher-Timme CA, Sancak Y, Bao XR, Strittmatter L, Goldberger O, Bogorad RL, Koteliansky V, Mootha VK. Integrative genomics identifies MCU as an essential component of the mitochondrial calcium uniporter. *Nature*. 2011 Jun 19;476(7360):341-5.
18. Raffaello A, De Stefani D, Rizzuto R. The mitochondrial Ca²⁺ uniporter. *Cell Calcium*. 2012 Jul;52(1):16-21.
19. Drago I, Pizzo P, Pozzan T. After half a century mitochondrial calcium in- and efflux machineries reveal themselves. *EMBO J*. 2011 Sep 20;30(20):4119-25.
20. Rutter GA, Denton RM. Regulation of NAD⁺-linked isocitrate dehydrogenase and 2-oxoglutarate dehydrogenase by Ca²⁺ ions within toluene-permeabilized rat heart mitochondria. Interactions with regulation by adenine nucleotides and NADH/NAD⁺ ratios. *Biochem J*. 1988 May 15;252(1):181-9.
21. McCormack JG, Halestrap AP, Denton RM. Role of calcium ions in regulation of mammalian intramitochondrial metabolism. *Physiol Rev*. 1990 Apr;70(2):391-425.
22. Glancy B, Balaban RS. Role of mitochondrial Ca²⁺ in the regulation of cellular energetics. *Biochemistry*. 2012 Apr 10;51(14):2959-73.
23. Yamada EW, Huzel NJ. Ca²⁺-binding properties of a unique ATPase inhibitor protein isolated from mitochondria of bovine heart and rat skeletal muscle. *Cell Calcium*. 1985 Dec;6(6):469-79.

24. McCormack JG, Halestrap AP, Denton RM. Role of calcium ions in regulation of mammalian intramitochondrial metabolism. *Physiol Rev.* 1990 Apr;70(2):391-425.
25. Szabadkai G, Duchen MR. Mitochondria: the hub of cellular Ca²⁺ signaling. *Physiology (Bethesda).* 2008 Apr;23:84-94.
26. Szydlowska K, Tymianski M. Calcium, ischemia and excitotoxicity. *Cell Calcium.* 2010 Feb;47(2):122-9.
27. Baffy G, Miyashita T, Williamson JR, Reed JC. Apoptosis induced by withdrawal of interleukin-3 (IL-3) from an IL-3-dependent hematopoietic cell line is associated with repartitioning of intracellular calcium and is blocked by enforced Bcl-2 oncogene production. *J Biol Chem.* 1993 Mar 25;268(9):6511-9.
28. Giacomello M, Drago I, Pizzo P, Pozzan T. Mitochondrial Ca²⁺ as a key regulator of cell life and death. *Cell Death Differ.* 2007 Jul;14(7):1267-74.
29. Pizzo P, Drago I, Filadi R, Pozzan T. Mitochondrial Ca²⁺ homeostasis: mechanism, role, and tissue specificities. *Pflugers Arch.* 2012 Jul;464(1):3-17.
30. Rizzuto R, Pozzan T. Microdomains of intracellular Ca²⁺: molecular determinants and functional consequences. *Physiol Rev.* 2006 Jan;86(1):369-408.
31. Vaux DL, Korsmeyer SJ. Cell death in development. *Cell.* 1999 Jan 22;96(2):245-54.
32. Hotchkiss RS, Strasser A, McDunn JE, Swanson PE. Cell death. *N Engl J Med.* 2009 Oct 15;361(16):1570-83.
33. Galluzzi L, Maiuri MC, Vitale I, Zischka H, Castedo M, Zitvogel L, Kroemer G. Cell death modalities: classification and pathophysiological implications. *Cell Death Differ.* 2007 Jul;14(7):1237-43.
34. Orrenius S, Zhivotovsky B, Nicotera P. Regulation of cell death: the calcium-apoptosis link. *Nat Rev Mol Cell Biol.* 2003 Jul;4(7):552-65.
35. Kerr JF, Wyllie AH, Currie AR. Apoptosis: a basic biological phenomenon with wide-ranging implications in tissue kinetics. *Br J Cancer.* 1972 Aug;26(4):239-57.
36. Desagher S, Martinou JC. Mitochondria as the central control point of apoptosis. *Trends Cell Biol.* 2000 Sep;10(9):369-77.
37. Tait SW, Green DR. Mitochondria and cell death: outer membrane permeabilization and beyond. *Nat Rev Mol Cell Biol.* 2010 Sep;11(9):621-32.
38. Sheridan C, Martin SJ. Commitment in apoptosis: slightly dead but mostly alive. *Trends Cell Biol.* 2008 Aug;18(8):353-7.
39. Lemasters JJ. Dying a thousand deaths: redundant pathways from different organelles to apoptosis and necrosis. *Gastroenterology.* 2005 Jul;129(1):351-60.
40. Green DR. Apoptotic pathways: ten minutes to dead. *Cell.* 2005 Jun 3;121(5):671-4.

41. Muzio M, Chinnaiyan AM, Kischkel FC, O'Rourke K, Shevchenko A, Ni J, Scaffidi C, Bretz JD, Zhang M, Gentz R, Mann M, Krammer PH, Peter ME, Dixit VM. FLICE, a novel FADD-homologous ICE/CED-3-like protease, is recruited to the CD95 (Fas/APO-1) death-inducing signaling complex. *Cell*. 1996 Jun 14;85(6):817-27
42. Newton K, Harris AW, Bath ML, Smith KG, Strasser A. A dominant interfering mutant of FADD/MORT1 enhances deletion of autoreactive thymocytes and inhibits proliferation of mature T lymphocytes. *EMBO J*. 1998 Feb 2;17(3):706-18.
43. Yu JW, Shi Y. FLIP and the death effector domain family. *Oncogene*. 2008 Oct 20;27(48):6216-27.
44. Susin SA, Lorenzo HK, Zamzami N, Marzo I, Snow BE, Brothers GM, Mangion J, Jacotot E, Costantini P, Loeffler M, Larochette N, Goodlett DR, Aebersold R, Siderovski DP, Penninger JM, Kroemer G. Molecular characterization of mitochondrial apoptosis-inducing factor. *Nature*. 1999 Feb 4;397(6718):441-6.
45. Li LY, Luo X, Wang X. Endonuclease G is an apoptotic DNase when released from mitochondria. *Nature*. 2001 Jul 5;412(6842):95-9.
46. Bernardi P, Azzone GF. Cytochrome c as an electron shuttle between the outer and inner mitochondrial membranes. *J Biol Chem*. 1981 Jul 25;256(14):7187-92.
47. Gottlieb E. OPA1 and PARL keep a lid on apoptosis. *Cell*. 2006 Jul 14;126(1):27-9.
48. Cipolat S, Rudka T, Hartmann D, Costa V, Serneels L, Craessaerts K, Metzger K, Frezza C, Annaert W, D'Adamio L, Derks C, Dejaegere T, Pellegrini L, D'Hooze R, Scorrano L, De Strooper B. Mitochondrial rhomboid PARL regulates cytochrome c release during apoptosis via OPA1-dependent cristae remodeling. *Cell*. 2006 Jul 14;126(1):163-75.
49. Scorrano L, Ashiya M, Buttle K, Weiler S, Oakes SA, Mannella CA, Korsmeyer SJ. A distinct pathway remodels mitochondrial cristae and mobilizes cytochrome c during apoptosis. *Dev Cell*. 2002 Jan;2(1):55-67.
50. Bernardi P, Petronilli V, Di Lisa F, Forte M. A mitochondrial perspective on cell death. *Trends Biochem Sci*. 2001 Feb;26(2):112-7.
51. Hunter DR, Haworth RA, Southard JH. Relationship between configuration, function, and permeability in calcium-treated mitochondria. *J Biol Chem*. 1976 Aug 25;251(16):5069-77.
52. Hunter DR, Haworth RA. The Ca²⁺-induced membrane transition in mitochondria. I. The protective mechanisms. *Arch Biochem Biophys*. 1979 Jul;195(2):453-9.
53. Haworth RA, Hunter DR. The Ca²⁺-induced membrane transition of rat liver mitochondria. II. Nature of the Ca²⁺ trigger site. *Arch Biochem Biophys*. 1979 Jul;195(2):460-7.
54. Hunter DR, Haworth RA. The Ca²⁺-induced membrane transition in mitochondria. III. Transitional Ca²⁺ release. *Arch Biochem Biophys*. 1979 Jul;195(2):468-77.

55. Massari S, Azzone GF. The equivalent pore radius of intact and damaged mitochondria and the mechanism of active shrinkage. *Biochim Biophys Acta*. 1972;283(1):23-9.
56. Lemasters JJ, Nieminen AL, Qian T, Trost LC, Elmore SP, Nishimura Y, Crowe RA, Cascio WE, Bradham CA, Brenner DA, Herman B. The mitochondrial permeability transition in cell death: a common mechanism in necrosis, apoptosis and autophagy. *Biochim Biophys Acta*. 1998 Aug 10;1366(1-2):177-96.
57. Crompton M. The mitochondrial permeability transition pore and its role in cell death. *Biochem J*. 1999 Jul 15;341 (Pt 2):233-49.
58. Fontaine E, Eriksson O, Ichas F, Bernardi P. Regulation of the permeability transition pore in skeletal muscle mitochondria. Modulation By electron flow through the respiratory chain complex I. *J Biol Chem*. 1998 May 15;273(20):12662-8.
59. Chauvin C, De Oliveira F, Ronot X, Mousseau M, Leverve X, Fontaine E. Rotenone inhibits the mitochondrial permeability transition-induced cell death in U937 and KB cells. *J Biol Chem*. 2001 Nov 2;276(44):41394-8.
60. Bernardi P, Scorrano L, Colonna R, Petronilli V, Di Lisa F. Mitochondria and cell death. Mechanistic aspects and methodological issues. *Eur J Biochem*. 1999 Sep;264(3):687-701.
61. Bernardi P, Krauskopf A, Basso E, Petronilli V, Blachly-Dyson E, Di Lisa F, Forte MA. The mitochondrial permeability transition from in vitro artifact to disease target. *FEBS J*. 2006 May;273(10):2077-99.
62. Fournier N, Ducet G, Crevat A. Action of cyclosporine on mitochondrial calcium fluxes. *J Bioenerg Biomembr*. 1987 Jun;19(3):297-303.
63. Crompton M, Ellinger H, Costi A. Inhibition by cyclosporin A of a Ca²⁺-dependent pore in heart mitochondria activated by inorganic phosphate and oxidative stress. *Biochem J*. 1988 Oct 1;255(1):357-60.
64. Hüser J, Blatter LA. Fluctuations in mitochondrial membrane potential caused by repetitive gating of the permeability transition pore. *Biochem J*. 1999 Oct 15;343 Pt 2:311-7.
65. Petronilli V, Miotto G, Canton M, Brini M, Colonna R, Bernardi P, Di Lisa F. Transient and long-lasting openings of the mitochondrial permeability transition pore can be monitored directly in intact cells by changes in mitochondrial calcein fluorescence. *Biophys J*. 1999 Feb;76(2):725-34.
66. Bernardi P, Petronilli V. The permeability transition pore as a mitochondrial calcium release channel: a critical appraisal. *J Bioenerg Biomembr*. 1996 Apr;28(2):131-8.
67. Bernardi P. Mitochondrial transport of cations: channels, exchangers, and permeability transition. *Physiol Rev*. 1999 Oct;79(4):1127-55.

68. Bernardi P, von Stockum S. The permeability transition pore as a Ca(2+) release channel: new answers to an old question. *Cell Calcium*. 2012 Jul;52(1):22-7.
69. Altschuld RA, Hohl CM, Castillo LC, Garleb AA, Starling RC, Brierley GP. Cyclosporin inhibits mitochondrial calcium efflux in isolated adult rat ventricular cardiomyocytes. *Am J Physiol*. 1992 Jun;262(6 Pt 2):H1699-704.
70. Elrod JW, Wong R, Mishra S, Vagnozzi RJ, Sakthivel B, Goonasekera SA, Karch J, Gabel S, Farber J, Force T, Brown JH, Murphy E, Molkentin JD. Cyclophilin D controls mitochondrial pore-dependent Ca(2+) exchange, metabolic flexibility, and propensity for heart failure in mice. *J Clin Invest*. 2010 Oct;120(10):3680-7.
71. Barsukova A, Komarov A, Hajnóczky G, Bernardi P, Bourdette D, Forte M. Activation of the mitochondrial permeability transition pore modulates Ca²⁺ responses to physiological stimuli in adult neurons. *Eur J Neurosci*. 2011 Mar;33(5):831-42.
72. Zamzami N, Kroemer G. The mitochondrion in apoptosis: how Pandora's box opens. *Nat Rev Mol Cell Biol*. 2001 Jan;2(1):67-71.
73. Nicolli A, Petronilli V, Bernardi P. Modulation of the mitochondrial cyclosporin A-sensitive permeability transition pore by matrix pH. Evidence that the pore open-closed probability is regulated by reversible histidine protonation. *Biochemistry*. 1993 Apr 27;32(16):4461-5.
74. Petronilli V, Cola C, Bernardi P. Modulation of the mitochondrial cyclosporin A-sensitive permeability transition pore. II. The minimal requirements for pore induction underscore a key role for transmembrane electrical potential, matrix pH, and matrix Ca²⁺. *J Biol Chem*. 1993 Jan 15;268(2):1011-16.
75. Bernardi P. Modulation of the mitochondrial cyclosporin A-sensitive permeability transition pore by the proton electrochemical gradient. Evidence that the pore can be opened by membrane depolarization. *J Biol Chem*. 1992 May 5;267(13):8834-9.
76. Petronilli V, Cola C, Massari S, Colonna R, Bernardi P. Physiological effectors modify voltage sensing by the cyclosporin A-sensitive permeability transition pore of mitochondria. *J Biol Chem*. 1993 Oct 15;268(29):21939-45.
77. Costantini P, Chernyak BV, Petronilli V, Bernardi P. Modulation of the mitochondrial permeability transition pore by pyridine nucleotides and dithiol oxidation at two separate sites. *J Biol Chem*. 1996 Mar 22;271(12):6746-51.
78. Petronilli V, Costantini P, Scorrano L, Colonna R, Passamonti S, Bernardi P. The voltage sensor of the mitochondrial permeability transition pore is tuned by the oxidation-reduction state of vicinal thiols. Increase of the gating potential by oxidants and its reversal by reducing agents. *J Biol Chem*. 1994 Jun 17;269(24):16638-42.
79. Costantini P, Chernyak BV, Petronilli V, Bernardi P. Selective inhibition of the mitochondrial permeability transition pore at the oxidation-reduction sensitive dithiol by monobromobimane. *FEBS Lett*. 1995 Apr 3;362(2):239-42.

80. Costantini P, Colonna R, Bernardi P. Induction of the mitochondrial permeability transition by N-ethylmaleimide depends on secondary oxidation of critical thiol groups. Potentiation by copper-ortho-phenanthroline without dimerization of the adenine nucleotide translocase. *Biochim Biophys Acta*. 1998 Jul 20;1365(3):385-92.
81. Petronilli V, Sileikyte J, Zulian A, Dabbeni-Sala F, Jori G, Gobbo S, Tognon G, Nikolov P, Bernardi P, Ricchelli F. Switch from inhibition to activation of the mitochondrial permeability transition during hematoporphyrin-mediated photooxidative stress. Unmasking pore-regulating external thiols. *Biochim Biophys Acta*. 2009 Jul;1787(7):897-904
82. Broekemeier KM, Dempsey ME, Pfeiffer DR. Cyclosporin A is a potent inhibitor of the inner membrane permeability transition in liver mitochondria. *J Biol Chem*. 1989 May 15;264(14):7826-30.
83. Halestrap AP, Davidson AM. Inhibition of Ca²⁺(+)-induced large-amplitude swelling of liver and heart mitochondria by cyclosporin is probably caused by the inhibitor binding to mitochondrial-matrix peptidyl-prolyl cis-trans isomerase and preventing it interacting with the adenine nucleotide translocase. *Biochem J*. 1990 May 15;268(1):153-60.
84. Clipstone NA, Crabtree GR. Identification of calcineurin as a key signalling enzyme in T-lymphocyte activation. *Nature*. 1992 Jun 25;357(6380):695-7.
85. Gomez L, Thibault H, Gharib A, Dumont JM, Vuagniaux G, Scalfaro P, Derumeaux G, Ovize M. Inhibition of mitochondrial permeability transition improves functional recovery and reduces mortality following acute myocardial infarction in mice. *Am J Physiol Heart Circ Physiol*. 2007 Sep;293(3):H1654-61.
86. Reutenauer J, Dorchies OM, Patthey-Vuadens O, Vuagniaux G, Ruegg UT. Investigation of Debio 025, a cyclophilin inhibitor, in the dystrophic mdx mouse, a model for Duchenne muscular dystrophy. *Br J Pharmacol*. 2008 Oct;155(4):574-84. doi: 10.1038/bjp.2008.285. Epub 2008 Jul 21.
87. Tiepolo T, Angelin A, Palma E, Sabatelli P, Merlini L, Nicolosi L, Finetti F, Braghetta P, Vuagniaux G, Dumont JM, Baldari CT, Bonaldo P, Bernardi P. The cyclophilin inhibitor Debio 025 normalizes mitochondrial function, muscle apoptosis and ultrastructural defects in Col6a1^{-/-} myopathic mice. *Br J Pharmacol*. 2009 Jul;157(6):1045-52.
88. Waldmeier PC, Feldtrauer JJ, Qian T, Lemasters JJ. Inhibition of the mitochondrial permeability transition by the nonimmunosuppressive cyclosporin derivative NIM811. *Mol Pharmacol*. 2002 Jul;62(1):22-9.
89. Liu Q, Rehman H, Harley RA, Lemasters JJ, Zhong Z. Small-for-Size Liver Transplantation Increases Pulmonary Injury in Rats: Prevention by NIM811. *HPB Surg*. 2012;2012:270372. doi: 10.1155/2012/270372.
90. Readnower RD, Pandya JD, McEwen ML, Pauly JR, Springer JE, Sullivan PG. Post-injury administration of the mitochondrial permeability transition pore inhibitor,

- NIM811, is neuroprotective and improves cognition after traumatic brain injury in rats. *J Neurotrauma*. 2011 Sep;28(9):1845-53. doi: 10.1089/neu.2011.1755.
91. Sloan RC, Moukdar F, Frasier CR, Patel HD, Bostian PA, Lust RM, Brown DA. Mitochondrial permeability transition in the diabetic heart: contributions of thiol redox state and mitochondrial calcium to augmented reperfusion injury. *J Mol Cell Cardiol*. 2012 May;52(5):1009-18.
 92. Basso E, Petronilli V, Forte MA, Bernardi P. Phosphate is essential for inhibition of the mitochondrial permeability transition pore by cyclosporin A and by cyclophilin D ablation. *J Biol Chem*. 2008 Sep 26;283(39):26307-11.
 93. Azzolin L, von Stockum S, Basso E, Petronilli V, Forte MA, Bernardi P. The mitochondrial permeability transition from yeast to mammals. *FEBS Lett*. 2010 Jun 18;584(12):2504-9.
 94. Jung DW, Bradshaw PC, Pfeiffer DR. Properties of a cyclosporin-insensitive permeability transition pore in yeast mitochondria. *J Biol Chem*. 1997 Aug 22;272(34):21104-12.
 95. Yamada A, Yamamoto T, Yoshimura Y, Gouda S, Kawashima S, Yamazaki N, Yamashita K, Kataoka M, Nagata T, Terada H, Pfeiffer DR, Shinohara Y. Ca²⁺-induced permeability transition can be observed even in yeast mitochondria under optimized experimental conditions. *Biochim Biophys Acta*. 2009 Dec;1787(12):1486-91.
 96. von Stockum S, Basso E, Petronilli V, Sabatelli P, Forte MA, Bernardi P. Properties of Ca²⁺ transport in mitochondria of *Drosophila melanogaster*. *J Biol Chem*. 2011 Dec 2;286(48):41163-70.
 97. Walter L, Nogueira V, Leverve X, Heitz MP, Bernardi P, Fontaine E. Three classes of ubiquinone analogs regulate the mitochondrial permeability transition pore through a common site. *J Biol Chem*. 2000 Sep 22;275(38):29521-7.
 98. Li B, Chauvin C, De Paulis D, De Oliveira F, Gharib A, Vial G, Lablanche S, Leverve X, Bernardi P, Ovize M, Fontaine E. Inhibition of complex I regulates the mitochondrial permeability transition through a phosphate-sensitive inhibitory site masked by cyclophilin D. *Biochim Biophys Acta*. 2012 Sep;1817(9):1628-34.
 99. Chappell JB, Crofts AR. Calcium ion accumulation and volume changes of isolated liver mitochondria. Calcium ion-induced swelling. *Biochem J*. 1965 May;95:378-86
 100. Crofts AR, Chappell JB. Calcium ion accumulation and volume changes of isolated liver mitochondria. Reversal of calcium ion-induced swelling. *Biochem J*. 1965 May;95:387-92.
 101. Gunter TE, Pfeiffer DR. Mechanisms by which mitochondria transport calcium. *Am J Physiol*. 1990 May;258(5 Pt 1):C755-86.

102. Pfeiffer DR, Schmid PC, Beatrice MC, Schmid HH. Intramitochondrial phospholipase activity and the effects of Ca²⁺ plus N-ethylmaleimide on mitochondrial function. *J Biol Chem.* 1979 Nov 25;254(22):11485-94.
103. Schmid PC, Pfeiffer DR, Schmid HH. Quantification of lysophosphatidylethanolamine in the nanomole range. *J Lipid Res.* 1981 Jul;22(5):882-6.
104. Beatrice MC, Stiers DL, Pfeiffer DR. The role of glutathione in the retention of Ca²⁺ by liver mitochondria. *J Biol Chem.* 1984 Jan 25;259(2):1279-87.
105. He L, Lemasters JJ. Regulated and unregulated mitochondrial permeability transition pores: a new paradigm of pore structure and function? *FEBS Lett.* 2002 Feb 13;512(1-3):1-7.
106. Fagian MM, Pereira-da-Silva L, Martins IS, Vercesi AE. Membrane protein thiol cross-linking associated with the permeabilization of the inner mitochondrial membrane by Ca²⁺ plus prooxidants. *J Biol Chem.* 1990 Nov 15;265(32):19955-60.
107. Kroemer G, Galluzzi L, Brenner C. Mitochondrial membrane permeabilization in cell death. *Physiol Rev.* 2007 Jan;87(1):99-163.
108. Beutner G, Ruck A, Riede B, Welte W, Brdiczka D. Complexes between kinases, mitochondrial porin and adenylate translocator in rat brain resemble the permeability transition pore. *FEBS Lett.* 1996 Nov 4;396(2-3):189-95.
109. Marzo I, Brenner C, Zamzami N, Susin SA, Beutner G, Brdiczka D, Rémy R, Xie ZH, Reed JC, Kroemer G. The permeability transition pore complex: a target for apoptosis regulation by caspases and bcl-2-related proteins. *J Exp Med.* 1998 Apr 20;187(8):1261-71.
110. Wieckowski MR, Brdiczka D, Wojtczak L. Long-chain fatty acids promote opening of the reconstituted mitochondrial permeability transition pore. *FEBS Lett.* 2000 Nov 3;484(2):61-4.
111. McEnery MW, Snowman AM, Trifiletti RR, Snyder SH. Isolation of the mitochondrial benzodiazepine receptor: association with the voltage-dependent anion channel and the adenine nucleotide carrier. *Proc Natl Acad Sci U S A.* 1992 Apr 15;89(8):3170-4.
112. Lê-Quôc K, Lê-Quôc D. Crucial role of sulfhydryl groups in the mitochondrial inner membrane structure. *J Biol Chem.* 1985 Jun 25;260(12):7422-8.
113. Szabó I, De Pinto V, Zoratti M. The mitochondrial permeability transition pore may comprise VDAC molecules. II. The electrophysiological properties of VDAC are compatible with those of the mitochondrial megachannel. *FEBS Lett.* 1993 Sep 13;330(2):206-10.
114. Szabó I, Zoratti M. The mitochondrial permeability transition pore may comprise VDAC molecules. I. Binary structure and voltage dependence of the pore. *FEBS Lett.* 1993 Sep 13;330(2):201-5.

115. Gincel D, Shoshan-Barmatz V. Glutamate interacts with VDAC and modulates opening of the mitochondrial permeability transition pore. *J Bioenerg Biomembr*. 2004 Apr;36(2):179-86.
116. Crompton M, Virji S, Ward JM. Cyclophilin-D binds strongly to complexes of the voltage-dependent anion channel and the adenine nucleotide translocase to form the permeability transition pore. *Eur J Biochem*. 1998 Dec 1;258(2):729-35.
117. Woodfield K, Rück A, Brdiczka D, Halestrap AP. Direct demonstration of a specific interaction between cyclophilin-D and the adenine nucleotide translocase confirms their role in the mitochondrial permeability transition. *Biochem J*. 1998 Dec 1;336 (Pt 2):287-90.
118. Fontaine E, Ichas F, Bernardi P. A ubiquinone-binding site regulates the mitochondrial permeability transition pore. *J Biol Chem*. 1998 Oct 2;273(40):25734-40.
119. Cesura AM, Pinard E, Schubanel R, Goetschy V, Friedlein A, Langen H, Polcic P, Forte MA, Bernardi P, Kemp JA. The voltage-dependent anion channel is the target for a new class of inhibitors of the mitochondrial permeability transition pore. *J Biol Chem*. 2003 Dec 12;278(50):49812-8.
120. Krauskopf A, Eriksson O, Craigen WJ, Forte MA, Bernardi P. Properties of the permeability transition in VDAC1(-/-) mitochondria. *Biochim Biophys Acta*. 2006 May-Jun;1757(5-6):590-5. Krauskopf A, Eriksson O, Craigen WJ, Forte MA, Bernardi P. Properties of the permeability transition in VDAC1(-/-) mitochondria. *Biochim Biophys Acta*. 2006 May-Jun;1757(5-6):590-5.
121. Baines CP, Kaiser RA, Sheiko T, Craigen WJ, Molkentin JD. Voltage-dependent anion channels are dispensable for mitochondrial-dependent cell death. *Nat Cell Biol*. 2007 May;9(5):550-5
122. Schultheiss HP, Klingenberg M. Immunochemical characterization of the adenine nucleotide translocator. Organ specificity and conformation specificity. *Eur J Biochem*. 1984 Sep 17;143(3):599-605.
123. Brustovetsky N, Klingenberg M. Mitochondrial ADP/ATP carrier can be reversibly converted into a large channel by Ca²⁺. *Biochemistry*. 1996 Jul 2;35(26):8483-8.
124. Kokoszka JE, Waymire KG, Levy SE, Sligh JE, Cai J, Jones DP, MacGregor GR, Wallace DC. The ADP/ATP translocator is not essential for the mitochondrial permeability transition pore. *Nature*. 2004 Jan 29;427(6973):461-5.
125. Leung AW, Halestrap AP. Recent progress in elucidating the molecular mechanism of the mitochondrial permeability transition pore. *Biochim Biophys Acta*. 2008 Jul-Aug;1777(7-8):946-52.
126. Leung AW, Varanyuwatana P, Halestrap AP. The mitochondrial phosphate carrier interacts with cyclophilin D and may play a key role in the permeability transition. *J Biol Chem*. 2008 Sep 26;283(39):26312-23.

127. Palmieri F. The mitochondrial transporter family (SLC25): physiological and pathological implications. *Pflugers Arch.* 2004 Feb;447(5):689-709.
128. Ko YH, Delannoy M, Hüllihen J, Chiu W, Pedersen PL. Mitochondrial ATP synthasome. Cristae-enriched membranes and a multiwell detergent screening assay yield dispersed single complexes containing the ATP synthase and carriers for Pi and ADP/ATP. *J Biol Chem.* 2003 Apr 4;278(14):12305-9.
129. Schroers A, Krämer R, Wohlrab H. The reversible antiport-uniport conversion of the phosphate carrier from yeast mitochondria depends on the presence of a single cysteine. *J Biol Chem.* 1997 Apr 18;272(16):10558-64.
130. Halestrap AP, Pasdois P. The role of the mitochondrial permeability transition pore in heart disease. *Biochim Biophys Acta.* 2009 Nov;1787(11):1402-15.
131. Halestrap AP. What is the mitochondrial permeability transition pore? *J Mol Cell Cardiol.* 2009 Jun;46(6):821-31.
132. Gutiérrez-Aguilar M, Pérez-Martínez X, Chávez E, Uribe-Carvajal S. In *Saccharomyces cerevisiae*, the phosphate carrier is a component of the mitochondrial unselective channel. *Arch Biochem Biophys.* 2010 Feb 15;494(2):184-91.
133. Wilson JE. Isozymes of mammalian hexokinase: structure, subcellular localization and metabolic function. *J Exp Biol.* 2003 Jun;206(Pt 12):2049-57.
134. Rasola A, Sciacovelli M, Pantic B, Bernardi P. Signal transduction to the permeability transition pore. *FEBS Lett.* 2010 May 17;584(10):1989-96.
135. Chiara F, Castellaro D, Marin O, Petronilli V, Brusilow WS, Juhaszova M, Sollott SJ, Forte M, Bernardi P, Rasola A. Hexokinase II detachment from mitochondria triggers apoptosis through the permeability transition pore independent of voltage-dependent anion channels. *PLoS One.* 2008 Mar 19;3(3):e1852.
136. Pastorino JG, Hoek JB, Shulga N. Activation of glycogen synthase kinase 3beta disrupts the binding of hexokinase II to mitochondria by phosphorylating voltage-dependent anion channel and potentiates chemotherapy-induced cytotoxicity. *Cancer Res.* 2005 Nov 15;65(22):10545-54.
137. Halestrap AP, Davidson AM. Inhibition of Ca²⁺(+)-induced large-amplitude swelling of liver and heart mitochondria by cyclosporin is probably caused by the inhibitor binding to mitochondrial-matrix peptidyl-prolyl cis-trans isomerase and preventing it interacting with the adenine nucleotide translocase. *Biochem J.* 1990 May 15;268(1):153-60.
138. McGuinness O, Yafei N, Costi A, Crompton M. The presence of two classes of high-affinity cyclosporin A binding sites in mitochondria. Evidence that the minor component is involved in the opening of an inner-membrane Ca²⁺(+)-dependent pore. *Eur J Biochem.* 1990 Dec 12;194(2):671-9.

139. Griffiths EJ, Halestrap AP. Further evidence that cyclosporin A protects mitochondria from calcium overload by inhibiting a matrix peptidyl-prolyl cis-trans isomerase. Implications for the immunosuppressive and toxic effects of cyclosporin. *Biochem J.* 1991 Mar 1;274 (Pt 2):611-4.
140. Nicolli A, Basso E, Petronilli V, Wenger RM, Bernardi P. Interactions of cyclophilin with the mitochondrial inner membrane and regulation of the permeability transition pore, and cyclosporin A-sensitive channel. *J Biol Chem.* 1996 Jan 26;271(4):2185-92.
141. Nakagawa T, Shimizu S, Watanabe T, Yamaguchi O, Otsu K, Yamagata H, Inohara H, Kubo T, Tsujimoto Y. Cyclophilin D-dependent mitochondrial permeability transition regulates some necrotic but not apoptotic cell death. *Nature.* 2005 Mar 31;434(7033):652-8.
142. Baines CP, Kaiser RA, Purcell NH, Blair NS, Osinska H, Hambleton MA, Brunskill EW, Sayen MR, Gottlieb RA, Dorn GW, Robbins J, Molkentin JD. Loss of cyclophilin D reveals a critical role for mitochondrial permeability transition in cell death. *Nature.* 2005 Mar 31;434(7033):658-62.
143. Schinzel AC, Takeuchi O, Huang Z, Fisher JK, Zhou Z, Rubens J, Hetz C, Danial NN, Moskowitz MA, Korsmeyer SJ. Cyclophilin D is a component of mitochondrial permeability transition and mediates neuronal cell death after focal cerebral ischemia. *Proc Natl Acad Sci U S A.* 2005 Aug 23;102(34):12005-10.
144. Basso E, Fante L, Fowlkes J, Petronilli V, Forte MA, Bernardi P. Properties of the permeability transition pore in mitochondria devoid of Cyclophilin D. *J Biol Chem.* 2005 May 13;280(19):18558-61.
145. Cereghetti GM, Stangherlin A, Martins de Brito O, Chang CR, Blackstone C, Bernardi P, Scorrano L. Dephosphorylation by calcineurin regulates translocation of Drp1 to mitochondria. *Proc Natl Acad Sci U S A.* 2008 Oct 14;105(41):15803-8.
146. Kang BH, Plescia J, Dohi T, Rosa J, Doxsey SJ, Altieri DC. Regulation of tumor cell mitochondrial homeostasis by an organelle-specific Hsp90 chaperone network. *Cell.* 2007 Oct 19;131(2):257-70.
147. Giorgio V, Bisetto E, Soriano ME, Dabbeni-Sala F, Basso E, Petronilli V, Forte MA, Bernardi P, Lippe G. Cyclophilin D modulates mitochondrial FOF1-ATP synthase by interacting with the lateral stalk of the complex. *J Biol Chem.* 2009 Dec 4;284(49):33982-8.
148. Eliseev RA, Malecki J, Lester T, Zhang Y, Humphrey J, Gunter TE. Cyclophilin D interacts with Bcl2 and exerts an anti-apoptotic effect. *J Biol Chem.* 2009 Apr 10;284(15):9692-9.
149. Giorgio V, Bisetto E, Soriano ME, Dabbeni-Sala F, Basso E, Petronilli V, Forte MA, Bernardi P, Lippe G. Cyclophilin D modulates mitochondrial FOF1-ATP synthase by interacting with the lateral stalk of the complex. *J Biol Chem.* 2009 Dec 4;284(49):33982-8.

150. Wang X, Carlsson Y, Basso E, Zhu C, Rousset CI, Rasola A, Johansson BR, Blomgren K, Mallard C, Bernardi P, Forte MA, Hagberg H. Developmental shift of cyclophilin D contribution to hypoxic-ischemic brain injury. *J Neurosci*. 2009 Feb 25;29(8):2588-96.
151. Griffiths EJ, Halestrap AP. Protection by Cyclosporin A of ischemia/reperfusion-induced damage in isolated rat hearts. *J Mol Cell Cardiol*. 1993 Dec;25(12):1461-9.
152. Piot C, Croisille P, Staat P, Thibault H, Rioufol G, Mewton N, Elbelghiti R, Cung TT, Bonnefoy E, Angoulvant D, Macia C, Raczka F, Sportouch C, Gahide G, Finet G, André-Fouët X, Revel D, Kirkorian G, Monassier JP, Derumeaux G, Ovize M. Effect of cyclosporine on reperfusion injury in acute myocardial infarction. *N Engl J Med*. 2008 Jul 31;359(5):473-81.
153. Friberg H, Ferrand-Drake M, Bengtsson F, Halestrap AP, Wieloch T. Cyclosporin A, but not FK 506, protects mitochondria and neurons against hypoglycemic damage and implicates the mitochondrial permeability transition in cell death. *J Neurosci*. 1998 Jul 15;18(14):5151-9.
154. Folbergrová J, Li PA, Uchino H, Smith ML, Siesjö BK. Changes in the bioenergetic state of rat hippocampus during 2.5 min of ischemia, and prevention of cell damage by cyclosporin A in hyperglycemic subjects. *Exp Brain Res*. 1997 Mar;114(1):44-50.
155. Uchino H, Elmér E, Uchino K, Li PA, He QP, Smith ML, Siesjö BK. Amelioration by cyclosporin A of brain damage in transient forebrain ischemia in the rat. *Brain Res*. 1998 Nov 23;812(1-2):216-26.
156. Matsumoto S, Friberg H, Ferrand-Drake M, Wieloch T. Blockade of the mitochondrial permeability transition pore diminishes infarct size in the rat after transient middle cerebral artery occlusion. *J Cereb Blood Flow Metab*. 1999 Jul;19(7):736-41.
157. Okonkwo DO, Povlishock JT. An intrathecal bolus of cyclosporin A before injury preserves mitochondrial integrity and attenuates axonal disruption in traumatic brain injury. *J Cereb Blood Flow Metab*. 1999 Apr;19(4):443-51.
158. Scheff SW, Sullivan PG. Cyclosporin A significantly ameliorates cortical damage following experimental traumatic brain injury in rodents. *J Neurotrauma*. 1999 Sep;16(9):783-92.
159. Forte M, Gold BG, Marracci G, Chaudhary P, Basso E, Johnsen D, Yu X, Fowlkes J, Rahder M, Stem K, Bernardi P, Bourdette D. Cyclophilin D inactivation protects axons in experimental autoimmune encephalomyelitis, an animal model of multiple sclerosis. *Proc Natl Acad Sci U S A*. 2007 May 1;104(18):7558-63. Epub 2007 Apr 26. Erratum in: *Proc Natl Acad Sci U S A*. 2007 Oct 30;104(44):17554.
160. Martin LJ, Gertz B, Pan Y, Price AC, Molkenstin JD, Chang Q. The mitochondrial permeability transition pore in motor neurons: involvement in the pathobiology of ALS mice. *Exp Neurol*. 2009 Aug;218(2):333-46.

161. Martin LJ, Gertz B, Pan Y, Price AC, Molkenin JD, Chang Q. The mitochondrial permeability transition pore in motor neurons: involvement in the pathobiology of ALS mice. *Exp Neurol*. 2009 Aug;218(2):333-46.
162. Lampe AK, Bushby KM. Collagen VI related muscle disorders. *J Med Genet*. 2005 Sep;42(9):673-85.
163. Jöbsis GJ, Keizers H, Vreijling JP, de Visser M, Speer MC, Wolterman RA, Baas F, Bolhuis PA. Type VI collagen mutations in Bethlem myopathy, an autosomal dominant myopathy with contractures. *Nat Genet*. 1996 Sep;14(1):113-5.
164. Camacho Vanegas O, Bertini E, Zhang RZ, Petrini S, Minosse C, Sabatelli P, Giusti B, Chu ML, Pepe G. Ullrich scleroatonic muscular dystrophy is caused by recessive mutations in collagen type VI. *Proc Natl Acad Sci U S A*. 2001 Jun 19;98(13):7516-21.
165. Merlini L, Martoni E, Grumati P, Sabatelli P, Squarzoni S, Urciuolo A, Ferlini A, Gualandi F, Bonaldo P. Autosomal recessive myosclerosis myopathy is a collagen VI disorder. *Neurology*. 2008 Oct 14;71(16):1245-53.
166. Bonaldo P, Braghetta P, Zanetti M, Piccolo S, Volpin D, Bressan GM. Collagen VI deficiency induces early onset myopathy in the mouse: an animal model for Bethlem myopathy. *Hum Mol Genet*. 1998 Dec;7(13):2135-40.
167. Irwin WA, Bergamin N, Sabatelli P, Reggiani C, Megighian A, Merlini L, Braghetta P, Columbaro M, Volpin D, Bressan GM, Bernardi P, Bonaldo P. Mitochondrial dysfunction and apoptosis in myopathic mice with collagen VI deficiency. *Nat Genet*. 2003 Dec;35(4):367-71. Epub 2003 Nov 16.
168. Palma E, Tiepolo T, Angelin A, Sabatelli P, Maraldi NM, Basso E, Forte MA, Bernardi P, Bonaldo P. Genetic ablation of cyclophilin D rescues mitochondrial defects and prevents muscle apoptosis in collagen VI myopathic mice. *Hum Mol Genet*. 2009 Jun 1;18(11):2024-31.
169. Grumati P, Coletto L, Sabatelli P, Cescon M, Angelin A, Bertaggia E, Blaauw B, Urciuolo A, Tiepolo T, Merlini L, Maraldi NM, Bernardi P, Sandri M, Bonaldo P. Autophagy is defective in collagen VI muscular dystrophies, and its reactivation rescues myofiber degeneration. *Nat Med*. 2010 Nov;16(11):1313-20.
170. Angelin A, Tiepolo T, Sabatelli P, Grumati P, Bergamin N, Golfieri C, Mattioli E, Gualandi F, Ferlini A, Merlini L, Maraldi NM, Bonaldo P, Bernardi P. Mitochondrial dysfunction in the pathogenesis of Ullrich congenital muscular dystrophy and prospective therapy with cyclosporins. *Proc Natl Acad Sci U S A*. 2007 Jan 16;104(3):991-6.
171. Merlini L, Angelin A, Tiepolo T, Braghetta P, Sabatelli P, Zamparelli A, Ferlini A, Maraldi NM, Bonaldo P, Bernardi P. Cyclosporin A corrects mitochondrial dysfunction and muscle apoptosis in patients with collagen VI myopathies. *Proc Natl Acad Sci U S A*. 2008 Apr 1;105(13):5225-9.

172. Millay DP, Sargent MA, Osinska H, Baines CP, Barton ER, Vuagniaux G, Sweeney HL, Robbins J, Molkentin JD. Genetic and pharmacologic inhibition of mitochondrial-dependent necrosis attenuates muscular dystrophy. *Nat Med*. 2008 Apr;14(4):442-7.
173. Anholt RR, Pedersen PL, De Souza EB, Snyder SH. The peripheral-type benzodiazepine receptor. Localization to the mitochondrial outer membrane. *J Biol Chem*. 1986 Jan 15;261(2):576-83.
174. Gavish M, Bachman I, Shoukrun R, Katz Y, Veenman L, Weisinger G, Weizman A. Enigma of the peripheral benzodiazepine receptor. *Pharmacol Rev*. 1999 Dec;51(4):629-50.
175. Papadopoulos V. Peripheral benzodiazepine receptor: structure and function in health and disease. *Ann Pharm Fr*. 2003 Jan;61(1):30-50.
176. Lacapère JJ, Papadopoulos V. Peripheral-type benzodiazepine receptor: structure and function of a cholesterol-binding protein in steroid and bile acid biosynthesis. *Steroids*. 2003 Sep;68(7-8):569-85.
177. Rupprecht R, Papadopoulos V, Rammes G, Baghai TC, Fan J, Akula N, Groyer G, Adams D, Schumacher M. Translocator protein (18 kDa) (TSPO) as a therapeutic target for neurological and psychiatric disorders. *Nat Rev Drug Discov*. 2010 Dec;9(12):971-88.
178. Bernassau JM, Reversat JL, Ferrara P, Caput D, Lefur G. A 3D model of the peripheral benzodiazepine receptor and its implication in intra mitochondrial cholesterol transport. *J Mol Graph*. 1993 Dec;11(4):236-44, 235.
179. Murail S, Robert JC, Coïc YM, Neumann JM, Ostuni MA, Yao ZX, Papadopoulos V, Jamin N, Lacapère JJ. Secondary and tertiary structures of the transmembrane domains of the translocator protein TSPO determined by NMR. Stabilization of the TSPO tertiary fold upon ligand binding. *Biochim Biophys Acta*. 2008 Jun;1778(6):1375-81.
180. Joseph-Liauzun E, Delmas P, Shire D, Ferrara P. Topological analysis of the peripheral benzodiazepine receptor in yeast mitochondrial membranes supports a five-transmembrane structure. *J Biol Chem*. 1998 Jan 23;273(4):2146-52.
181. Korkhov VM, Sachse C, Short JM, Tate CG. Three-dimensional structure of TspO by electron cryomicroscopy of helical crystals. *Structure*. 2010 Jun 9;18(6):677-87.
182. Braestrup C, Squires RF. Specific benzodiazepine receptors in rat brain characterized by high-affinity (3H)diazepam binding. *Proc Natl Acad Sci U S A*. 1977 Sep;74(9):3805-9.
183. Braestrup C, Albrechtsen R, Squires RF. High densities of benzodiazepine receptors in human cortical areas. *Nature*. 1977 Oct 20;269(5630):702-4. PubMed PMID: 22814.
184. Papadopoulos V, Baraldi M, Guilarte TR, Knudsen TB, Lacapère JJ, Lindemann P, Norenberg MD, Nutt D, Weizman A, Zhang MR, Gavish M. Translocator protein

- (18kDa): new nomenclature for the peripheral-type benzodiazepine receptor based on its structure and molecular function. *Trends Pharmacol Sci.* 2006 Aug;27(8):402-9.
185. Casellas P, Galiegue S, Basile AS. Peripheral benzodiazepine receptors and mitochondrial function. *Neurochem Int.* 2002 May;40(6):475-86.
186. Scarf AM, Ittner LM, Kassiou M. The translocator protein (18 kDa): central nervous system disease and drug design. *J Med Chem.* 2009 Feb 12;52(3):581-92.
187. Gatliff J, Campanella M. The 18 kDa translocator protein (TSPO): a new perspective in mitochondrial biology. *Curr Mol Med.* 2012 May;12(4):356-68.
188. Qi X, Xu J, Wang F, Xiao J. Translocator Protein (18 kDa): A Promising Therapeutic Target and Diagnostic Tool for Cardiovascular Diseases. *Oxid Med Cell Longev.* 2012;2012:162934. Epub 2012 Nov 28.
189. Papadopoulos V, Miller WL. Role of mitochondria in steroidogenesis. *Best Pract Res Clin Endocrinol Metab.* 2012 Dec;26(6):771-90.
190. Li H, Papadopoulos V. Peripheral-type benzodiazepine receptor function in cholesterol transport. Identification of a putative cholesterol recognition/interaction amino acid sequence and consensus pattern. *Endocrinology.* 1998 Dec;139(12):4991-7.
191. Taketani S, Kohno H, Furukawa T, Tokunaga R. Involvement of peripheral-type benzodiazepine receptors in the intracellular transport of heme and porphyrins. *J Biochem.* 1995 Apr;117(4):875-80.
192. Wendler G, Lindemann P, Lacapère JJ, Papadopoulos V. Protoporphyrin IX binding and transport by recombinant mouse PBR. *Biochem Biophys Res Commun.* 2003 Nov 28;311(4):847-52.
193. Taketani S, Kohno H, Okuda M, Furukawa T, Tokunaga R. Induction of peripheral-type benzodiazepine receptors during differentiation of mouse erythroleukemia cells. A possible involvement of these receptors in heme biosynthesis. *J Biol Chem.* 1994 Mar 11;269(10):7527-31.
194. Ajioka RS, Phillips JD, Kushner JP. Biosynthesis of heme in mammals. *Biochim Biophys Acta.* 2006 Jul;1763(7):723-36.
195. Yeliseev AA, Kaplan S. TspO of rhodobacter sphaeroides. A structural and functional model for the mammalian peripheral benzodiazepine receptor. *J Biol Chem.* 2000 Feb 25;275(8):5657-67.
196. Verma A, Nye JS, Snyder SH. Porphyrins are endogenous ligands for the mitochondrial (peripheral-type) benzodiazepine receptor. *Proc Natl Acad Sci U S A.* 1987 Apr;84(8):2256-60.

197. Snyder SH, Verma A, Trifiletti RR. The peripheral-type benzodiazepine receptor: a protein of mitochondrial outer membranes utilizing porphyrins as endogenous ligands. *FASEB J.* 1987 Oct;1(4):282-8.
198. Verma A, Snyder SH. Characterization of porphyrin interactions with peripheral type benzodiazepine receptors. *Mol Pharmacol.* 1988 Dec;34(6):800-5.
199. Ricchelli F. Photophysical properties of porphyrins in biological membranes. *J Photochem Photobiol B.* 1995 Aug;29(2-3):109-18.
200. Moan J, Berg K. The photodegradation of porphyrins in cells can be used to estimate the lifetime of singlet oxygen. *Photochem Photobiol.* 1991 Apr;53(4):549-53.
201. Scarf AM, Ittner LM, Kassiou M. The translocator protein (18 kDa): central nervous system disease and drug design. *J Med Chem.* 2009 Feb 12;52(3):581-92. doi: 10.1021/jm8011678.
202. Lacapère JJ, Delavoie F, Li H, Péranzi G, Maccario J, Papadopoulos V, Vidic B. Structural and functional study of reconstituted peripheral benzodiazepine receptor. *Biochem Biophys Res Commun.* 2001 Jun 8;284(2):536-41.
203. Le Fur G, Perrier ML, Vaucher N, Imbault F, Flamier A, Benavides J, Uzan A, Renault C, Dubroeuq MC, Guérémy C. Peripheral benzodiazepine binding sites: effect of PK 11195, 1-(2-chlorophenyl)-N-methyl-N-(1-methylpropyl)-3-isoquinolinecarboxamide. I. In vitro studies. *Life Sci.* 1983 Apr 18;32(16):1839-47.
204. Le Fur G, Vaucher N, Perrier ML, Flamier A, Benavides J, Renault C, Dubroeuq MC, Guérémy C, Uzan A. Differentiation between two ligands for peripheral benzodiazepine binding sites, [3H]RO5-4864 and [3H]PK 11195, by thermodynamic studies. *Life Sci.* 1983 Aug 1;33(5):449-57.
205. Bolger GT, Weissman BA, Luëddens H, Basile AS, Mantione CR, Barrett JE, Witkin JM, Paul SM, Skolnick P. Late evolutionary appearance of 'peripheral-type' binding sites for benzodiazepines. *Brain Res.* 1985 Jul 15;338(2):366-70.
206. Basile AS, Klein DC, Skolnick P. Characterization of benzodiazepine receptors in the bovine pineal gland: evidence for the presence of an atypical binding site. *Brain Res.* 1986 Nov;387(2):127-35.
207. Farges R, Joseph-Liauzun E, Shire D, Caput D, Le Fur G, Loison G, Ferrara P. Molecular basis for the different binding properties of benzodiazepines to human and bovine peripheral-type benzodiazepine receptors. *FEBS Lett.* 1993 Dec 13;335(3):305-8.
208. Farges R, Joseph-Liauzun E, Shire D, Caput D, Le Fur G, Ferrara P. Site-directed mutagenesis of the peripheral benzodiazepine receptor: identification of amino acids implicated in the binding site of Ro5-4864. *Mol Pharmacol.* 1994 Dec;46(6):1160-7.

209. Rao VL, Butterworth RF. Characterization of binding sites for the omega3 receptor ligands [3H]PK11195 and [3H]RO5-4864 in human brain. *Eur J Pharmacol.* 1997 Dec 4;340(1):89-99.
210. Romeo E, Auta J, Kozikowski AP, Ma D, Papadopoulos V, Puia G, Costa E, Guidotti A. 2-Aryl-3-indoleacetamides (FGIN-1): a new class of potent and specific ligands for the mitochondrial DBI receptor (MDR). *J Pharmacol Exp Ther.* 1992 Sep;262(3):971-8.
211. Anzini M, Cappelli A, Vomero S, Seeber M, Menziani MC, Langer T, Hagen B, Manzoni C, Bourguignon JJ. Mapping and fitting the peripheral benzodiazepine receptor binding site by carboxamide derivatives. Comparison of different approaches to quantitative ligand-receptor interaction modeling. *J Med Chem.* 2001 Apr 12;44(8):1134-50.
212. Hirsch T, Decaudin D, Susin SA, Marchetti P, Larochette N, Resche-Rigon M, Kroemer G. PK11195, a ligand of the mitochondrial benzodiazepine receptor, facilitates the induction of apoptosis and reverses Bcl-2-mediated cytoprotection. *Exp Cell Res.* 1998 Jun 15;241(2):426-34.
213. Bono F, Lamarche I, Prabonnaud V, Le Fur G, Herbert JM. Peripheral benzodiazepine receptor agonists exhibit potent antiapoptotic activities. *Biochem Biophys Res Commun.* 1999 Nov 19;265(2):457-61.
214. Chelli B, Falleni A, Salvetti F, Gremigni V, Lucacchini A, Martini C. Peripheral-type benzodiazepine receptor ligands: mitochondrial permeability transition induction in rat cardiac tissue. *Biochem Pharmacol.* 2001 Mar 15;61(6):695-705.
215. Chelli B, Salvetti A, Da Pozzo E, Rechichi M, Spinetti F, Rossi L, Costa B, Lena A, Rainaldi G, Scatena F, Vanacore R, Gremigni V, Martini C. PK 11195 differentially affects cell survival in human wild-type and 18 kDa translocator protein-silenced ADF astrocytoma cells. *J Cell Biochem.* 2008 Oct 15;105(3):712-23.
216. Pastorino JG, Simbula G, Gilfor E, Hoek JB, Farber JL. Protoporphyrin IX, an endogenous ligand of the peripheral benzodiazepine receptor, potentiates induction of the mitochondrial permeability transition and the killing of cultured hepatocytes by rotenone. *J Biol Chem.* 1994 Dec 9;269(49):31041-6.
217. Azarashvili T, Grachev D, Krestinina O, Evtodienko Y, Yurkov I, Papadopoulos V, Reiser G. The peripheral-type benzodiazepine receptor is involved in control of Ca²⁺-induced permeability transition pore opening in rat brain mitochondria. *Cell Calcium.* 2007 Jul;42(1):27-39.
218. Krestinina OV, Grachev DE, Odinkova IV, Reiser G, Evtodienko YV, Azarashvili TS. Effect of peripheral benzodiazepine receptor (PBR/TSP0) ligands on opening of Ca²⁺-induced pore and phosphorylation of 3.5-kDa polypeptide in rat brain mitochondria. *Biochemistry (Mosc).* 2009 Apr;74(4):421-9.
219. Ostuni MA, Ducroc R, Péranzi G, Tonon MC, Papadopoulos V, Lacapere JJ. Translocator protein (18 kDa) ligand PK 11195 induces transient mitochondrial

- Ca²⁺ release leading to transepithelial Cl⁻ secretion in HT-29 human colon cancer cells. *Biol Cell*. 2007 Nov;99(11):639-47.
220. Leducq N, Bono F, Sulpice T, Vin V, Janiak P, Fur GL, O'Connor SE, Herbert JM. Role of peripheral benzodiazepine receptors in mitochondrial, cellular, and cardiac damage induced by oxidative stress and ischemia-reperfusion. *J Pharmacol Exp Ther*. 2003 Sep;306(3):828-37.
221. Parker MA, Bazan HE, Marcheselli V, Rodriguez de Turco EB, Bazan NG. Platelet-activating factor induces permeability transition and cytochrome c release in isolated brain mitochondria. *J Neurosci Res*. 2002 Jul 1;69(1):39-50.
222. Bernardi P, Forte M. The mitochondrial permeability transition pore. *Novartis Found Symp*. 2007;287:157-64; discussion 164-9.
223. Gonzalez-Polo RA, Carvalho G, Braun T, Decaudin D, Fabre C, Larochette N, Perfettini JL, Djavaheri-Mergny M, Youlyouz-Marfak I, Codogno P, Raphael M, Feuillard J, Kroemer G. PK11195 potently sensitizes to apoptosis induction independently from the peripheral benzodiazepin receptor. *Oncogene*. 2005 Nov 17;24(51):7503-13.
224. Hans G, Wislet-Gendebien S, Lallemand F, Robe P, Rogister B, Belachew S, Nguyen L, Malgrange B, Moonen G, Rigo JM. Peripheral benzodiazepine receptor (PBR) ligand cytotoxicity unrelated to PBR expression. *Biochem Pharmacol*. 2005 Mar 1;69(5):819-30.
225. Kletsas D, Li W, Han Z, Papadopoulos V. Peripheral-type benzodiazepine receptor (PBR) and PBR drug ligands in fibroblast and fibrosarcoma cell proliferation: role of ERK, c-Jun and ligand-activated PBR-independent pathways. *Biochem Pharmacol*. 2004 May 15;67(10):1927-32.
226. Papadopoulos V, Amri H, Boujrad N, Cascio C, Culty M, Garnier M, Hardwick M, Li H, Vidic B, Brown AS, Reversa JL, Bernassau JM, Drieu K. Peripheral benzodiazepine receptor in cholesterol transport and steroidogenesis. *Steroids*. 1997 Jan;62(1):21-8.
227. Sternberg N, Hamilton D, Hoess R. Bacteriophage P1 site-specific recombination. II. Recombination between loxP and the bacterial chromosome. *J Mol Biol*. 1981 Aug 25;150(4):487-507.
228. Sauer B, Henderson N. Site-specific DNA recombination in mammalian cells by the Cre recombinase of bacteriophage P1. *Proc Natl Acad Sci USA*. 1988 Jul;85(14):5166-70.
229. Nagy A. Cre recombinase: the universal reagent for genome tailoring. *Genesis*. 2000 Feb;26(2):99.
230. McLeod M, Craft S, Broach JR. Identification of the crossover site during FLP-mediated recombination in the *Saccharomyces cerevisiae* plasmid 2 microns circle. *Mol Cell Biol*. 1986 Oct;6(10):3357-67.

231. Wigley P, Becker C, Beltrame J, Blake T, Crocker L, Harrison S, Lyons I, McKenzie Z, Tearle R, Crawford R, et al. Site-specific transgene insertion: an approach. *Reprod Fertil Dev.* 1994;6(5):585-8.
232. Sadowski PD. The Flp recombinase of the 2-microns plasmid of *Saccharomyces cerevisiae*. *Prog Nucleic Acid Res Mol Biol.* 1995; 51:53-91.
233. Gornall AG, Bardawill CJ and David MM. Determination of Serum Proteins by means of the Biuret Reaction. *J Biol Chem.* 1949 Feb;177(2):751-66.
234. Chance B, Williams GR. Respiratory enzymes in oxidative phosphorylation. III. The steady state. *J Biol Chem.* 1955 Nov;217(1):409-27.
235. Emaus RK, Grunwald R, Lemasters JJ. Rhodamine 123 as a probe of transmembrane potential in isolated rat-liver mitochondria: spectral and metabolic properties. *Biochim Biophys Acta.* 1986 Jul 23;850(3):436-48.
236. Scaduto RC Jr, Grotyohann LW. Measurement of mitochondrial membrane potential using fluorescent rhodamine derivatives. *Biophys J.* 1999 Jan;76(1 Pt 1):469-77.
237. Tedeschi H, Harris DL. Some observations on the photometric estimation of mitochondrial volume. *Biochim Biophys Acta.* 1958 May;28(2):392-402.
238. Sileikyte J, Petronilli V, Zulian A, Dabbeni-Sala F, Tognon G, Nikolov P, Bernardi P, Ricchelli F. Regulation of the inner membrane mitochondrial permeability transition by the outer membrane translocator protein (peripheral benzodiazepine receptor). *J Biol Chem.* 2011 Jan 14;286(2):1046-53.
239. Salet C, Moreno G, Ricchelli F, Bernardi P. Singlet oxygen produced by photodynamic action causes inactivation of the mitochondrial permeability transition pore. *J Biol Chem.* 1997 Aug 29;272(35):21938-43.
240. Hirsch JD, Beyer CF, Malkowitz L, Beer B, Blume AJ. Mitochondrial benzodiazepine receptors mediate inhibition of mitochondrial respiratory control. *Mol Pharmacol.* 1989 Jan;35(1):157-63.
241. Nakazawa F, Alev C, Shin M, Nakaya Y, Jakt LM, Sheng G. PBRL, a putative peripheral benzodiazepine receptor, in primitive erythropoiesis. *Gene Expr Patterns.* 2009 Feb;9(2):114-21.
242. Papadopoulos V, Boujrad N, Ikonovic MD, Ferrara P, Vidic B. Topography of the Leydig cell mitochondrial peripheral-type benzodiazepine receptor. *Mol Cell Endocrinol.* 1994 Aug;104(1):R5-9
243. Garnier M, Dimchev AB, Boujrad N, Price JM, Musto NA, Papadopoulos V. In vitro reconstitution of a functional peripheral-type benzodiazepine receptor from mouse Leydig tumor cells. *Mol Pharmacol.* 1994 Feb;45(2):201-11.

244. Ankarcrona M, Dypbukt JM, Bonfoco E, Zhivotovsky B, Orrenius S, Lipton SA, Nicotera P. Glutamate-induced neuronal death: a succession of necrosis or apoptosis depending on mitochondrial function. *Neuron*. 1995 Oct;15(4):961-73.
245. Pastorino JG, Hoek JB. Hexokinase II: the integration of energy metabolism and control of apoptosis. *Curr Med Chem*. 2003 Aug;10(16):1535-51.
246. Ricchelli F, Sileikytė J, Bernardi P. Shedding light on the mitochondrial permeability transition. *Biochim Biophys Acta*. 2011 May;1807(5):482-90.
247. Cleary J, Johnson KM, Opiari AW Jr, Glick GD. Inhibition of the mitochondrial F1F0-ATPase by ligands of the peripheral benzodiazepine receptor. *Bioorg Med Chem Lett*. 2007 Mar 15;17(6):1667-70.
248. Blatt NB, Bednarski JJ, Warner RE, Leonetti F, Johnson KM, Boitano A, Yung R, Richardson BC, Johnson KJ, Ellman JA, Opiari AW Jr, Glick GD. Benzodiazepine-induced superoxide signals B cell apoptosis: mechanistic insight and potential therapeutic utility. *J Clin Invest*. 2002 Oct;110(8):1123-32.
249. Batarseh A, Papadopoulos V. Regulation of translocator protein 18 kDa (TSPO) expression in health and disease states. *Mol Cell Endocrinol*. 2010 Oct 7;327(1-2):1-12.

5. Appendix



Switch from inhibition to activation of the mitochondrial permeability transition during hematoporphyrin-mediated photooxidative stress. Unmasking pore-regulating external thiols

Valeria Petronilli^a, Justina Šileikytė^{b,1}, Alessandra Zulian^c, Federica Dabbeni-Sala^c, Giulio Jori^b, Silvano Gobbo^b, Giuseppe Tognon^b, Peter Nikolov^d, Paolo Bernardi^a, Fernanda Ricchelli^{b,*}

^a C.N.R. Institute of Neurosciences at the Department of Biomedical Sciences, University of Padova, Italy

^b C.N.R. Institute of Biomedical Technologies at the Department of Biology, University of Padova, Italy

^c Department of Pharmacology and Anesthesiology/Pharmacology Division, University of Padova, Italy

^d Bulgarian Academy of Sciences, Institute of Organic Chemistry, Sofia, Bulgaria

ARTICLE INFO

Article history:

Received 22 October 2008

Received in revised form 17 March 2009

Accepted 19 March 2009

Available online 1 April 2009

Keywords:

Mitochondria

Permeability transition pore

External thiols

Porphyrin

Photooxidation

ABSTRACT

We have studied the mitochondrial permeability transition pore (PTP) under oxidizing conditions with mitochondria-bound hematoporphyrin, which generates reactive oxygen species (mainly singlet oxygen, $^1\text{O}_2$) upon UV/visible light-irradiation and promotes the photooxidative modification of vicinal targets. We have characterized the PTP-modulating properties of two major critical sites endowed with different degrees of photosensitivity: (i) the most photovulnerable site comprises critical histidines, whose photomodification by vicinal hematoporphyrin causes a drop in reactivity of matrix-exposed (internal), PTP-regulating cysteines thus stabilizing the pore in a closed conformation; (ii) the most photoresistant site coincides with the binding domains of (external) cysteines sensitive to membrane-impermeant reagents, which are easily unmasked when oxidation of internal cysteines is prevented. Photooxidation of external cysteines promoted by vicinal hematoporphyrin reactivates the PTP after the block caused by histidine photodegradation. Thus, hematoporphyrin-mediated photooxidative stress can either inhibit or activate the mitochondrial permeability transition depending on the site of hematoporphyrin localization and on the nature of the substrate; and selective photomodification of different hematoporphyrin-containing pore domains can be achieved by fine regulation of the sensitizer/light doses. These findings shed new light on PTP modulation by oxidative stress.

© 2009 Elsevier B.V. All rights reserved.

1. Introduction

The mitochondrial permeability transition (PT) features an abrupt increase of mitochondrial inner membrane permeability to solutes with molecular masses up to about 1500 Da. If long-lasting, this event is followed by membrane depolarization, matrix swelling, depletion of

matrix pyridine nucleotides (PN), outer membrane rupture and release of intermembrane proteins, including cytochrome *c*, thus leading to cell death [1,2]. The PT is due to the opening of a protein channel, the CsA-sensitive permeability transition pore (PTP), whose structure has yet to be identified. The most studied candidates have been the adenine nucleotide translocator (ANT), the voltage-dependent anion channel (VDAC), and cyclophilin D (CyP-D) [1–4]. However, recent studies on the response of mouse mitochondria devoid of CyP-D [5–7], of ANT1 and ANT2 [8], and of the three VDAC isoforms [9] have shown that a functional PTP can still be formed in the absence of each of these proteins (see ref. [10] for a review). In spite of these uncertainties on the molecular nature of the PTP, its role as a mechanism for the execution of cell death is no longer questioned (reviewed in refs. [4] and [11]).

The PT can be favoured by a variety of structurally unrelated compounds and conditions. In spite of the inducer heterogeneity, a large body of data indicates that the PT is a regulated process, and that inducers converge on one or more discrete regulatory step(s) [12]. A key feature of the system is the regulation by both ΔpH and $\Delta\Psi_{\text{m}}$ components of the mitochondrial protonmotive force. Critical

Abbreviations: ANT, adenine nucleotide translocase; CsA, cyclosporin A; Cyp-D, cyclophilin D; Cu(OP)₂, copper-*o*-phenanthroline; Cys, cysteine; DTT, dithiothreitol; EGTA, [ethylenbis(oxoethylenitrilo)] tetraacetic acid; His, histidine; HP, hematoporphyrin IX; IMM, inner mitochondrial membrane; MBM⁺, trimethylammonium monobromobimane; MOPS, 4-morpholinepropanesulfonic acid; $^1\text{O}_2$, singlet oxygen; OMM, outer mitochondrial membrane; PhAsO, phenylarsine oxide; PT, permeability transition; PTP, permeability transition pore; RCR, respiratory control ratio; ROS, reactive oxygen species; TEM, transmission electron microscopy; VDAC, voltage-dependent anion channel

* Corresponding author. C.N.R. Institute of Biomedical Technologies/Padova Unit, Department of Biology, University of Padova, Via Ugo Bassi 58B, 35121 Padova, Italy. Tel.: +39 049 827 6336; fax: +39 049 827 6348.

E-mail address: rchielli@mail.bio.unipd.it (F. Ricchelli).

¹ Present address: Laser Research Center, Vilnius University, Sauletekio ave 9, bldg 3, 10222 Vilnius, Lithuania.

histidine (His) residues located on the matrix side of the inner membrane make the pore responsive to pH (matrix acidification favoring pore closure through His protonation) [13]. A voltage sensor which is influenced by various effectors is proposed to make the pore opening sensitive to $\Delta\Psi_m$ (depolarization favoring pore opening) [14].

A major role in tuning the voltage sensor of the PTP is played by the oxidation-reduction state of vicinal thiols in cysteinyl (Cys) residues. Disulfide formation (as well as dithiol cross-linking) at a critical site (dubbed the “S-site”) located in the matrix is associated with a higher probability of PT activation through a shift of the threshold potential at which pore opening occurs [15,16]. In addition, a class of pore-regulating thiols, which are sensitive to membrane-impermeant reagents (external thiols) has been also described. External thiols could be either located on the outer surface of the inner membrane, or on intermembrane/outer membrane regulatory protein(s), possibly at contact sites [17].

In 1997, Salet et al. [18] used a novel methodological approach to explore the regulatory properties of PTP-critical sites. Their method took advantage of the ability of porphyrins to bind to mitochondria and produce reactive oxygen species [ROS, mainly singlet oxygen (1O_2)] upon irradiation with UV/visible light [19]. The 1O_2 transient photogenerated *in situ* can easily oxidize electron-rich protein targets, including Cys and His, provided that the substrate and the sensitizer are situated in close proximity [20,21]. Using the porphyrin photosensitizing properties, Salet et al. [18] demonstrated that hematoporphyrin (HP) localizes to strategic matrix sites containing PTP-regulating His. In the first example of PTP desensitization by ROS, His degradation by 1O_2 generated by vicinal photoactivated HP maintained the pore in a closed conformation, in sharp contrast with what is generally observed with oxidizing agents (see also refs. [22,23]).

Herein we find that pore inhibition following His photodegradation can be ascribed to a drop of reactivity of the internal PTP-activating thiols (the “S” site), which are no longer reactive with cross-linkers and oxidants. We have exploited this inactivation of the “S” site to study the contribution to PTP regulation of an additional class of sulfhydryls, which can also trigger the PT after oxidation or reaction with cross-linkers. Based on the PT-desensitizing effect of membrane-impermeant, thiol-protective reagents and on the PT-activating effect of copper-*o*-phenanthroline, we conclude that this group of thiols is located on the external side of the inner membrane.

2. Materials and methods

2.1. Reagents

Hematoporphyrin IX (HP) was obtained from Frontier Scientific (Logan, UT, USA). Stock solutions were prepared in dimethylsulfoxide (DMSO). Trimethylammonium monobromobimane (MBM⁺) was a product of Calbiochem, UK. Copper-*o*-phenanthroline [Cu(OP)₂] was prepared just before use by mixing CuSO₄ with *o*-phenanthroline in a molar ratio of 1:2 in bidistilled water. All chemicals were of the highest purity commercially available.

2.2. Preparation of mitochondria

Liver mitochondria from Wistar rats were prepared by standard differential centrifugation. The final pellet was suspended in 0.25 M sucrose to give a protein concentration of 80–100 mg/ml, as measured by the biuret method. The functionality of mitochondria was established by measuring the respiratory control ratio (RCR) between the rate of oxygen consumption in state 3 (in the presence of 0.3 mM ADP) and in state 4 (in the absence of ADP) in a thermostatted ($T=25\text{ }^\circ\text{C}$), water-jacketed vessel, using a Clark electrode connected to a recorder. The incubation buffer contained 100 mM sucrose, 50 mM KCl, 10 mM Tris–Mops, 10 mM KH₂PO₄, 2 mM MgCl₂, 1 mM

EDTA, 2 μM rotenone, pH 7.4. Succinate (5 mM) was used as the energizing substrate. Only mitochondrial suspensions with a RCR ≥ 3.0 were used.

2.3. Mitochondrial permeability transition

Mitochondrial PT was induced at 25 $^\circ\text{C}$ in a medium containing 200 mM sucrose, 10 mM Tris–Mops, 5 mM succinate, 1 mM P_i, 10 μM EGTA–Tris, 0.5 $\mu\text{g/ml}$ oligomycin, 2 μM rotenone, pH 7.4 (standard medium) [14]. Ca²⁺, phenylarsine oxide (PhAsO) and copper-*o*-phenanthroline [Cu(OP)₂] were used as PT inducers.

PT-induced osmotic swelling of mitochondrial suspensions was followed as the decrease in 90 $^\circ$ light scattering at 540 nm, measured with a Perkin-Elmer LS 50 spectrophotofluorimeter [22].

The calcium retention capacity (CRC), i.e., the amount of Ca²⁺ accumulated and retained by mitochondria before the occurrence of the PT [24], was measured with a Ca²⁺-selective electrode (Elektrode ISE Calcium, Crison Instruments, Barcelona, Spain).

2.4. Photosensitization of HP-labelled mitochondria

Mitochondria (0.5 mg/ml) were incubated for 1–2 min in the dark with the desired concentration of HP and then irradiated at 365 nm in a thermostated glass reaction vessel with a Philips HPW 125-W lamp (Philips, Eindhoven, The Netherlands). The fluence rate at the level of the preparations (40 W/m²) was measured with a calibrated quantum-photo-radiometer (Delta OHM HD 9021). All irradiations were performed at 25 $^\circ\text{C}$ under magnetic stirring. Proper controls were carried out indicating that neither incubation with the photosensitizer in the dark nor illumination under identical experimental conditions but in the absence of porphyrin produced any appreciable changes in the parameters under study.

2.5. Transmission electron microscopy (TEM) of mitochondria

Mitochondria in the various experimental conditions were fixed for 30 min at 4 $^\circ\text{C}$ using glutaraldehyde at a final concentration of 1.5% (V/V) in 0.1 M cacodilate buffer (pH 7.2), then post-fixed with 1% OsO₄. Thin sections (60–80 nm) were stained with uranyl acetate in alcohol (50%) and lead citrate. Observations were made by using a FEI Tecnai F12 transmission electron microscope.

3. Results and discussion

3.1. Inhibition of the mitochondrial PT by HP-mediated photooxidative stress. Degradation of PTP-regulating His

We studied the effects of photoactivated HP on mitochondrial Ca²⁺ uptake and membrane permeabilization to sucrose. Mitochondria labelled with 3 μM HP were incubated for 2 min at 25 $^\circ\text{C}$ and the PT was triggered by Ca²⁺ after irradiation for increasing times at a fluence rate of 40 W/m². Non-irradiated mitochondria did not retain a 80 μM Ca²⁺ pulse, and a fast process of Ca²⁺ release readily followed the initial phase of Ca²⁺ uptake (Fig. 1A, trace a). This fast process of Ca²⁺ release was due to the opening of the PTP since it was accompanied by swelling (Fig. 1B, trace a), and the Ca²⁺ threshold was more than doubled in the presence of 1 μM CsA (not shown). After 20 s of irradiation (total light dose = 0.08 J/cm²) mitochondria readily accumulated the initial 80 μM Ca²⁺ pulse, whereas Ca²⁺ efflux was triggered by a further 60 μM Ca²⁺ load (Fig. 1A, trace b) and the rate of membrane permeabilization was significantly decreased (Fig. 1B, trace b). After irradiation for 45 s (total light dose = 0.18 J/cm²), the ability of mitochondria to take up and retain Ca²⁺ was further improved (Fig. 1A, trace c), and the inner mitochondrial membrane became impermeable to sucrose (Fig. 1B, trace c).

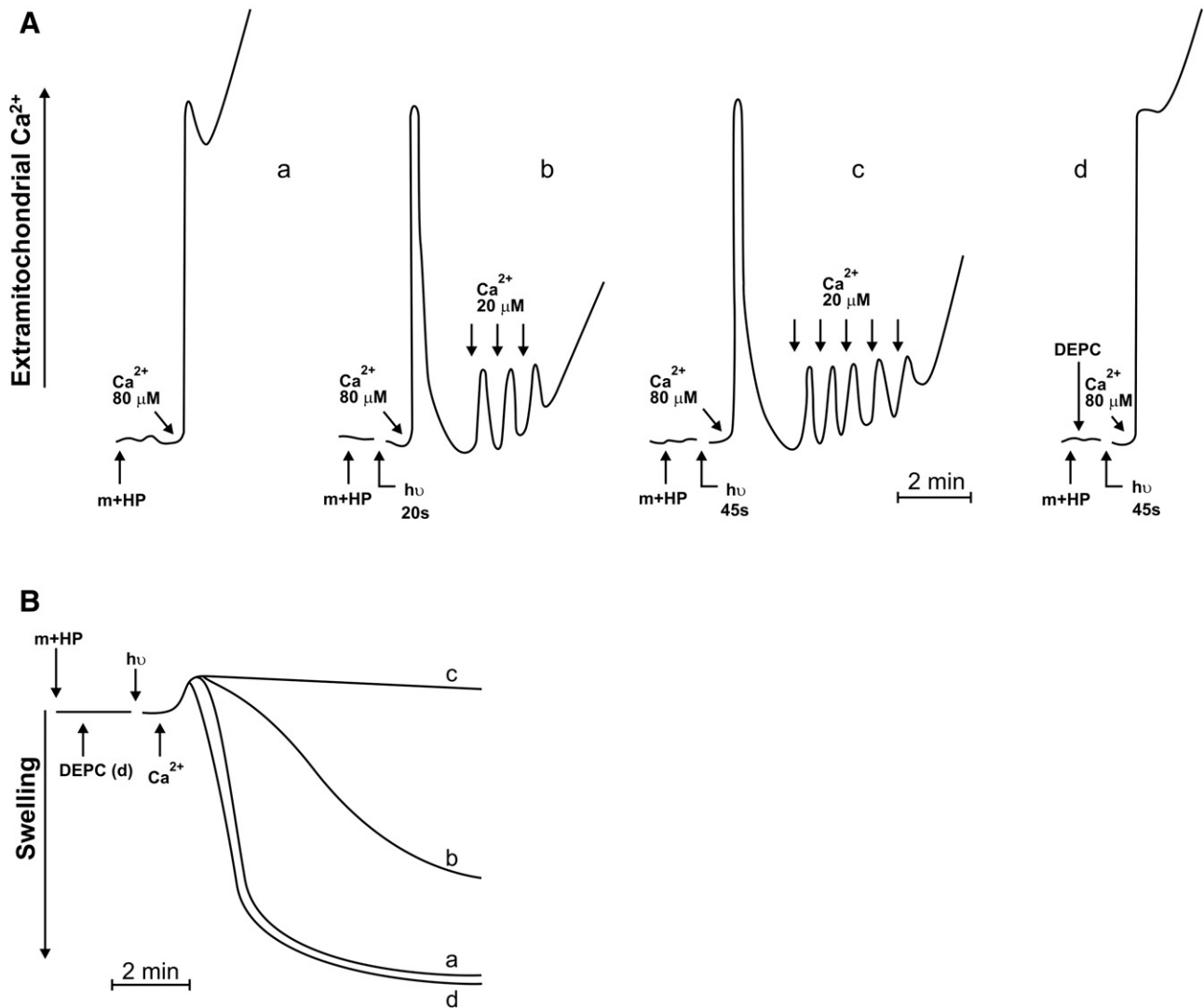


Fig. 1. Progressive mitochondrial PT inhibition at increasing irradiation times in HP-loaded mitochondria, as followed by the changes in PT-induced Ca^{2+} release (A) and matrix swelling (B). Mitochondria (0.5 mg/ml) labelled with HP (3 μM) (m+HP) were incubated for 2 min at 25 °C in the standard medium. Irradiation ($h\nu$) was performed for the indicated periods of time at a fluence rate of 40 W/m^2 . Where indicated (trace d) mitochondria were supplemented with DEPC (200 μM). Panel A: Ca^{2+} pulses were added to the mitochondrial suspensions as indicated by arrows. Extramitochondrial Ca^{2+} was monitored by a Ca^{2+} -selective electrode. Panel B: the PT was triggered by 80 μM Ca^{2+} . Matrix swelling was followed as the decrease of 90° light scattering at 540 nm.

Maintenance of the pore in the closed state after mitochondrial irradiation in the presence of HP was previously attributed to photodegradation of matrix-exposed, PTP-regulating His residues [18,22,23]. Involvement of His as the photosensitive substrate is demonstrated by the antagonizing effects of pretreatment of mitochondria with diethyl pyrocarbonate (DEPC), which prevented the effects of photoirradiation (Fig. 1A and B, traces d). DEPC reacts with His, thereby hindering the addition of $^1\text{O}_2$ to the $\text{C}_2\text{--C}_3$ bond of the imidazole ring and its irreversible degradation [23].

3.2. Functional state of PTP-regulating thiols after His photodegradation. Unmasking external thiols

Under conditions leading to PT inhibition HP-mediated photo-damage was selective to His, and PTP opening could still be triggered through other critical sites of the pore. As an example, the experiments reported in Fig. 2 show that non-irradiated mitochondria were permeabilized to sucrose by 80 μM Ca^{2+} (trace a), whereas irradiated mitochondria maintained their permeability barrier when challenged with an identical Ca^{2+} load (trace b), yet underwent permeabilization and swelling upon addition of the dithiol cross-

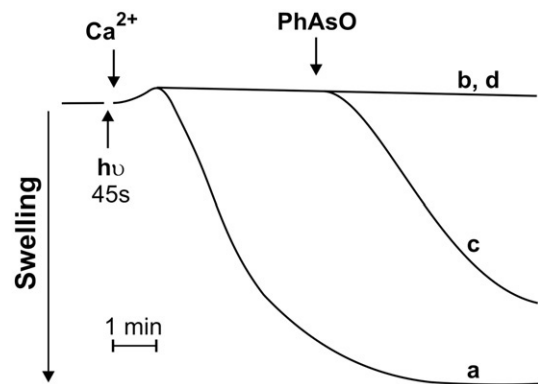


Fig. 2. Activation of the PTP by PhAsO in HP-loaded, irradiated mitochondria. Trace a: the PT was induced by 80 μM Ca^{2+} in HP (3 μM)-labelled, non-irradiated mitochondria. Trace b: the Ca^{2+} -induced PT was inhibited by irradiation at 40 W/m^2 for 45 s (total light dose = 0.18 J/cm^2). Trace c: opening of the PTP was triggered in irradiated mitochondria by addition of 10 μM PhAsO. Trace d: 1 μM CsA was present in the incubation medium under the various experimental conditions. The PT trend was followed by the changes in 90° light scattering intensity at 540 nm, due to the changes of mitochondrial volume.

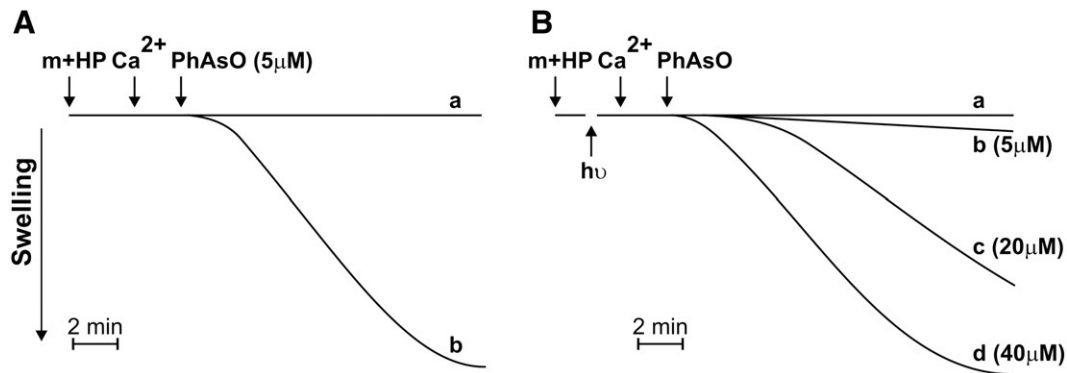


Fig. 3. Induction of the PT by PhAsO in HP-loaded, non-irradiated (A) and irradiated (B) mitochondria. Mitochondria (0.5 mg/ml) labelled with 3 μM HP, either in the dark (panel A) or irradiated for 45 s at 40 W/m^2 (total light dose = 0.18 J/cm^2) (panel B), were supplemented with a small Ca^{2+} pulse (5 μM), which was unable to induce PTP opening per se (panels A and B, traces a), followed by addition of PhAsO at concentration: 5 μM (panels A and B, traces b), 20 μM (panel B, trace c) or 40 μM (panel B, trace d). The PT was followed by the changes in 90° light scattering intensity at 540 nm.

linker PhAsO (trace c), in a process that maintained full sensitivity to CsA (trace d). These findings indicate that the pore remained competent for opening through critical thiols, which must have maintained the reduced state during the His photooxidation process (see also ref. [18]). Since photodamage is strictly localized to substrates that are in close proximity to the sensitizer, it follows that the PhAsO-reactive thiols and HP were beyond the critical distance (less than 0.02 μm , according to Moan and Berg, [20]) required for an efficient oxidative photoprocess (otherwise cysteine should be oxidized to cystine by $^1\text{O}_2$).

The -SH groups insensitive to the photoprocess could belong to the matrix-facing, critical cysteines (“S” site), as suggested by their availability to cross-linking reactions by the membrane-permeant PhAsO. Alternatively, His photodegradation could modify the pore-regulatory activity of the “S” site and lead to unmasking an additional class of thiols. The following set of experiments was aimed at discriminating between these two possibilities.

HP-labelled mitochondria, either non-irradiated (Fig. 3A) or exposed to a light dose of 0.18 J/cm^2 (40 W/m^2 for 45 s) (Fig. 3B), were supplemented with a small Ca^{2+} pulse (5 μM) unable to induce PTP opening per se (Fig. 3A, B, traces a), followed by PhAsO. In non-irradiated mitochondria, 5 μM PhAsO was sufficient to trigger the PT (Fig. 3A, trace b), a concentration that was instead ineffective in irradiated mitochondria (Fig. 3B, trace b). Remarkably, much higher PhAsO concentrations were necessary to induce swelling in irradiated mitochondria (Fig. 3B, traces c, d). Similar results were obtained with

the membrane-permeant thiol oxidant diamide (DIA) (data not shown). These results suggest that the accessibility of PhAsO-reactive thiols was altered during irradiation, probably as a consequence of a conformational change brought about by His photooxidation [18,23].

To identify the class of thiols involved in the photoirradiation-dependent events we performed a set of experiments using DTT and MBM^+ as -SH protective agents. Monobromobimane (MBM^+) and the cationic derivative MBM^+ were introduced by Costantini et al. [25] as PTP-thiol reagents which neither inhibit the phosphate carrier, nor interfere with Ca^{2+} transport, energy coupling or ATP production and transport.

The process of PT activation by PhAsO (Fig. 4A, B, traces a) was prevented by treatment with 200 μM DTT in both non-irradiated (Fig. 4A, trace b) and irradiated (Fig. 4B, trace b) mitochondria. MBM^+ (up to 200 μM) was ineffective at blocking the DTT-sensitive site in non-irradiated mitochondria (Fig. 4A, trace c). Since this cationic species is impermeant to (or slowly permeating) cell membranes [26] we conclude that PhAsO interacted with internal thiols that could not be protected by MBM^+ . In striking contrast, 10 μM MBM^+ significantly delayed opening of the pore in irradiated mitochondria (Fig. 4B, trace c). Protection of the PhAsO-reactive thiols by MBM^+ strongly suggests that in irradiated mitochondria PhAsO triggered the PT mainly via an external site. In keeping with this interpretation, addition of up to 0.5 mM MBM^+ to mitochondria did not cause any perturbation of the membrane potential as measured through the fluorescence changes of Pyronin G [22,23] (results not shown), in contrast to what observed

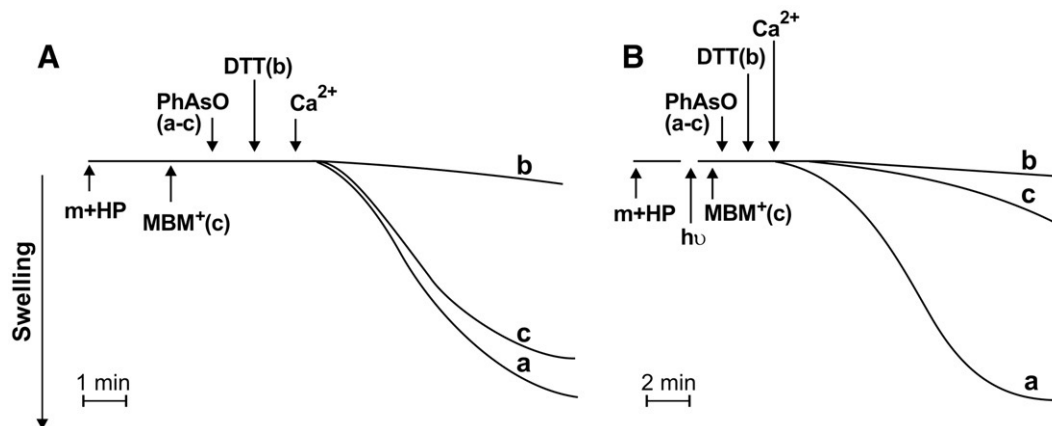


Fig. 4. Induction of the PT by PhAsO in HP-loaded, non-irradiated (A) and irradiated (B) mitochondria in the absence and in the presence of thiol-protective reagents. HP (3 μM)-labelled mitochondria (0.5 mg/ml), either non-irradiated (panel A) or irradiated for 45 s at 40 W/m^2 (total light dose = 0.18 J/cm^2) (panel B), were supplemented with 10 μM PhAsO, then 10 μM Ca^{2+} (a concentration not sufficient to induce PTP opening per se) was added (panels A and B, traces a). Where indicated, 200 μM DTT (panels A and B, traces b) or MBM^+ (10–200 μM in panel A and 10 μM in panel B, traces c) were also added. The PT was followed by the changes in 90° light scattering intensity at 540 nm.

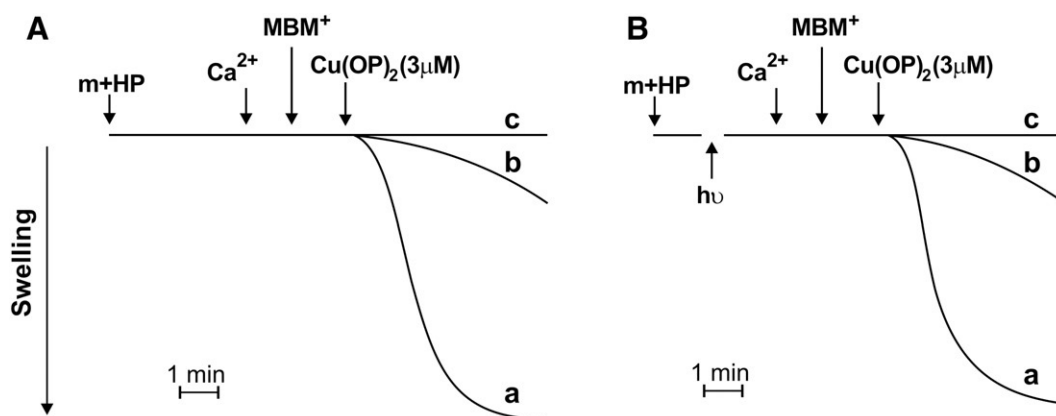


Fig. 5. Induction of the PT by $\text{Cu}(\text{OP})_2$ in HP-loaded, non-irradiated (A) and irradiated (B) mitochondria in the absence and in the presence of the thiol-protective reagent, MBM^+ . HP ($3 \mu\text{M}$)-labelled mitochondria (0.5 mg/ml), either non-irradiated (panel A) or irradiated for 45 s at 40 W/m^2 (total light dose = 0.18 J/cm^2) (panel B), were supplemented with $10 \mu\text{M}$ Ca^{2+} (a concentration not sufficient to induce PTP opening per se), then $\text{Cu}(\text{OP})_2$ ($3 \mu\text{M}$) was added (panels A and B, traces a). Where indicated, $10 \mu\text{M}$ MBM^+ (panels A and B, traces b) were also added. In traces c, the various experiments were carried out in the presence of $1 \mu\text{M}$ CsA. The PT was followed by the changes in 90° light scattering intensity at 540 nm .

with Ca^{2+} [23] or with membrane-permeant lipophilic cations [27]. Thus, it appears that MBM^+ is not transported across the inner membrane; and that the MBM^+ -inhibitable sites unmasked by irradiation are not located in the matrix, also based on the effects of membrane-impermeant $\text{Cu}(\text{OP})_2$ (see below).

To further probe the involvement of external thiols in mitochondrial PT activation after His photooxidation, we used a PTP-triggering, membrane-impermeant reagent. In the next set of experiments HP-loaded mitochondria were assayed using the thiol oxidant $\text{Cu}(\text{OP})_2$ as the PT inducer. It was previously shown that $\text{Cu}(\text{OP})_2$ stimulates the PT by catalyzing the dithiol-disulfide interconversion of a class of external thiols [17]. Both non-irradiated (Fig. 5A) and irradiated (Fig. 5B) mitochondria underwent matrix swelling after exposure to $3 \mu\text{M}$ $\text{Cu}(\text{OP})_2$ (Fig. 5A, B, traces a), in a process sensitive to CsA (Fig. 5A, B, traces c). In both cases, the effects of $\text{Cu}(\text{OP})_2$ could be prevented by thiol reaction with MBM^+ (Fig. 5A, B, traces b). These results clearly indicate that PT induction and PT inhibition by MBM^+ in irradiated mitochondria was indeed due to the activation and protection of external thiols, respectively. These groups were not affected by any structural rearrangement after His photodegradation, because the concentration of $\text{Cu}(\text{OP})_2$ required to induce the PT was identical in irradiated and non-irradiated mitochondria.

Taken together, these findings suggest that: (i) in non-irradiated mitochondria, pore opening via cross-linking of $-\text{SH}$ groups by low PhAsO concentrations is mainly regulated by the internal, matrix-facing sites; (ii) His photodegradation causes a drop in reactivity of internal but not of external thiols, thus allowing to study the specific contribution of the latter to PT regulation. This class of thiols readily reacts with membrane-impermeant reagents, such as $\text{Cu}(\text{OP})_2$, whereas more drastic conditions are necessary for the interaction with membrane-permeant compounds, such as PhAsO and DIA, which partition in both surface and internal mitochondrial membrane domains.

3.3. HP-mediated photooxidation of external thiols

The next set of experiments was aimed at determining whether HP-binding sites were also present near the external thiol domains, and could modify their reactivity upon irradiation. Since under the experimental conditions used thus far ($3 \mu\text{M}$ HP, 45 s irradiation at 40 W/m^2) only HP-binding sites interfering with the critical His could be detected, we explored the effects of different times of irradiation and HP concentrations on the PT, as measured with the sensitive CRC assay (Fig. 6). These experiments revealed that the effect of irradiation was biphasic in all the experimental conditions used. Inhibition of the PT increased with the irradiation time up to a maximum, followed by a

decreased inhibition at longer irradiation times. In all cases, HP-mediated photodamage causing PT inhibition could be ascribed to His photodegradation, as indicated by the counteracting effect of DEPC (results not shown). These findings suggest that the HP-binding sites adjacent to the critical His are highly selective for the porphyrin, being the most photovulnerable in the whole range of effective HP concentrations.

The CRC values rapidly decreased upon increase of the light dose. We found that the CRC decrease below control values could still be largely counteracted by CsA. As an example, Fig. 7 shows that 0.5 mg/ml of mitochondria incubated with $3 \mu\text{M}$ HP and supplemented with $40 \mu\text{M}$ Ca^{2+} (which does not affect the membrane permeability per se), then irradiated for 100 s at 40 W/m^2 (total light dose = 0.4 J/cm^2) underwent a large amplitude swelling (trace a) that was prevented by CsA (trace b). Similarly to most PTP inducers, HP + light needed Ca^{2+} as a permissive factor for PTP opening (see in trace c the lack of effect obtained in the absence of Ca^{2+}). Thus, in these protocols, PTP opening was due to a HP-dependent photooxidation process of a PTP-regulating site that is less photosensitive than His. This site coincides with the external critical thiols, as shown by the antagonizing effect of the membrane-impermeant thiol reagent MBM^+ (trace d). This result

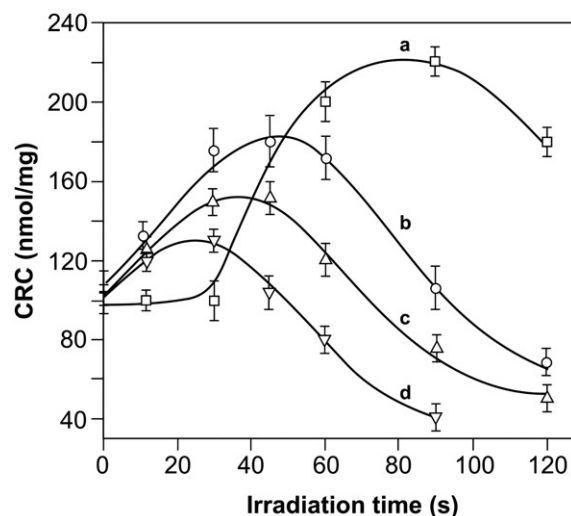


Fig. 6. Effects of irradiation on the PT in HP-loaded mitochondria at different HP concentrations and light doses. Mitochondria (0.5 mg/ml) were incubated for 2 min at 25°C in the standard medium after labelling with: $1 \mu\text{M}$ (a), $3 \mu\text{M}$ (b), $4 \mu\text{M}$ (c), or $5 \mu\text{M}$ (d) HP. After irradiation for the indicated periods of time at a fluence rate of 40 W/m^2 , mitochondria were loaded with a series of $10 \mu\text{M}$ Ca^{2+} pulses at 1 min intervals. PTP opening was determined as the CRC measured with a Ca^{2+} -selective electrode.

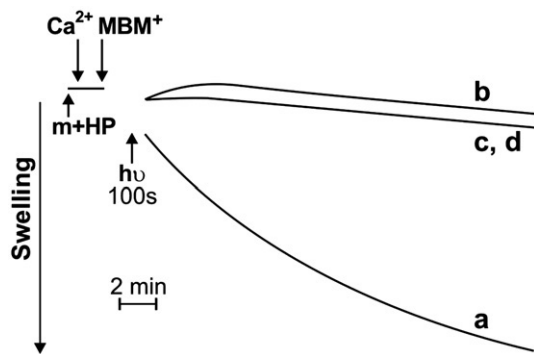


Fig. 7. Induction of mitochondrial PT after 100 s irradiation of HP-loaded mitochondria. HP (3 μM)-labelled mitochondria (0.5 mg/ml) after addition of 40 μM Ca^{2+} (a concentration not sufficient to induce PTP opening per se), were irradiated for 100 s at 40 W/m^2 (total light dose = 0.4 J/cm^2) (trace a). In trace b, 1 μM CsA was present in the incubation medium; in trace c, irradiation was performed in the absence of added Ca^{2+} ; in trace d, 10 μM MBM⁺ was added before irradiation. The PT was followed by the changes in 90° light scattering intensity at 540 nm.

is remarkable because it demonstrates that photooxidative stress mediated by the same sensitizer (HP) can either inhibit (through His degradation) or activate (through external thiol oxidation) the PT, depending on the interplay between light and sensitizer dose.

3.4. Effects of HP and irradiation on mitochondrial ultrastructure

We studied the effects of photooxidative events mediated by HP on mitochondrial ultrastructure, as analysed by TEM. Mitochondria maintained their integrity after loading with HP in the dark, as demonstrated by their regular shape with a well defined outer membrane and rich inner membrane infolding to define the cristae (Fig. 8A and B). Following PTP opening by 80 μM Ca^{2+} , mitochondria

appeared swollen with decreased matrix electron density and increased volume (Fig. 8C). The mitochondrial membranes were well preserved when Ca^{2+} was added after exposure to 0.18 J/cm^2 light dose (40 W/m^2 for 45 s) (Fig. 8D), mitochondrial morphology being closely comparable to that obtained by pretreatment with 1 μM CsA (Fig. 8E).

HP-loaded mitochondria had normal morphology and folding of the inner membrane after exposure to 0.4 J/cm^2 light dose (40 W/m^2 for 100 s) in the absence of added Ca^{2+} (Fig. 8F) (i.e. a condition under which the PTP was in the closed state, Fig. 7). Addition of 40 μM Ca^{2+} , which induced PTP opening (Fig. 7), caused matrix swelling and expansion of the mitochondrial volume (Fig. 8G). These effects were prevented by pretreatment with 10 μM MBM⁺ (Fig. 8H). It should be noted that the outer membrane could not be clearly detected after HP + light treatment when the PTP did not open (Fig. 8F and H); yet, the activity of monoaminoxidase was fully retained, indicating that impermeability barrier to proteins was fully maintained (data not shown). It appears likely that the observed structural reorganization is concomitant with the marked decrease of oxidative phosphorylation efficiency after prolonged irradiation times [18]. This would be consistent with the observations of Hackenbrock [28,29], which indicate that the internal mitochondrial structure is rather flexible, and linked to the metabolic state of the organelle.

4. Summary and conclusions

In photosensitization of biological materials by reactive oxygen species (including $^1\text{O}_2$) the photodamage is strictly limited to the immediate surroundings of the sensitizer because of the short diffusion distance and high reactivity of the photogenerated species. On this basis, selective targeting of photosensitive substrates located at or near the sensitizer binding sites is thus possible. This peculiar oxidation mechanism has provided more detailed information on residues regulating the PT than is possible to achieve with other

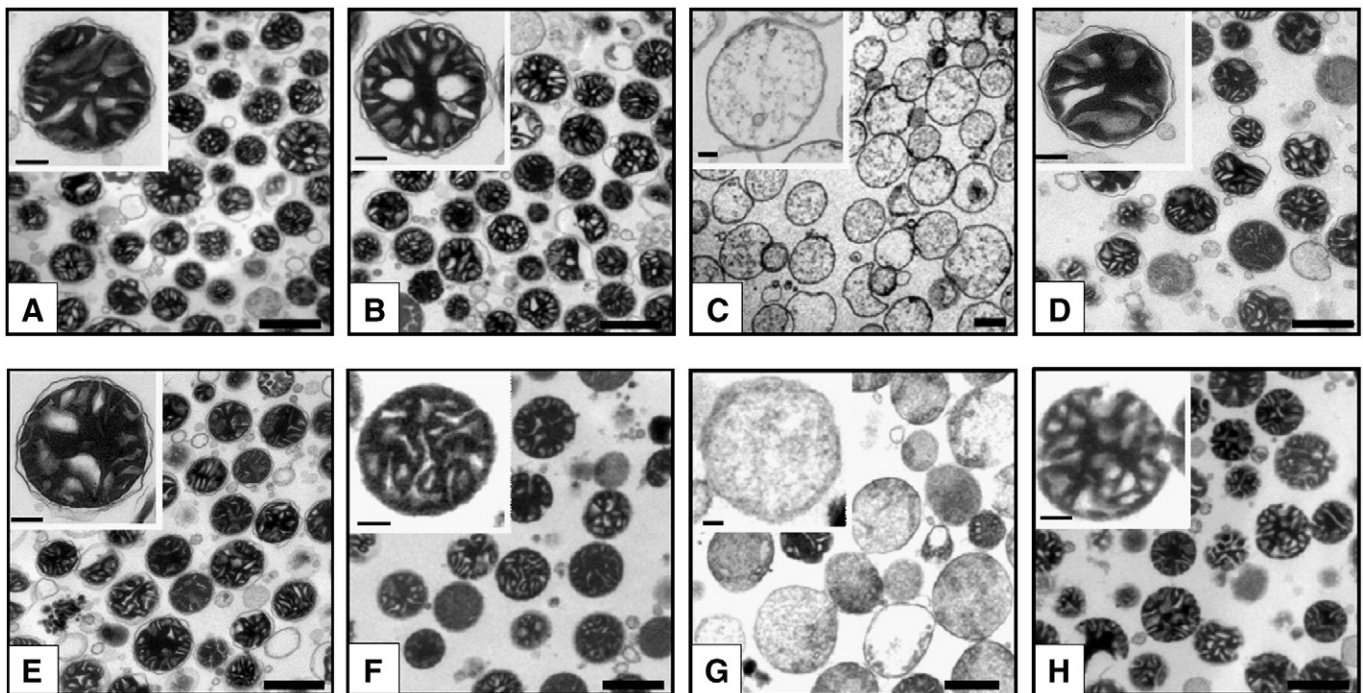


Fig. 8. Effects of HP loading and different light doses on mitochondrial ultrastructure. Mitochondria (0.5 mg/ml) were incubated for 2 min at 25 °C in the standard medium without (panel A) or with 3 μM HP (panels B–H). HP-loaded mitochondria were treated as follows: kept in the dark (panel B); supplemented with 80 μM Ca^{2+} to induce PTP opening (panel C); exposed to 0.18 J/cm^2 light dose (40 W/m^2 for 45 s) before addition of 80 μM Ca^{2+} (panel D); pretreated with 1 μM CsA before addition of 80 μM Ca^{2+} (panel E); exposed to 0.4 J/cm^2 light dose (40 W/m^2 for 100 s) in the absence of added Ca^{2+} (panel F); supplemented with 40 μM Ca^{2+} before exposure to 0.4 J/cm^2 light dose (panel G); supplemented with 40 μM Ca^{2+} plus 10 μM MBM⁺ before exposure to 0.4 J/cm^2 light dose (panel H). Bars correspond to 1 μm (main figure) or 0.2 μm (insets).

oxidizing agents or conditions. In this study, whose results are summarized in Fig. 9, we were able to characterize the PTP-modulating properties of two sites which exhibited different sensitivity towards oxidation by vicinal, photoactivated HP.

Under basal conditions (step 1) the PTP favors the closed conformation, and the presence of HP does not affect the reactivity and pore-modulating properties of internal (matrix-exposed) and external cysteines (for clarity, the latter are represented as located on the outer surface of the IMM); indeed, an increased probability of PTP opening can be easily elicited by complex formation with PhAsO (which reacts with both sites) or $\text{Cu}(\text{OP})_2$, a membrane-impermeant reagent that only oxidizes the external site (step 2). Photoirradiation for short periods of time hits the most photovulnerable site, which comprises matrix-exposed His (see also ref. [18]), and causes a secondary drop of reactivity of internal, pore-activating Cys, thus stabilizing the PTP in the closed conformation (step 3); indeed, matrix Cys can no longer react with PhAsO, probably because of a conformational rearrangement of the “S” site which makes these residues distant or poorly accessible to reagents. On this basis, the key His residues appear to play a role in PT activation as modulators of the conformation of internal thiol domains. In agreement, literature data indicate that protonation of the key His is associated with less extensive thiol oxidation [30] or cross-linking [23]. Thus, it appears that any modification of the His site interferes with the activity of the “S” site, suggesting that they are closely related both structurally and functionally.

The functional inactivation of internal Cys by His photodegradation in turn allows to study the role of external regulatory Cys, which can still undergo oxidation by $\text{Cu}(\text{OP})_2$ (or complex formation by PhAsO, omitted for clarity) and thus increase the probability of PTP opening (step 4). Finally, photoirradiation for times longer than necessary to

oxidize His causes direct oxidation of the external Cys, which is followed by PTP opening (step 5).

In conclusion, oxidative stress mediated by $^1\text{O}_2$ photogenerated in the presence of HP can either trigger or inhibit the mitochondrial PT depending on porphyrin localization and nature of the photosubstrate. The importance of the sensitizer binding site for the effects of $^1\text{O}_2$ on the PT was already demonstrated by comparative studies with two structurally different photoactivated dyes, HP (PT inhibition) and 4,5',8-trimethylpsoralen (PT induction) [21]. In addition, the present data demonstrate that the photoprocess stimulated by the same sensitizer can switch the mitochondrial PT from inhibition to activation by a fine tuning of light intensity/sensitizer concentration combinations.

The identity of the mitochondrial proteins which bind the two PTP-regulating, photosensitive substrates remains undefined. Yet, some indications could arise from previous studies of mitochondrial function under irradiation. At increasing light doses, oxidative phosphorylation was the first function to be lost, whereas respiration, Ca^{2+} cycling, OMM-, matrix- and intermembrane-enzyme activities were more resistant in this order. Among the identified $^1\text{O}_2$ -targets of the IMM, ANT inactivation was largely responsible for the decline of oxidative phosphorylation at short irradiation times [18,31]. Thus, it is tempting to speculate that ANT domains exposed to the matrix side might contain the highly photosensitive, critical His. Such His location would also agree with the desensitizing effect caused by His photodegradation on the oxidation of the vicinal, internal thiol groups if these are exposed to the matrix side of the ANT as well, as suggested by some authors [3,32–36]. This interpretation would be in agreement with a PT-regulatory role of ANT, but of course PTP photoinactivation may well involve other critical targets of the phosphorylation cycle, including the P_i carrier, which was recently postulated to contain PTP-critical thiol groups [37]. Work aimed at

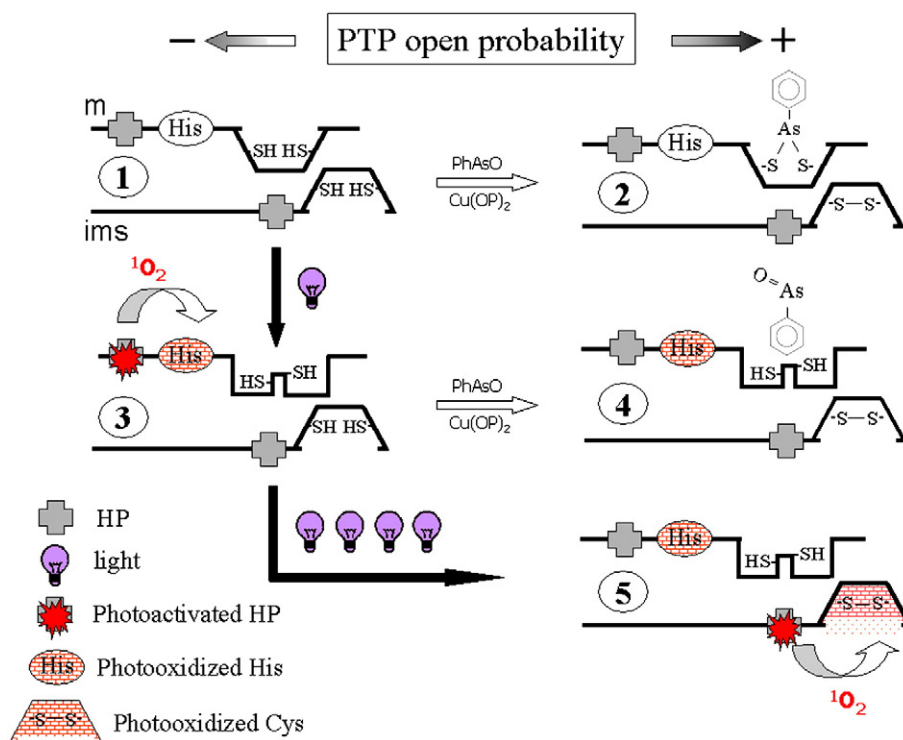


Fig. 9. Summary of the photodynamic events mediated by HP at PTP-regulating His and Cys residues. Matrix-facing (m) IMM HP-binding sites are located in close proximity to critical His residues. Additional HP-binding sites are adjacent to external, critical thiols. For clarity, external thiols are represented as located on the outer surface of the inner membrane facing the intermembrane space (ims). In the dark, HP does not affect the structural properties of His- and Cys-containing domains (step 1) and PTP can be opened through selective activation of internal or external Cys when low concentrations of PhAsO or $\text{Cu}(\text{OP})_2$ are used (step 2; reaction of external Cys with PhAsO is not shown for clarity). After mitochondrial irradiation with moderate light doses, m-located photoactivated HP generates $^1\text{O}_2$. The photoprocess causes oxidation of the key His and a structural rearrangement of the internal thiol binding sites, which hinders the cross-linking reaction with PhAsO leading to PT inhibition (step 3). The PT can be reactivated through external thiols by oxidation with $\text{Cu}(\text{OP})_2$ (step 4) or by cross-linking with PhAsO (not shown). Irradiation with high light doses causes photoactivation of ims-located HP leading to oxidation of ims-facing Cys by $^1\text{O}_2$ photogenerated *in situ* (step 5). For further explanation see text.

identifying the relevant protein targets of HP-mediated photooxidation is under way in our laboratories.

Acknowledgements

This research was supported by the Italian National Research Council (CNR) within the framework of the Italy–Bulgaria (BAN) bilateral cooperation and, partially, by a MIUR/FIRB project, code CINECA RBAU01YL5R.

References

- [1] J.J. Lemasters, T. Qian, C.A. Bradham, D.A. Brenner, W.E. Cascio, L.C. Trost, Y. Nishimura, A.L. Nieminen, B. Herman, Mitochondrial dysfunction in the pathogenesis of necrotic and apoptotic cell death, *J. Bioenerg. Biomembr.* 31 (1999) 305–319.
- [2] M. Crompton, The mitochondrial permeability transition pore and its role in cell death, *Biochem. J.* 341 (1999) 233–249.
- [3] A.W. Leung, A.P. Halestrap, Recent progress in elucidating the molecular mechanism of the mitochondrial permeability transition pore, *Biochim. Biophys. Acta* 1777 (7–8) (2008) 946–952.
- [4] P. Bernardi, A. Krauskopf, E. Basso, V. Petronilli, E. Blachly-Dyson, F. Di Lisa, M.A. Forte, The mitochondrial permeability transition from in vitro artifact to disease target, *FEBS J.* 273 (2006) 2077–2099.
- [5] C.P. Baines, R.A. Kaiser, N.H. Purcell, N. Scott Blair, H. Osinska, M.A. Hambleton, E.W. Brunskill, M.R. Sayen, R.A. Gottlieb, G.W. Dorn II, J. Robbins, J.D. Molkenin, Loss of cyclophilin D reveals a critical role for mitochondrial permeability transition in cell death, *Nature* 434 (2005) 658–662.
- [6] E. Basso, L. Fante, J. Fowlkes, V. Petronilli, M.A. Forte, P. Bernardi, Properties of the permeability transition pore in mitochondria devoid of cyclophilin D, *J. Biol. Chem.* 280 (2005) 18558–18561.
- [7] E. Basso, V. Petronilli, M.A. Forte, P. Bernardi, Phosphate is essential for inhibition of the mitochondrial permeability transition pore by cyclosporin A and by cyclophilin D ablation, *J. Biol. Chem.* 283 (2008) 26307–26311.
- [8] J.E. Kokoszka, K.G. Waymire, S.E. Levy, J.E. Sligh, J. Cai, D.P. Jones, G.R. MacGregor, D.C. Wallace, The ADP/ATP translocator is not essential for the mitochondrial permeability transition pore, *Nature* 427 (2004) 461–465.
- [9] C.P. Baines, R.A. Kaiser, T. Sheiko, W.J. Craigen, J.D. Molkenin, Voltage-dependent anion channels are dispensable for mitochondrial-dependent cell death, *Nat. Cell. Biol.* 9 (2007) 550–555.
- [10] P. Bernardi, M. Forte, The mitochondrial permeability transition pore, *Novartis Found Symp.* 287 (2007) 157–164.
- [11] A. Rasola, P. Bernardi, The mitochondrial permeability transition pore and its involvement in cell death and in disease pathogenesis, *Apoptosis* 12 (2007) 815–833.
- [12] P. Bernardi, The permeability transition pore. Control points of a cyclosporin A-sensitive mitochondrial channel involved in cell death, *Biochim. Biophys. Acta* 1275 (1996) 5–9.
- [13] A. Nicolli, V. Petronilli, P. Bernardi, Modulation of the mitochondrial cyclosporin A-sensitive permeability transition pore by matrix pH. Evidence that the pore open-closed probability is regulated by reversible histidine protonation, *Biochemistry* 32 (1993) 4461–4465.
- [14] V. Petronilli, C. Cola, S. Massari, R. Colonna, P. Bernardi, Physiological effectors modify voltage sensing by the cyclosporin A-sensitive permeability transition pore of mitochondria, *J. Biol. Chem.* 268 (1993) 21939–21945.
- [15] V. Petronilli, P. Costantini, L. Scorrano, R. Colonna, S. Passamonti, P. Bernardi, The voltage sensor of the mitochondrial permeability transition pore is tuned by the oxidation-reduction state of vicinal thiols. Increase of the gating potential by oxidants and its reversal by reducing agents, *J. Biol. Chem.* 269 (1994) 16638–16642.
- [16] P. Costantini, B.V. Chernyak, V. Petronilli, P. Bernardi, Modulation of the mitochondrial permeability transition pore by pyridine nucleotides and dithiol oxidation at two separate sites, *J. Biol. Chem.* 271 (1996) 6746–6751.
- [17] P. Costantini, R. Colonna, P. Bernardi, Induction of the mitochondrial permeability transition by N-ethylmaleimide depends on secondary oxidation of critical thiol groups. Potentiation by copper-ortho-phenanthroline without dimerization of the adenine nucleotide translocase, *Biochim. Biophys. Acta* 1365 (1998) 385–392.
- [18] C. Salet, G. Moreno, F. Ricchelli, P. Bernardi, Singlet oxygen produced by photodynamic action causes inactivation of the mitochondrial permeability transition pore, *J. Biol. Chem.* 272 (1997) 21938–21943.
- [19] J. Morgan, A.R. Oseroff, Mitochondria-based photodynamic anti-cancer therapy, *Adv. Drug Deliv. Rev.* 49 (2001) 71–86.
- [20] J. Moan, K. Berg, The photodegradation of porphyrins in cells can be used to estimate the lifetime of singlet oxygen, *Photochem. Photobiol.* 53 (1991) 353–359.
- [21] G. Moreno, K. Poussin, F. Ricchelli, C. Salet, The effects of singlet oxygen produced by photodynamic action on the mitochondrial permeability transition differ in accordance with the localization of the sensitizer, *Arch. Biochem. Biophys.* 386 (2001) 243–250.
- [22] F. Ricchelli, S. Gobbo, G. Moreno, C. Salet, Changes of the fluidity of mitochondrial membranes induced by the permeability transition, *Biochemistry* 38 (1999) 9295–9300.
- [23] F. Ricchelli, G. Jori, S. Gobbo, P. Nikolov, V. Petronilli, Discrimination between two steps in the mitochondrial permeability transition process, *Int. J. Biochem. Cell Biol.* 37 (2005) 1858–1868.
- [24] E. Fontaine, F. Ichas, P. Bernardi, A ubiquinone-binding site regulates the mitochondrial permeability transition pore, *J. Biol. Chem.* 273 (1998) 25734–25740.
- [25] P. Costantini, B.V. Chernyak, V. Petronilli, P. Bernardi, Selective inhibition of the mitochondrial permeability transition pore at the oxidation-reduction sensitive dithiol by monobromobimane, *FEBS Lett.* 362 (1995) 239–242.
- [26] N.S. Kosower, N.M. Kosower, G.L. Newton, H.M. Ranney, Bimane fluorescent labels: labeling of normal human red cells under physiological conditions, *Proc. Natl. Acad. Sci. U.S.A.* 76 (1979) 3382–3386.
- [27] A. Zulian, V. Petronilli, S. Bova, F. Dabbeni-Sala, G. Cargnelli, M. Cavalli, D. Rennison, J. Ståb, O. Laita, M.A. Brimble, B. Hopkins, P. Bernardi, F. Ricchelli, Assessing the molecular basis for rat-selective induction of the mitochondrial permeability transition by norbormide, *Biochim. Biophys. Acta Bioenerg.* 1767 (2007) 980–988.
- [28] C.R. Hackenbrock, Ultrastructural bases for metabolically linked mechanical activity in mitochondria. II. Electron transport-linked ultrastructural transformations in mitochondria, *J. Cell Biol.* 37 (1968) 345–369.
- [29] C.R. Hackenbrock, Energy-linked ultrastructural transformations in isolated liver mitochondria and mitoplasts. Preservation of configurations by freeze-cleaving compared to chemical fixation, *J. Cell Biol.* 53 (1972) 450–465.
- [30] B.M. Teixeira, A.J. Kowaltowski, R.F. Castilho, A.E. Vercesi, Inhibition of mitochondrial permeability transition by low pH is associated with less extensive membrane protein thiol oxidation, *Oncogene* 19 (2) (1999) 525–533.
- [31] C. Salet, G. Moreno, Photosensitization of mitochondria. Molecular and cellular aspects, *J. Photochem. Photobiol., B. Biol.* 5 (2) (1990) 133–150.
- [32] P. Costantini, A.-S. Belzacq, H.L.A. Vieira, N. Larochette, M.A. de Pablo, N. Zamzami, S.A. Susin, C. Brenner, G. Kroemer, Oxidation of a critical thiol residue of the adenine nucleotide translocator enforces Bcl-2-independent permeability transition pore opening and apoptosis, *Oncogene* 19 (2) (2000) 307–314.
- [33] T. Kanno, E.E. Sato, S. Muranaka, H. Fujita, T. Fujiwara, T. Utsumi, M. Inoue, K. Utsumi, Oxidative stress underlines the mechanism for Ca²⁺-induced permeability transition of mitochondria, *Free Rad. Res.* 38 (1) (2004) 27–35.
- [34] A.J. Kowaltowski, A.E. Vercesi, R.F. Castilho, Mitochondrial membrane protein thiol reactivity with N-ethylmaleimide or mersalyl is modified by Ca²⁺: correlation with mitochondrial permeability transition, *Biochim. Biophys. Acta.* 1318 (3) (1997) 395–402.
- [35] G.P. McStay, S.J. Clarke, A.P. Halestrap, Role of critical thiol groups on the matrix surface of the adenine nucleotide translocase in the mechanism of the mitochondrial permeability transition pore, *Biochem. J.* 36 (2002) 541–548.
- [36] A.P. Halestrap, K.Y. Woodfield, C.P. Connern, Oxidative stress, thiol reagents, and membrane potential modulate the mitochondrial permeability transition by affecting nucleotide binding to the adenine nucleotide translocase, *J. Biol. Chem.* 272 (6) (1997) 3346–3354.
- [37] A.W. Leung, P. Varanyuwatana, A.P. Halestrap, The mitochondrial phosphate carrier interacts with cyclophilin D and may play a key role in the permeability transition, *J. Biol. Chem.* 283 (39) (2008) 26312–26323.



Contents lists available at SciVerse ScienceDirect

Biochimica et Biophysica Acta

journal homepage: www.elsevier.com/locate/bbambio

The translocator protein (peripheral benzodiazepine receptor) mediates rat-selective activation of the mitochondrial permeability transition by norbormide

Alessandra Zulian^{a,1}, Justina Šileikytė^{a,1}, Valeria Petronilli^a, Sergio Bova^b, Federica Dabbeni-Sala^b, Gabriella Cargnelli^b, David Rennison^c, Margaret A. Brimble^c, Brian Hopkins^d, Paolo Bernardi^{a,*}, Fernanda Ricchelli^{e,**}

^a C.N.R. Institute of Neurosciences at the Department of Biomedical Sciences, University of Padova, Padova, Italy

^b Department of Pharmacology and Anesthesiology/Pharmacology Division, University of Padova, Padova, Italy

^c Department of Chemistry, University of Auckland, Auckland, New Zealand

^d Landcare Research, Canterbury Agriculture and Science Centre, Lincoln, New Zealand

^e C.N.R. Institute of Biomedical Technologies at the Department of Biology, University of Padova, Padova, Italy

ARTICLE INFO

Article history:

Received 14 June 2011

Received in revised form 29 July 2011

Accepted 10 August 2011

Available online 26 August 2011

Keywords:

Mitochondria

Mitoplast

Permeability transition

Norbormide

TSPO

ABSTRACT

We have investigated the mechanism of rat-selective induction of the mitochondrial permeability transition (PT) by norbormide (NRB). We show that the inducing effect of NRB on the PT (i) is inhibited by the selective ligands of the 18 kDa outer membrane (OMM) translocator protein (TSPO, formerly peripheral benzodiazepine receptor) protoporphyrin IX, *N,N*-dihexyl-2-(4-fluorophenyl)indole-3-acetamide and 7-chloro-5-(4-chlorophenyl)-1,3-dihydro-1-methyl-2H-1,4-benzodiazepin-2-one; and (ii) is lost in digitonin mitoplasts, which lack an intact OMM. In mitoplasts the PT can still be induced by the NRB cationic derivative OL14, which contrary to NRB is also effective in intact mitochondria from mouse and guinea pig. We conclude that selective NRB transport into rat mitochondria occurs via TSPO in the OMM, which allows its translocation on PT-regulating sites in the inner membrane. Thus, species-specificity of NRB toward the rat PT depends on subtle differences in the structure of TSPO or of TSPO-associated proteins affecting its substrate specificity.

© 2011 Elsevier B.V. All rights reserved.

1. Introduction

Norbormide (NRB, 5-(α -hydroxy- α -2-pyridylbenzyl)-7-(α -2-pyridylbenzylidene)-5-norbornene-2,3-dicarboximide) is a synthetic compound introduced as a specific rat toxicant in 1964 [1]. It is endowed with unique pharmacodynamic properties inducing species-selective contraction of rat peripheral blood vessels, likely

Abbreviations: CsA, cyclosporin A; Cu(OP)₂, copper-*o*-phenanthroline; Cys, cysteine; EGTA, [ethylenedis(oxoethylenitrilo)] tetraacetic acid; FGIN1-27, *N,N*-dihexyl-2-(4-fluorophenyl)indole-3-acetamide; HP, hematoporphyrin IX; IMM, inner mitochondrial membrane; MOPS, 4-morpholinepropanesulfonic acid; NRB, 5-(α -hydroxy- α -2-pyridylbenzyl)-7-(α -2-pyridylbenzylidene)-5-norbornene-2,3-dicarboximide; OL14, 5-(α -hydroxy- α -2-pyridylbenzyl)-7-(*N*-pivaloyloxymethyl- α -2-pyridylbenzylidene)-5-norbornene-2,3-dicarboximide; OMM, outer mitochondrial membrane; PhAsO, phenylarsine oxide; PT, permeability transition; PTP, permeability transition pore; Ro5-4864 4'-chlorodiazepam, 7-chloro-5-(4-chlorophenyl)-1,3-dihydro-1-methyl-2H-1,4-benzodiazepin-2-one; TSPO, 18 kDa translocator protein (peripheral benzodiazepine receptor)

* Correspondence to: P. Bernardi, Department of Biomedical Sciences, University of Padova, Viale Giuseppe Colombo 3, I-35121 Padova, Italy. Fax: +39 0498276361.

** Correspondence to: F. Ricchelli, Consiglio Nazionale delle Ricerche Institute of Biomedical Technologies at the Department of Biology, University of Padova, Viale Giuseppe Colombo 3, I-35121 Padova, Italy. Fax: +39 0498276348.

E-mail addresses: bernardi@bio.unipd.it (P. Bernardi), rchielli@bio.unipd.it (F. Ricchelli).

¹ A.Z. and J.S. contributed equally to this work.

by acting on a phospholipase C (PLC)-coupled receptor, which is abundantly or exclusively expressed in the myocytes of these vessels [2]. NRB instead elicits a relaxing action in rat aorta and non-vascular smooth muscles, as well as in blood vessels of species other than the rat, possibly because of reduced Ca²⁺ influx through voltage-dependent L-type Ca²⁺ channels [1–7]. NRB is a mixture of eight racemic stereoisomers, which differ in their vasoconstrictor activity and toxicity [8–10]. Detailed studies of each individual stereoisomer demonstrate that both drug-induced contractile activity and lethality in rats are strongly stereospecific, with only the *endo* configurations retaining the effects elicited by the mixture [8]. Moreover, investigations over a series of NRB fragments derived from the “deconstruction” of the parent molecule suggest that integrity of the molecule must be retained, in order for NRB-type vasoconstriction to be conserved [11].

Intriguingly, NRB also causes rat-selective mitochondrial dysfunction that can be traced to opening of the permeability transition (PT) pore (PTP) [12,13]. The PTP is a high conductance channel of the inner mitochondrial membrane (IMM), whose opening leads to an increase of permeability to ions and solutes with an exclusion size of about 1500 Da. This potentially catastrophic event has long been known, yet the molecular bases for its occurrence remain unsolved despite its established importance in several *in vivo* models of pathology [14–17]. The key structural feature responsible for PTP activation by

NRB is its 2-(1-phenylvinyl)pyridine fragment (DR166) [13]. The relationship between lethal vasoconstriction and the PTP-inducing effect is not obvious, because both lethal (*endo*-) and non lethal (*exo*-) NRB isomers display comparable stimulatory effects on the PT in isolated mitochondria [13].

In order to better understand the mode of action of NRB, and the possible correlation between the various rat-selective effects, this study examines the mechanisms causing species-specificity for PTP activation. It has already been shown that rat selectivity of NRB toward the PT is not due to a different PTP structure/target in the various animal species, but rather involves a transport system allowing selective penetration of the drug in the IMM/matrix of rat mitochondria [12,13]. Indeed, the cationic NRB derivative 5-(α -hydroxy- α -2-pyridylbenzyl)-7-(*N*-pivaloyloxymethyl- α -2-pyridylbenzylidene)-5-norbornene-2,3-dicarboximide (OL14), which permeates through the IMM driven by the inside negative membrane potential, is as effective in mouse and guinea pig as it is in rat mitochondria [13]. The present paper reports on whether the putative NRB carrier is located in the outer mitochondrial membrane (OMM) by comparing the PTP-regulatory properties of the drug in mitochondria and in digitonin-treated mitoplasts. Our data demonstrate that an intact OMM is necessary for the PTP-inducing effects of NRB, and strongly suggest that the drug permeates through domains of the 18 kDa translocator protein (TSPO, formerly known as peripheral benzodiazepine receptor, [18]), or of TSPO-associated protein(s), that are unique to the rat.

2. Materials and methods

NRB was purchased from I.N.D.I.A. Industria Chimica, Padova while its cationic derivative OL14 was synthesized and purified by Drs. David Rennison and Olivia Laita, Department of Chemistry, University of Auckland (New Zealand). The structure of these compounds is depicted in Fig. 1. Hematoporphyrin IX, protoporphyrin IX, deuteroporphyrin IX, and coproporphyrin III were obtained from Frontier Scientific (Logan, UT, U.S.A.) and stock solutions were prepared in dimethylsulfoxide. *N,N*-dihexyl-2-(4-fluorophenyl)indole-3-acetamide (FGIN1-27), (4'-chlorodiazepam;7-chloro-5-(4-chlorophenyl)-1,3-dihydro-1-methyl-2H-1,4-benzodiazepin-2-one) (Ro5-4864), digitonin, phenylarsine oxide (PhAsO) and etioporphyrin I were purchased from Sigma. Copper-*o*-phenanthroline ($\text{Cu}(\text{OP})_2$) was prepared just before use by mixing CuSO_4 with *o*-phenanthroline in a molar ratio of 1:2 in bidistilled water. All chemicals were of the highest purity commercially available.

Liver mitochondria from Albino Wistar rats, CD1 mice and Albino guinea pigs (from Charles River, Italy) were prepared by standard differential centrifugation. The final pellet was suspended in 0.25 M sucrose to give a protein concentration of 80–100 mg/ml, as measured by the biuret method. The quality of mitochondrial preparations was established by the value of the respiratory control ratio (RCR), as described previously [13].

Mitoplasts were prepared by treatment of mitochondria with 0.09 mg of digitonin/mg of mitochondrial protein, and purity of the

preparations was checked by enzymatic and electron microscopy assays, as described in detail in Ref. [19].

Mitochondrial PT was induced at 25 °C in a standard medium (250 mM sucrose, 10 mM Tris-Mops pH 7.4, 5 mM succinate-Tris, 1 mM P_i -Tris, 10 μM EGTA-Tris, 1 μM rotenone, 0.5 $\mu\text{g}/\text{ml}$ oligomycin). Ca^{2+} , phenylarsine oxide (PhAsO) and $\text{Cu}(\text{OP})_2$ were used as PT inducers. PT-induced osmotic swelling of mitochondrial suspensions was followed as the decrease in 90° light scattering at 540 nm, measured with a Perkin-Elmer LS 50 spectrophotofluorimeter [12]. Permeabilization rates were calculated as the rate of change of light scattering immediately after addition of inducer. The calcium retention capacity (CRC), i.e., the amount of Ca^{2+} accumulated and retained by mitochondria before the occurrence of the PT [20] was measured with 0.5 μM Calcium Green-5N as an indicator of the Ca^{2+} concentration in the external medium (excitation at 480 nm and emission at 530 nm) [13].

3. Results

3.1. Effects of NRB and OL14 on the mitochondrial and mitoplast PT

We compared the effects of NRB and its cationic derivative, OL14, on mitochondria and mitoplasts prepared by extraction with 0.09 mg digitonin \times mg^{-1} of protein, i.e. a condition yielding mitoplasts that maintain a high IMM integrity as assessed by development of a membrane potential, ability to take up Ca^{2+} , and maintenance of a permeability barrier to solutes [19]. We tested the ability of both organelles to undergo the PT with the sensitive calcium retention capacity (CRC) test, which measures the threshold Ca^{2+} load required to open the pore. Incubation of mitochondria with 40 nmol/mg protein of NRB for 5 min decreased the Ca^{2+} load required for PTP opening without affecting the rate of Ca^{2+} uptake (Fig. 2A trace b, compare with trace a), an effect that was also seen with OL14 (Fig. 2A, trace c). In striking contrast, NRB did not affect the CRC in mitoplasts (Fig. 2A', trace b, compare with trace a) while OL14 was as effective as it was in mitochondria. The concentration-dependence of the effects of NRB and OL14 in mitochondria and mitoplasts is presented in Fig. 3. These findings indicate that NRB requires an intact OMM to be effective; yet its site of action must be at the IMM or matrix, because its PTP-inducing effects in mitochondria are retained by the permeant cationic OL14 (see also Refs. [12,13]). The higher doses necessary to induce PT activation in mitoplasts suggest that access of OL14 to the mitochondrial matrix is also facilitated by the OMM.

We next tested if the differential effects of NRB on PTP in mitochondria and mitoplasts could also be detected by modifying two classes of IMM (matrix- and surface-exposed) PT-regulating sulfhydryls, which can be discriminated based on their reactivity with the membrane-permeant dithiol cross-linker phenylarsine oxide (PhAsO) and the membrane-impermeant thiol oxidant copper-*o*-phenanthroline ($\text{Cu}(\text{OP})_2$), respectively [21–23]. We first assessed the response to PhAsO. In these protocols, a permissive Ca^{2+} load that does not cause PTP opening per se was allowed to accumulate first (Fig. 4A, A', trace a); ruthenium red (RR) was then added to prevent Ca^{2+} redistribution, and finally PTP opening was triggered by PhAsO and the process was monitored as the ensuing Ca^{2+} release (Fig. 4A, A', trace b), which was indeed fully inhibited by CsA (Fig. 4A, A', trace c). Treatment with NRB caused an earlier onset of PTP opening in mitochondria (Fig. 4A, trace d) but not in mitoplasts, where the release rate was indistinguishable from that of PhAsO alone (Fig. 4A', trace d). Consistent with what was observed with Ca^{2+} -dependent PT (Figs. 2, 3), OL14 caused PhAsO to induce immediate triggering of PTP opening in both preparations (Fig. 4A, A', trace e). The response to $\text{Cu}(\text{OP})_2$ gave results superimposable to those obtained with PhAsO, as PTP opening was stimulated by NRB in mitochondria but not in mitoplasts, while OL14 was equally effective (Fig. 4B, B', trace labeling is identical to panels A, A').

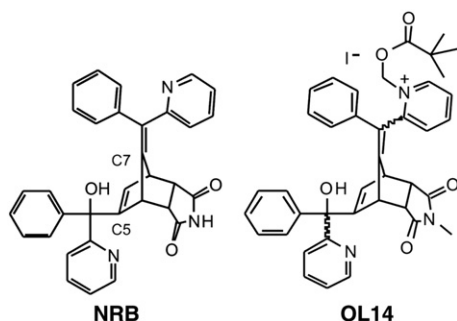


Fig. 1. Chemical structures of NRB and OL14.

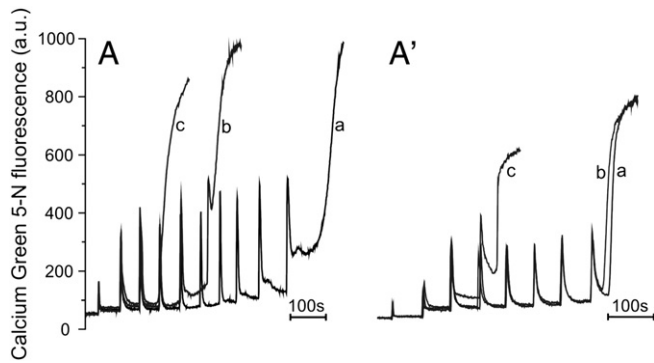


Fig. 2. Effects of NRB and OL14 on the Ca^{2+} retention capacity of rat liver mitochondria and mitoplasts. One milligram per milliliter of rat liver mitochondria (A) or mitoplasts (A') was suspended in the standard incubation medium in the presence of $0.5 \mu\text{M}$ Calcium Green-5N, then loaded with a train of 10 (A) or 5 (A') μM Ca^{2+} pulses at 1-min intervals (trace a). In traces b,c the organelles were preincubated for 5 min with 40 nmol/mg of NRB (b) or OL14 (c). Extramitochondrial Ca^{2+} was monitored as the fluorescence emission of Calcium Green-5N ($\lambda_{\text{excitation}} = 480 \text{ nm}$; $\lambda_{\text{emission}} = 530 \text{ nm}$).

3.2. Effects of NRB on the thiol-regulated mitochondrial PT in the presence of high affinity TSPO-ligands

It has been previously demonstrated that the OMM regulates the PT and that PTP regulatory sites are contributed by TSPO [19]. To test whether NRB transport could occur through TSPO we studied the effects of NRB on the PT induced by PhAsO and $\text{Cu}(\text{OP})_2$ in the presence or absence of hematoporphyrin IX (HP), a dicarboxylic porphyrin with high affinity for TSPO that at the concentration used here ($3 \mu\text{M}$) does not affect the PTP per se [19,21,24]. Mitochondria were incubated with NRB for 5 or 2 min depending on whether PhAsO or $\text{Cu}(\text{OP})_2$ was used as PT inducer because at these incubation times NRB displayed the maximal effect with each thiol reagent (data not shown). To evaluate the extent of stimulation by NRB, the permeabilization rates of NRB-treated mitochondria were normalized to those of NRB-untreated mitochondria. In the case of PhAsO HP suppressed the stimulatory effect of NRB up to 25–30 nmol/mg (Fig. 5A). The effect was even larger in the case of PTP induction by $\text{Cu}(\text{OP})_2$, where HP caused a marked inhibition of the PT up to 20–30 nmol/mg NRB (Fig. 5B). Consistent with competition for TSPO binding, NRB above 20–30 nmol/mg regained its potentiating ability on the PTP.

Similar effects have been observed in the presence of other protoporphyrin IX-like dicarboxylic porphyrins, such as deuteroporphyrin IX and protoporphyrin IX itself, which display even higher affinity than HP in binding TSPO [24]. However, in this study no effect on

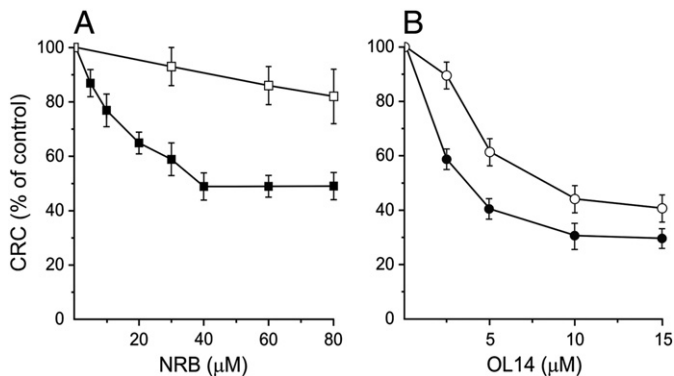


Fig. 3. CRC of rat liver mitochondria and mitoplasts loaded with NRB and OL14. The CRC was calculated according to the experimental procedure described in the legend to Fig. 2 after the addition of NRB (A) or OL14 (B) to rat liver mitochondria (closed symbols) or mitoplasts (open symbols). PTP opening was determined as the Ca^{2+} retention capacity (CRC, expressed as the % of the CRC of organelles not treated with NRB or OL14). Values are mean \pm S.D. of three experiments.

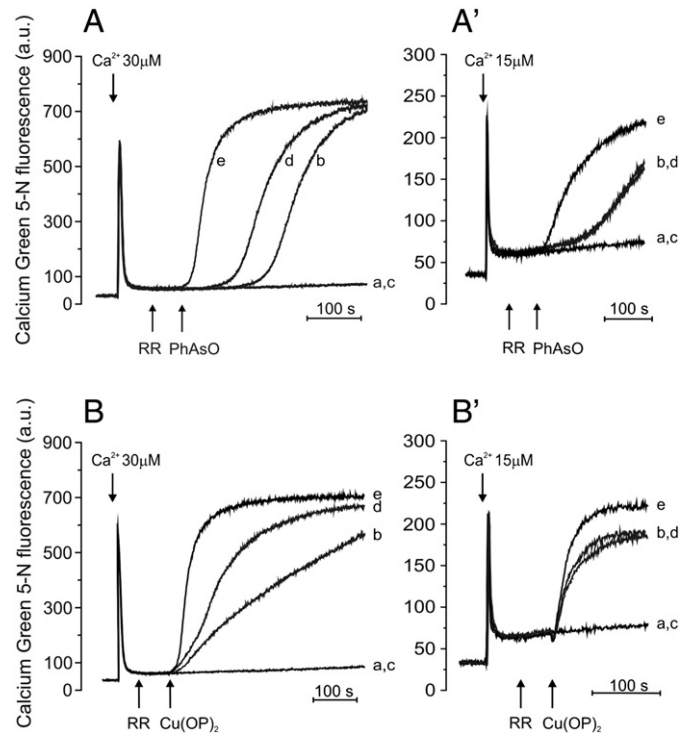


Fig. 4. Effects of NRB and OL14 on PT-dependent Ca^{2+} release in rat liver mitochondria and mitoplasts. One milligram per milliliter of rat liver mitochondria (A) or mitoplasts (A') was incubated in the standard medium containing $0.5 \mu\text{M}$ Calcium Green-5N and allowed to accumulate a Ca^{2+} load (30 and 15 nmol/mg of protein, respectively) that was not sufficient for spontaneous PTP opening (trace a). PTP opening was then triggered by $5 \mu\text{M}$ PhAsO (traces b–e). In the experiments of trace c $1 \mu\text{M}$ CsA was also present, and in those of traces d and e the organelles were supplemented with 40 nmol/mg of NRB and OL14, respectively, and incubated for 5 min prior to the addition of Ca^{2+} . Where indicated, Ca^{2+} was added followed by $0.1 \mu\text{M}$ ruthenium red (RR) and by PhAsO. B, B', the experimental conditions were the same as those described in A, A', except that $3 \mu\text{M}$ $\text{Cu}(\text{OP})_2$ was used as PT inducer.

the NRB-stimulated PT was observed with PP-unrelated porphyrins, such as the tetracarboxylic coproporphyrin III, whose binding to TSPO is very weak, or etioporphyrin I, which lacks carboxylic groups (data not shown). These results suggest that, at low NRB concentrations, interference between NRB and TSPO-porphyrin binding sites causes (i) a drop of reactivity of the external thiols, and (ii) blockade of drug translocation into internal PTP-regulating sites. Other selective TSPO-ligands, such as Ro5-4864 and FGIN1-27 [18,25,26], at concentrations ($\leq 10 \mu\text{M}$) not sufficient to induce the PT per se (data not

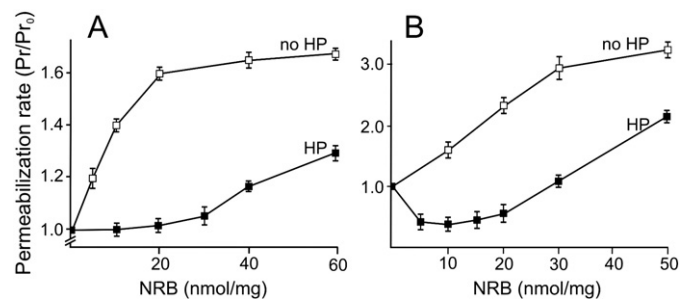


Fig. 5. Effects of NRB and their inhibition by HP, on the PT induced by PhAsO and $\text{Cu}(\text{OP})_2$ in rat liver mitochondria. Mitochondria (0.5 mg/ml) were incubated with the indicated concentrations of NRB for 5 min (panel A) or 2 min (panel B) in standard medium at 25°C , both in the absence (no HP) or presence (HP) of $3 \mu\text{M}$ HP; then $10 \mu\text{M}$ Ca^{2+} (a Ca^{2+} pulse not sufficient to induce the PT per se) was added followed by $5 \mu\text{M}$ PhAsO (A) or $3 \mu\text{M}$ $\text{Cu}(\text{OP})_2$ (B). Spreading of the PT was followed as the decrease in light scattering intensity at 540 nm . The data are expressed as the ratio between the permeabilization rates of NRB-treated (Pr) and -untreated (Pr_0) mitochondria. Values are mean \pm S.D. of three experiments.

shown but see Ref. [19]), were able to suppress the potentiating effects of NRB on the PT induced by both PhAsO and Cu(OP)_2 (Fig. 6). In summary, these results suggest that in the presence of specific TSPO-ligands NRB accumulates in the contact regions between IMM and OMM, and perturbation of these regions does not allow NRB to reach its sites of action at the IMM/matrix.

The experiments described above were performed also in mouse and guinea pig liver mitochondria. Irrespective of whether PhAsO or Cu(OP)_2 was used, or whether TSPO ligands were present, no effect of NRB was observed, while the PT could be induced by the positively charged OL14 (results not shown). These data confirm that in animal species different from the rat the drug-sensitive sites of the mitochondrial PTP are not accessible to NRB [12,13].

4. Discussion

In this paper we have demonstrated that rat-selective opening of the PTP by NRB in liver mitochondria requires an intact OMM, and obtained compelling evidence that the effect of NRB is specifically mediated by the OMM protein, TSPO.

The regulatory role of the OMM is demonstrated by the lack of PT-promoting effect of NRB in mitoplasts, i.e. in the absence of an intact OMM irrespective of whether PTP opening is induced by Ca^{2+} plus Pi, or by reaction with internal (PhAsO-sensitive) or external (Cu(OP)_2 -sensitive) sulfhydryls. We deduce that in rat mitochondria NRB is transferred from the OMM to the IMM through a transport system that is lost in mitoplasts. OMM TSPO appears to be the key element mediating mitochondrial internalization of NRB, as suggested by the findings that, at NRB concentrations up to $30 \mu\text{M}$ (i) high-affinity ligands of TSPO, such as protoporphyrin IX-like dicarboxylic porphyrins, Ro5-4864 and FGIN1-27, are able to abolish the effects of NRB at the internal, PhAsO-reactive sites; and (ii) co-administration of porphyrins and NRB to mitochondria drastically reduces the reactivity of the external, Cu(OP)_2 -sensitive sites, which we know to be in close contact with the binding site of porphyrins on TSPO [19]. These effects are likely a consequence of competition between NRB and TSPO-ligands for specific sites on TSPO, which both alters the external, Cu(OP)_2 -sensitive PTP domains and prevents NRB transfer to the matrix. These findings suggest that NRB interacts with TSPO sites adjacent to or overlapping with those of porphyrins, Ro5-4864 and FGIN1-27.

The cationic OL14 is active on both mitochondria and mitoplasts of all species and is more potent than NRB. These data suggest that both agents act from the matrix and thus must cross both the OMM and IMM. Indeed, NRB cationic derivatives transiently depolarize the mitochondrial inner membrane and then activate the PT also in mouse

and guinea pig, consistent with transport to the matrix [13]. It is also noteworthy that cationic NRB derivatives that do not bear the active core still depolarize the inner membrane but are not able to activate the PT [13]. But why should NRB require TSPO to get to the IMM and not OL14? We think that the amount of (neutral) NRB taken up by mitochondria via passive diffusion may not be sufficient to stimulate the PT unless the drug first binds the OMM (via TSPO) and then is transferred to the IMM. It is not inconceivable that the cationic OL14 can instead be attracted by the huge driving force provided by the IMM proton electrochemical gradient (predicted equilibrium accumulation of 1000 if the membrane potential is -180 mV , negative inside).

When administered to mitochondria at 30 nmol/mg protein or more, NRB regains its ability to potentiate the PT irrespective of the presence of selective TSPO-ligands. TSPO is still required, because these concentrations of NRB do not affect the PT in mitoplasts. A likely explanation is that NRB at high concentrations is able to bind to lower affinity secondary sites on TSPO, overcoming the inhibition produced by TSPO ligands occupying the primary binding site. The presence of two populations of (high and low affinity) drug-binding sites is common to other TSPO-ligands, and this observation has been used to explain the dose-dependent pro-apoptotic and anti-apoptotic effects, and modulation of muscle contractility of many TSPO-ligands [27–31]. Although in our interpretation TSPO allows NRB to be transported to its internal matrix site(s) of action (see also Ref. [13]), we cannot exclude that, after interaction with NRB, TSPO per se might mediate PTP opening.

In conclusion, the present data support previous results demonstrating a key role of TSPO in PT regulation [19,32]. The absence of demonstrable effects of NRB on the PTP of mouse and guinea pig mitochondria suggests that selectivity may depend on one or more residues of TSPO that are unique to the rat. Of note, and in spite of the high degree of TSPO sequence homology, changes in only 3 amino acid residues cause remarkable differences in the binding potency of the archetypal TSPO-ligand Ro5-4864 in different species [33–36], and mutation of only one critical residue at the interface between OMM and cytoplasm results in complete loss of ligand binding activity [37].

Alignment of the rat and mouse primary sequences revealed that the proteins have a high level of identity, with only 8 amino acid substitutions (Fig. 7). Since mouse and guinea pig are both resistant to NRB, amino acids that have changed during evolution between these species should not be critical. If this hypothesis is correct, the only relevant difference between the NRB-sensitive rat and NRB-insensitive mouse and guinea pig would be at position 113, where in the rat a methionine interrupts a stretch of 3 leucine residues within a highly conserved DLLLVS motif (Fig. 7A). We analyzed all NRB-insensitive species [3] and found that, as well as mouse and guinea pig, the LLL sequence is conserved in ox, cat, chicken, dog, horse, monkey, rabbit, and sheep. Based on the predicted protein membrane topology [38] the DLLLVS motif is located at the interface between the OMM and the cytosol (Fig. 7B), where it could serve as a selectivity filter for the transported species. This issue can be addressed by proper receptor swap and mutagenesis experiments that are under way in our laboratories.

Acknowledgements

This manuscript is in partial fulfillment of the requirements for the PhD of JS, who was supported by a Fellowship from the Fondazione Cariparo, Padova. The work was supported in part by grants from the Ministry for University and Research (MIUR/PRIN) and Fondazione Cariparo Progetti di Eccellenza “Models of Mitochondrial Diseases”. The authors also wish to thank Landcare Research for financial support and assistance.

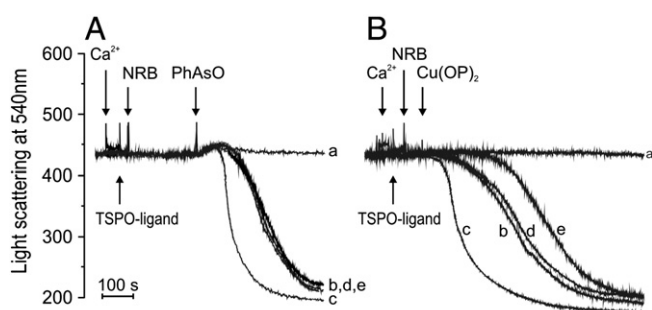


Fig. 6. Effects of NRB, and their inhibition by Ro5-4864 and FGIN1-27, on the PT induced by PhAsO and Cu(OP)_2 in rat liver mitochondria. Mitochondria (1 mg/ml) suspended in the standard medium at 25°C were loaded with a small Ca^{2+} load ($10 \mu\text{M}$) that was not sufficient for spontaneous PTP opening (trace a) followed by $5 \mu\text{M}$ PhAsO (A, traces b–e) or $3 \mu\text{M}$ Cu(OP)_2 (B, traces b–e). In traces c–e, mitochondria were supplemented with 10 (A) or 30 (B) nmol/mg NRB, and with the TSPO ligand Ro5-4864 ($10 \mu\text{M}$, trace d only) or FGIN1-27 ($10 \mu\text{M}$, trace e only). The PT was followed as the decrease in light scattering intensity at 540 nm .

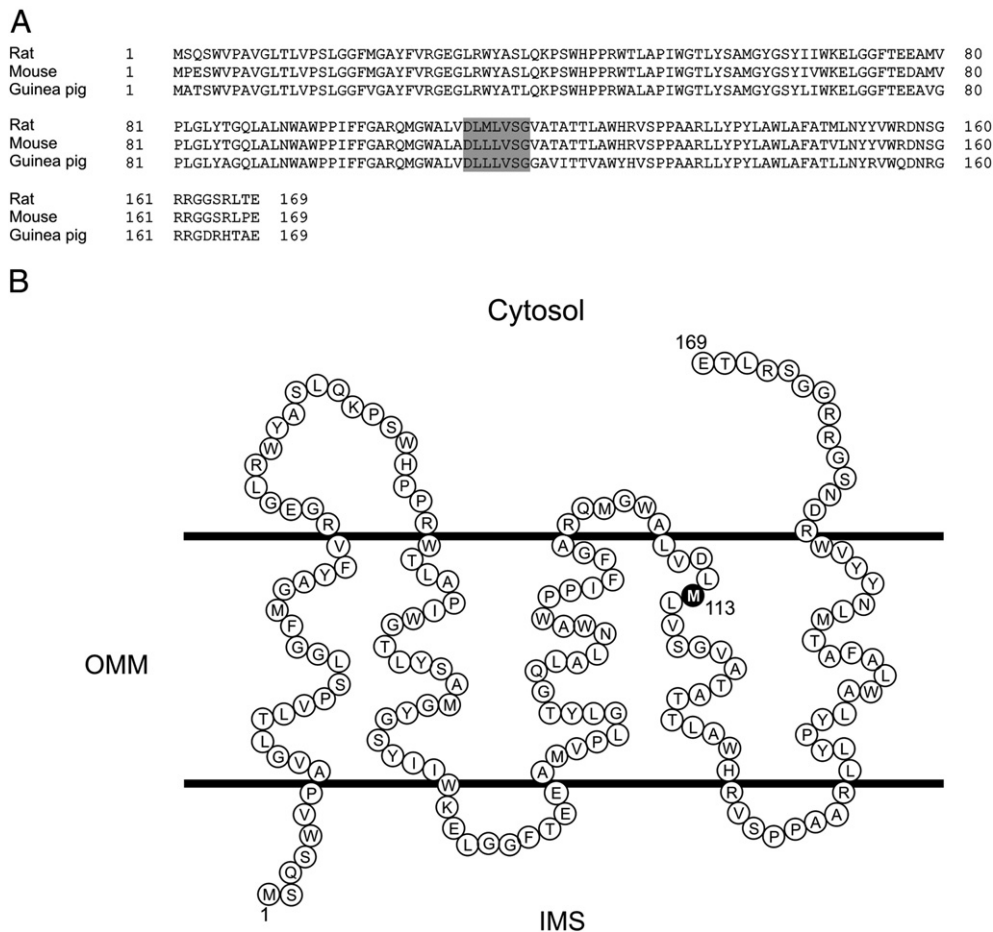


Fig. 7. Comparison of the primary sequence of rat, mouse and guinea pig TSPO and schematic membrane topology of the rat protein. Panel A, alignment of the rat, mouse and guinea pig TSPO sequences. Panel B, schematic view of rat TSPO [38] where the methionine at position 113 is highlighted. For explanation see text.

References

- [1] A.P. Roszkowski, G.I. Poos, R.J. Mohrbacher, Selective rat toxicant, *Science* 144 (1964) 412–413.
- [2] S. Bova, L. Trevisi, L. Cima, S. Luciani, V. Golovina, G. Cargnelli, Signaling mechanisms for the selective vasoconstrictor effect of norbormide on the rat small arteries, *J. Pharmacol. Exp. Ther.* 296 (2001) 458–463.
- [3] A.P. Roszkowski, The pharmacological properties of norbormide, a selective rat toxicant, *J. Pharmacol. Exp. Ther.* 149 (1965) 288–299.
- [4] S. Bova, L. Trevisi, P. Debetto, L. Cima, M. Furnari, S. Luciani, R. Padrini, G. Cargnelli, Vasorelaxant properties of norbormide, a selective vasoconstrictor agent for the rat microvasculature, *Br. J. Pharmacol.* 117 (1996) 1041–1046.
- [5] S. Bova, G. Cargnelli, E. D'Amato, S. Forti, Q. Yang, L. Trevisi, P. Debetto, L. Cima, S. Luciani, R. Padrini, Calcium-antagonist effects of norbormide on isolated perfused heart and cardiac myocytes of guinea-pig: a comparison with verapamil, *Br. J. Pharmacol.* 120 (1997) 19–24.
- [6] F. Fusi, S. Saponara, G. Sgaragli, G. Cargnelli, S. Bova, Ca^{2+} entry blocking and contractility promoting actions of norbormide in single rat caudal artery myocytes, *Br. J. Pharmacol.* 137 (2002) 323–328.
- [7] S. Bova, M. Cavalli, L. Cima, S. Luciani, S. Saponara, G. Sgaragli, G. Cargnelli, F. Fusi, Relaxant and Ca^{2+} channel blocking properties of norbormide on rat non-vascular smooth muscles, *Eur. J. Pharmacol.* 470 (2003) 185–191.
- [8] G.I. Poos, R.J. Mohrbacher, E.L. Carson, V. Paragamian, B.M. Puma, C.R. Rasmussen, A.P. Roszkowski, Structure-activity studies with the selective rat toxicant norbormide, *J. Med. Chem.* 9 (1966) 537–540.
- [9] M.A. Brimble, V.J. Muir, B. Hopkins, S. Bova, Synthesis and evaluation of vasoconstrictor and vasorelaxant activity of norbormide isomers, *ARKIVOC* (i) (2004) 1–11.
- [10] P.J. Steel, M.A. Brimble, B. Hopkins, D. Rennison, Two stereoisomers of the rat toxicant norbormide, *Acta Crystallogr. C* 60 (2004) o374–o376.
- [11] D. Rennison, S. Bova, M. Cavalli, F. Ricchelli, A. Zulian, B. Hopkins, M.A. Brimble, Synthesis and activity studies of analogues of the rat selective toxicant norbormide, *Bioorg. Med. Chem.* 15 (2007) 2963–2974.
- [12] F. Ricchelli, F. Dabbeni-Sala, V. Petronilli, P. Bernardi, B. Hopkins, S. Bova, Species-specific modulation of the mitochondrial permeability transition by norbormide, *Biochim. Biophys. Acta* 1708 (2005) 178–186.
- [13] A. Zulian, V. Petronilli, S. Bova, F. Dabbeni-Sala, G. Cargnelli, M. Cavalli, D. Rennison, J. Stáb, O. Laita, D.J. Lee, M.A. Brimble, B. Hopkins, P. Bernardi, F. Ricchelli, Assessing the molecular basis for rat-selective induction of the mitochondrial permeability transition by norbormide, *Biochim. Biophys. Acta* 1767 (2007) 980–988.
- [14] P. Bernardi, A. Krauskopf, E. Basso, V. Petronilli, E. Blachly-Dyson, F. Di Lisa, M.A. Forte, The mitochondrial permeability transition from in vitro artifact to disease target, *FEBS J.* 273 (2006) 2077–2099.
- [15] A. Rasola, P. Bernardi, The mitochondrial permeability transition pore and its involvement in cell death and in disease pathogenesis, *Apoptosis* 12 (2007) 815–833.
- [16] J.J. Lemasters, T. Qian, C.A. Bradham, D.A. Brenner, W.E. Cascio, L.C. Trost, Y. Nishimura, A.L. Nieminen, B. Herman, Mitochondrial dysfunction in the pathogenesis of necrotic and apoptotic cell death, *J. Bioenerg. Biomembr.* 31 (1999) 305–319.
- [17] M. Crompton, The mitochondrial permeability transition pore and its role in cell death, *Biochem. J.* 341 (1999) 233–249.
- [18] V. Papadopoulos, M. Baraldi, T.R. Guilarte, T.B. Knudsen, J.J. Lacapere, P. Lindemann, M.D. Norenberg, D. Nutt, A. Weizman, M.R. Zhang, M. Gavish, Translocator protein (18 kDa): new nomenclature for the peripheral-type benzodiazepine receptor based on its structure and molecular function, *Trends Pharmacol. Sci.* 27 (2006) 402–409.
- [19] J. Sileikyte, V. Petronilli, A. Zulian, F. Dabbeni-Sala, G. Tognon, P. Nikolov, P. Bernardi, F. Ricchelli, Regulation of the inner membrane mitochondrial permeability transition by the outer membrane translocator protein (peripheral benzodiazepine receptor), *J. Biol. Chem.* 286 (2011) 1046–1053.
- [20] E. Fontaine, F. Ichas, P. Bernardi, A ubiquinone-binding site regulates the mitochondrial permeability transition pore, *J. Biol. Chem.* 273 (1998) 25734–25740.
- [21] V. Petronilli, J. Sileikyte, A. Zulian, F. Dabbeni-Sala, G. Jori, S. Gobbo, G. Tognon, P. Nikolov, P. Bernardi, F. Ricchelli, Switch from inhibition to activation of the mitochondrial permeability transition during hematoxylin-mediated photooxidative stress. Unmasking pore-regulating external thiols, *Biochim. Biophys. Acta* 1787 (2009) 897–904.
- [22] V. Petronilli, P. Costantini, L. Scorrano, R. Colonna, S. Passamonti, P. Bernardi, The voltage sensor of the mitochondrial permeability transition pore is tuned by the oxidation–reduction state of vicinal thiols. Increase of the gating potential by oxidants and its reversal by reducing agents, *J. Biol. Chem.* 269 (1994) 16638–16642.
- [23] P. Costantini, R. Colonna, P. Bernardi, Induction of the mitochondrial permeability transition pore by N-ethylmaleimide depends on secondary oxidation of critical thiol groups. Potentiation by copper-*ortho*-phenanthroline without dimerization

- of the adenine nucleotide translocase, *Biochim. Biophys. Acta* 1365 (1998) 385–392.
- [24] A. Verma, J.S. Nye, S.H. Snyder, Porphyrins are endogenous ligands for the mitochondrial (peripheral-type) benzodiazepine receptor, *Proc. Natl. Acad. Sci. U. S. A.* 84 (1987) 2256–2260.
- [25] G. Le Fur, N. Vaucher, M.L. Perrier, A. Flamier, J. Benavides, C. Renault, M.C. Dubroeuq, C. Gueremy, A. Uzan, Differentiation between two ligands for peripheral benzodiazepine binding sites, [³H]RO5-4864 and [³H]PK 11195, by thermodynamic studies, *Life Sci.* 33 (1983) 449–457.
- [26] E. Romeo, J. Auta, A.P. Kozikowski, D. Ma, V. Papadopoulos, G. Puia, E. Costa, A. Guidotti, 2-Aryl-3-indoleacetamides (FGIN-1): a new class of potent and specific ligands for the mitochondrial DBI receptor (MDR), *J. Pharmacol. Exp. Ther.* 262 (1992) 971–978.
- [27] L. Veenman, M. Gavish, The peripheral-type benzodiazepine receptor and the cardiovascular system. Implications for drug development, *Pharmacol. Ther.* 110 (2006) 503–524.
- [28] J.P. Hullihan, S. Spector, T. Taniguchi, J.K. Wang, The binding of [³H]-diazepam to guinea-pig ileal longitudinal muscle and the in vitro inhibition of contraction by benzodiazepines, *Br. J. Pharmacol.* 78 (1983) 321–327.
- [29] P. Erme, M. Chiesi, S. Longoni, J. Fulbright, K. Hermsmeyer, Relaxation of rat vascular muscle by peripheral benzodiazepine modulators, *J. Clin. Invest.* 84 (1989) 493–498.
- [30] D. Raeburn, L.G. Miller, W.R. Summer, Peripheral type benzodiazepine receptor and airway smooth muscle relaxation, *J. Pharmacol. Exp. Ther.* 245 (1988) 557–562.
- [31] M. Holck, W. Osterrieder, The peripheral, high affinity benzodiazepine binding site is not coupled to the cardiac Ca²⁺ channel, *Eur. J. Pharmacol.* 118 (1985) 293–301.
- [32] F. Ricchelli, J. Sileikyte, P. Bernardi, Shedding light on the mitochondrial permeability transition, *Biochim. Biophys. Acta* 1807 (2011) 482–490.
- [33] A. Verma, S.H. Snyder, Characterization of porphyrin interactions with peripheral type benzodiazepine receptors, *Mol. Pharmacol.* 34 (1988) 800–805.
- [34] M. Awad, M. Gavish, Binding of [³H]Ro 5-4864 and [³H]PK 11195 to cerebral cortex and peripheral tissues of various species: species differences and heterogeneity in peripheral benzodiazepine binding sites, *J. Neurochem.* 49 (1987) 1407–1414.
- [35] M. Awad, M. Gavish, Species differences and heterogeneity of solubilized peripheral-type benzodiazepine binding sites, *Biochem. Pharmacol.* 38 (1989) 3843–3849.
- [36] R. Sprengel, P. Werner, P.H. Seeburg, A.G. Mukhin, M.R. Santi, D.R. Grayson, A. Guidotti, K.E. Krueger, Molecular cloning and expression of cDNA encoding a peripheral-type benzodiazepine receptor, *J. Biol. Chem.* 264 (1989) 20415–20421.
- [37] R. Farges, E. Joseph-Liauzun, D. Shire, D. Caput, G. Le Fur, P. Ferrara, Site-directed mutagenesis of the peripheral benzodiazepine receptor: identification of amino acids implicated in the binding site of Ro5-4864, *Mol. Pharmacol.* 46 (1994) 1160–1167.
- [38] M.B. Rone, J. Liu, J. Blonder, X. Ye, T.D. Veenstra, J.C. Young, V. Papadopoulos, Targeting and insertion of the cholesterol-binding translocator protein into the outer mitochondrial membrane, *Biochemistry* 48 (2009) 6909–6920.